Investigating the substrate specificity of 3-deoxy-D-*arabino*-heptulosonate 7-phosphate (DAH7P) synthase

A thesis

submitted in partial fulfilment

of the requirements for the degree

of

Doctor of Philosophy in Chemistry

at the

University of Canterbury

by

David Tran

UNIVERSITY OF CANTERBURY
Te Whare Wānanga o Waitaha
CHRISTCHURCH NEW ZEALAND

November 2011

When a chemist determines the structure of a different natural product or synthesises a new compound, the effect of a small chemical change — a double bond moved here, an oxygen atom substituted there, an alteration to a side group — often seems of little consequence. It is only with hindsight that we recognise the momentous effect that very small chemical changes can have.

– *Penny Le Couteur*, Napoleon's Buttons

Acknowledgements

I would like to immensely thank my supervisor Emily Parker for all her guidance during my studies. Without your support, advice, encouragement and words of wisdom, finishing this PhD would not have been possible.

Thanks to all the technical staff in the Department of Chemistry for all the wonderful help that was provided throughout my studies: from fixing broken glassware to repairing fumehoods, especially to Marie Squire and Meike Holzenkaempfer for their magical mass-spec powers.

Thanks to Michael Hunter, Tim Allison, Richard Hutton and Andy Pratt for checking, editing and helping me out with the fabrication of this thesis. Without your useful discussions and "constructive" criticisms this thesis may never had been finished.

Thanks to the past members of the Parker research group: Scott Walker, Aidan Harrison, Steve McNabb and Hemi Cummings. The lab was busy and vibrant when you guys were around, but has been very empty since you all left. To the present members of the Parker research group, it has been a barrel of laughs running around with you crazy people. I will miss the conversations, dinners, conferences and miscellaneous things that we did as a group. In addition to the Parker research group, cheers to Fez's research group (Sam McKenize, Evan Nimmo and Davey Lim), having other synthetic organic chemists around to discuss things made working in this department highly entertaining.

Finally, thanks to all my friends and family for your support during this long chapter of my life. Thank goodness it is all over now.

Abstract

The shikimate pathway is a biosynthetic pathway that is responsible for producing a variety of organic compounds that are necessary for life in plants and microorganisms. The pathway consists of seven enzyme catalysed reactions beginning with the condensation reaction between D-erythrose 4-phosphate (E4P) and phosphoenolpyruvate (PEP) to give the seven-carbon sugar DAH7P.

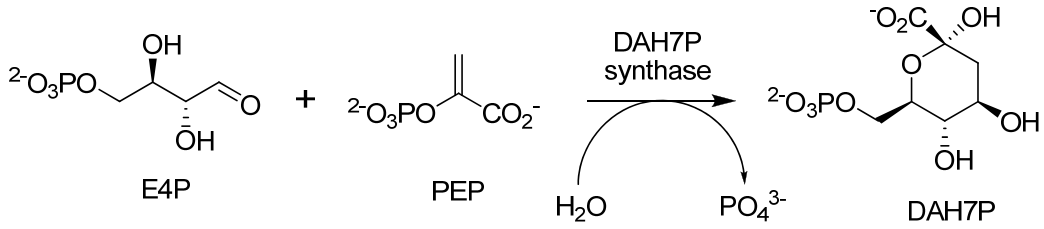

This thesis describes the design, synthesis and evaluation of a range of alternative non-natural four-carbon analogues of E4P to help to probe the substrate specificity of the different types of DAH7P synthases.

Chapter 2 describes the synthesis of 2- and 3-deoxyE4P and their evaluation on the type II DAH7P synthase from *M. tuberculosis*. These E4P analogues were found to be substrates for this type II enzyme, indicating that removal of either the C2 or C3 hydroxyl groups on E4P does not completely disrupt catalysis.

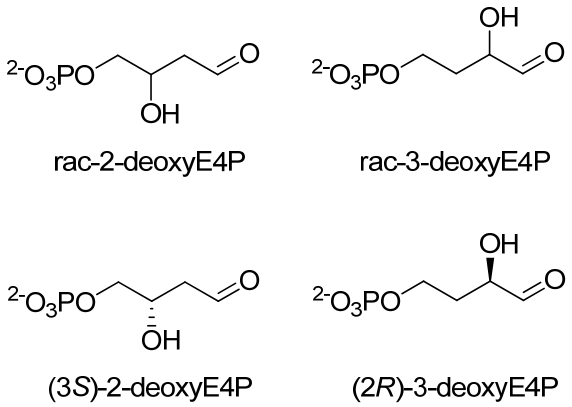

In Chapter 3, the synthesis of 3-methylE4P and the attempts to synthesise 2-methylE4P are described. 3-MethylE4P was prepared in nine steps from DL-malic acid and was found not to be a substrate for the type Iα DAH7P synthase (phe) from *E. coli*.

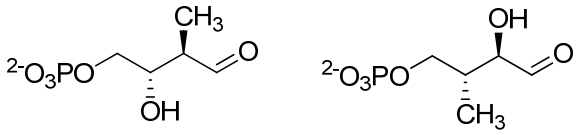

2-methylE4P 3-methylE4P

Chapter 4 describes the synthesis of 2,3-dideoxy erythrose 4-phosphonate **4.38** and the attempts at synthesising the phosphonate analogue of E4P, D-erythrose 4-phosphonate. Compound **4.38** was prepared in overall eight steps from butan-1,4-diol. Evaluation of compound **4.38** on the type Iα DAH7P synthase (phe) from *E. coli* found that it was not a substrate for this enzyme.

D-erythrose 4-phosphonate **4.38**

In Chapter 5, the substrate specificity of DAH7P synthases are discussed and interpreted. Predicted outcomes for 2-methylE4P and D-erythrose 4-phosphonate are also included. Several approaches are described for the completion and advancement of the studies presented here in this thesis.

Table of Contents

Abbreviations

A. aeolicus	*Aquifex aeolicus*
BTP	1,3-bis(tris(hydroxymethyl)methylamino)propane/bis-tris propane
IBX	2-iodoxybenzoic acid
DHQ	3-dehydroquinate
DAH7P	3-deoxy D-*arabino*-heptulosonate 7-phosphate
KDO	3-deoxy-D-*manno*-octulosonate
KDO8P	3-deoxy-D-*manno*-octulosonate 8-phosphate
EPSP	5-enolpyruvylshikimate-3-phosphate
Ac_2O	acetic anhydride
ATP	adenosine 5-triphosphate
ADP	adenosine diphosphate
ap	apparent
aq	aqueous
A5P	arabinose 5-phosphate
Ar	argon
atm	atmosphere
B. subtilis	*Bacillus subtilis*
Bn	benzyl
BTCA	benzyl 2,2,2-trichloroacetimidate
BnBr	benzyl bromide
br.s.	broad singlet
COSY	correlation spectroscopy
DMP	Dess-Martin periodinane
DCM	dichloromethane
DIBALH	diisobutylaluminium hydride
DMF	dimethylformamide
d	doublet
ddd	doublet of doublet of doublets
dd	doublet of doublets
ESI	electrospray ionisation
E4P	erythrose 4-phosphate
E. coli	*Escherichia coli*
EtOH	ethanol
Et	ethyl
EtOAc	ethyl acetate
EDCP	ethyl dichlorophosphite
EDPP	ethyl diphenylphosphate
EDTA	ethylenediaminetetraacetic acid
H. pylori	*Helicobacter pylori*
HMBC	heteronuclear multiple bond coherence
HSQC	heteronuclear single quantum coherence

HRMS	high resolution mass spectrometry
Im	imidazole
k_{cat}	turnover number
K_i	inhibition constant
Pi	inorganic phosphate
LPS	lipopolysaccharide
LDA	lithium diisopropylamine
m.p.	melting point
mRNA	messenger ribonucleic acid
MeOH	methanol
Me	methyl
K_M	Michaelis constant
m	multiplet
M. tuberculosis	*Mycobacterium tuberculosis*
NBS	*N*-bromosuccinimide
NMR	nuclear magnetic resonance
PABA	para-aminobenzoic acid
ppm	parts per million
Pet ether	petroleum ether
Ph	phenyl
phe	phenylalanine
PEP	phosphoenolpyruvate
p-TsOH	p-toluenesulfonic acid
P. furiosus	*Pyrococcus furiosus*
R_f	retention factor
RNA	ribonucleic acid
S. cerevisiae	*Saccharomyces cerevisiae*
sat.	saturated
s	singlet
NaAc	sodium acetate
NaH	sodium hydride
^{t}Bu	tert-butyl
TBDPSCl	tert-butyl diphenylchlorosilane
TBDMSCl	tert-butyldimethylchlorosilane
TBDMS	tert-butyldimethylsilyl
TBDPS	tert-butyldiphenylsilyl
TBAI	tetrabutylammonium iodide
THF	tetrahydrofuran
TBAF	tetra-n-butylammonium fluoride
IC_{50}	the half maximal inhibitory concentration
T. maritima	*Thermotoga maritima*
TLC	thin layer chromatography
T4P	threose 4-phosphate

Tf	triflic
TfOH	trifluoromethanesulfonic acid or triflic acid
TIPS	triisopropylsilyl
TIPSCl	triisopropylsilyl chloride
TMSBr	trimethylsilyl bromide
TMSCl	trimethylsilyl chloride
t	triplet
TCEP	tris(2-carboxyethyl)phosphine
trp	tryptophan
tyr	tyrosine
UV	ultra violet
v/v	volume per volume
wt	weight
w/v	weight per volume

Amino acid three-letter codes

Ala	alanine	Glu	glutamate	Leu	leucine	Ser	serine
Arg	arginine	Gln	glutamine	Lys	lysine	Thr	threonine
Asn	asparagine	Gly	glycine	Met	methionine	Trp	tryptophan
Asp	aspartate	His	histidine	Phe	phenylalanine	Tyr	tyrosine
Cys	cysteine	Ile	isoleucine	Pro	proline	Val	valine

Chapter 1: Introduction

1.1 The shikimate pathway

The shikimate pathway (Figure 1.1) is a biosynthetic pathway that is responsible for producing a variety of organic compounds that are necessary for life in plants and microorganisms. The pathway consists of seven enzyme catalysed reactions beginning with the condensation reaction between D-erythrose 4-phosphate (E4P) and phosphoenolpyruvate (PEP), and ultimately ending with the synthesis of chorismate.[1-3]

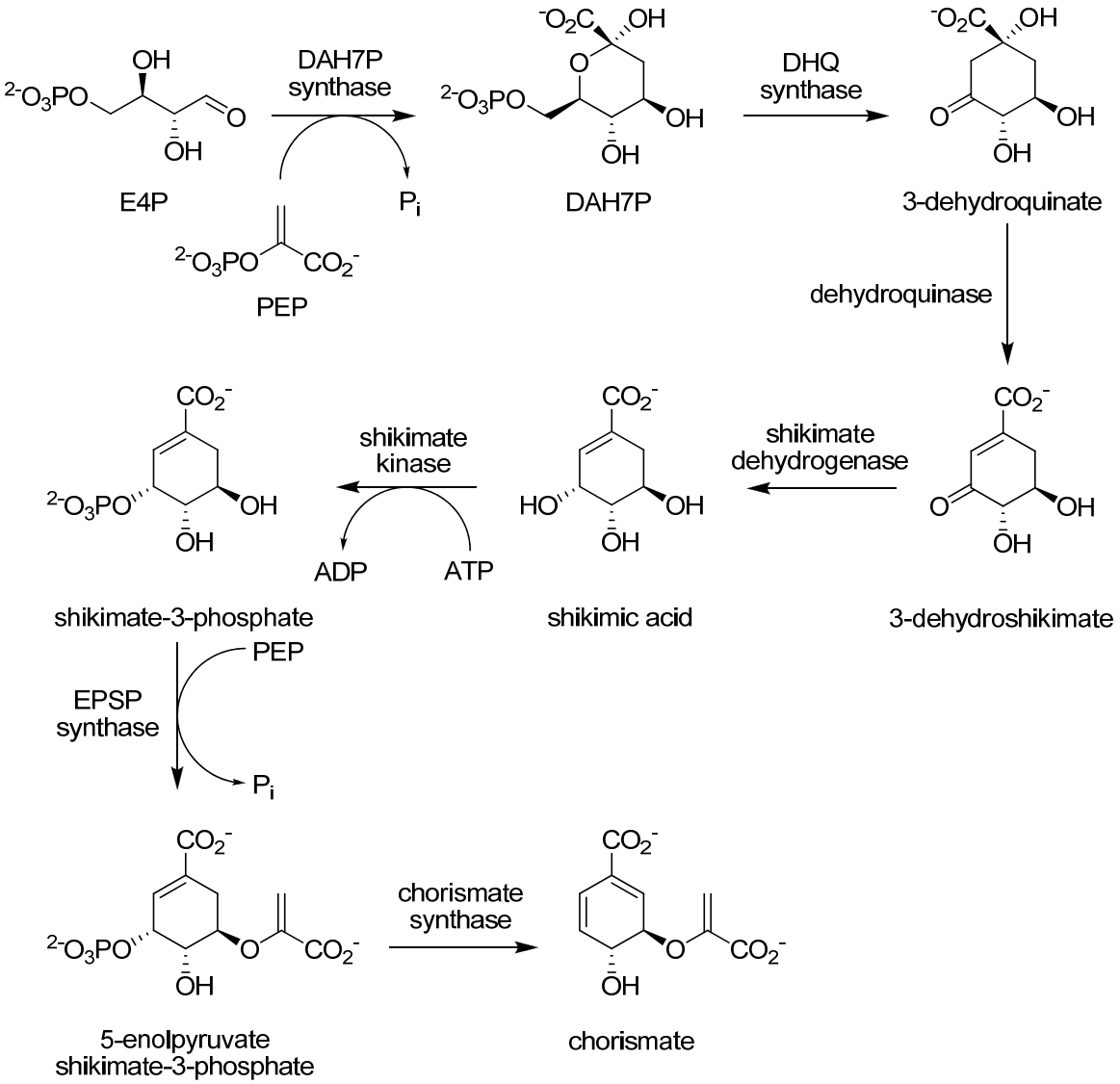

Figure 1.1: The shikimate pathway.

The shikimate pathway is named after its central metabolic intermediate, shikimic acid, which was first isolated from *Illicium religiosum* (in Japanese, shik-imi-no-ki) in 1885.[4] However, the structure and stereochemistry of shikimic acid was not determined until the 1930s and it was not till the 1950s that the structure of shikimic acid was noted to be similar to that of aromatic compounds. Subsequently, shikimic acid was found to be an important intermediate in the biosynthesis of aromatic compounds.[5,6]

Chorismate, the end product of the shikimate pathway, is a highly important precursor for the synthesis of the essential aromatic amino acids phenylalanine, tyrosine and tryptophan, as well as other important aromatic compounds such as ubiquinones (an electron transfer agent used in cellular respiration) and *para*-aminobenzoic acid (PABA) which is converted into folates (Figure 1.2).[7,8]

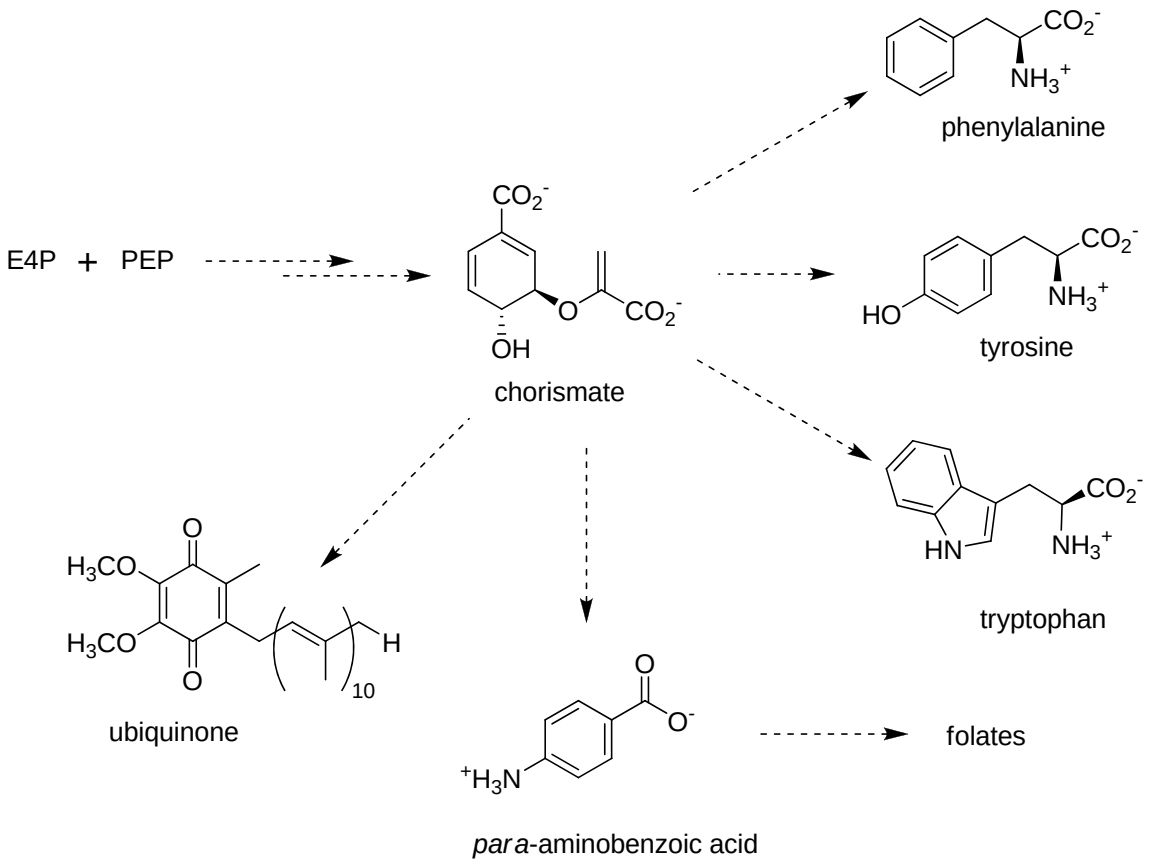

Figure 1.2: Chorismate is a key precursor for the biosynthesis of aromatic amino acids, ubiquinones and folates.

The shikimate pathway is essential for the production of the aromatic amino acids in plants, bacteria and fungi, but the pathway is absent in animals. The absence of this pathway in animals makes this pathway an important target for the action of herbicides and

antibiotics.[9-11] One such example is the herbicide glyphosate (Roundup®, Sigma)[1,9,12], a compound of enormous commercial and agricultural importance as it inhibits the sixth enzyme of the pathway (Figure 1.3), 5-enolpyruvyl-shikimate 3-phosphate (EPSP) synthase. In addition to being a potent broad spectrum herbicide it has been successfully tested on mice as a therapeutic agent against diseases such as toxoplasmosis and malaria.[1,13,14]

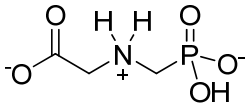

Figure 1.3: The structure of *N*-(phosphonomethyl) glycine (Glyphosate), a broad spectrum herbicide used to kill weeds. Also know as Roundup®.

1.2 DAH7P synthase

The first step of the shikimate pathway is catalysed by the enzyme 3-deoxy-D-*arabino*-heptulosonate 7-phosphate (DAH7P) synthase. The enzyme catalyses the condensation reaction between E4P, an intermediate of the pentose-phosphate cycle, and PEP, an intermediate of the glycolytic pathway, to give the seven carbon sugar DAH7P (Figure 1.4).[12,15] It constitutes the first committed step in the biosynthesis of aromatic amino acids, various aromatic cofactors and secondary metabolites that are formed in microorganisms, plants and fungi. The reaction catalysed by DAH7P synthase was first demonstrated experimentally in 1959 in *Escherichia coli* cellular extracts.[16,17]

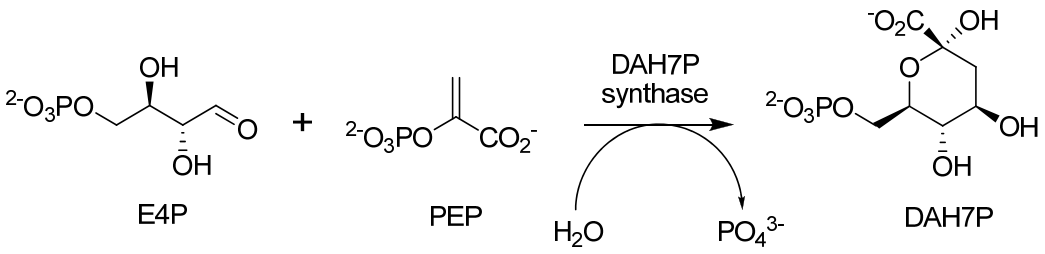

Figure 1.4: The reaction catalysed by the first enzyme, DAH7P synthase, in the shikimate pathway.

There is also a very closely related enzyme to DAH7P synthase, 3-deoxy-D-*manno*-octulosaonate 8-phosphate (KDO8P) synthase. KDO8P synthase catalyses a similar reaction to that of DAH7P synthase, except that D-arabinose 5-phosphate (A5P) is used in place of

E4P to form 3-deoxy-D-*manno*-octulosonate 8-phosphate (KDO8P), an eight carbon analogue of DAH7P. This enzyme is described in a later section (page 21).

1.2.1 Classification

The family of DAH7P synthases can be broadly divided into two groups based on amino acid sequence and molecular mass, and are classified as type I or type II DAH7P synthases according to Walker *et al*. (Figure 1.5).[18] The type I and type II DAH7P synthases have also been referred to as the $AroA_I$ and $AroA_{II}$ families, respectively, by Gosset *et al*.[19]

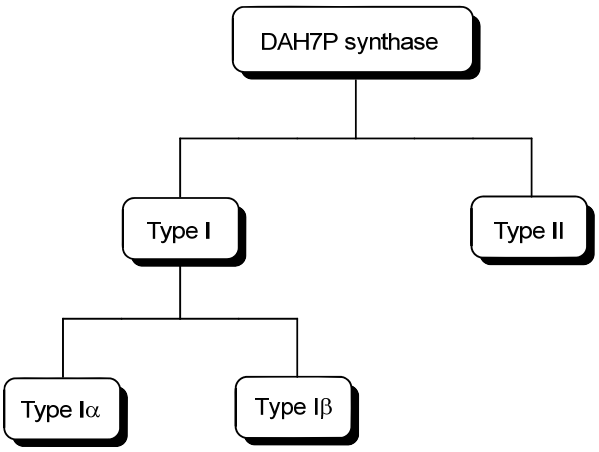

Figure 1.5: The families of DAH7P synthases, based on sequence relationships.

Type I DAH7P synthases are defined as having an *E. coli*-like sequence with molecular masses of less than 40 kDa; and represent the most well characterised family of DAH7P synthases. The type I DAH7P synthases can be further divided into two subfamilies, denoted Iα and Iβ, based on sequence similarity.[20] Subfamily Iα consist entirely of DAH7P synthases and include the structurally characterised enzymes from *E. coli*[21-24] and *Saccharomyces cerevisiae*.[25-27] Subfamily Iβ on the other hand contain both DAH7P synthases (subfamily $I\beta_D$) and KDO8P synthases (subfamily $I\beta_K$), based on sequence similarities.[28] The Iβ subfamily is also considered to be ancestral to all DAH7P and KDO8P synthases with ancient lineages such as *Pyrococcus furiosus* and *Thermotoga maritima*.[29] The $I\beta_D$ are functionally related to the Iα enzymes (catalysing the same reaction between E4P and PEP) but bear more structural similarities with the $I\beta_K$ enzymes.[20] The $I\beta_K$ enzymes can also be further divided into metallo[30] and non-metallo enzymes.[31] All DAH7P synthase are metallo enzymes.

Type II DAH7P synthases are defined as "plant-like" homologues with a molecular mass around 54 kDa. Additionally, type II DAH7P synthases were originally identified in plant proteins, they are now known to encompass a diverse set of microbial protein and include the bacterial DAH7P synthases from *Mycobacterium tuberculosis* and *Streptomyces*.[12,19]

A phylogenetic tree based on sequence similarity between type I enzymes has been constructed by Jensen *et al*. (Figure 1.6).[29] The subfamily Iα contains only DAH7P synthases. All of which have feedback regulation. Subfamily Iβ consists of the subfamilies $I\beta_D$ and $I\beta_K$, representing the DAH7P and KDO8P synthases, respectively. Among the structurally characterised members of subfamily Iβ, only the *T. maritima* DAH7P synthase has feedback regulation. Birck *et al.*[28] have suggested that DAH7P and KDO8P synthases are evolutionally related by divergent evolution from a common ancestor and are based on the two enzymes having similar proposed mechanisms and very similar monomer structures. Gosset *et al*.[19] proposed that due to the widely distributed Iβ enzymes found in nature, the ancestral form of DAH7P synthase must be a Iβ-like protein. Subramaniam *et al.*[20] proposed that substrate specificity could explain the differences between the Iα and Iβ subfamilies, and that ancient proteins had broad substrate specificities which narrowed over time. For example, the enzyme from *P. furiosus*, a $I\beta_D$ DAH7P synthase, is considered one of the most closely related enzymes to the ancestral enzyme, and displays a broad substrate specificity and no feedback regulation.[32]

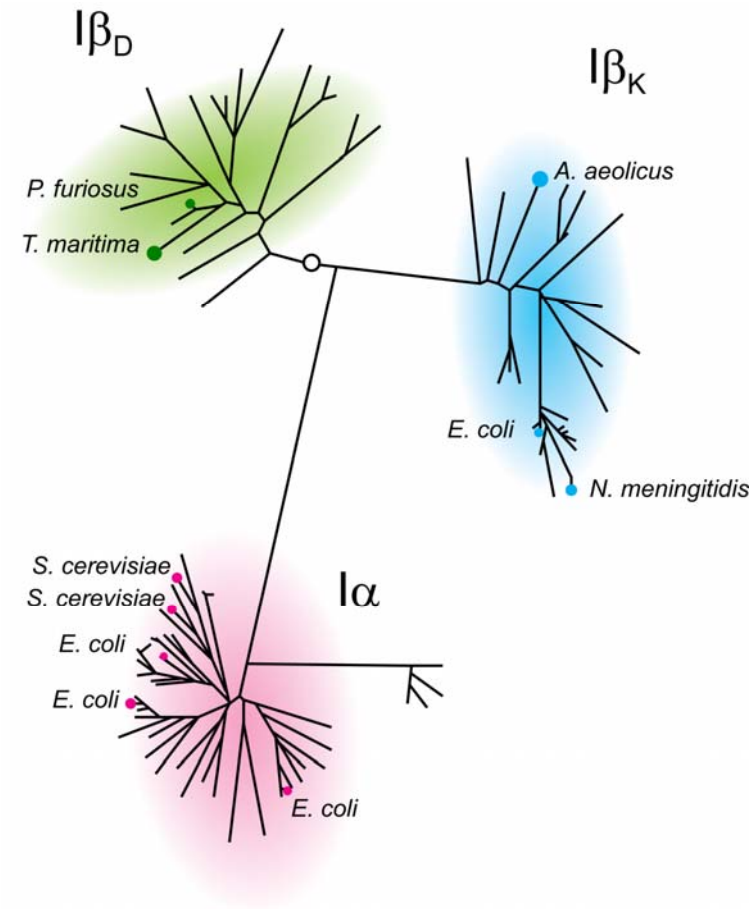

Figure 1.6: Phylogentic tree of homology type I proteins consisting of subfamilies Iα and Iβ modified from Jensen *et al.*[29] Subfamily Iα contain only DAH7P synthase proteins that have feedback regulation. Subfamily Iβ consists of subfamily Iβ$_D$ (DAH7P synthases) and subfamily Iβ$_K$ (KDO8P synthases). The white circle indicates the hypothetical root.

1.2.2 Feedback regulation

The first step of the shikimate pathway, catalysed by DAH7P synthase, regulates carbon flow though the entire pathway by feedback regulation. In addition, the shikimate pathway is responsible for up to 30% of the total carbon flux within the cell, so this makes DAH7P synthase a vital part of the overall control of cellular carbon flux.[15] *E. coli* DAH7P synthase has three isozymes, each sensitive to feedback regulation by one of the three aromatic amino acid products of the pathway; phenylalanine, tyrosine or tryptophan. DAH7P synthase (phe), the phenylalanine inhibited isozyme of DAH7P synthase, is responsible for about 80% of the total activity in *E. coli*.[15] The rest of the activity is made up from the tyrosine-sensitive isozyme, DAH7P synthase (tyr), and the tryptophan-sensitive isozyme, DAH7P synthase (trp), which accounts for ~20% and <1% activity, respectively.[33] The structural genes, *aroG*,

aroF and *aroH* are scattered over the *E. coli* chromosome and encode the phenylalanine-, tyrosine-, and tryptophan-sensitive DAH7P synthases, respectively.[34]

Not all DAH7P synthases are inhibited by the three aromatic amino acids in the same way as the enzymes from *E. coli*. Different microorganisms express between one and three isozymes of DAH7P synthase which are inhibited by end products or intermediates of the pathway, or a combination of the two, while some enzymes are entirely unregulated.[18] For example, DAH7P synthase from the hyperthermophile *T. maritima* is inhibited by phenylalanine or tyrosine, but not by tryptophan, and the enzyme from the extremophile *P. furiosus* is not inhibited by phenylalanine, tyrosine or tryptophan.[7,35]

Structural and kinetic studies have provided some insight into the mechanism by which this feedback regulation works. All DAH7P synthases characterised to date, except *P. furiosus*, have some kind of decoration on the basic $(\beta/\alpha)_8$ barrel (Figure 1.7).[25] The Iα proteins from *E. coli* and *S. cerevisiae* have an N-terminal extension and a β-sheet inserted between the α5 and β6 strands of the barrel. The type II enzyme from *M. tuberculosis* has a major extension at the N-terminus and a pair of α-helices inserted into the α2-β3 connecting loop. Evidence based on studies with *S. cerevisiae*, *P. furiosus* and *M. tuberculosis* suggests that these decorations contain the binding sites for allosteric inhibitors (Figure 1.7).[36-39] Studies on the tyrosine-sensitive *S. cerevisiae* DAH7P synthase showed that by deleting the N-terminal extensions the enzyme becomes unregulated.[25] The lack of feedback regulation of the *P. furiosus* enzyme can be explained by the absence of the regulatory extensions on the enzyme.[35] Like *P. furiosus* DAH7P synthase, KDO8P synthases have only a basic barrel structure and are unregulated.[31]

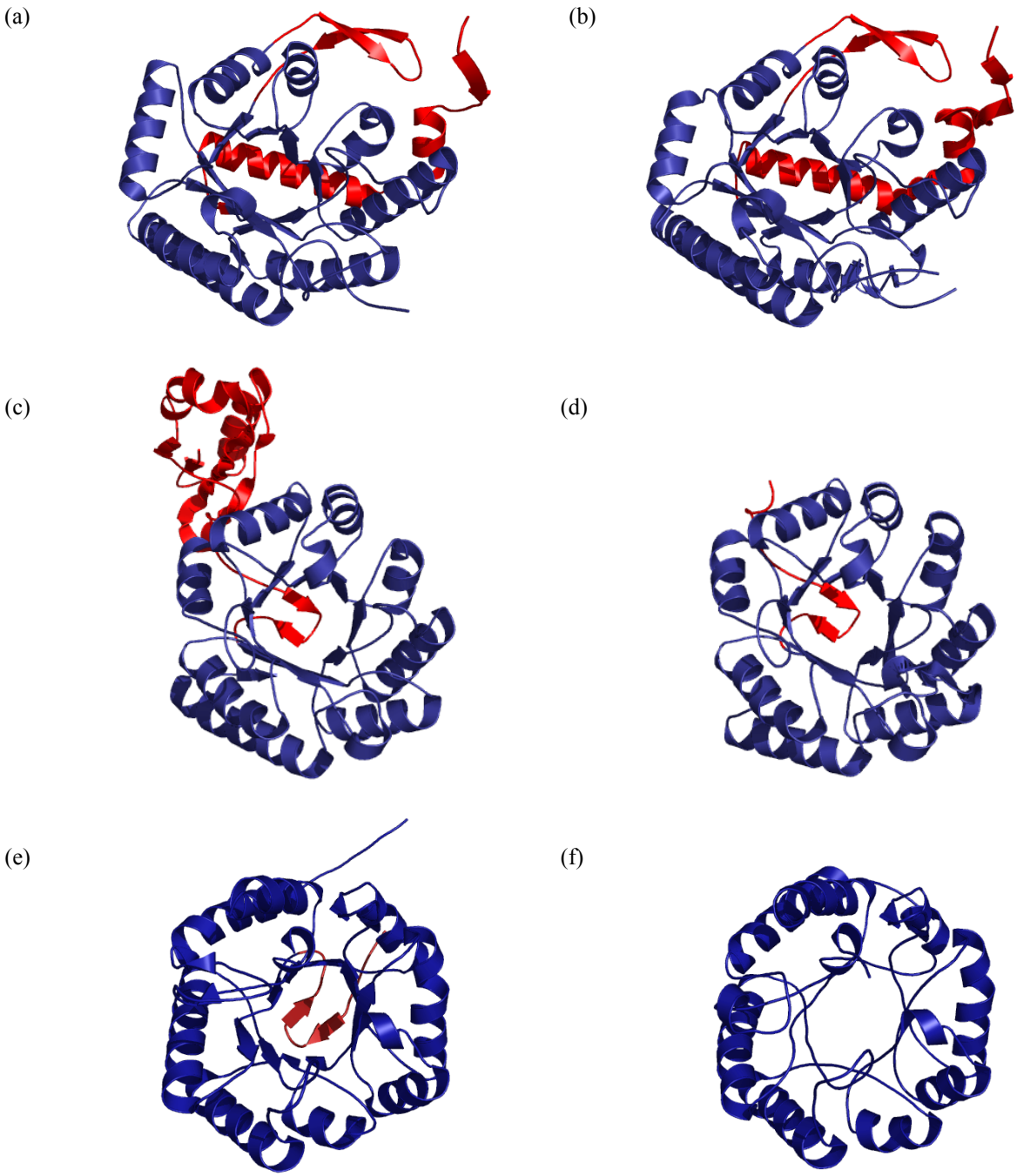

Figure 1.7: The monomer structures of (a) *E. coli* DAH7P synthase (phe) (PDB code 1KFL), (b) *S. cerevisiae* DAH7P synthase (tyr) (PDB code 1OF6), (c) *T. maritima* DAH7P synthase (PDB code 1RZM), (d) *P. furiosus* DAH7P synthase (PDB code 1ZCO), (e) *E. coli* KDO8P synthase (PDB code 1D9E), and (f) *Aquifex aeolicus* KDO8P synthase (PDB code 1FWW). Structures from Meekyung Ahn.[40] The views of the structures are looking down their $(\beta/\alpha)_8$-barrel. The overall structures of *T. maritima* and *P. furiosus* DAH7P synthases appear to be more similar to those of *E. coli* and *A. aeolicus* KDO8P synthases than those of *E. coli* and *S. cerevisiae* DAH7P synthases. The helices and loops are highlighted in blue and N-terminal extension, along with extended loops, is highlighted in red. The extra extension and loops are implicated in feedback regulation. *P. furiosus* DAH7P synthase, and *E. coli* and *A. aeolicus* KDO8P synthases do not have feedback regulation and lack N-terminal extensions.

A structure of *E. coli* DAH7P synthase (phe) with the phenylalanine inhibitor bound has been solved and provides some insight onto how feedback regulation functions in the type Iα family.[21,41] The structure shows phenylalanine bound in a cavity on the outer side of the barrel, near the N-terminus, in each monomer. The binding of phenylalanine appears to initiate a transmission pathway in which an inhibitory signal is transmitted from the β6a/β6b segment, which binds phenylalanine, to the β2–α2 segment which contains both PEP and E4P binding residues (Figure 1.8). This transmission is thought to result in significant conformational changes in the enzyme causing the enzyme to lose the ability to bind E4P and causing of PEP to be bound in a flipped orientation.[21]

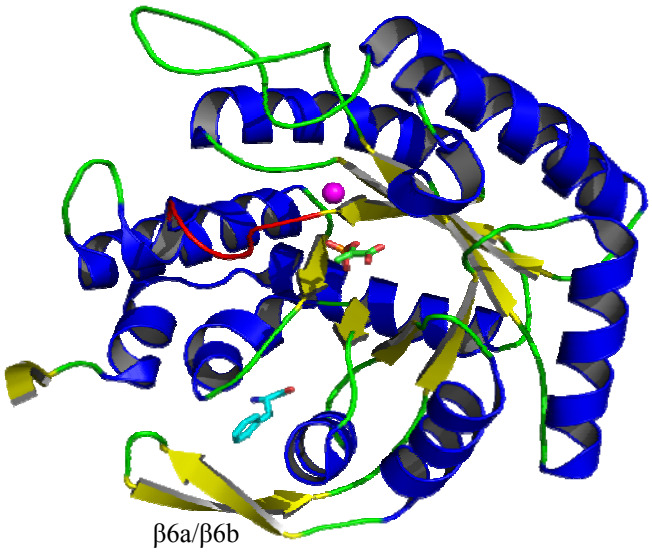

Figure 1.8: *E. coli* DAH7P synthase (phe) monomer structure showing the α-helices (blue) and β-sheets (yellow) of the basic $(\beta/\alpha)_8$ TIM barrel (PDB code 1KFL). The β2–α2 loop is in red. Phenylalanine (cyan/pink/blue), PEP (green/orange/pink), Mn^{2+} (magenta).

1.2.3 Metal activation

Studies testing the sensitivity of DAH7P synthases to the presence of metal ions and to the metal chelator ethylenediaminetetraacetic acid (EDTA), have found that all DAH7P synthases characterised to date require a divalent metal ion for activity.[22,42-46] Although the role of the divalent metal ion for the reaction catalysed by DAH7P synthase is still unclear. These studies showed that DAH7P synthases completely lost activity in the presence of EDTA and were reactivated by the addition of metal ions. Additionally, sequence alignments have shown that all identified DAH7P synthases possess the metal-binding residues Cys, His, Glu and Asp.[46]

Although DAH7P synthases appear to have an absolute requirement for the presence of a divalent metal ion, there is considerable variation in the ability of different metal ions to activate the enzyme after treatment with a metal chelator. The extent to which a given metal ion can do this *in vitro* differs from species to species and also in the different isozymes of the same organism.[35,38,47] For example, the tyrosine regulated isozyme of *S. cerevisiae* is most activated by Co^{2+}, whilst the phenylalanine regulated isozyme is most activated by Mn^{2+}.[26]

The three isozymes of DAH7P synthase from *E. coli* and their specific reactions by various metal ions has been reported by Stephens *et al.*[48]; with the order of activation as follows: $Mn^{2+} > Cd^{2+}$, $Fe^{2+} > Co^{2+} > Ni^{2+}$, Cu^{2+}, $Zn^{2+} >> Ca^{2+}$. Interestingly, although Mn^{2+} showed the highest activity with all three isozymes of DAH7P synthase from *E. coli*, the Mn^{2+} bound to the enzymes is highly labile and can be displaced by other metals. In contrast, the Fe^{2+}, Co^{2+} and Zn^{2+} enzyme complexes are considerably less labile. These workers suggested that Fe^{2+} and perhaps Zn^{2+} may be the preferred metal cofactors *in vivo*.

There has been an ongoing debate in literature regarding the nature of the metal ion at the active site of DAH7P synthase *in vivo*. A variety of metal ions have been proposed to reside at the active site under physiological conditions.[7,49] The metal present in *E. coli* DAH7P synthase (phe) from *in vivo* studies was thought to be Co^{2+} or Fe^{2+} or even Cu^{2+} as these metals were found in the enzyme solution after purification.[42,43,50,51] Analysis of purified samples of *E. coli* DAH7P synthase (phe) using atomic absorption spectroscopy by Stephens *et al.*[48], indicated Fe^{2+}, Zn^{2+}, Cu^{2+}, Mn^{2+} and Co^{2+} metal ions to be present in the enzyme. As mentioned before, it was suggested that Fe^{2+} and perhaps Zn^{2+}, may be the preferred metal

cofactors *in vivo* and was based on the presence of these two metals before removal by chelation, their high bioavailability, and the high affinity of the enzymes for these metal ions *in vitro*.[48]

It is clear from these studies that DAH7P synthases are activated by a wide range of divalent metal ions and that all DAH7P synthases, to date, require a metal for enzyme activity. However, after more than 30 years of research, the nature of the physiological metal ion at the active site is still an open question and the metal ion is likely to depend on various factors such as bioavailability and growth conditions.[7]

The presence of high concentrations of metal ions in enzymes can also cause the inactivation of the enzyme, in particular it has been shown that in the absence of the substrate PEP, redox-active metal ions (e.g. Cu^{2+} and Fe^{2+}) catalyse the inactivation of *E. coli* DAH7P synthase (phe).[52] The inactivation of this enzyme is caused by the metal-catalysed oxidation of two cysteine residues, Cys61 and Cys328, which is not seen when the enzyme is treated with EDTA. The presence of high metal concentrations allows a conformational change in the active site of the enzyme, causing the thiol groups of Cys61 and Cys328 to be orientated in a position to enable disulfide bond formation. The binding of PEP in the active site presumably hinders this conformational change.[20,52,53] Studies on *M. tuberculosis* DAH7P synthase have identified the formation of disulfide bonds between the metal-binding Cys61 and other Cys residues.[37] Reducing agents such as *tris*(2-carboxyethyl)phosphine (TCEP) have to be added to reactions in order to maintain full enzyme activity.[38,47]

1.2.4 Mechanism

The mechanism of DAH7P synthase has been investigated widely in literature and several studies have provided valuable information on the mechanism. Analysis of the product of the reaction utilising stereospecifically labelled PEP has shown that the addition of PEP to E4P proceeds stereospecifically with the *si* face of PEP attacking the *re* face of E4P (Figure 1.9) to produce the seven carbon sugar DAH7P.[54,55]

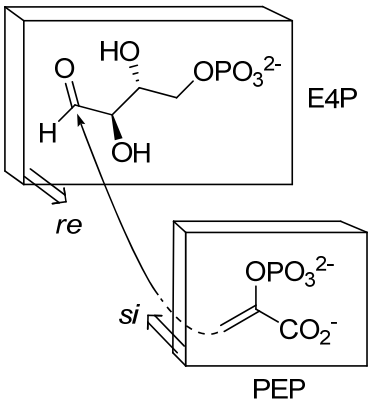

Figure 1.9: The stereospecific reaction between PEP onto E4P catalysed by DAH7P synthase.

Labelling studies using ^{18}O have shown that DAH7P synthase catalyses the unusual cleavage of the C-O bond rather the P-O bond of PEP.[56] Typical enzymes utilising PEP make use of the high energy contained in the phosphate ester bond ($\Delta G^{o} = -62$ kJ mol^{-1}) by cleavage of the P-O bond of PEP; only a few enzymes such as EPSP synthase and UDP-*N*-acetyl-glucosamine enolpyruvyltransferase (MurA), cleave via the C-O bond in PEP.[57,58]

It was originally thought the reaction between E4P and PEP catalysed by DAH7P synthase followed a ping-pong mechanism[59], but this was eventually disproven through detailed kinetic studies.[45] In fact, the reaction proceeds though an ordered sequential mechanism, with PEP binding first before E4P, followed by the release of phosphate and then DAH7P.[45]

The exact mechanism of DAH7P synthase has been the subject of ongoing controversy. Two possible mechanisms have been proposed (Figure 1.10). These differ by the order in which water adds to PEP and PEP adds to E4P.

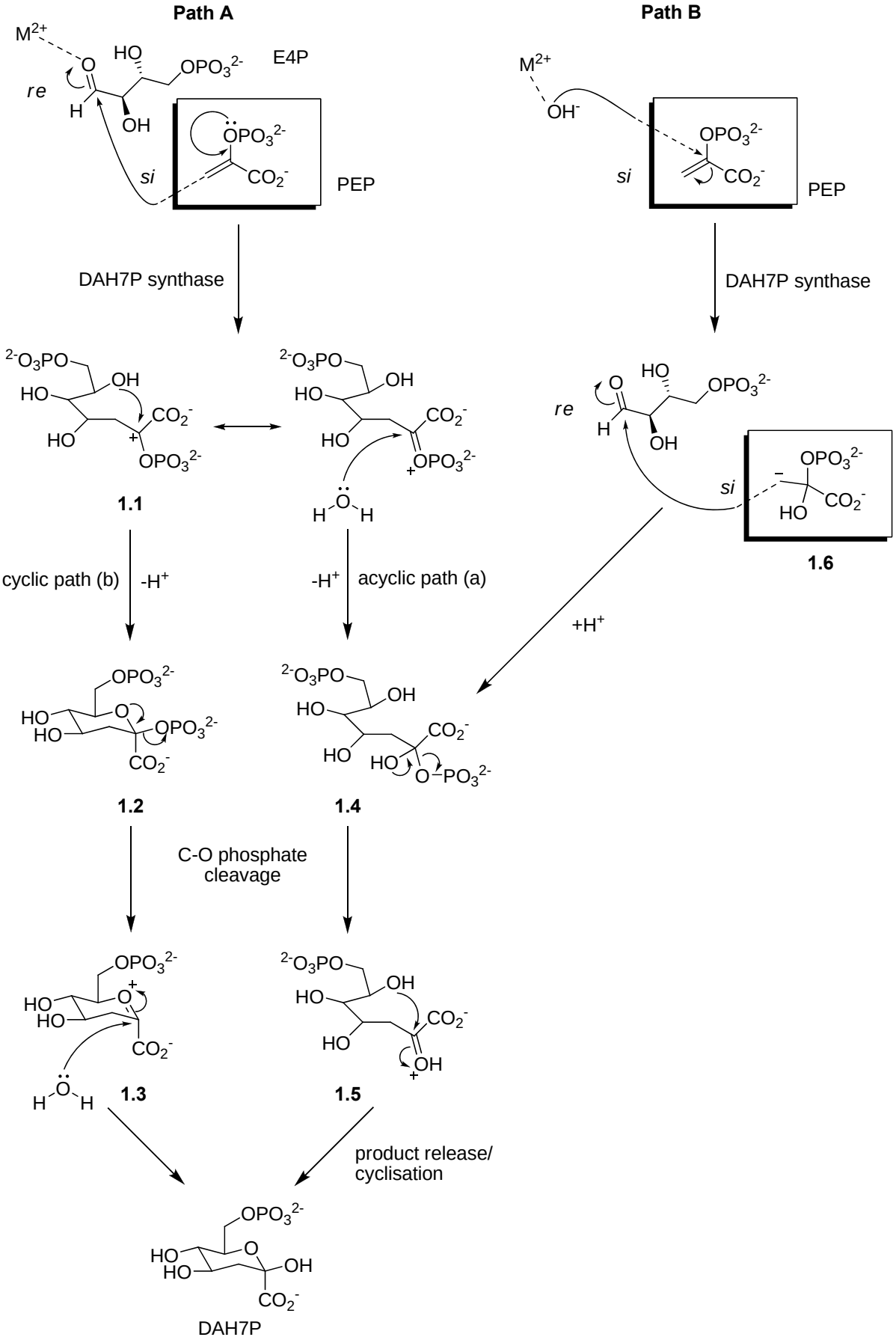

Figure 1.10: Proposed mechanisms for DAH7P synthase.

In path A (Figure 1.10), the C3 of PEP attacks the metal-activated carbonyl group of E4P to form the oxocarbenium ion intermediate **1.1**. The mechanism then diverges into two possible pathways for the synthesis of DAH7P, the acyclic path (a) and the cyclic path (b). In the acyclic pathway, the intermediate **1.1** is attacked by water to give the labile phosphate hemiketal intermediate **1.4**. This intermediate then undergoes loss of phosphate forming the acyclic DAH7P **1.5**, and giving the observed C-O phosphate bond cleavage. The DAH7P sugar is then released, followed by spontaneous cyclisation in solution to give the more stable hemiacetal form of DAH7P. In the cyclic pathway (Path A, Figure 1.10) the oxocarbenium ion intermediate **1.1** cyclises to give the cyclic hemiketal biphosphate compound **1.2**. Cyclisation is achieved by the hydroxyl group on C3 of E4P attacking the carbocation formed at C2 of PEP. The biphosphate compound **1.2** then undergoes a C-O bond cleavage to give the cyclic oxonium ion **1.3**, with the release of inorganic phosphate. Water then attacks the C2 position of the oxonium ion **1.3** to give the cyclic form of DAH7P.[56,58,60,61]

The proposed mechanism shown in path B (Figure 1.10) begins with the formation of a carbanion intermediate **1.6** that is formed by the attack of a hydroxide ion onto the C2 position of PEP (the hydroxide ion is produced by the deprotonation of a metal-water complex). The carbanion **1.6** then attacks the carbonyl group of E4P to give the labile phosphate hemiketal intermediate **1.4**. Intermediate **1.4** then follows the same route as the acyclic path (a) mentioned before, eventually giving the cyclic DAH7P.[45,61-64]

Both path B and the cyclic pathway of path A have been discredited due to a number of factors and the most plausible mechanistic route is seen in the acyclic pathway of path A. Path B requires the existence of an unstabilised carbanion, with a likely pK_a of > 30, inside the enzyme active site that contains carbon-hydrogen bonds of greater acidity in addition to water molecules, carboxylic acids and ammonium ions. Any of these species in the active site could potentially and immediately quench the carbanion long before it has a chance to attack E4P making path B an implausible mechanism.[65] The cyclic pathway in path A, has been discredited by a number of observations. Firstly, the compound 3-deoxyE4P has been shown, by Dr Amy Pietersma[66] and in this thesis (Chapter 2), to be a substrate for DAH7P synthase. If only the cyclic mechanism operated, then 3-deoxyE4P should not be a substrate as the C3-hydroxy group in E4P is required for cyclisation in this pathway. Therefore, this cyclic pathway is not the exclusive mechanism for the formation of DAH7P. Secondly, studies of the structure of DAH7P synthase active site has shown the active site to be a long linear

pocket in which there is insufficient room for intramolecular cyclisation making this cyclic pathway implausible.[21,32,38,63]

1.2.5 Enzyme structure

The most well characterised examples of DAH7P synthases are those from *E. coli*. As previously mentioned, *E. coli* DAH7P synthase has three isozymes all of which belong to the type Iα family of DAH7P synthases. The structure of *E. coli* DAH7P synthase (phe) has been investigated by X-ray crystallography and the first structure of this enzyme was determined as a Pb^{2+}-PEP complex at 2.6 Å resolution by Shumilin *et al.* in 1999 (Figure 1.11).[21]

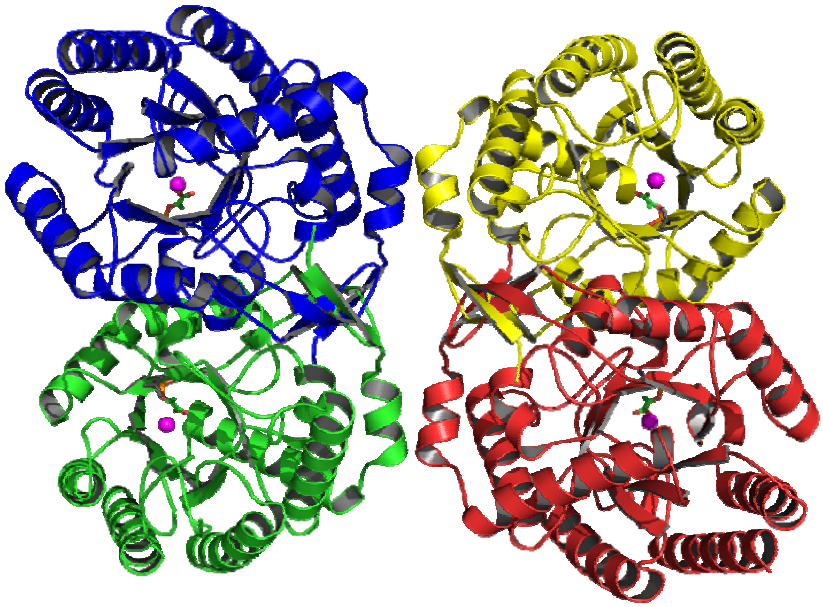

Figure 1.11: Structure of the *E. coli* DAH7P synthase (phe)- Pb^{2+}-PEP tetramer (PDB code 1QR7). PEP substrate (green/orange/pink, stick model), lead ion (magenta) and sulphate ion (grey).

The enzyme crystallised as a tetramer consisting of two tight dimers. Each monomer is a $(\beta/\alpha)_8$ barrel enhanced by a N-terminal extension of 53 residues, as well as a two-stranded antiparallel β-sheet, β6a/β6b inserted between the α5 and β6 strands of the barrel. These two additional structural elements have been shown to be essential for feedback regulation (Figure 1.12).[25,41] The active site of the enzyme is located at the C-terminal end of the β strands of the $(\beta/\alpha)_8$ barrel and contains the binding sites for PEP, metal and E4P.

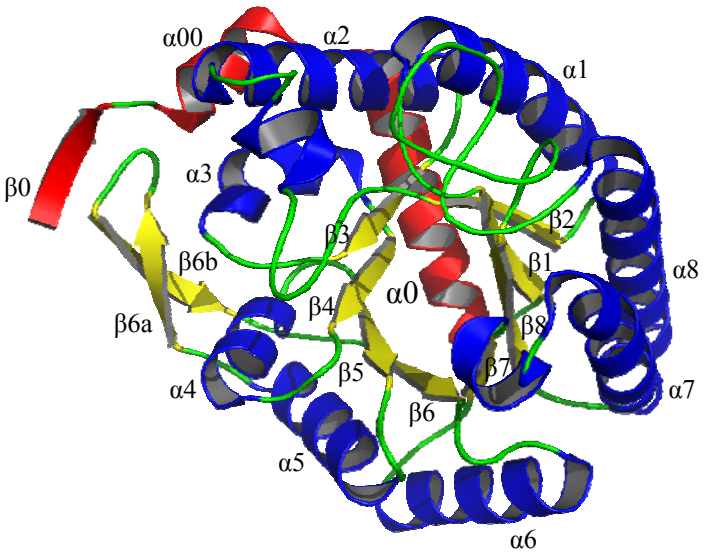

Figure 1.12: *E. coli* DAH7P synthase (phe) monomer structure with α-helices and β-sheets of the basic $(\beta/\alpha)_8$ TIM barrel labelled (PDB code 1KFL). N-terminal extension coloured red.

Pb^{2+} is bound at the active site of DAH7PS near the C-terminal end of the barrel. The metal ion is held in distorted trigonal bipyramidal geometry, coordinated to four protein side chains (Cys61, His268, Glu302 and Asp326), PEP and a water bridging to Lys97. PEP is found at the bottom of the active site cleft surrounded by six positively charged residues which anchor the substrate with either multiple salt bridges (Arg92, Lys97, Arg165, Lys186 and Arg234) or conjugated π bonds (His268). Each of the three anionic oxygens of the phosphate of PEP is bonded with two or three nitrogen atoms of Arg165, Lys186 or Arg234. The oxygen atoms of the carboxylate group of PEP forms salt bridges with the nitrogen atoms of Arg92 and Lys186 (Figure 1.13).

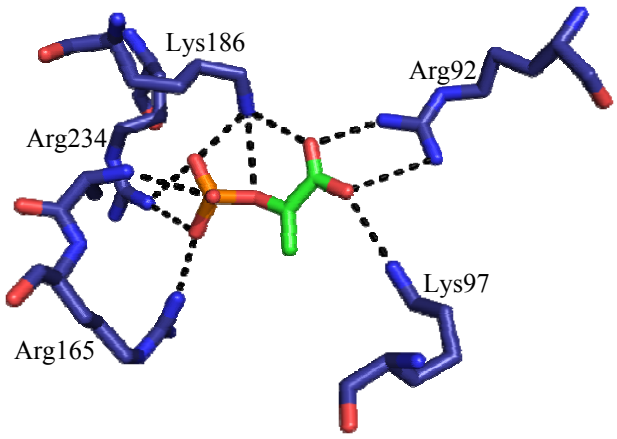

Figure 1.13: Coordination of PEP in *E. coli* DAH7P synthase (phe) active site (PDB code 1QR7). Dashed lines indicate polar interactions between PEP (green/orange/pink) and surrounding residues.

There is a channel leading to PEP from the top of the $(\beta/\alpha)_8$ barrel in the active site of *E. coli* DAH7P synthase. C3 of PEP, which forms a covalent bond with C1 of E4P in the condensation reaction (Figure 1.10, page 13), is pointed towards this opening. Additionally, the structure shows a sulphate ion in this channel and it has been suggested that this sulphate ion occupies the binding site of the phosphate of E4P.[21,63] When the phosphate group of E4P is docked to the sulphate ion binding site, E4P in the extended conformation fits into the channel leading to the bound PEP molecule. The C1 of E4P can approach to within 3.0 Å of C3 of PEP.[21]

While to date there is no structure that shows E4P bound in the active site of DAH7P synthase in a manner competent for reaction, the structure of *S. cerevisiae* DAH7P synthase (tyr) has been determined containing bound Co^{2+}, PEP and D-glycerol 3-phosphate (G3P) (Figure 1.14) and provides some insight into the probable binding site of E4P.[61]

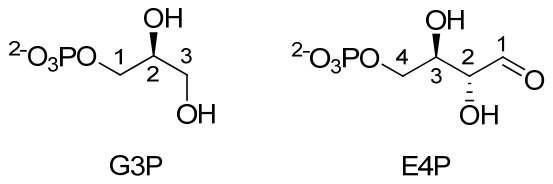

Figure 1.14: Structures of G3P and E4P.

In the active site of *S. cerevisiae* DAH7P synthase (tyr)-Co^{2+}-PEP complex (Figure 1.15), the C3 hydroxyl group in G3P, corresponding to C2 hydroxyl group of E4P, is hydrogen bonded to Asp342 and the C2 hydroxyl group of G3P, corresponding to C3 hydroxyl group of E4P, is hydrogen bonded to the main chain carbonyl group of Pro113. The position of G3P in this structure has been used to infer information about the binding of E4P in the active site. Pro113 has been found to be a conserved residue in all DAH7P synthases and is part of a conserved LysProArgThr(Ser) motif found in all DAH7P synthases. The phosphate moiety of G3P forms salt bridges to the guanidino group of Arg114 and hydrogen bonds to both the N and O atom of Thr115. This phosphate binding site coincides with the sulphate binding site in the structure of *E. coli* DAH7P synthase (phe).

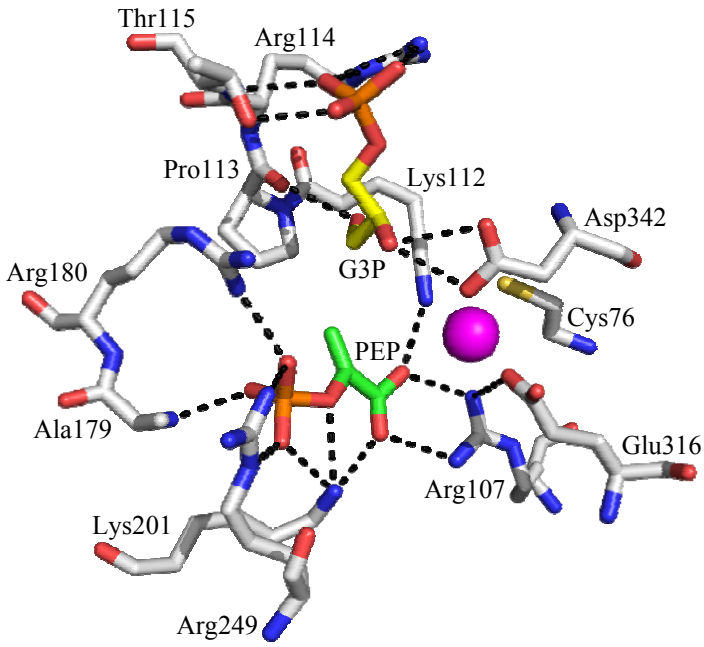

Figure 1.15: Active site in *S. cerevisiae* DAH7P synthase Co^{2+}-PEP-G3P complex (PDB code 1OF8). Polar interactions are indicated by dashed lines, Co^{2+} is shown as a magenta sphere, PEP (green/pink/orange) and G3P (yellow/pink/orange) are labelled.[61]

Konig *et al.*[61] have modelled a bound E4P molecule into the active site of the *S. cerevisiae* DAH7P synthase (tyr)-Co^{2+}-PEP-G3P-complex (Figure 1.16). Modelling of E4P in this site indicates that C1 of E4P can approach within 2.7 Å of the C3 of PEP and that the *si* face of PEP faces the *re* face of E4P, in accordance with the established stereochemistry. It also places the carbonyl of E4P in a position where it can coordinate to the metal ion, activating it for attack and supporting the mechanism in the acyclic pathway (Figure 1.10, page 13).[61]

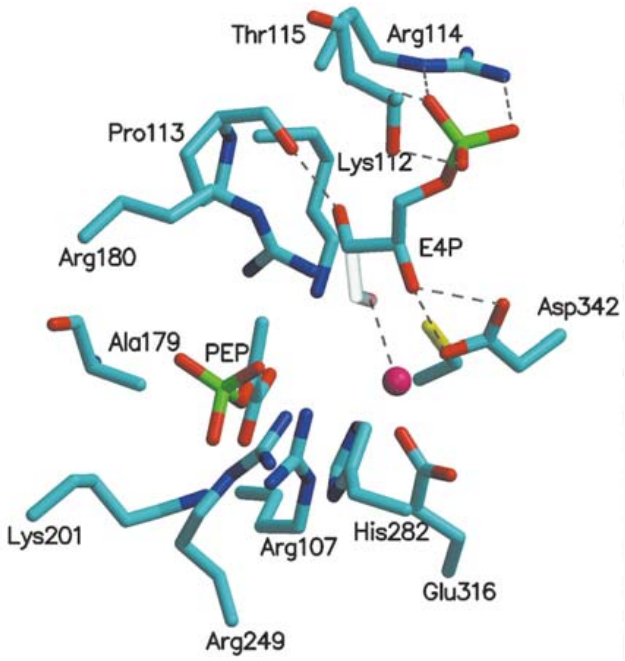

Figure 1.16: Active site in the DAH7P synthase Co^{2+}-PEP-G3P complex from *S. cerevisiae* (tyr) after replacement of G3P by E4P and modelling of the carbonyl group of E4P. Diagram from Konig *et al.*[61]

The structure of the type II DAH7P synthase from *M. tuberculosis* was recently solved by Webby *et al.*[38] as a PEP-Mn^{2+} complex. The quaternary structure is a homotetramer consisting of two tight dimers (Figure 1.17). Each dimer consists of a $(\beta/\alpha)_8$ TIM barrel, as is found in type I DAH7P synthases and the closely related KDO8P synthases. As is typical for TIM-barrel enzymes like *E. coli* DAH7P synthase (phe), the active site of *M. tuberculosis* DAH7P synthase is located at the C-terminal end of the barrel at the bottom of a deep cavity with Mn^{2+} and PEP bound.

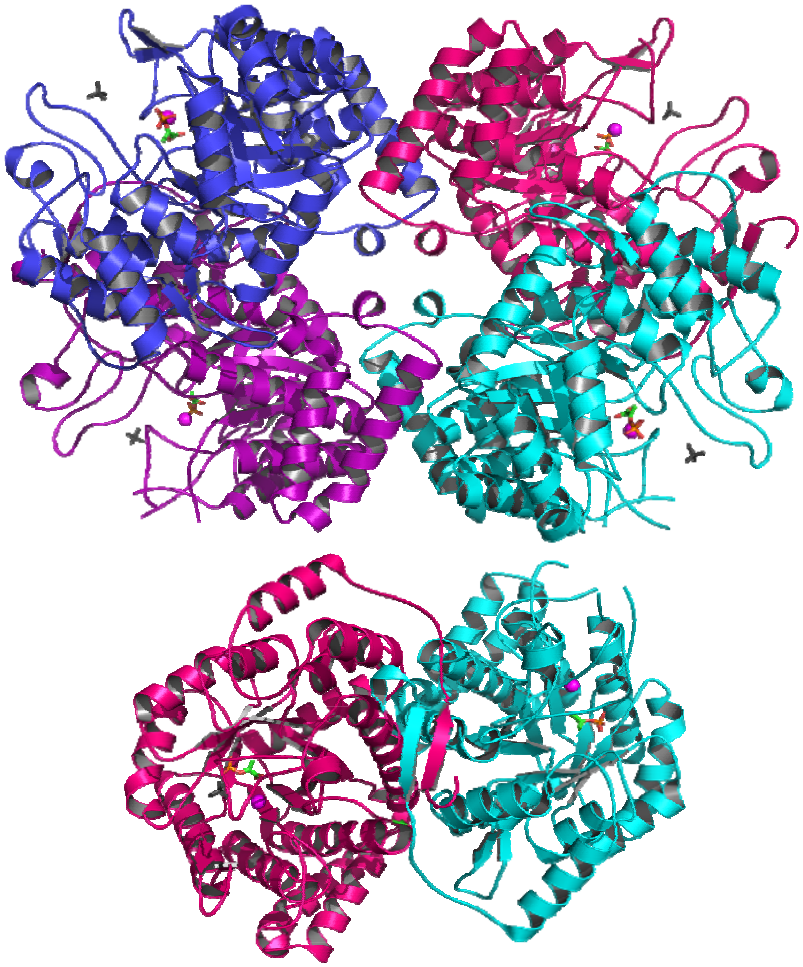

Figure 1.17: *M. tuberculosis* DAH7P synthase structure (PDB code 2B7O). (Top) The homotetramer structure of *M. tuberculosis* DAH7P synthase. (Bottom) Dimer structure of *M. tuberculosis* DAH7P synthase. The two monomers exchange N-terminal strands to form an antiparallel ribbon. PEP (green/orange, stick model), manganese ion (magenta, spheres) and sulphate ion (grey).

The metal is coordinated in an approximate trigonal bipyramidal geometry coordinated to four protein ligands Cys87, His369, Glu411 and Asp441 in the active site of *M. tuberculosis* DAH7P synthase. The PEP binding site is defined by a network of hydrogen bonds between the protein and the PEP phosphate and carboxylate groups. The phosphate group of PEP is hydrogen bonded by the amino acids Glu283, Arg284, Lys306, Arg337 and two water molecules. The carboxylate group of PEP is hydrogen bonded to Arg126, Lys306 and a water molecule (Figure 1.18). Also in the active site region, near its opening and ~10 Å further out from PEP, is a bound sulphate ion. This ion marks the likely position of the E4P phosphate.

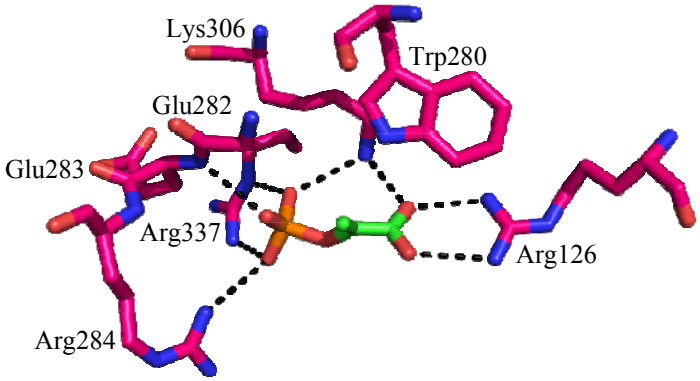

Figure 1.18: Active site of *M. tuberculosis* DAH7P with PEP bound (PDB code 2B7O). Dashed lines indicate interactions between PEP (green/orange/pink) and surrounding residues.

Surprisingly, despite the large variations in sequence and size across the DAH7P synthase family (type Iα[67], Iβ[32], and II[38] DAH7P synthases), all DAH7P synthases so far characterised share common traits such as the $(\beta/\alpha)_8$ TIM barrel fold, arrangement of key residues in the active site and the binding modes of PEP and Mn^{2+}; indicating a common ancestry for the type I and II DAH7P synthases. Additions of various decorations on the core $(\beta/\alpha)_8$ fold such as different regulatory domains determines the major structural differences between species and families.[65]

1.2.6 A related enzyme: KDO8P synthase

Along with the enzyme DAH7P synthase, there is another closely related enzyme KDO8P synthase, which also catalyses a similar reaction. This enzyme catalyses the condensation reaction between the five carbon sugar A5P, and PEP to give the eight carbon sugar KDO8P (Figure 1.19). Inorganic phosphate is also released.

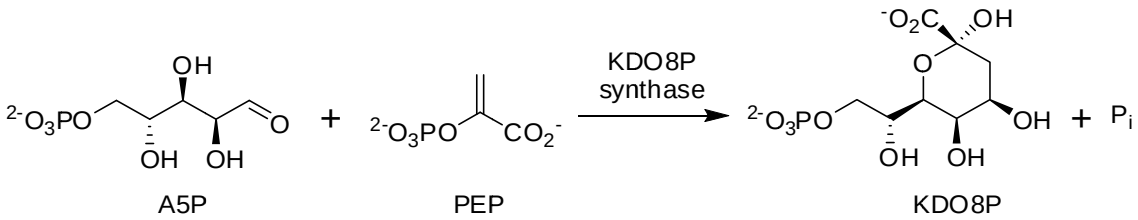

Figure 1.19: The reaction catalysed by KDO8P synthase.

KDO8P synthase catalyses the second step in formation of the sugar 3-deoxy-D-*manno*-octulosonate (KDO) from ribulose 5-phosphate (Figure 1.20). KDO is an integral part of

various glycolipids coating the surface of the outer membrane of Gram-negative organisms, including the lipopolysaccharide (LPS) region.[24,68,69] As the formation of the LPS is essential for the growth and virulence of Gram-negative organisms, KDO8P synthase has been a target for the development of novel anti-infective agents.[70-72]

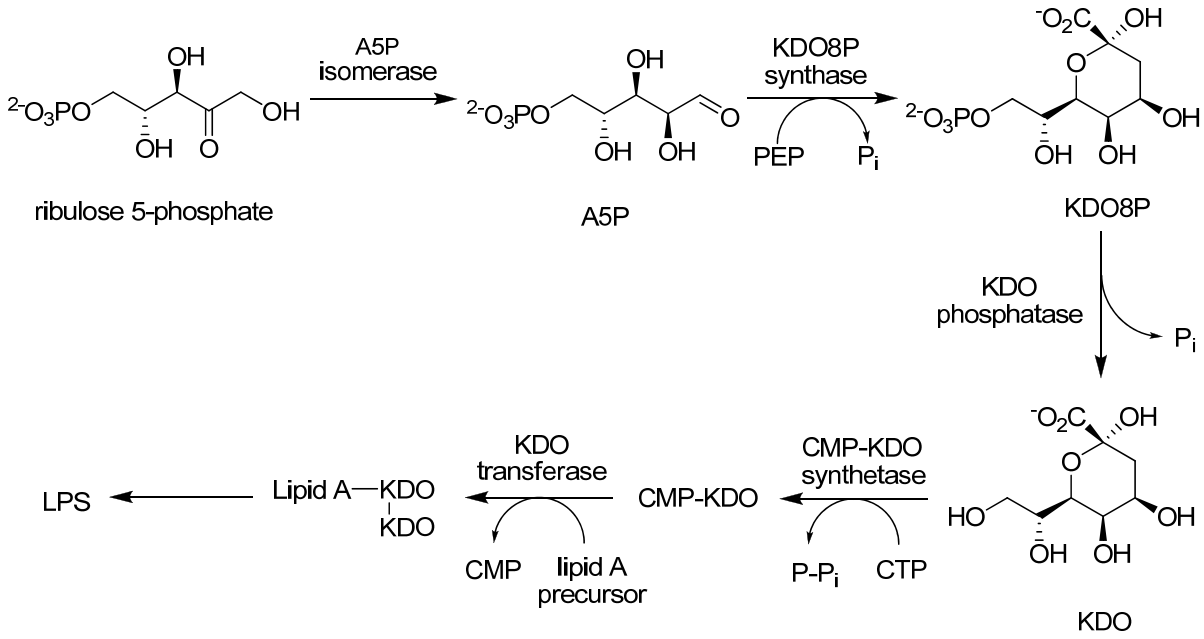

Figure 1.20: Biosynthesis of Lipid A from ribose 5-phosphate.

The two substrates, A5P and E4P, are similar with only a difference in carbon chain length and stereochemistry; A5P is longer by one carbon length and the stereochemistry at C2 is inverted compared to E4P (Figure 1.21). Both enzymes catalyse an aldol-like condensation reaction of which the *si* face of PEP attacks the *re* face of their respective phosphorylated monosaccharide and are part of a unique class of PEP-utilising enzymes in which loss of the phosphate moiety of PEP occurs through cleavage of the C-O bond rather than through the more common mode in which the O-P bond is broken.[24]

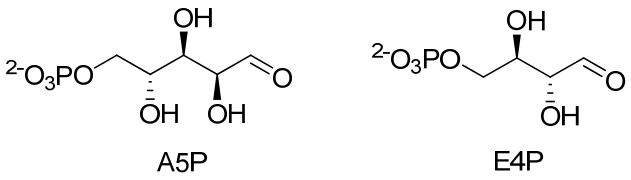

Figure 1.21: Structures of A5P and E4P.

DAH7P and KDO8P synthases catalyse different reactions and there is very little primary sequence similarity between the two enzymes e.g. only 13% of the residues are identical

between the *E. coli* KDO8P synthase and the *E. coli* DAH7P synthase. Despite these differences, the two enzymes have strong similarities in regards to their mechanism and structures.[20] Due to these similarities these enzymes are often compared.[24,31]

1.2.7 Inhibitors

The design of inhibitors for DAH7P synthase has been of great interest in our laboratory and in literature.[73-75] As previously mentioned, DAH7P synthase is the first enzyme in the shikimate pathway, which leads to the synthesis of aromatic amino acids and other aromatic metabolites in microorganisms and plants. The disruption of this pathway leads to death of microorganisms and plants and makes it an attractive target for the development of new anti-infectious agents without side effects. Unfortunately, little has been published on inhibitors of DAH7P synthase.[75-77]

Designing inhibitors that mimic the transition state or intermediates can lead to very high potencies and the best ligand for an enzyme is likely to be the transition state or a high energy intermediate for the reaction, rather than the substrate or products.[65,78]

KDO8P synthase and DAH7P synthase share strong mechanistic similarities between their respective reactions and it has been proposed that it should be possible to inhibit DAH7P synthase by mimicking the oxocarbenium ion intermediate **1.1** involved in the DAH7P synthase reaction (Figure 1.10, page 13). This was the basis of several of the inhibitors synthesised by Scott Walker in our laboratory.[65] One such inhibitor that was synthesised and tested is the bisubstrate inhibitor **1.7** which mimics the oxocarbenium ion **1.1** (Figure 1.22). The inhibitor **1.7** was based on another inhibitor, the aminophosphonate inhibitor **1.9**, which inhibits *E. coli* KDO8P synthase strongly (K_i = 50±8 μM, Figure 1.22).[76,77] Inhibitor **1.7** was shown to be a very slow binding inhibitor of *E. coli* DAH7P synthase (phe) with an IC_{50} value of 6.6 μM.[79]

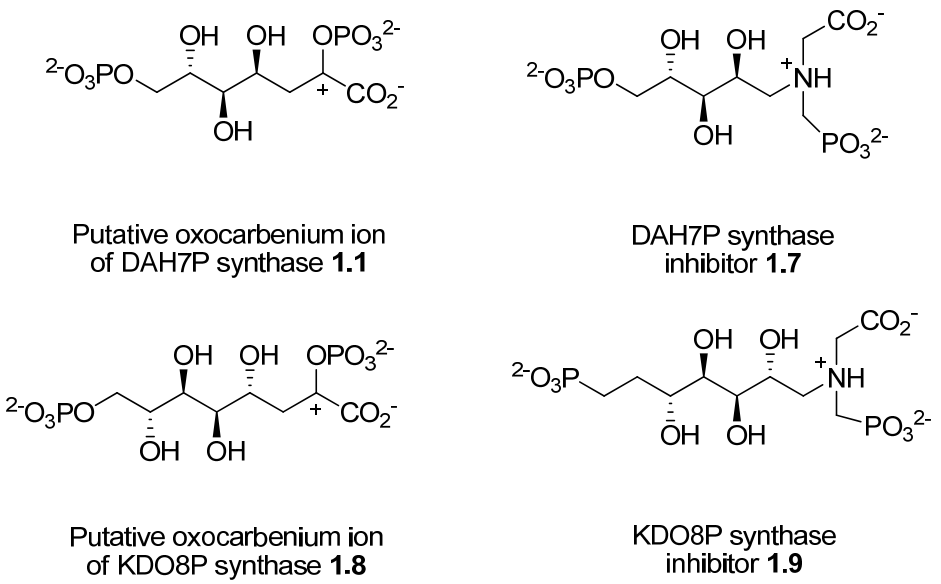

Figure 1.22: Inhibitors of KDO8P synthase and DAH7P synthase and their putative oxocarbenium ion intermediates.

Several PEP mimicking inhibitors of DAH7P synthase were synthesised as part of Scott Walker[65] and Hemi Cumming's[80] thesis work, beginning with the (*R*)- and (*S*)-phospholactates **1.10** and **1.11** (Figure 1.23) which were designed based on their similarity to the oxocarbenium ion intermediate **1.1** (Figure 1.10 and Figure 1.22).[81] Both phospholactates had previously been synthesised in a study of PEP utilising enzymes and were found to be moderately effective inhibitors of PEP carboxykinase, pyruvate kinase and enolase.[82] Other inhibitors included the PEP mimics **1.12**–**1.15**. All the compounds were found to be competitive inhibitors of *E. coli* DAH7P synthase (phe) (with respect to PEP), with the exception of compound **1.14** which did not inhibit the enzyme (Figure 1.23).

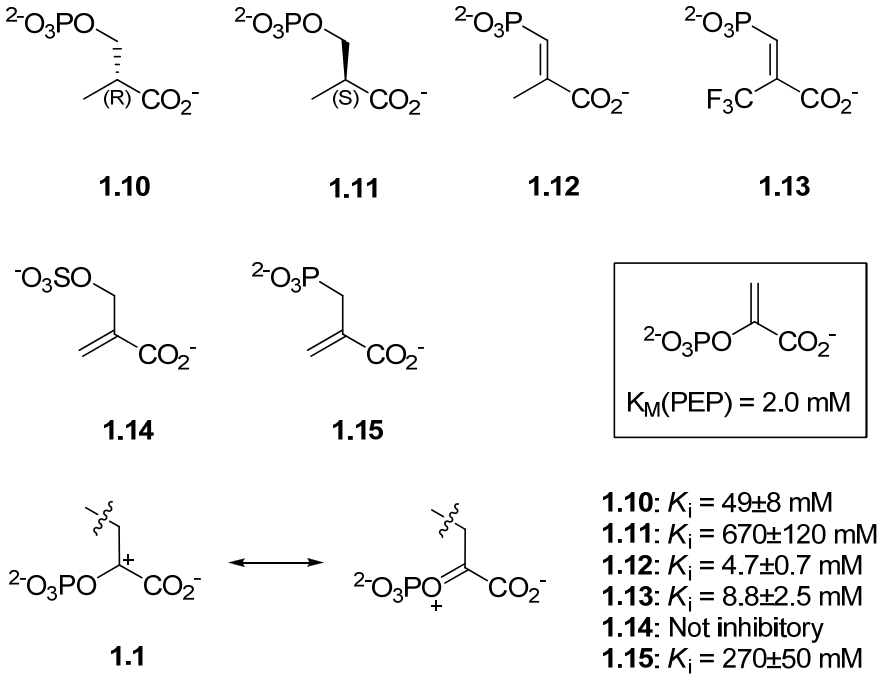

Figure 1.23: PEP-mimicking inhibitors. All compounds inhibited *E. coli* DAH7P synthase (phe) except 1.14.

Grison *et al.*[75] have synthesised a mechanism based inhibitor mimicking the open chain hemiketal intermediate **1.4**. This inhibitor, compound **1.16**, differs from the intermediate **1.4** in that the labile C-O phosphate bond is replaced by a more stable C-C linkage i.e. a phosphonate moiety (Figure 1.24).

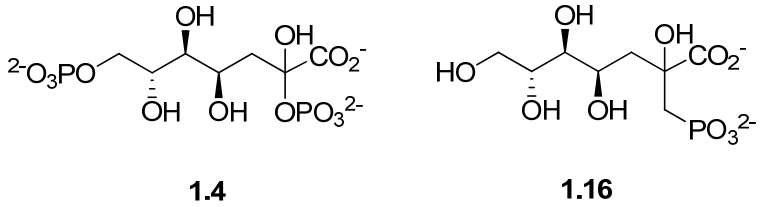

Figure 1.24: The hemiketal intermediate 1.4 and the inhibitor 1.16 synthesised by Grison *et al.*[75]

Although no kinetic data was reported for the above mechanistic inhibitor by Grison *et al.*, the authors did report that this compound had antibacterial activity inhibiting the growth of *E. coli*, *Yersinia enterocolitica* and *Pseudomonas aeruginosa* Gram-negative bacteria on Mueller-Hinton agar plates.[75]

1.3 Substrate specificity of DAH7P synthase

Substrate analogues are a tool that has been used widely in literature and in our research laboratory for studying enzyme-substrate interactions, and for the investigation into enzymatic reaction mechanisms. PEP and E4P are the natural substrates for DAH7P synthase but this enzyme has been shown to accept a wide range of alternative non-natural substrates (to varying degrees) and the substrate specificity is described in the next sections.

1.3.1 PEP analogues

Substrate specificity studies have been performed using substrate analogues of PEP on DAH7P synthase. These include the C3-substituted PEP analogues (*Z*)-3-chloroPEP **1.17**, (*Z*)-3-bromoPEP **1.18**, (Z)-3-methylPEP **1.19**, (*Z*)-3-fluoroPEP **1.20** and (*E*)-3-fluoroPEP **1.21** (Figure 1.25).[83] These four PEP analogues were tested as substrates for *E. coli* DAH7P synthase (phe) and was found that both isomers of (*Z*)- and (*E*)-3-fluoroPEP were substrates for DAH7P synthase (phe) with K_M values of 4.0 and 18 μM, respectively (Table 1.1). These higher K_M values, coupled with the extremely low k_{cat} values, suggests that (*Z*)- and (*E*)-3-fluoroPEP are poorer substrates for *E. coli* DAH7P synthase (phe) when compared to the natural substrate PEP.

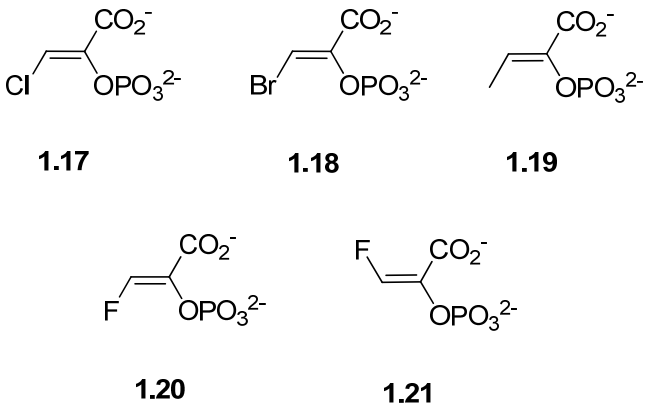

Figure 1.25: PEP analogues 1.17–1.21.

The (*Z*)-3-chloroPEP **1.17**, (*Z*)-3-bromoPEP **1.18** and (*Z*)-3-methylPEP **1.19** analogues of PEP were not substrates for *E. coli* DAH7P synthase (phe), and were found to be only weak reversible competitive inhibitors (Table 1.1). This indicates that the size of the substituent on C3 of PEP is a factor, as fluorine is the only substituent that is comparable in size with the hydrogen that it is replacing.

Substrate	K_M (μM)	K_i (μM)	k_{cat} (s^{-1})	k_{cat}/K_M ($s^{-1}\mu M^{-1}$)
PEP	2.0±0.2		71±3	36
(*E*)-3-fluoroPEP **1.21**	4.0±0.4		1.0±0.2	0.3
(*Z*)-3-fluoroPEP **1.20**	18±1		4.1±0.2	0.2
(*Z*)-3-chloroPEP **1.17**		31±6		
(*Z*)-3-methylPEP **1.19**		160±30		
(*Z*)-3-bromoPEP **1.18**		250±50		

Table 1.1: Analogues of PEP as substrates and inhibitors of *E. coli* DAH7P synthase (phe).[83]

Along with the C3-substituted PEP analogues, the difluoromethylenephosphonate **1.22**, and phosphoamidate **1.23** analogues of PEP have been tested as substrates on *E. coli* DAH7P synthase (phe) (Figure 1.26). None of these analogues were substrates for DAH7P synthase indicating the intolerance to changes in the phosphate moiety of PEP.[83]

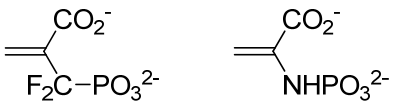

1.22 **1.23**

Figure 1.26: PEP analogues 1.22 and 1.23.

1.3.2 E4P analogues

Three, five and six carbon sugar analogues of E4P have been used to probe the substrate specificity of three different families of DAH7P synthase and include *E. coli* DAH7P synthase (phe) (type Iα), *P. furiosus* DAH7P synthase (type Iβ) and *Helicobacter pylori* DAH7P synthase (type II).[24,32,47] A summary of the kinetic data for these enzymes is shown in Table 1.2.

Substrate	DAH7P Source								
	***E. coli* (phe) (type Iα)**			***P. furiosus* (type Iβ)**			***H. pylori* (type II)**		
	K_M (μM)	k_{cat} (s^{-1})	k_{cat}/K_M ($s^{-1}\mu M^{-1}$)	K_M (μM)	k_{cat} (s^{-1})	k_{cat}/K_M ($s^{-1}\mu M^{-1}$)	K_M (μM)	k_{cat} (s^{-1})	k_{cat}/K_M ($s^{-1}\mu M^{-1}$)
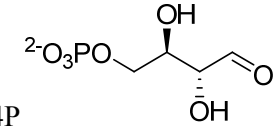 E4P	141	10	0.07	9±1	1.4±0.1	0.2	6±1	3.3±0.3	0.6
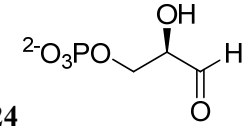 **1.24**	NS			NS			NS		
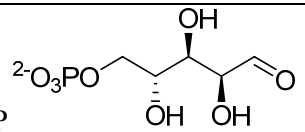 A5P	30	0.054	0.002	2700±200	1.1±0.1	0.0004	4800±360	0.3±0.01	0.00006
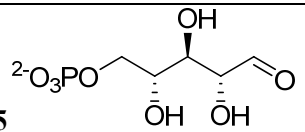 **1.25**	6000	0.72	0.0001	1580±110	2.5±0.1	0.002	1700±400	3.5±0.2	0.002
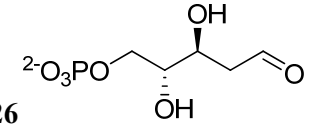 **1.26**	6800	0.46	0.00007	2500±150	1.7±0.1	0.0007	2300±500	0.95±0.06	0.0004
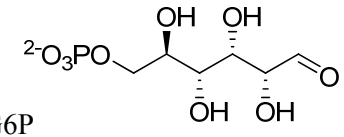 G6P	NS			NS			NS		

Table 1.2: Kinetic constants of *E. coli*, *P. furiosus* and *H. pylori* DAH7P synthases with alternative substrates of E4P. *E. coli* DAH7P synthase (phe) kinetic data from Sheflyan *et al.*[24] *P. furiosus* DAH7P synthase kinetic data from Schofield *et al.*[32] *H. pylori* DAH7P synthase kinetic data from Webby *et al.*[47] NS = not a substrate.

Sheflyan *et al.*[24] have determined that the type Iα *E. coli* DAH7P synthase can accept the five carbon sugars ribose 5-phosphate **1.25** (R5P, with the same C2 configuration as the natural substrate E4P), 2-deoxyribose 5-phosphate **1.26** (with no C2-hydroxyl) and A5P (with the opposite C2 stereochemistry to E4P) as substrates for this enzyme and produce KDO8P-like products. Although, the five carbon analogues were accepted as substrates by this type Iα enzyme, the K_M values were significantly higher and the k_{cat} values were extremely low compared to those obtained with E4P, indicating that these five carbon analogues were significantly poorer substrates for *E. coli* DAH7P synthase (phe) than the natural substrate.

Schofield *et al.*[32] have determined that the type Iβ *P. furiosus* DAH7P synthase was able to utilised the five carbon sugars **1.25**, **1.26** and A5P as substrates. It was found that these five carbon sugars had similar k_{cat} values as the natural substrate E4P. This is in contrast to the studies carried out on the Iα enzyme from *E. coli* by Sheflyan *et al.*, which is only able to utilise these five carbon sugars with k_{cat} values comparable to E4P. This indicates that this type Iβ *P. furiosus* DAH7P synthase is a more promiscuous enzyme compared to the type Iα *E. coli* DAH7P synthase.

The substrate specificity of the type II *H. pylori* DAH7P synthase was examined by Webby *et al.*[47] *H. pylori* DAH7P synthase was found to be able to utilise all three five carbon sugar analogues **1.25**, **1.26** and A5P with greatly elevated K_M values compared to E4P. Additionally, the k_{cat} values for A5P and compound **1.26** were significantly lower than E4P, with the exception of compound **1.25** whose k_{cat} value is comparable to E4P. The higher K_M values and lower k_{cat} values seen for the five carbon sugars on *H. pylori* DAH7P synthase were similar to the trends seen for the type Iα and Iβ enzymes (Table 1.2) i.e. all three families of DAH7P synthase had significantly higher K_M values for these substrates when compared to E4P. This indicates that the five carbon sugar analogues examined were poorer substrate for all three families of DAH7P synthases, with the type Iβ enzyme being the most promiscuous, followed by the type II enzyme, while the type Iα enzyme showing the least tolerance to changes in substrate.

Although all five carbon sugars were found to be substrates for type Iα, Iβ and II DAH7P synthases, none of these enzymes were able to utilise the three and six carbon sugars (D-glyceraldehyde 3-phosphate **1.24** and D-glucose 6-phosphate (G6P) respectively). These findings are consistent with crystal structure studies of the active site of *E. coli* DAH7P

synthase (phe) with G3P bound by Shumilin *et al.*[21] i.e. if a shorter carbon chain is bound in the active site, then the aldehyde is not close enough to react with C3 of PEP as the phosphate moiety of the aldose phosphate binds in the same position. A carbon chain longer than five carbons would be unlikely to fit in the active site.[24]

Sheflyan *et al.*[24] also discovered that the phosphate group on the sugars appeared to be absolutely essential for enzyme activity as the non-phosphorylated forms of the substrates E4P, A5P, **1.25** and **1.26** were not substrates for *E. coli* DAH7P synthase (phe) (Figure 1.27). Crystal structures have shown that the phosphate group has many binding interactions, so the phosphate group may be important for positioning the substrate into the proper location in the active site, thus orientating the carbonyl group for attack by PEP.[24]

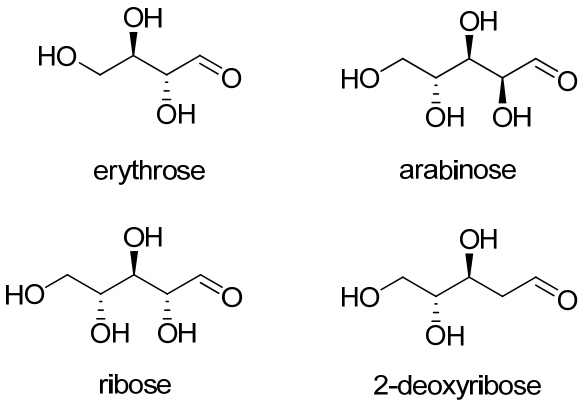

Figure 1.27: The non-phosphorylated versions of E4P, A5P, R5P (1.25) and 2-deoxyR5P (1.26). Erythrose, arabinose, ribose and 2-deoxyribose were all tested on *E. coli* DAH7P synthase (phe) and found not to be substrates for this enzyme.

The tolerance of DAH7P synthase to configurational changes at C2 or C3 of natural substrate E4P has been previously studied in our laboratory by Meekyung Ahn.[40] D-Threose 4-phosphate (T4P) and L-threose 4-phosphate have been prepared synthetically from D-diethyl tartaric acid and L-diethyl tartaric acid respectively. These two substrate analogues of E4P have the opposite stereochemistry at C2 (D-T4P) or C3 (L-T4P) with respect to E4P (Figure 1.28).

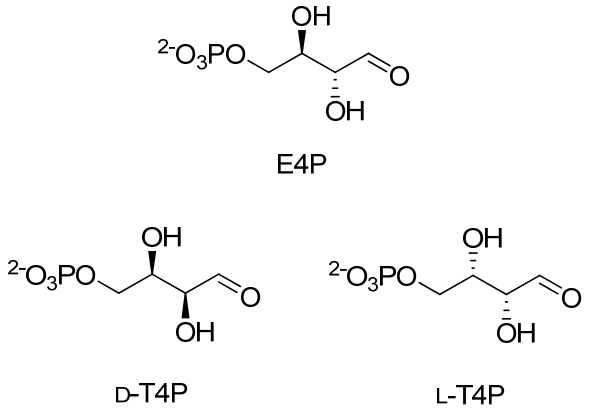

Figure 1.28: Substrate analogues of E4P with the opposite stereochemistry at C2 (D-T4P) or C3 (L-T4P).

Substrate specificity tests on *E. coli* (type Iα) and *P. furiosus* (type Iβ) DAH7P synthases showed that both D- and L-T4P were alternative substrates for the two enzymes. The seven-carbon phosphorylated sugar products of the enzymatic reactions for both D- and L-T4P were isolated and characterised by both NMR spectroscopy and mass spectrometry and were identified as the expected 3-deoxy D-*lyxo* heptulosonate 7-phosphate and 3-deoxy L-*xylo* heptulosonate 7-phosphate respectively. For *E. coli* DAH7P synthase (phe), a significant increase in the K_M value was recorded with both substrates, whereas D- and L-T4P were utilised with a comparable catalytic efficiency to the natural substrate E4P for *P. furiosus* DAH7P synthase (Table 1.3).

Substrate	***E. coli* DAH7P synthase (phe) (type Iα)**			***P. furiosus* DAH7P synthase (type Iβ)**		
	K_M (μM)	**k_{cat} (s^{-1})**	**k_{cat}/K_M ($s^{-1}\mu M^{-1}$)**	**K_M (μM)**	**k_{cat} (s^{-1})**	**k_{cat}/K_M ($s^{-1}\mu M^{-1}$)**
E4P	39±4	26±2	0.7	9±1	1.4±0.1	0.2
D-T4P	390±13	2.5±0.1	0.006	21±1	2.4±0.1	0.1
L-T4P	750±10	1.5±0.1	0.002	47±3	4.0±0.1	0.09

Table 1.3: Kinetic parameters of *E. coli* DAH7P synthase (phe) and *P. furiosus* DAH7P synthase with D- and L-T4P.

The results with D- and L-T4P suggest that both enzymes can tolerate configurational changes to either the C2 or C3 hydroxyl groups from the natural substrate E4P. These observations suggest that the configurations of the C2 and C3 hydroxyl groups on E4P do not play a critical role in the DAH7P synthase enzymatic reaction.

1.4 Properties and preparation of E4P

E4P is an extremely unstable and difficult to handle compound in solution.[84] In aqueous solutions of ~1.0 M, E4P consists of a mixture of monomeric aldehyde, hydrated aldehyde and three major contributing dimeric forms (Figure 1.29). In dilute solutions of ~0.04 M only the hydrate monomer is predominant and the dimeric forms are not detectable at this concentration by NMR.[85] The two major dimers of E4P, I and II, are asymmetrically substituted 1,3-dioxane and 1,3-dioxolane structures, respectively, and dimer III is the α-anomer of dimer I. Although these dimers are not normally significant at biological concentrations, as the concentrations used are very low, they could interfere in some of the *in vitro* enzymatic studies using E4P as a substrate.[86] Frozen preparations of the compound should be allowed sufficient time to reach equilibrium before use and freeze-dried samples or samples that have been evaporated to dryness to give solid E4P have a tendency to dephosphorylate on concentration. Overall, this instability of E4P poses particular difficulties with the isolation and purification of this compound and with the synthesis of analogues of this molecule.

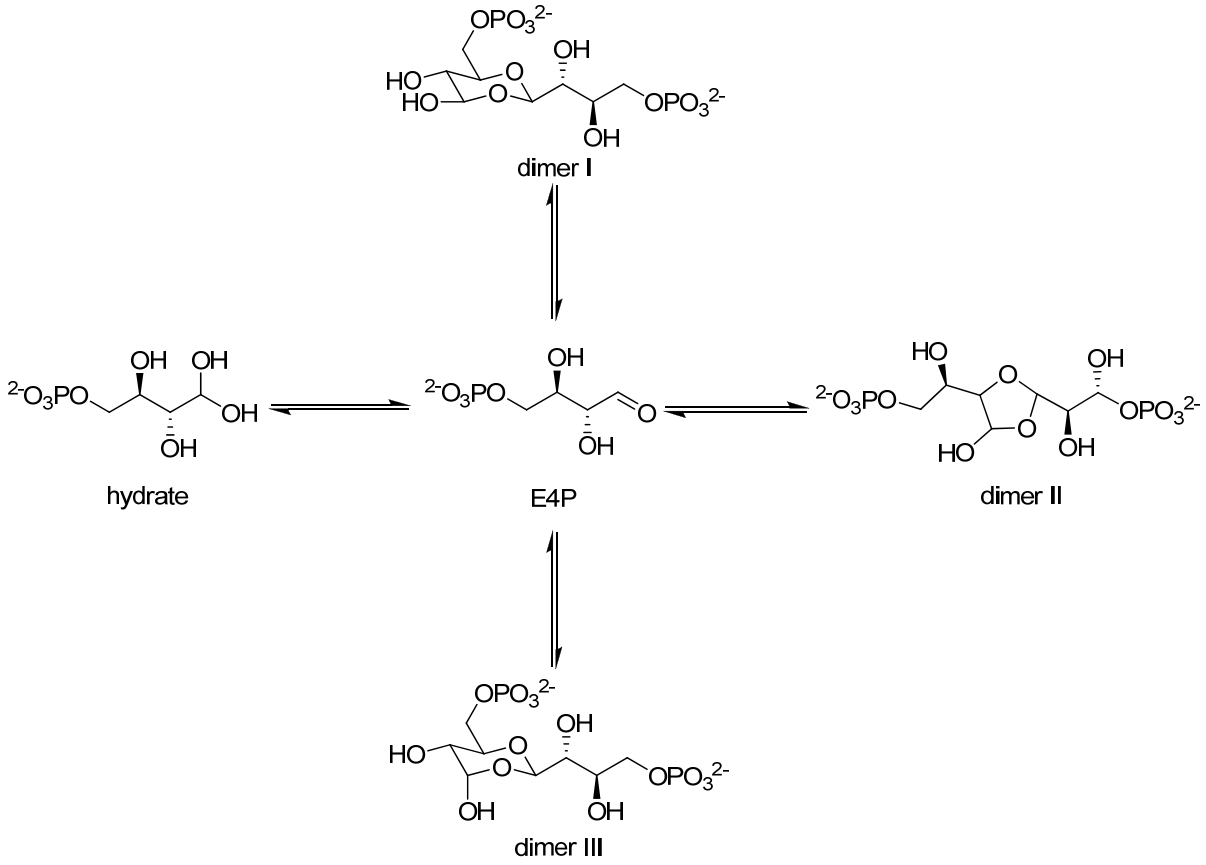

Figure 1.29: The monomeric and dimeric forms of E4P in solution determined by Duke *et al.*[85]

E4P can be brought commercially but the cost of purchasing this compound is extremely high; approximately $1700 NZD for 100 mg of E4P (Sigma-Aldrich). Therefore, to able to synthesis E4P by other means would be highly advantageous.

Two methods can be used to synthesis E4P, enzymatically from the enzyme transketolase or synthetically from the precursor D-glucose 6-phosphate.[87-90] In the enzymatic route, the enzyme transketolase catalyses the reaction between D-fructose and **1.25** to produce E4P, sedoheptulonase 7-phosphate and other sugar phosphates at equilibrium (Figure 1.30). However, it has been reported to be highly difficult to purify E4P from this mixture.[87]

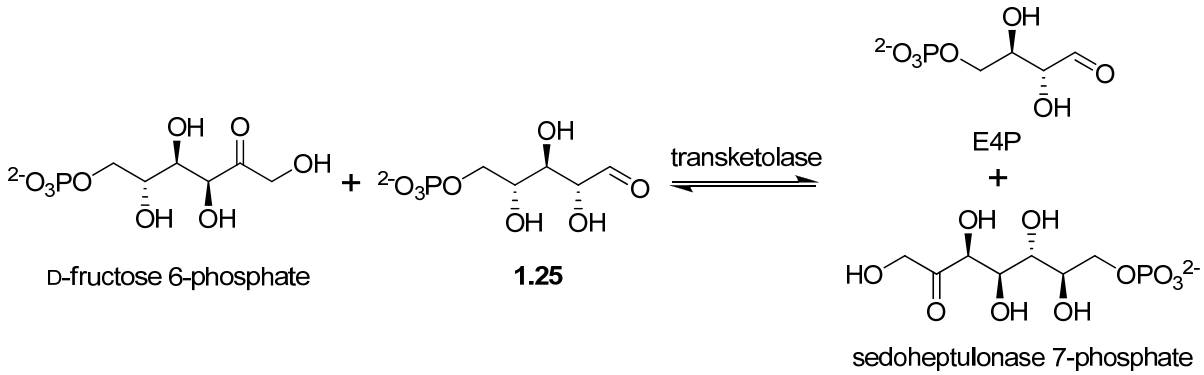

Figure 1.30: Synthesis of E4P using the enzyme transketolase.

E4P can also be prepared by oxidative cleavage of D-glucose 6-phosphate with lead tetraacetate (Figure 1.31).[89] This is a convenient one step procedure and it is the commonly used method for the synthesis of E4P. By using this method E4P can be obtained in a good yield (63%). Substrate analogues such as D- and L-T4P were prepared by this lead tetraacetate method.

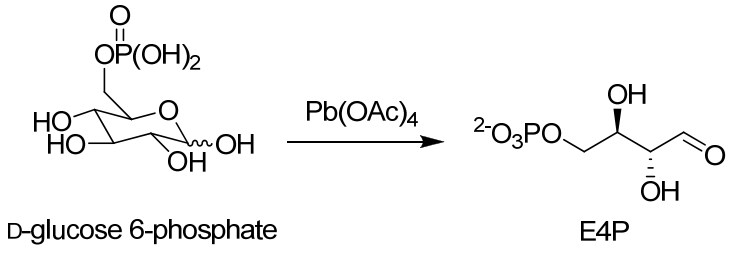

Figure 1.31: Synthesis of E4P from oxidative cleavage of D-glucose 6-phoshate.

Although this method can be high yielding, there are a couple of drawbacks. These include a long and tedious experimental procedure and non-selective cleavage of carbon atoms as the oxidative cleavage is not 100% selective for cleaving only two carbons to give E4P. The

reaction also produces D-glyceraldehyde 3-phosphate from over oxidation, and D-arabinose 5-phosphate from under oxidation (Figure 1.32).[91] Optimisation studies in our laboratory conducted by Meekyung Ahn[40] showed that only 1.7 equivalents of lead tetraacetate had to be used in the reaction to achieved a high 73% yield for E4P, compared to the stoichiometric two equivalents that is usually required to cleave two carbons. The use of fewer or more equivalents of lead tetraacetate resulted in lower yields of E4P and more side-products.

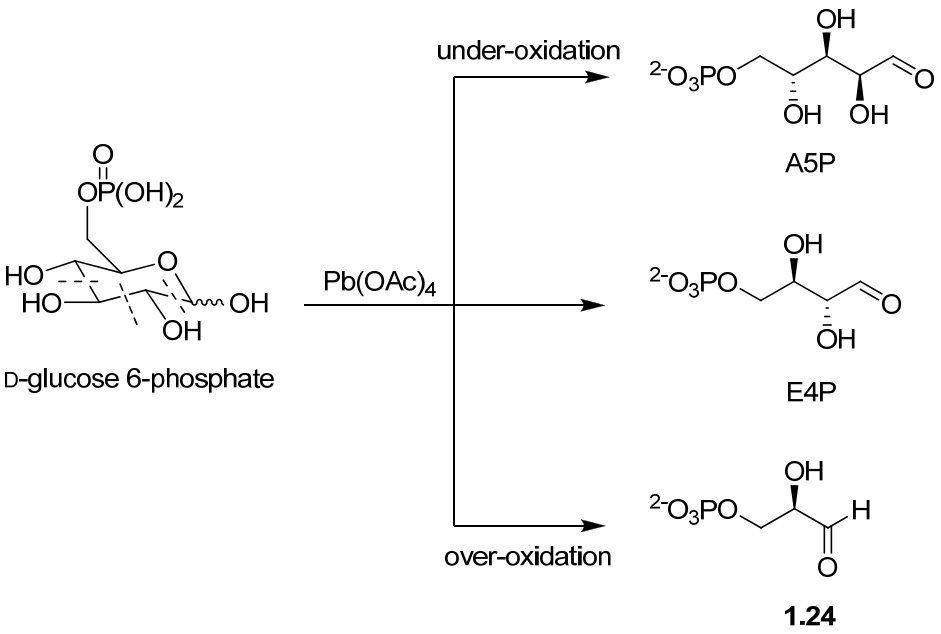

Figure 1.32: Oxidative cleavage of D-glucose 6-phosphate to give E4P and unwanted side-products. Cleavage of one carbon gives D-arabinose 5-phosphate, two carbons gives E4P and three carbons gives D-glyceraldehyde 3-phosphate 1.24.

1.5 The project

DAH7P synthase is the first enzyme of the shikimate pathway, catalysing the reaction between three carbon PEP and the four carbon sugar E4P. This pathway exists in plants and microorganisms, but not mammals, making it a potential target for novel fungicides, herbicides and antibiotics. Although there has been a lot of work done on the substrate specificity of PEP analogues on this enzyme, little work has been done on the substrate specificity of alternative four carbon sugars of E4P.

Therefore, the aim of this project was to synthesise a range of alternative non-natural four carbon analogues of E4P for DAH7P synthase to help to probe the substrate specificity of the

different types of DAH7P synthase. This would allow us to further understand how variations in sequence relate to variations in substrate selection and reaction chemistry in this group of enzymes. In particular, we wished to investigate the importance of the C2 and C3 hydroxyl groups in E4P and the effect of changing the phosphate groups in E4P to their phosphonate analogues. Specific goals of the project were to (Figure 1.33):

- Chemically synthesise both 2- and 3-deoxy analogues of E4P.
- Chemically synthesise both 2- and 3-methyl analogues of E4P.
- Chemically synthesise the phosphonate analogue of E4P.
- Chemically synthesise the dideoxyphosphonate analogue of E4P.
- To examine the tolerance of DAH7P synthase to changes in the C2 or C3 hydroxyl group of E4P.
- To examine the tolerance of DAH7P synthase to changes in the phosphate moiety of E4P.
- To characterise the products of the DAH7P synthase reactions where these compounds do act as alternative substrates to E4P.

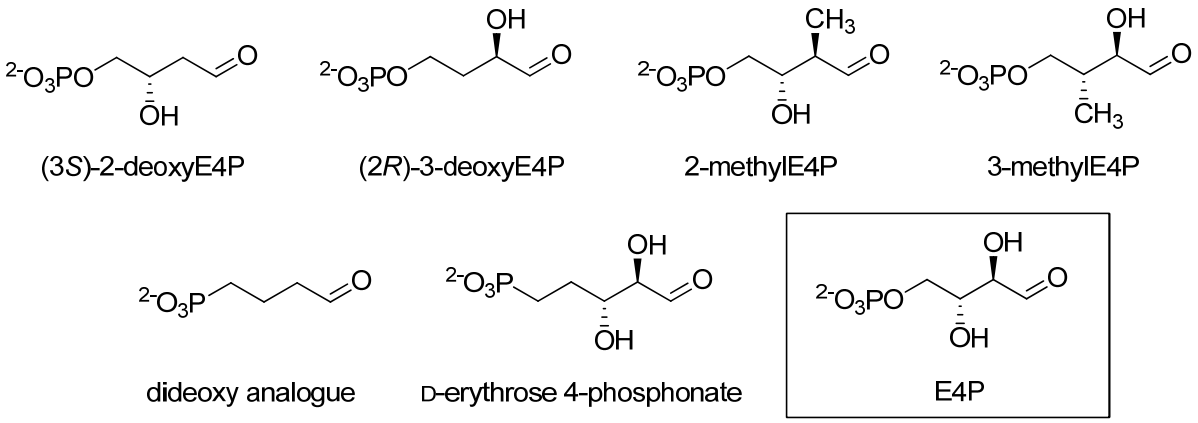

Figure 1.33: Target compounds for DAH7P synthase (analogues of E4P).

Chapter 2: Deoxy analogues of E4P

2.1 Introduction

As introduced in Chapter 1, we are interested in how sensitive DAH7P synthase is to structural changes in the E4P moiety. In particular, the importance of the hydroxyl groups on C2 and C3 of E4P for binding and catalysis in the active site.

Substrate specificity studies on D- and L-threose 4-phosphate (T4P), in which the stereochemistry is reversed at the C2 and C3 positions with respect to E4P (Figure 2.1), were part of Meekyung Ahn's PhD studies.[40] These studies demonstrated that both analogues were alternative substrates for the type I *E. coli* (phe) and *P. furiosus* DAH7P synthases, indicating the correct configuration of the hydroxyl groups at C2 and C3 of E4P is not critical to allow the enzymatic reaction to proceed.

Following Meekyung Ahn's studies, investigations were carried out to determine whether the deoxy analogues of E4P were possible substrates for DAH7P synthase. The deoxy analogues corresponding to the removal of the hydroxyl groups of the C2 or C3 position of E4P to give 2- and 3-deoxyE4P respectively, were investigated as part of Amy Pietersma's PhD studies (Figure 2.1).[66]

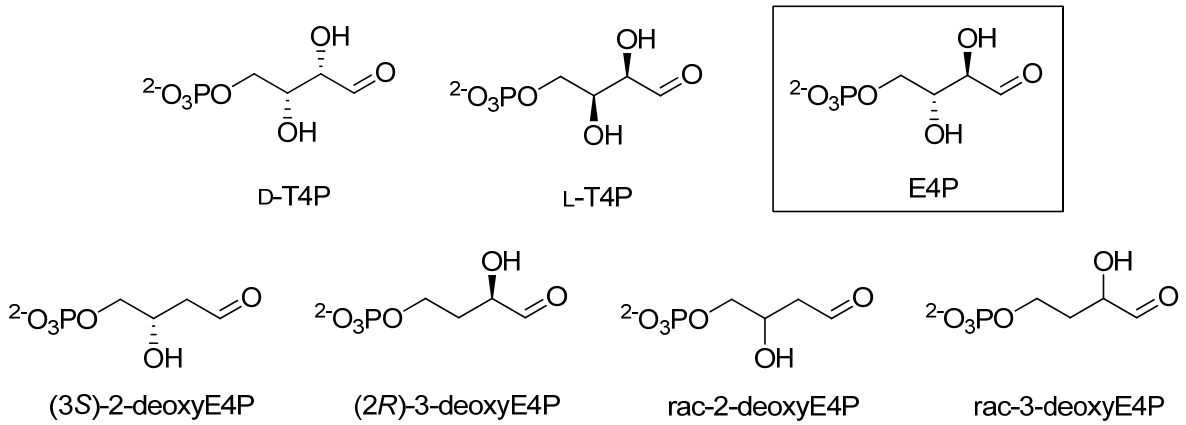

Figure 2.1: Substrate analogues of E4P investigated on type I DAH7P synthases. D- and L-T4P were investigated by Dr Ahn.[40] The enantiopure and racemic deoxy substrates of E4P were investigated by Dr Pietersma.[66]

Dr Pietersma demonstrated that the enantiopure analogues (3*S*)-2-deoxyE4P and (2*R*)-3-deoxyE4P were all found to be substrates for the type I *E. coli* (phe), *N. meningitidis* and *P. furiosus* DAH7P synthases. Studies on the racemic substrates with *E. coli* DAH7P synthase (phe) found that both rac-2-deoxyE4P and rac-3-deoxyE4P were substrates for this enzyme. Interestingly, rac-3-deoxyE4P was found not to be a substrate for *P. furiosus* DAH7P synthases (Table 2.1).

Substrate	**DAH7P synthase source**		
	***E. coli* (phe)**	***P. furiosus***	***N. meningitidis***
(3*S*)-2-deoxyE4P	✓	✓	✓
(2*R*)-3-deoxyE4P	✓	✓	✓
rac-2-deoxyE4P	✓	ND	ND
rac-3-deoxyE4P	✓	✗	ND

Table 2.1: Substrate specificity tests on (3*S*)-2-deoxyE4P, (2*R*)-3-deoxyE4P, rac-2-deoxyE4P and rac-3-deoxyE4P on type I DAH7P synthases.[66] ND = not determined.

Although the majority of substrate specificity investigations have been done on type I DAH7P synthases, little work has been done on the type II DAH7P synthases. The *M. tuberculosis* enzyme is a type II enzyme, and therefore is significantly different in sequence compared to the type I DAH7P synthases. The investigation of how sensitive this particular enzyme is to structural changes and the importance of the hydroxyl groups on C2 and C3 of E4P for binding and catalysis in the active site of this enzyme could be valuable information for the design of inhibitors for DAH7P synthase. Additionally, investigations into the substrate specificity of 2- and 3-deoxyE4P on this type II enzyme would also give a platform for which we can compare the substrate specificities of type I DAH7P synthases with the type II enzyme.

Preliminary studies on the role of the hydroxyl groups of E4P on *M. tuberculosis* DAH7P synthase were investigated by Dr Pietersma[66], but these investigations was not completed. For example, the determination of the kinetic data for racemic 2- and 3-deoxyE4P analogues was not accomplished. In addition, the investigations into whether *M. tuberculosis* DAH7P synthase could accept both enantiomers from racemic 2- and 3-deoxyE4P as substrates were not performed. Therefore, as part of the studies described in this thesis it was decided to synthesise the racemic and enantiopure forms of 2- and 3-deoxyE4P, and to further examine

the substrate specificity of the type II DAH7P synthase from *M. tuberculosis*. Additionally, synthesis of these deoxy analogues would allow the development of the chemistry that is required for the synthesis of more complex analogues such as the methyl-substituted analogues. This work is described in Chapter 3.

2.1.1 Outline of chapter

This chapter is divided into four main sections. The first section describes the synthesis of the enantiopure and racemic substrates, 2- and 3-deoxyE4P, using a modification of a synthetic route previously reported by Dr Pietersma.[66] Rac-3-deoxyE4P was synthesised using DL-malic acid whereas (2*R*)-3-deoxyE4P was synthesised from (2*R*)-malic acid. Rac-2-deoxyE4P was synthesised from a readily available precursor **2.18** (Figure 2.15, page 47) that was previously synthesised by Dr Rachel Williamson.[92] Synthesis of enantiopure (3*S*)-2-deoxyE4P and (2*R*)-3-deoxyE4P allow for direct comparison with the natural substrate E4P, as these two analogues have the same C2 and C3 hydroxyl configurations as E4P, respectively.

The second section provides evidence for the formation of the 6-deoxyDAH7P sugar that is formed from the reaction between 3-deoxyE4P with PEP catalysed by DAH7P synthase. Prior work by Dr Pietersma[66] had demonstrated the formation of 5-deoxyDAH7P from the reaction between 2-deoxyE4P and PEP catalysed by DAH7P synthase.

The third section describes the investigations into the enantiomer utilisation of racemic 2- and 3-deoxyE4P by *M. tuberculosis* DAH7P synthase. Standard enzyme assays, Lanzetta assays[93] and ^{31}P NMR spectroscopy were used to determine the concentrations of the racemic mixtures. Once an accurate concentration of each substrate was known, the investigation of whether *M. tuberculosis* DAH7P synthase was utilising one or both enantiomers of the racemic mixtures were determined.

The fourth section describes the kinetic studies that were undertaken for the reaction of enantiopure and racemic 2- and 3-deoxyE4P with PEP catalysed by *M. tuberculosis* DAH7P synthase. A comparison of the substrate specificities of these deoxy analogues on the type II DAH7P synthase from *M. tuberculosis*, with type I DAH7P synthases is also described.

2.2 Synthesis of the deoxy analogues of E4P

2.2.1 Synthesis of 3-deoxyE4P

Rac-3-deoxyE4P was previously synthesised by Dr Pietersma using the synthetic route shown in Scheme 2.1.[66] DL-Malic acid was esterified by MeOH and concentrated H_2SO_4 to give diester **2.1**. The secondary alcohol group was then protected as the benzyl ether, and the ester functionalities were reduced using $LiAlH_4$ to give diol **2.3**. Phosphorylation of this diol produced monophosphorylated compound **2.4**. Oxidation of phosphate **2.4** using Dess-Martin periodinane (DMP) gave aldehyde **2.7**. The aldehyde functionality was protected as its dimethyl acetal prior to hydrogenolysis. Deprotection of compound **2.8** gave rac-3-deoxyE4P.

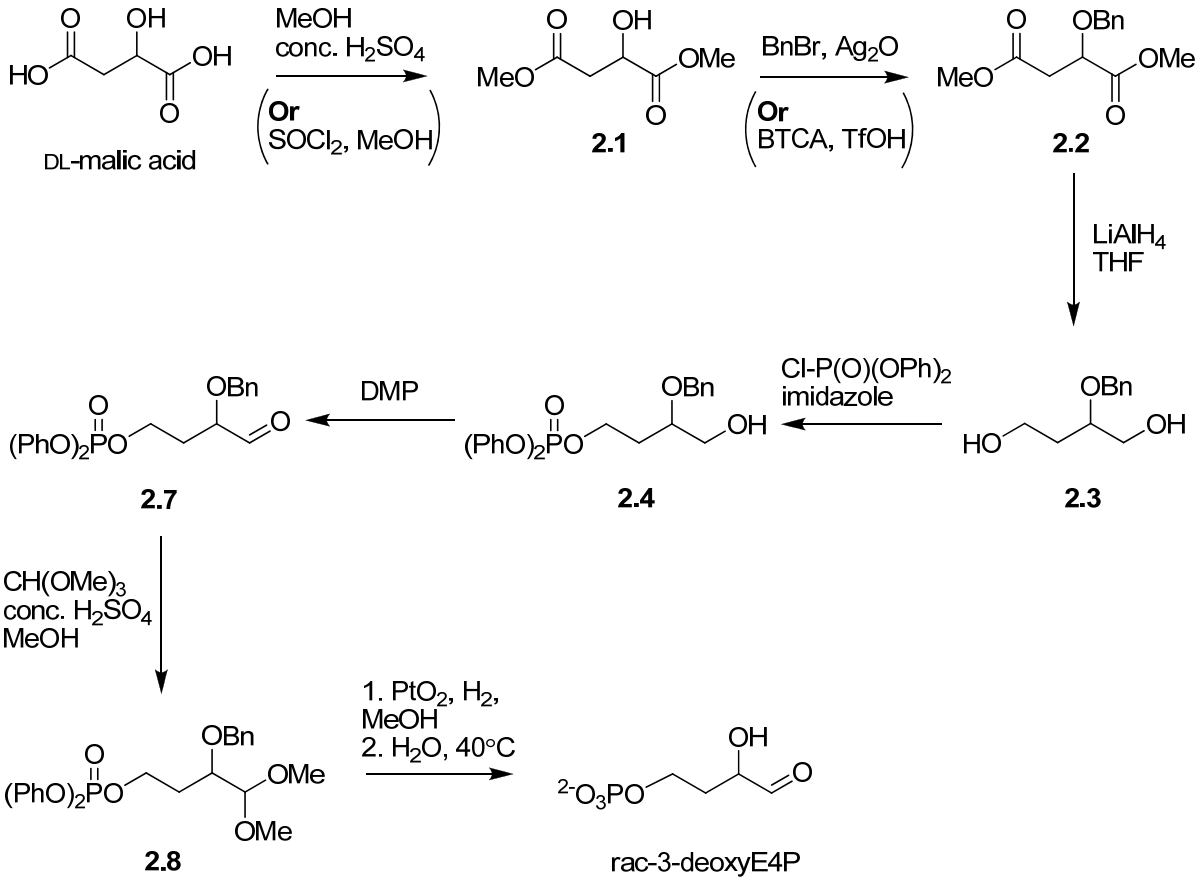

Scheme 2.1: Synthetic route used by Dr Pietersma to synthesise rac-3-deoxyE4P. Modifications were made to steps 1 and 2 for the synthesis of diester 2.1 and compound 2.2 respectively. All other steps were identical to Dr Pietersma's[66] synthetic route for the synthesis of rac-3-deoxyE4P.

Although the synthetic route in Scheme 2.1 was used by Dr Pietersma to synthesise rac-3-deoxyE4P in the work described in this thesis, complications arose for the synthesis of diester **2.1** and compound **2.2**. Due to these complications, modifications were made for the synthesis of these two compounds, and the reasons for these modifications are described in the next section.

2.2.1.1 Synthesis of rac-3-deoxyE4P from DL-malic acid

DL-Malic acid was first esterified by treatment with MeOH and concentrated H_2SO_4 under reflux conditions to give diester **2.1** (Scheme 2.1). The resulting yields from this method ranged from 50–96% following purification of the product by flash chromatography. Due to this inconsistency, the procedure was carried out via the initial formation of the acyl chloride using $SOCl_2$, and subsequent esterification using MeOH to give diester **2.1**. The yields obtained were consistent and higher using the $SOCl_2$ method: diester **2.1** was obtained in 90–99% yield following purification by flash chromatography (Figure 2.2). ^{1}H NMR spectroscopy confirmed the synthesis of diester **2.1**, with the appearance of the methyl resonances at 3.82 and 3.72 ppm in the spectrum.

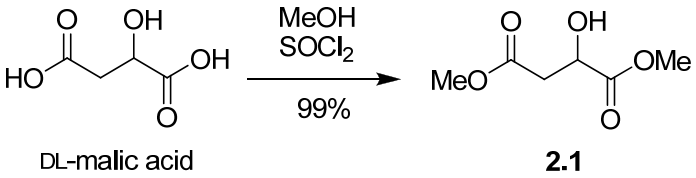

Figure 2.2: Synthesis of diester 2.1 using $SOCl_2$ and MeOH.

Benzylation of diester **2.1** was first carried out using BnBr and freshly prepared Ag_2O, and gave multiple unidentifiable side-products (as detected by TLC analysis). These unknown impurities were separated from the desired compound **2.2** (26% yield) by flash chromatography (Figure 2.3). Base-catalysed hydrolysis of the ester functionality could possibly be a cause for the low yield of compound **2.2**. It is possible that cleavage may be occurring due to contamination of the Ag_2O with NaOH (Ag_2O was prepared from NaOH and $AgNO_3$).[94] The ^{1}H NMR spectrum of the crude unidentifiable products showed that one or both of the ester group methyl resonances at 3.82 and 3.72 ppm were no longer present, indicating the loss of the methyl group(s).

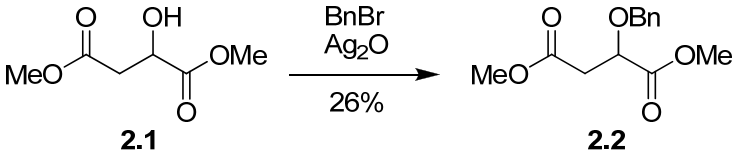

Figure 2.3: Benzylation of diester 2.1 using BnBr and Ag_2O.

To improve the yield of the benzylation reaction and to avoid the possibility of side-products, an acid-catalysed benzylation reaction was used instead. Diester **2.1** was benzylated using benzyl 2,2,2-trichloroacetimidate (BTCA) and trifluoromethanesulfonic acid (TfOH) to give compound **2.2** in 75% yield following purification by flash chromatography (Figure 2.4). Benzylation using this method was found to be considerably more reliable and higher yielding than the $BnBr/Ag_2O$ method.

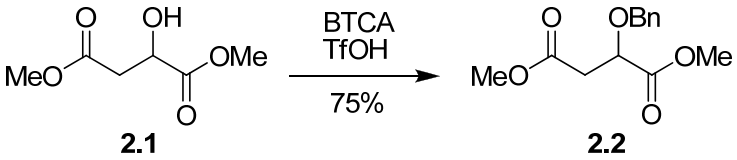

Figure 2.4: Benzylation of diester 2.1 using BTCA and triflic acid.

Reduction of compound **2.2** using $LiAlH_4$ provided the diol **2.3** in 63% yield (Figure 2.5). NMR spectroscopy confirmed that the reduction had occurred with the disappearance of the ester group methyl resonances at 3.77 and 3.69 ppm in the ^1H NMR spectrum, and the disappearance of the carbonyl resonances at 172.1 and 170.7 ppm in the ^{13}C NMR spectrum.

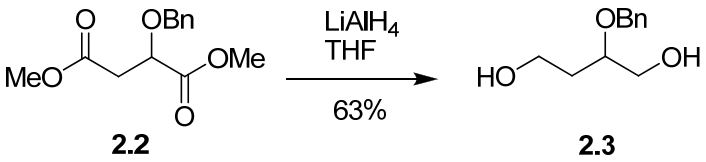

Figure 2.5: Synthesis of diol 2.3.

Diol **2.3** was phosphorylated using diphenyl chlorophosphate and imidazole to give phosphate **2.4**. The yield of the desired phosphate **2.4** was 18%, compared to 6% for the other monophosphorylated product **2.5** (Figure 2.6). A large amount of starting material, diol **2.3** (24%), was also recovered along with diphosphorylated compound **2.6** (6%). The ^1H, ^{13}C and ^{31}P NMR spectra of phosphate **2.4** matched those previously described by Dr Pietersma.[66] It was found, as expected, the benzyl group of diol **2.3** offered some directing effect for

monophosphorylation due to the steric hindrance that it would provide at C1 of diol **2.3**.[66] The bulkiness of the phosphorylating reagent may also aid in this directing effect by encouraging reaction at the less hindered primary alcohol.

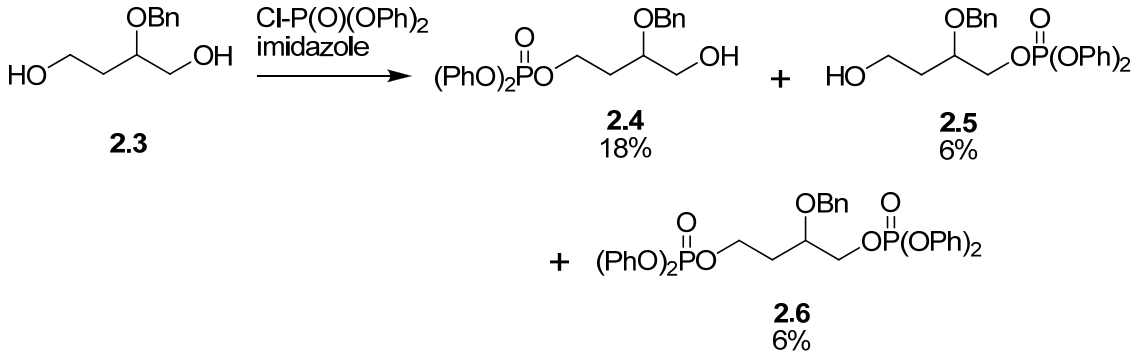

Figure 2.6: Phosphorylation of diol 2.3 to give a mixture of compounds 2.4–2.6.

The remaining primary hydroxyl group of phosphate **2.4** was oxidised using freshly prepared DMP to give aldehyde **2.7** (85% yield, Figure 2.7). The ^{1}H and ^{13}C NMR spectra confirmed the presence of the aldehyde resonance with signals at 9.62 and 202.5 ppm respectively.

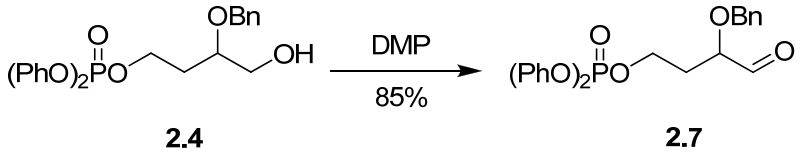

Figure 2.7: Oxidation of phosphate 2.4 to give aldehyde 2.7.

Aldehyde **2.7** was protected as the dimethyl acetal, using trimethyl orthoformate and concentrated H_2SO_4 to afford the fully protected analogue **2.8** in 94% yield (Figure 2.8). ^{1}H NMR spectroscopy confirmed the synthesis of compound **2.8**, with the appearance of the diastereotopic methoxy group proton resonances at 3.43 and 3.39 ppm in the spectrum.

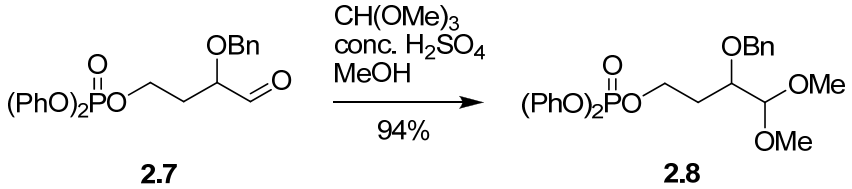

Figure 2.8: Synthesis of protected analogue 2.8.

The protected analogue **2.8** was hydrogenated at room temperature and monitored using TLC analysis until no UV active compound was present, indicating the phenyl groups had been cleaved. A small sample was then taken and concentrated under vacuum for ^{1}H NMR analysis. The ^{1}H NMR spectrum of this sample showed that all aromatic proton resonances between 7.41–7.09 ppm in the spectrum had gone, confirming the deprotection of the phenyl groups in compound **2.8**. Acetal **2.9** was then immediately hydrolysed to remove the acetal protecting group to give rac-3-deoxyE4P (Figure 2.9), where the phosphate group of acetal **2.9** provided the acidity required to cleave the acetal groups in water. ^{1}H NMR spectroscopy showed the disappearance of the methoxy proton resonances at 3.43 and 3.39 ppm in the spectrum. Additionally, mass spectrometry detected rac-3-deoxyE4P as a compound with a molecular mass of 207.0038 (calc. $C_4H_9NaO_6P$ $[M+Na]^+$: 207.0029). Rac-3-deoxyE4P was then used in enzyme assays without further purification.

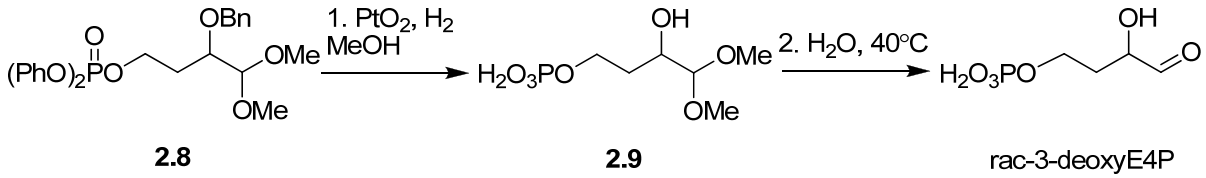

Figure 2.9: Synthesis of rac-3-deoxyE4P.

The enantiopure (2*R*)-3-deoxyE4P was also synthesised using the same route described in this section, but starting with (2*R*)-malic acid instead of DL-malic acid. Similar yields and identical spectroscopic data were obtained for the synthesis of (2*R*)-3-deoxyE4P as for rac-3-deoxyE4P. Once (2*RS*)-3-deoxyE4P and (2*R*)-3-deoxyE4P were synthesised, both were tested as substrates for DAH7P synthase from *M. tuberculosis*.

2.2.2 Synthesis of 2-deoxyE4P

(3*S*)-2-DeoxyE4P was previously synthesised by Dr Pietersma using the synthetic route shown in Scheme 2.2.[66] β-hydroxy-γ-butyrolactone was protected as its benzyl ether to give compound **2.11**. Compound **2.11** was then reduced to give lactol **2.12**. Subsequent protection of lactol **2.12** to give compound **2.14**, followed by phosphorylation of the exposed hydroxyl group gives compound **2.16**. Deprotection of compound **2.16** gives (3*S*)-2-deoxyE4P.

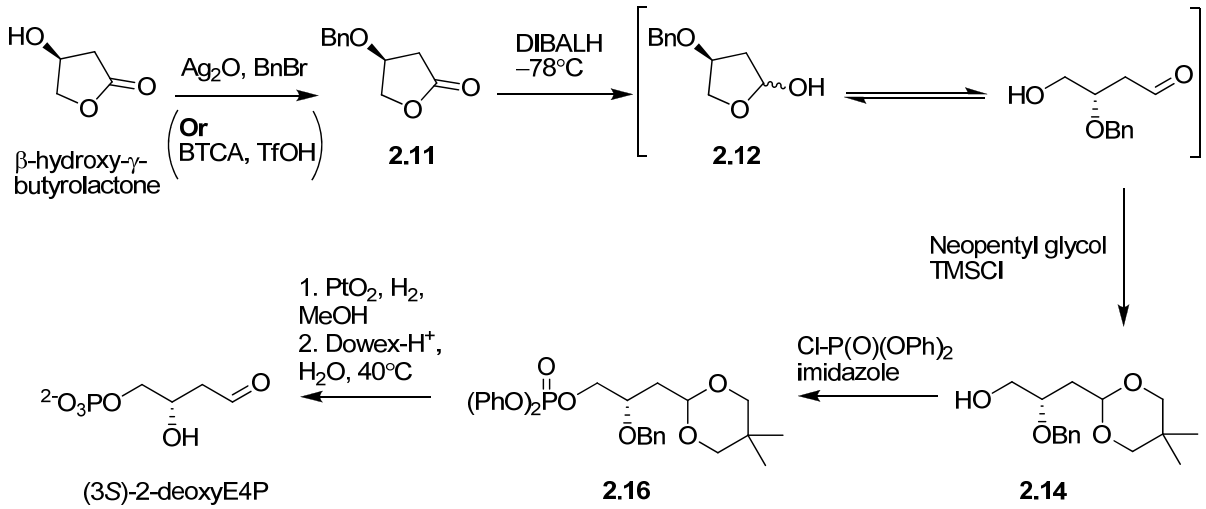

Scheme 2.2: Synthetic route used by Dr Pietersma[66] to synthesise (3*S*)-2-deoxyE4P. Only step 1 was modified. All other steps were identical to Dr Pietersma's synthetic route for the synthesis of (3*S*)-2-deoxyE4P.

Although the synthetic route in Scheme 2.2 was used by Dr Pietersma to synthesise (3*S*)-2-deoxyE4P, complications arose for the synthesis of compound **2.11** and modifications were made for the synthesis of this compound (described in the next section).

2.2.2.1 Synthesis of (3S)-2-deoxyE4P from β-hydroxy-γ-butyrolactone

Benzylation of β-hydroxy-γ-butyrolactone was carried out using BnBr and freshly prepared Ag_2O (Scheme 2.2). When the reaction was carried out in this way, lactone **2.11** was obtained in 7% yield, in addition with several unidentifiable products were formed (as detected by TLC analysis). Similar yields and results were also found during the synthesis of compound **2.2** for the synthesis of 3-deoxyE4P, and a marked improvement was observed by switching to the reagents BTCA and TfOH. When BTCA and TfOH was used for the benzylation of β-hydroxy-γ-butyrolactone (Figure 2.10), the lactone **2.11** was obtained in a much higher yield of 71%. This was a marked improvement in the reaction outcome compared to the BnBr/Ag_2O method. Lactone **2.11** was confirmed by a ^{1}H NMR spectrum showing the aromatic proton resonances between 7.41–7.24 ppm.

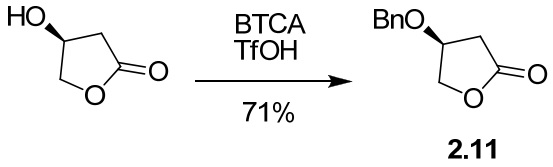

Figure 2.10: Synthesis of compound 2.11.

The next step in the synthetic scheme involved the reduction of lactone **2.11** to the corresponding lactol **2.12**. Lactol **2.12** is in equilibrium with its open-chain form, and this allows access to both the aldehyde functionality and the primary alcohol (Figure 2.11). The reduction was carried out at −78°C in order to prevent over reduction of the lactone to the alcohol, and DIBALH was added dropwise till no starting material was detectable by TLC analysis. Analysis of the reaction by ^{1}H NMR spectroscopy determined that reduction had occurred to give a mixture of diastereoisomers of lactol **2.12** (62% yield). The two acetal proton resonances were observed as either a multiplet between 5.84–5.61 ppm or a doublet of doublets at 5.44 ppm (J = 5.1, 10.6 Hz) in the spectrum. The two diastereoisomers were present in a 3:2 ratio. Evidence for the existence of the open-chain aldehyde was also present in the ^{1}H and ^{13}C spectra with small peaks (1:4 ratio, open-chain:major lactol) observable at 9.80 ppm and 208.8 ppm respectively.

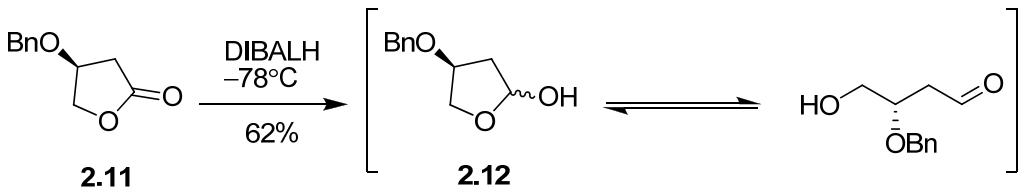

Figure 2.11: Reduction of lactone 2.11 with DIBAL to give lactol 2.12.

Ring opening of lactol **2.12** using neopentyl glycol and chlorotrimethylsilane (TMSCl) gave a mixture of products. The desired six membered ring product **2.14** was produced in 79% yield, along with a mixture of diastereoisomers of the five membered ring product **2.15** in 2% yield (Figure 2.12). The TMSCl acts as both a dehydrating agent and the acid catalyst in the reaction, eliminating the need to add molecular sieves or other drying agents and the products were separated by flash chromatography.[95]

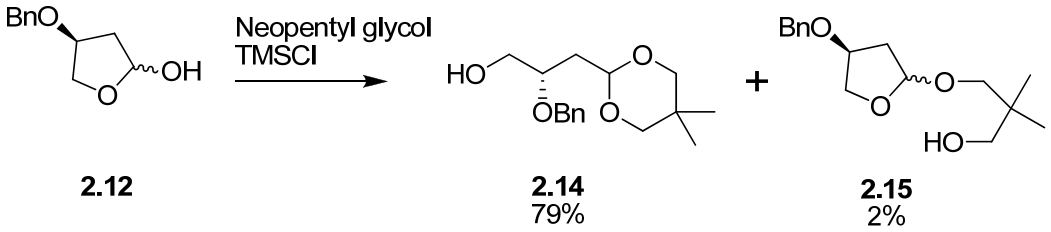

2.12 **2.14** 79% **2.15** 2%

Figure 2.12: The synthesis of the six and five membered ring products from lactone 2.12. Products were separated by flash chromatography.

With the aldehyde protected as its cyclic acetal, the exposed primary alcohol could now be phosphorylated. The phosphorylation was carried out using diphenyl chlorophosphate and imidazole to afford phosphate **2.16** in 95% yield following purification (Figure 2.13). The ^{1}H, ^{13}C and ^{31}P NMR spectra of phosphate **2.16** matched those previously reported by Dr Pietersma.[66]

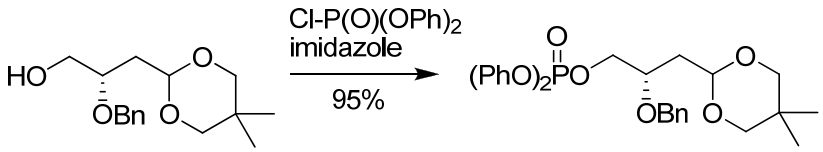

2.14 **2.16**

Figure 2.13: Synthesis of phosphate 2.16.

The benzyl and phenyl protecting groups of phosphate **2.16** were removed by hydrogenolysis using a platinum catalyst. The reaction mixture was stirred at room temperature until TLC analysis showed no UV active compound was present. A small sample was then taken and concentrated under vacuum for ^{1}H NMR analysis. The ^{1}H NMR spectrum of this sample showed that all aromatic signals between 7.37–7.14 ppm had been removed to give acetal **2.17**. Acetal **2.17** was then deprotected by the treatment with Dowex-H^{+} cation exchange resin and heating to 40°C in water overnight to give (3*S*)-2-deoxyE4P (Figure 2.14). Mass spectrometry detected the mass for (3*S*)-2-deoxyE4P with a molecular mass of 183.0060 ($C_4H_8O_6P$ $[M-H]^-$: 183.0064). (3*S*)-2-DeoxyE4P was then used in enzyme assays without further purification.

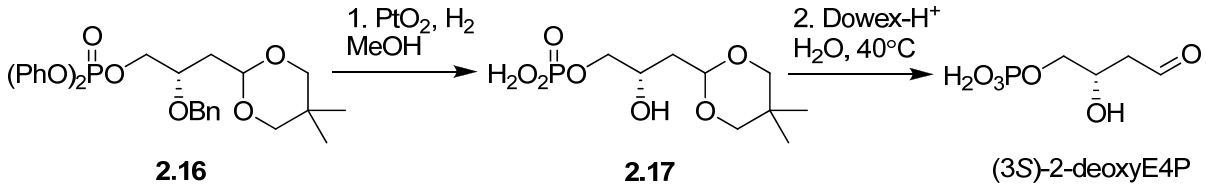

Figure 2.14: Synthesis of (3*S*)-2-deoxyE4P.

The synthesis of rac-2-deoxyE4P was previously carried out by Dr Rachel Williamson.[92] Only the final deprotection step using Dowex-H^+ resin was carried out in these studies as the precursor **2.18** was already available for use (Figure 2.15). Rac-2-deoxyE4P was then used in enzyme assays without further purification.

Figure 2.15: The synthesis of rac-2-deoxyE4P from precursor 2.18.

The 2-deoxy analogues of E4P, (3*RS*)-2-deoxyE4P and (3*S*)-2-deoxyE4P, were synthesised and both these analogues of E4P were then assayed as substrates on DAH7P synthase from *M. tuberculosis*.

2.3 Evidence for product identity in the *M. tuberculosis* DAH7P synthase catalysed reaction between 3-deoxyE4P and PEP

A standard enzyme assay carried out on 3-deoxyE4P shows that DAH7P synthase is utilising 3-deoxyE4P as a substrate. The standard enzyme assay used to monitor the reaction catalysed by DAH7P synthase monitors only the loss of PEP (at 232 nm) and does not confirm the formation of the seven carbon product. When 3-deoxyE4P is used in place of E4P, instead of DAH7P, the expected product is 6-deoxyDAH7P (Figure 2.16). To confirm formation of 6-deoxyDAH7P, an alternate thiobarbituric acid assay method was employed.[96]

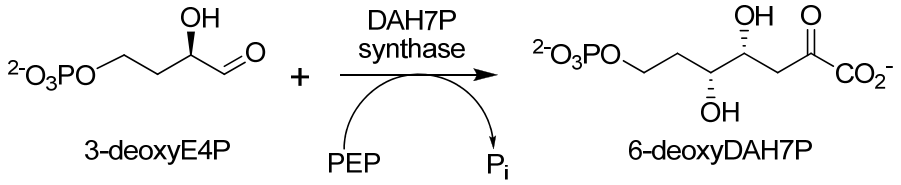

Figure 2.16: Synthesis of 6-deoxyDAH7P from 3-deoxyE4P and PEP catalysed by DAH7P synthase.

2.3.1 Thiobarbituric acid assay

The thiobarbituric acid assay is a colourimetric method for the detection of molecules that contain a specific 1,2-diol moiety (Figure 2.17).[96]

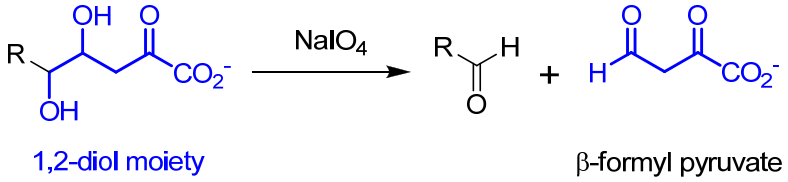

Figure 2.17: General structure of a molecule with the 1,2-diol moiety (blue) required to form β-formyl pyruvate from oxidative cleavage of this moiety.

In the assay, a molecule containing the 1,2-diol moiety is first oxidatively cleaved using $NaIO_4$ to generate β-formyl pyruvate. Thiobarbituric acid is then added, which reacts with β-formyl pyruvate to give a product with a characteristic pink chromophore (λ_{max} = 549 nm). The pink chromophore is due to the reaction of β-formyl pyruvate with thiobarbituric acid (Figure 2.18), and is a positive test for the presence of the 1,2-diol moiety.[97] If the 1,2-diol moiety is absent in the structure of the molecule, β-formyl pyruvate will not be formed and the assay will give a negative result.

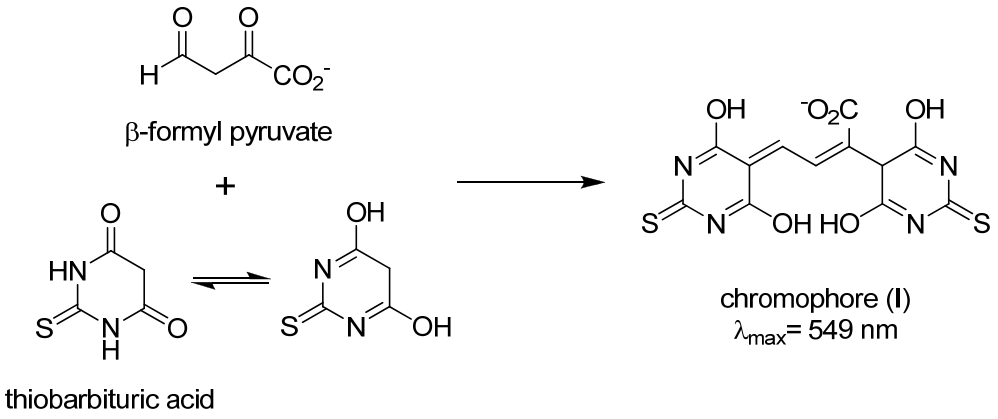

Figure 2.18: Structures of β-formyl pyruvate, thiobarbituric acid and chromophore I.[97] A pink complex is formed between β-formyl pyruvate and two molecules of thiobarbituric acid.

The seven carbon product of DAH7P synthase, DAH7P, which contains the requisite 1,2-diol moiety, has previously been detected using the thiobarbituric acid assay.[17,98] Oxidative cleavage of the diol between C4 and C5 of DAH7P using $NaIO_4$ gives β-formyl pyruvate, which after reaction with thiobarbituric acid results in formation of the pink chromophore (Figure 2.19).

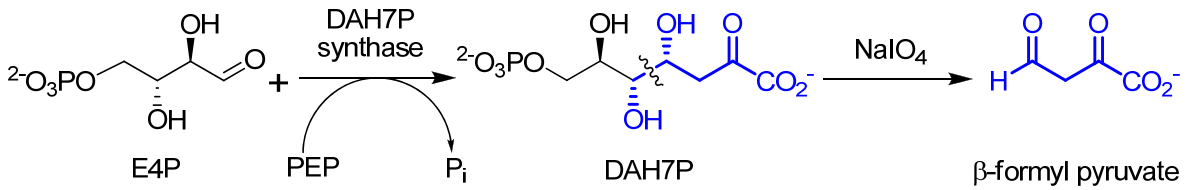

Figure 2.19: Enzyme catalysed reaction of E4P with PEP by DAH7P synthase to give DAH7P. Oxidative cleavage with $NaIO_4$ between C4 and C5 would give β-formyl pyruvate. The 1,2-diol moiety in DAH7P is shown in blue.

2.3.2 Detection of 6-deoxyDAH7P by thiobarbituric acid assay

Formation of 6-deoxyDAH7P, predicted to be formed in the reaction between 3-deoxyE4P and PEP catalysed by DAH7P synthase, can also be measured by the thiobarbituric acid assay as it contains the required 1,2-diol moiety (Figure 2.20).

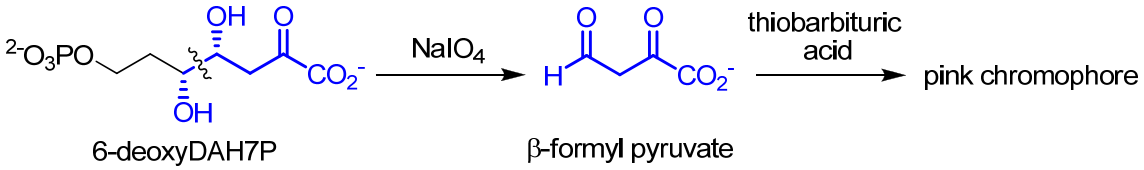

Figure 2.20: Thiobarbituric acid assay test on 6-deoxyDAH7P. The 1,2-diol moiety in 6-deoxyDAH7P is shown in blue.

A positive control using the thiobarbituric acid assay was carried out to detect the formation of DAH7P. The experiment involved the reaction between E4P and PEP, catalysed by *M. tuberculosis* DAH7P synthase, to form DAH7P, followed by analysis of the sample by the thiobarbituric acid assay. A pink coloured solution was observed that had an absorption maximum at 549 nm, corresponding to the pink chromophore. This indicated the formation of DAH7P from the reaction between E4P and PEP catalysed by *M. tuberculosis* DAH7P synthase.

An analogous reaction was carried out, but with 3-deoxyE4P instead of E4P. The characteristic absorption maximum at 549 nm from the pink chromophore was also detected. This was consistent with the formation of 6-deoxyDAH7P from the reaction between 3-deoxyE4P and PEP catalysed by *M. tuberculosis* DAH7P synthase.

2.4 Enantiomer utilisation

Enantiomer utilisation studies were carried out in order to confirm whether the enzyme *M. tuberculosis* DAH7P synthase is utilising either one or both of the 3-deoxyE4P enantiomers present in the assay when racemic 3-deoxyE4P was employed. By comparing the total concentration of racemic 3-deoxyE4P in solution with the amount of 3-deoxyE4P consumed in the enzyme assay, the enantioselectivity of the enzyme can be determined. This was also investigated for racemic 2-deoxyE4P with the *M. tuberculosis* enzyme.

2.4.1 Determination of the utilisation of racemic 3-deoxyE4P by *M. tuberculosis* DAH7P synthase

Two experimental methods were employed to investigate enantiomer utilisation of rac-3-deoxyE4P by *M. tuberculosis* DAH7P synthase. The first was a standard enzyme assay and the second used ^{31}P NMR spectroscopy. The amount of rac-3-deoxyE4P being utilised by *M. tuberculosis* DAH7P synthase was determined using a standard enzyme assay. The assay was carried out using the substrate rac-3-deoxyE4P, metal ($MnSO_4$), PEP (in excess), and was initiated by the addition of *M. tuberculosis* DAH7P synthase. The loss of absorbance due to the consumption of PEP at 232 nm was monitored using a UV-Visible spectrophotometer. As PEP was present in excess in the assay, the loss of absorbance is proportional to the amount of rac-3-deoxyE4P being consumed by the catalysed reaction. To convert absorbance into concentration, Beer's Law was applied ($A = \varepsilon cl$, $\varepsilon_{PEP} = 2.8 \times 10^3$ $M^{-1}cm^{-1}$ at 25°C). The stock solution concentration of utilised 3-deoxyE4P from rac-3-deoxyE4P was determined by this method to be 22.9 mM.

The concentration of rac-3-deoxyE4P in solution was determined by integrating the phosphorus resonances of a standard solution of glucose 6-phosphate (G6P) with rac-3-deoxyE4P in the ^{31}P NMR spectrum. The exact rac-3-deoxyE4P concentration could then be determined, as the relative concentrations of G6P and rac-3-deoxyE4P were known from the ^{31}P NMR spectrum. An accurate concentration of G6P was determined using a Lanzetta assay.[93] Although ^{31}P NMR spectra are not routinely integrated, there are examples in the literature where this has been carried out successfully.[99-101] A ^{31}P-^{1}H-decoupled NMR spectrum was collected and the phosphorus resonance of G6P at 1.7 ppm was integrated with

the phosphorus resonance of rac-3-deoxyE4P at 3.4 ppm to give a relative concentration of G6P:rac-3-deoxyE4P. The concentration determined for rac-3-deoxyE4P by this method was 40.2 mM, and represents the total concentration of rac-3-deoxyE4P in solution.

2.4.1.1 Conclusions

The results from these experiments showed that the concentration determined from the use of 3-deoxyE4P by *M. tuberculosis* DAH7P synthase, is approximately half (0.57) that of the total concentration. This was consistent with *M. tuberculosis* DAH7P synthase only using one enantiomer. It was expected that the (2*R*)-enantiomer of rac-3-deoxyE4P i.e. the one with the same C2 hydroxyl configuration as E4P, was the enantiomer being used based on the kinetic results for (2*R*)-3-deoxyE4P (Table 2.2, page 54).

2.4.2 Determination of the utilisation of racemic 2-deoxyE4P by *M. tuberculosis* DAH7P synthase

Two experimental methods were employed to investigate enantiomer utilisation of rac-2-deoxyE4P by *M. tuberculosis* DAH7P synthase. The first was a standard enzyme assay and the second was the Lanzetta assay. The amount of rac-2-deoxyE4P being utilised by *M. tuberculosis* DAH7P synthase was determined using a standard enzyme assay. The assay was analogous to that described for rac-3-deoxyE4P, except rac-2-deoxyE4P was used instead of rac-3-deoxyE4P. The stock solution concentration of utilised 2-deoxyE4P from rac-2-deoxyE4P was determined by this method to be 13.2 mM.

The Lanzetta assay is a colourimetric method for the detection of phosphate.[93] A positive test for phosphate results in a green complex being formed between phosphate and the ammonium molybdate–malachite green–Triton X-100 reagent (Lanzetta reagent). Although the structure of this complex was not reported by Lanzetta *et al*.[93], the absorbance of this green complex is measured at 630 nm and compared to a calibration curve to determine phosphate concentration. A modified form of this assay was used to quantify phosphate containing molecules. The samples were digested using calf alkaline phosphatase to free the phosphate, which was then detected using the Lanzetta assay.

The Lanzetta assay was employed to determine the concentration of rac-2-deoxyE4P in solution. The concentration determined for rac-2-deoxyE4P by this method was 23.6 mM, and represents the total concentration of rac-2-deoxyE4P in solution.

2.4.2.1 Conclusions

The results from these experiments showed that the concentration determined from the use of 2-deoxyE4P by *M. tuberculosis* DAH7P synthase, is approximately half (0.56) that of the total concentration. This was consistent with *M. tuberculosis* DAH7P synthase only using one enantiomer. It was expected that the (3*S*)-enantiomer of rac-2-deoxyE4P i.e. the one with the same C3 hydroxyl configuration as E4P, was the enantiomer being used based on the kinetic results for (3*S*)-2-deoxyE4P in the next section.

2.5 Kinetic studies on the deoxy analogues of E4P

The kinetic data for both the enantiopure and racemic 2- and 3-deoxyE4P with *M. tuberculosis* DAH7P synthase were determined by monitoring the loss of PEP at 232 nm using a UV-Visible spectrophotometer. The kinetic data were calculated by fitting the initial data to the Michaelis–Menten equation using GraFit (Erithacus Software). The Michaelis–Menten and Lineweaver–Burk plots for racemic and enantiopure 2- and 3-deoxyE4P can be found in Figure 2.21 and Figure 2.22, respectively. A summary of these results can be found in Table 2.2, along with the kinetic data for *E. coli* (phe) (type Iα) and *P. furiosus* (type Iβ) DAH7P synthase for comparison.

Substrate	DAH7P synthase source								
	***E. coli* (phe) (type Iα)**			***P. furiosus* (type Iβ)**			***M. tuberculosis* (type II)**		
	K_M (μM)	k_{cat} (s^{-1})	k_{cat}/K_M ($s^{-1}\mu M^{-1}$)	K_M (μM)	k_{cat} (s^{-1})	k_{cat}/K_M ($s^{-1}\mu M^{-1}$)	K_M (μM)	k_{cat} (s^{-1})	k_{cat}/K_M ($s^{-1}\mu M^{-1}$)
E4P 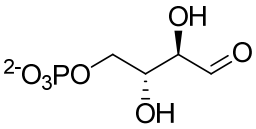	39±4	26±2	0.67	9±1	1.4±0.1	0.16	37±2	5.4±0.1	0.15
(3*S*)-2-deoxyE4P 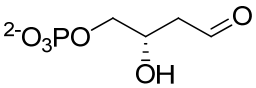	410±40	19±1	0.05	6±1	3.0±0.1	0.49	46±5	4.9±0.2	0.11
rac-2-deoxyE4P[(a)] 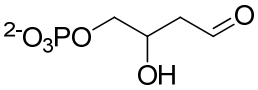	650±30	1.4±0.1	0.02	ND			85±7	6.8±0.2	0.14
(2*R*)-3-deoxyE4P 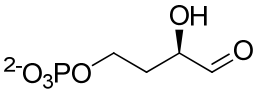	2700±140	4.5±0.1	0.002	200±30	2.1±0.1	0.01	77±9	2.4±0.1	0.031
rac-3-deoxyE4P[(a)] 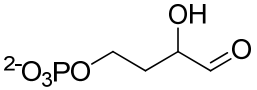	2600±330	4.5±0.1	0.002	NS			663±51	1.7±0.04	0.044

Table 2.2: Comparison of type I DAH7P synthases with the type II *M. tuberculosis* DAH7P synthase. [(a)] Kinetic data for racemic substrates were determined from the total concentration of the racemic mixture. *E. coli* DAH7P synthase (phe) kinetic data were determined by Dr Pietersma.[66] *P. furiosus* DAH7P synthase kinetic data determined by Dr Schofield.[32] ND = not determined. NS = not a substrate.

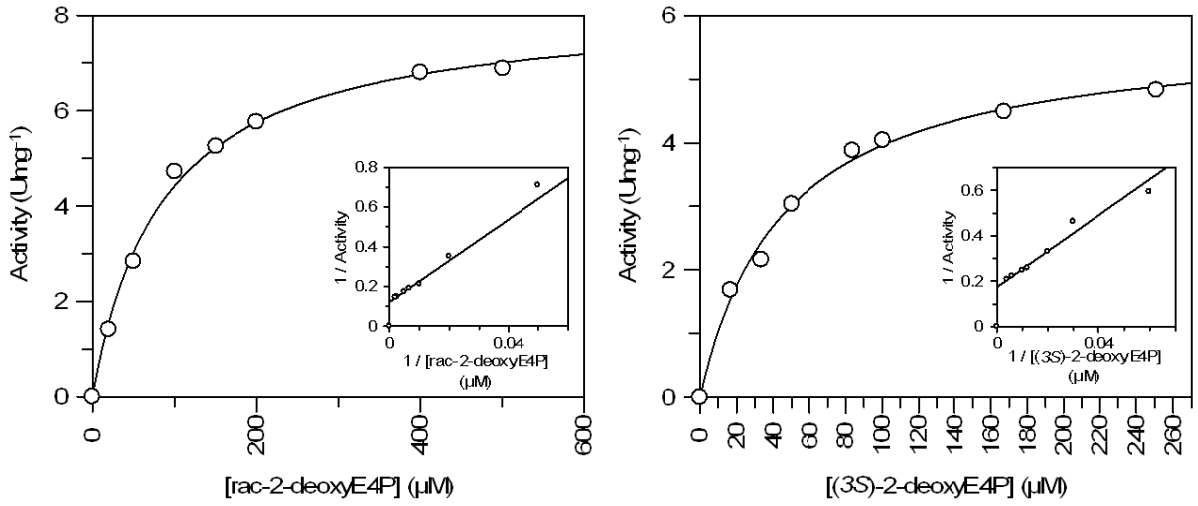

Figure 2.21: Michaelis–Menten and Lineweaver–Burk plots for the determination of K_M values for rac-2-deoxyE4P (left) and (3*S*)-2-deoxyE4P (right) with *M. tuberculosis* DAH7P synthase. The reaction mixtures for the determination of the K_M values of rac-2-deoxyE4P consisted of PEP (150 µM), $MnSO_4$ (100 µM), and rac-2-deoxyE4P (19–500 µM), in 50 mM BTP buffer, pH 7.5. The reaction mixtures for the determination of the K_M values of (3*S*)-2-deoxyE4P consisted of PEP (150 µM), $MnSO_4$ (100 µM), and (3*S*)-2-deoxyE4P (16–251 µM), in 50 mM BTP buffer, pH 7.5. The reaction was initiated by the addition of purified *M. tuberculosis* DAH7P synthase (3 µL, 1.4 mg/mL) and carried out at 30°C in a total volume of 1 mL. K_M and k_{cat} values were determined by fitting the data to the Michaelis–Menten equation using GraFit (Erithacus Software).

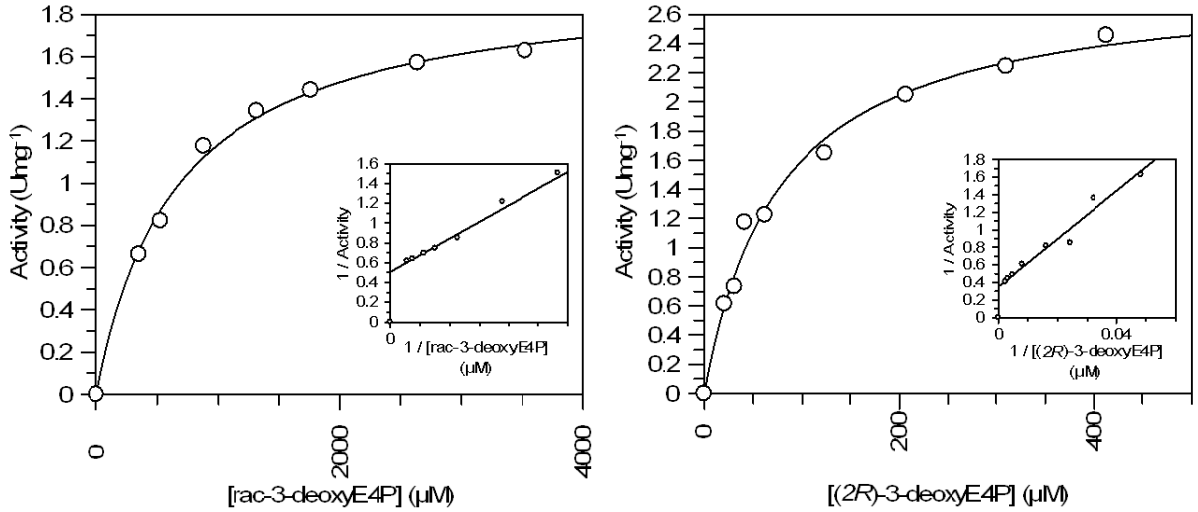

Figure 2.22: Michaelis–Menten and Lineweaver–Burk plots for the determination of K_M values for rac-3-deoxyE4P (left) and (2*R*)-3-deoxyE4P (right) with *M. tuberculosis* DAH7P synthase. The reaction mixtures for the determination of the K_M values of rac-3-deoxyE4P consisted of PEP (150 µM), $MnSO_4$ (100 µM), and rac-3-deoxyE4P (880–3526 µM), in 50 mM BTP buffer, pH 7.5. The reaction mixtures for the determination of the K_M values of (2*R*)-3-deoxyE4P consisted of PEP (150 µM), $MnSO_4$ (100 µM), and (2*R*)-3-deoxyE4P (21–414 µM), in 50 mM BTP buffer, pH 7.5. The reaction was initiated by the addition of purified *M. tuberculosis* DAH7P synthase (3 µL, 1.4 mg/mL) and carried out at 30°C in a total volume of 1 mL. K_M and k_{cat} values were determined by fitting the data to the Michaelis–Menten equation using GraFit (Erithacus Software).

2.5.1 *M. tuberculosis* DAH7P synthase

The concentration studies of rac-3-deoxyE4P carried out on *M. tuberculosis* (type II) DAH7P synthase showed the enzyme was only utilising one enantiomer in the racemic mixture. Comparison of the kinetic data obtained for (2*R*)-3-deoxyE4P and rac-3-deoxyE4P indicated that only the (2*R*)-enantiomer of the racemic mixture was being utilised by the enzyme. The K_M value of rac-3-deoxyE4P with *M. tuberculosis* DAH7P synthase was found to be approximately nine (8.6) times higher than (2*R*)-3-deoxyE4P, and the k_{cat} values were found to be similar to each other. These results suggest that the (2*S*)-enantiomer in the racemic mixture may be acting as a competitive inhibitor towards the enzyme. To confirm whether the (2*S*)-enantiomer was a competitive inhibitor, the (2*S*)-3-deoxyE4P substrate could be synthesised in the future and investigated with *M. tuberculosis* DAH7P synthase. Additionally, the higher K_M and lower k_{cat} values for 3-deoxyE4P indicates that it is a poorer substrate compared to E4P and 2-deoxyE4P, with *M. tuberculosis* DAH7P synthase.

Concentration studies conducted on *M. tuberculosis* DAH7P synthase with rac-2-deoxyE4P found that the enzyme only utilised one enantiomer of the racemic mixture. Comparison of the K_M values of rac-2-deoxyE4P with *M. tuberculosis* DAH7P synthase found that only the (3*S*)-enantiomer of the racemic mixture was being utilised by the enzyme. Although the k_{cat} values were different, the discrepancy was thought to be due to a more active batch of *M. tuberculosis* DAH7P synthase being used on rac-2-deoxyE4P. The K_M value for rac-2-deoxyE4P was found to be about twice (1.8) that of (3*S*)-2-deoxyE4P and suggests that only the (3*S*)-enantiomer is being utilised, with the (3*R*)-enantiomer having no affect on the kinetic parameters of the enzyme. Interestingly, the kinetic data for (3*S*)-2-deoxyE4P were comparable to that of E4P, indicating that the C2 hydroxyl group plays no significant role in the catalysis reaction by *M. tuberculosis* DAH7P synthase.

2.5.2 Type I and type II DAH7P synthases

The kinetic data in Table 2.2 shows that the 2- and 3-deoxyE4P analogues of E4P are substrates for enzymes of each of the three families of DAH7P synthase.

The type Iα DAH7P synthase from *E. coli* was found to be able to utilise both the enantiopure and racemic 2- and 3-deoxyE4P as substrates, but with significantly higher K_M and lower k_{cat} values compared to E4P.[66] In contrast, the K_M value for (3*S*)-2-deoxyE4P was found to be lower than E4P, and the k_{cat} was more than twice that of E4P for the type Iβ (*P. furiosus*) enzyme. This indicates that (3*S*)-2-deoxyE4P was a better substrate for *P. furiosus* DAH7P synthase than E4P. Furthermore, the type II DAH7P synthase from *M. tuberculosis* was found to be able to utilise (3*S*)-2-deoxyE4P with a similar catalytic efficiency as E4P, as indicated by the K_M and k_{cat} values. Both the type Iβ (*P. furiosus*) and II (*M. tuberculosis*) enzymes were overall more promiscuous than the type Iα (*E. coli*) enzyme in utilising the deoxy substrates.

Studies on rac-3-deoxyE4P on the type Iα DAH7P synthases from *E. coli* found that the type Iα enzyme utilises both enantiomers of the racemic mixture with no detectable change in the rate of reaction between rac-3-deoxyE4P and (2*R*)-3-deoxyE4P.[66] In contrast, the type II enzyme from *M. tuberculosis* utilised only the (2*R*)-enantiomer. Interestingly, rac-3-deoxyE4P was not a substrate for the type Iβ enzyme from *P. furiosus*, consistent with significant inhibition of this enzyme and non-productive binding with (2*S*)-3-deoxyE4P preventing productive binding by (2*R*)-3-deoxyE4P (Table 2.3).[32,66] This result was unexpected given the tolerance of this enzyme to the loss of the C2 hydroxyl group.

Studies on rac-2-deoxyE4P with the type Iα[66] and II DAH7P synthase from *E. coli* and *M. tuberculosis* respectively, showed that both enzymes only took the (3*S*)-enantiomer of the racemic mixture. Interestingly, the results for the type Iα (*E. coli*) enzyme indicated that the (3*R*)-enantiomer of the racemic mixture was inhibiting the enzyme, whereas the type II (*M. tuberculosis*) enzyme indicated the (3*R*)-enantiomer had no affect on the kinetic parameters of the enzyme (Table 2.3).

Substrate	**DAH7P synthase source**		
	***E. coli* (phe) (type Iα)**	***P. furiosus* (type Iβ)**	***M. tuberculosis* (type II)**
(2*R*)-3-deoxyE4P	✓	✓	✓
rac-3-deoxyE4P	(*R*) & (*S*)	✖	(*R*) only
(3*S*)-2-deoxyE4P	✓	✓	✓
rac-2-deoxyE4P	(*S*) only	ND	(*S*) only

Table 2.3: Summary of enantiomer utilisation and substrate studies on type Iα[66], Iβ[32] and II DAH7P synthases. ND = not determined.

Comparisons of all three families of DAH7P synthase have shown that the C2 and the C3 hydroxyl group on E4P are not essential for catalysis and binding in the enzymes. The results in Table 2.2 also show that 3-deoxyE4P is a poorer substrate for the DAH7P synthases from *E. coli*, *P. furiosus* and *M. tuberculosis* compared to 2-deoxyE4P. This indicates that the C2 hydroxyl group on E4P is less significant for binding and catalysis in the active site than the C3 hydroxyl group. Additionally, the type Iβ and II DAH7P synthase from *P. furiosus* and *M. tuberculosis* (respectively) were found to be the most promiscuous enzymes, with the type Iα DAH7P synthase from *E. coli* showing the least tolerance to the loss of the hydroxyl groups of E4P.

2.6 Summary

The synthesis of the enantiopure and racemic forms of 3-deoxyE4P was completed in eight steps from (2*R*)-malic acid and DL-malic acid respectively. The overall synthetic scheme that was used for the synthesis of rac-3-deoxyE4P is summarised below (Figure 2.23).

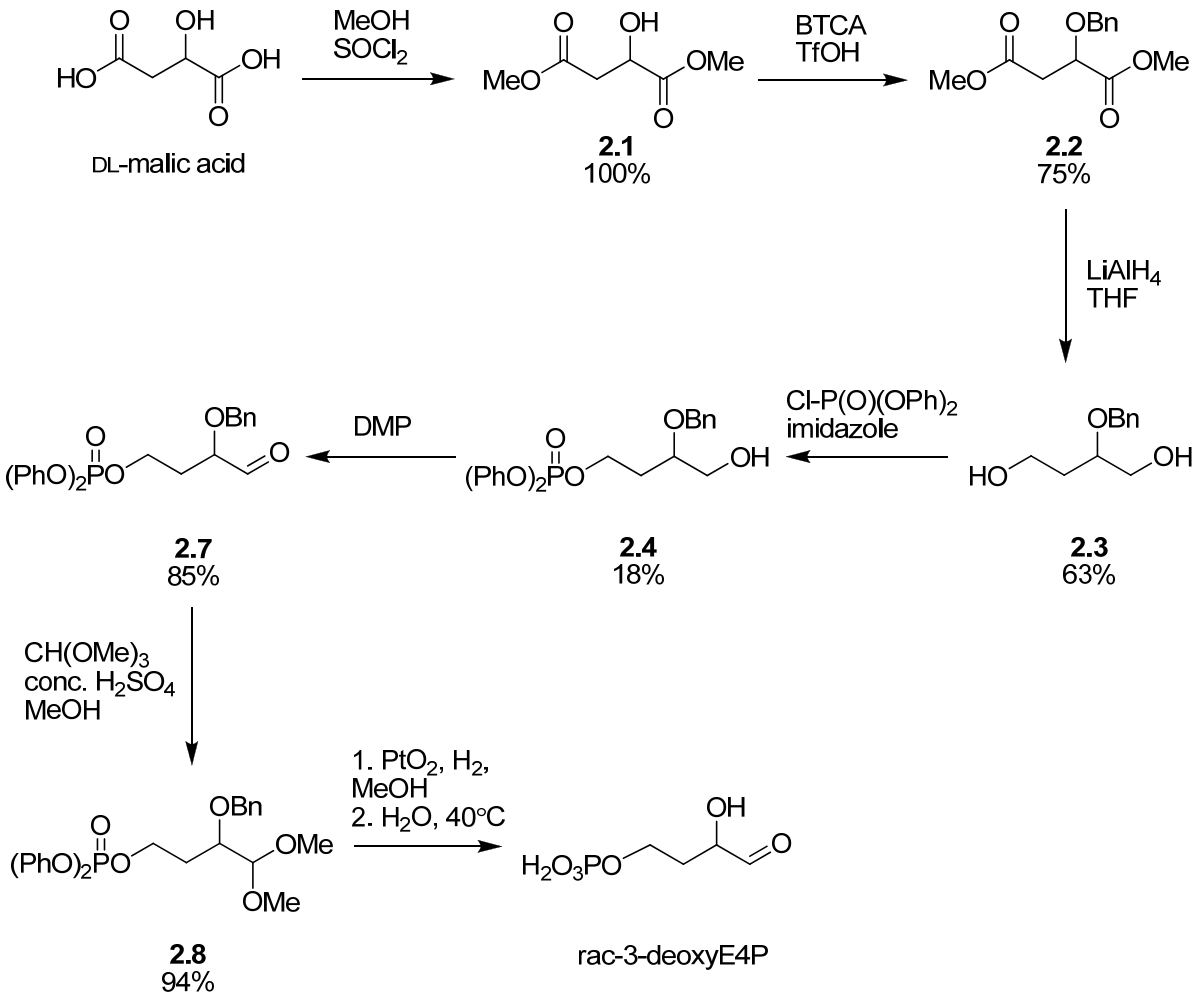

Figure 2.23: Overall synthetic scheme used to synthesise rac-3-deoxyE4P.

The yields of each step in the synthesis of rac-3-deoxyE4P were generally high, with the exception of the reaction for the formation of phosphate **2.4**. Similar yields were obtained for both the synthesis of enantiopure and racemic 3-deoxyE4P.

The low yield attributed to phosphate **2.4** is due to the formation of the side-products **2.5** (6%) and **2.6** (6%), and the recovery of a large amount of unreacted starting material **2.3** (24%). The monophosphorylated product **2.5** could also be useful in the potential synthesis of

2-deoxyE4P (Figure 2.24). Additionally, future work could involve investigations into bulkier protecting groups for the secondary alcohol of compound **2.3**, such as the sterically demanding TIPS group.[102,103] This group could potentially increase the yield of the desired phosphate **2.4**, and decrease the amount of side-products by adding to the steric hindrance for the phosphate group reacting at the other end of the molecule.

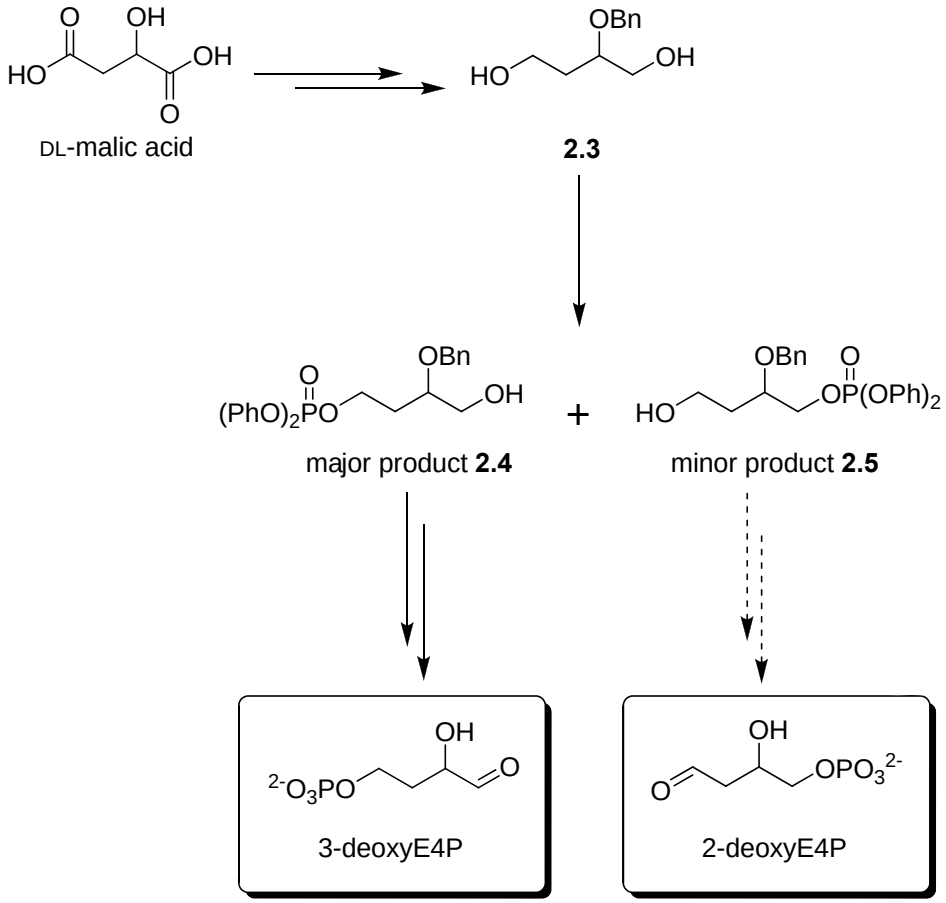

Figure 2.24: Potential route for the synthesis of 2-deoxyE4P starting with DL-malic acid.

The synthesis of (3*S*)-2-deoxyE4P was completed in six steps using the synthetic route in Scheme 2.2, and is summarised below (Figure 2.25). The yields of each step in the synthesis of (3*S*)-2-deoxyE4P were generally high.

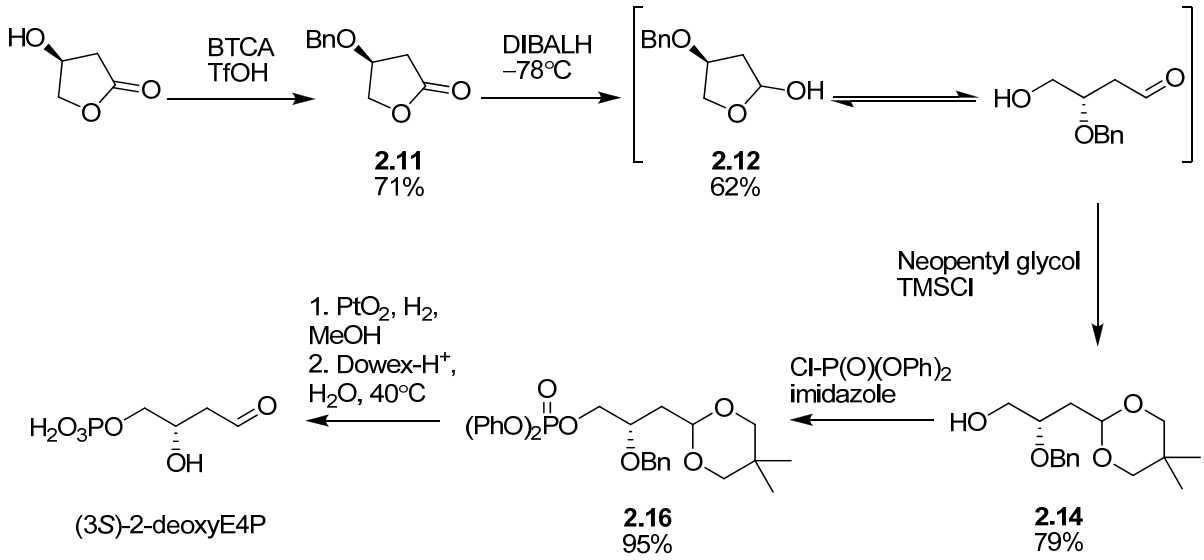

Figure 2.25: Overall synthetic scheme used to synthesise (3*S*)-2-deoxyE4P.

The successful synthesis of 2- and 3-deoxyE4P analogues (enantiopure and racemic substrates) has allowed for evaluation of their behaviour with *M. tuberculosis* DAH7P synthase, a type II enzyme. It has found that both 2- and 3-deoxyE4P are substrates for *M. tuberculosis* DAH7P synthase with the 3-deoxyE4P substrate being a worse substrate for the enzyme as indicated by its higher K_M value. The implication of these results for the kinetic mechanisms of DAH7P synthase is discussed in Chapter 5.

Chapter 3: Methyl analogues of E4P

3.1 Introduction

Carbon-carbon bond formation lies at the heart of organic synthesis. For complex, multifunctional target structures that are difficult to prepare by conventional means, asymmetric framework construction by enzymatic catalysis could be an attractive alternative to standard chemical methods.[104] The use of enzymes in organic synthesis has the advantage of being able to carry out reactions under mild conditions, allows a high degree of stereochemical control, and does not require the use of protecting group chemistry.[105] The DAH7P synthases could have potential use in this field, as the reaction between E4P and PEP results in the stereospecific formation of a new stereogenic centre and carbon-carbon bond (Figure 3.1). In addition, this enzyme has already been shown to have a broad tolerance for non-natural substrates taking the place of E4P[24,32,40,47] and could provide organic chemists with a useful synthetic tool for carrying out stereospecific aldol reactions with other aldehydic substrates.

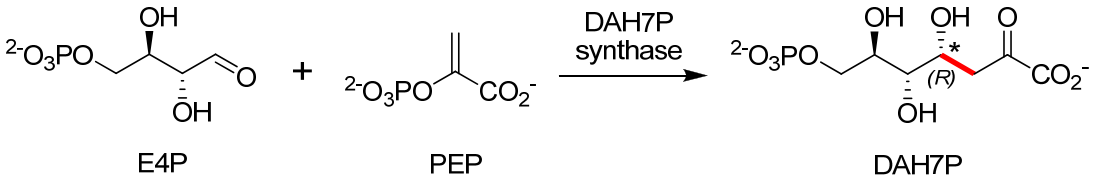

Figure 3.1: Catalysed reaction between E4P and PEP by DAH7P synthase to give the seven carbon sugar DAH7P. A new carbon-carbon bond (red) and a new stereocentre (*) is formed in DAH7P.

DAH7P synthase is able to utilise E4P analogues where the:

- configuration of the hydroxyl groups on the C2 and C3 positions of E4P are inverted (e.g. D/L-T4P)[40]
- hydroxyl group at either C2 or C3 has been removed (e.g. 2/3-deoxyE4P)[66]
- sugar is up to one carbon longer than E4P (compounds **1.25**, **1.26** and A5P)[24,32,47]

However, the presence of the phosphate and aldehyde groups in a potential substrate is essential for enzyme activity (Figure 3.2).[24,61]

These results suggest that the C2 and C3 hydroxyl groups of E4P are not necessary for substrate placement. Therefore the C2 and C3 hydroxyl groups of E4P and the active site residues they interact with have a limited role to play in substrate selection by the enzyme.

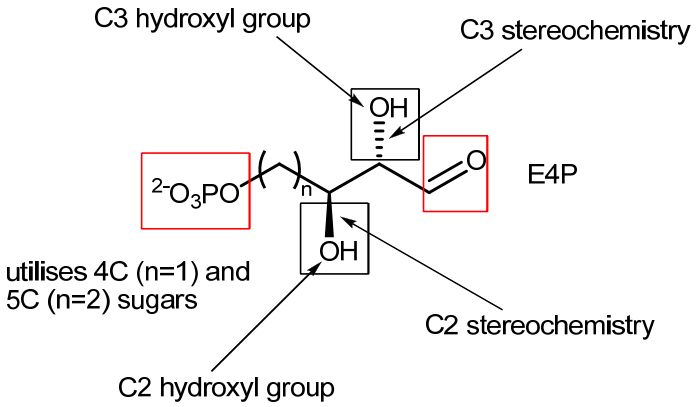

Figure 3.2: Structural requirements of E4P for binding and catalysis in the active site of DAH7P synthase. Red boxes indicate essential groups for binding and catalysis. Black boxes indicate non-essential groups for binding and catalysis.

Although the E4P analogues mentioned above (where the C2 or C3 hydroxyls are inverted or removed) were all substrates for DAH7P synthase, studies where these hydroxyl groups are replaced by different substituents (e.g. alkyl or halide groups) have not been investigated. Therefore, target analogues where the hydroxyl groups on C2 or C3 of E4P are replaced with methyl groups to give 2-methylE4P and 3-methylE4P respectively, were chosen as substrate analogues to synthesise for testing as substrates (Figure 3.3).

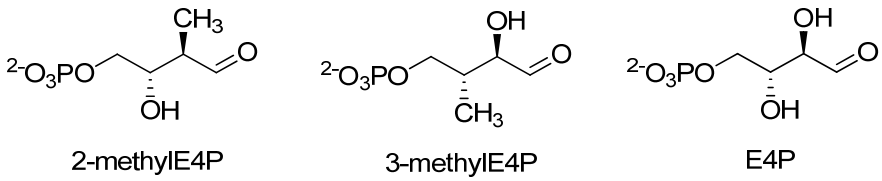

Figure 3.3: 2- and 3-methylE4P analogues of E4P.

The synthesis and evaluation of the 3-methylE4P analogue as a substrate for DAH7P synthase, and the attempts to synthesise the 2-methylE4P analogue are described in this chapter.

3.2 Synthesis of 3-methylE4P

DL-Malic acid was chosen as the starting material for the synthesis of 3-methylE4P. By examining the structure of DL-malic acid we can see that it has the potential to be readily chemically manipulated into 3-methylE4P (Figure 3.4). DL-Malic acid contains four carbons, has a hydroxyl group at the C2 position, an acidic α-proton on C3 which can be removed to form an enolate, so that the carbon can be readily alkylated, and the two carboxylic acid groups can be reduced to either aldehyde or primary alcohol functionalities. The primary alcohol group can be phosphorylated to give the phosphate functionality. Additionally, DL-malic acid had already been used for the synthesis of rac-3-deoxyE4P (Chapter 2), and the chemistry used for the synthesis of rac-3-deoxyE4P could also be applied here for the synthesis of 3-methylE4P.

Another advantage of DL-malic acid is that it is available commercially as both the racemic mixture and the enantiopure (2*R*) and (2*S*) forms, providing the option to use this as a starting material for the synthesis of enantiopure versions of 3-methylE4P. DL-Malic acid is also relatively inexpensive (500g for ~$70 NZD, Aldrich) which means the synthesis can be carried out on a multigram scale.

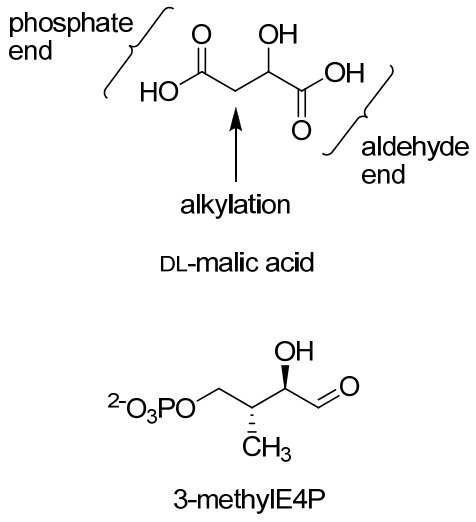

Figure 3.4: Structural analysis of DL-malic acid.

Shown in Scheme 3.1 is the synthetic route that was initially developed for the synthesis of 3-methylE4P. It was proposed that DL-malic acid would be converted into diester **2.1**, this would then be alkylated to give the α-alkylated diester **3.1**. The free hydroxyl group on

diester **3.1** would then be protected to give benzyl ether **3.2**, which would be reduced using $LiAlH_4$ to give diol **3.3**. Diol **3.3** would need to be phosphorylated at the C1 hydroxyl end and oxidised at the other to give compounds **3.4** and **3.7** respectively. The aldehyde group on compound **3.7** would then be protected as an acetal, to prevent reduction from the hydrogenation step, followed by two deprotection steps to give 3-methylE4P.

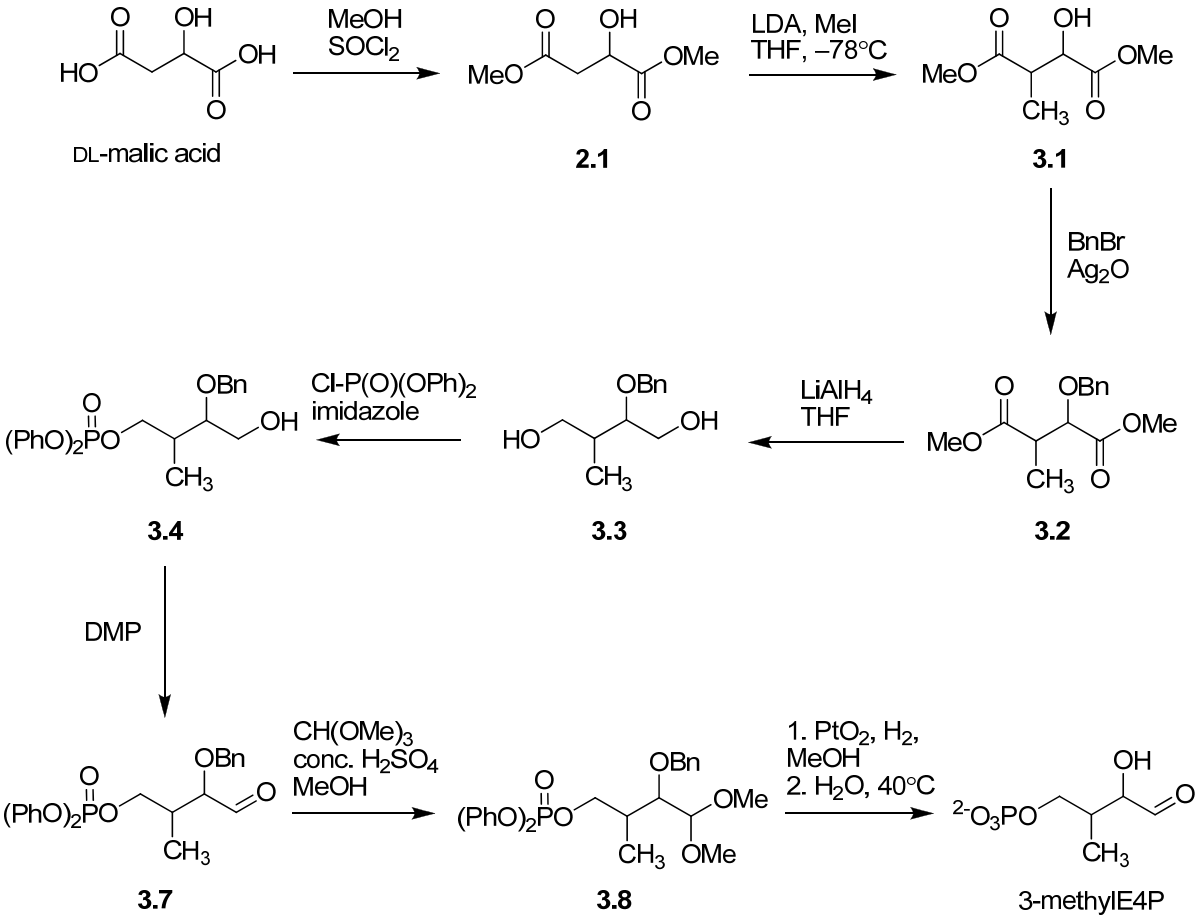

Scheme 3.1: The proposed synthetic route for the synthesis of 3-methylE4P from DL-malic acid.

3.2.1 Synthesis of 3-methylE4P from DL-malic acid

Following the successful synthesis of diester **2.1** (Chapter 2), diester **2.1** was alkylated using the method described by Seebach *et al.*[106,107] to give two diastereoisomers of diester **3.1** (66% yield) with diastereoselectivity of 6:1 (Figure 3.5). The formation of both diastereoisomers of diester **3.1** was confirmed by two sets of doublets in the ^1H NMR spectrum at 1.26 and 1.14 ppm corresponding to the new methyl resonances on the two products (Figure 3.6). However, the diastereomers could not be separated by flash chromatography and the mixture was used

in the next step. The stereo-selection in the reaction to form diester **3.1** is discussed in the next section.

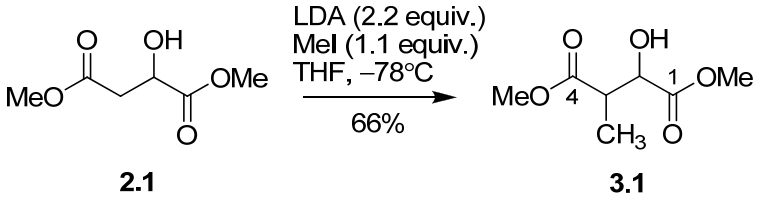

2.1 **3.1**

Figure 3.5: Alkylation of diester 2.1 to give a mixture of diastereoisomers of diester 3.1.

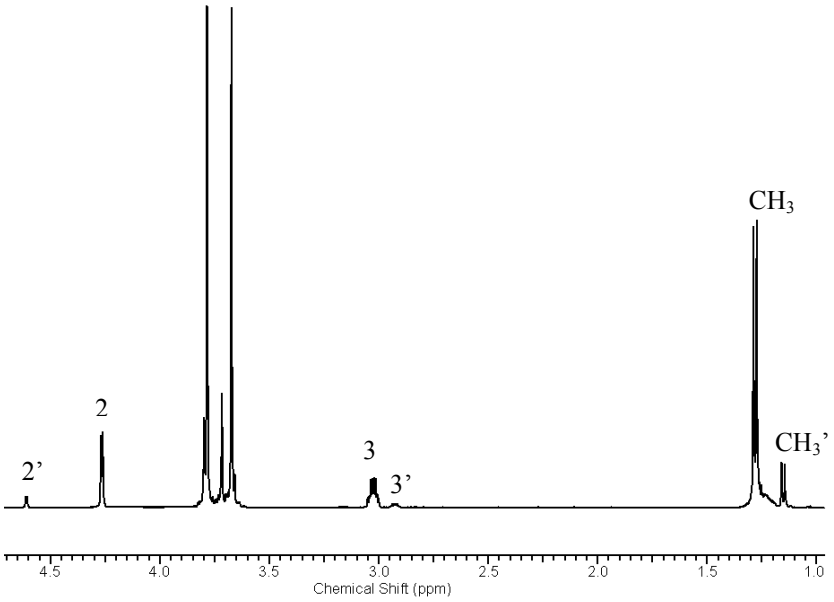

Figure 3.6: ^{1}H NMR spectrum of compound 3.1. Two sets of doublets corresponding to each methyl group on the diastereoisomers of diester 3.1.

Hydroxyl groups can participate in numerous transformations under mild conditions such as oxidation, halogenations and elimination reactions.[108-112] For this reason it was decided to protect the hydroxyl group of diester **3.1**. The benzyl ether protecting group was chosen due to its successful use for the synthesis of 2- and 3-deoxyE4P. Diester **3.1** was protected under mild conditions using freshly prepared Ag_2O and BnBr to give compound **3.2** in 79% yield (Figure 3.7).[113-115] Compound **3.2** was confirmed by an ^{1}H NMR spectrum showing the aromatic proton resonances between 7.35–7.26 ppm.

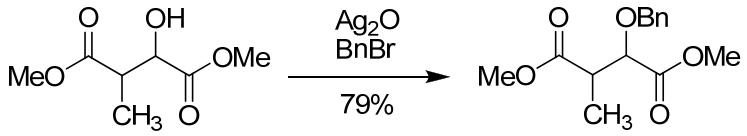

3.1 **3.2**

Figure 3.7: Benzylation of the α-alkylated diester 3.1 to give compound 3.2.

Reduction of compound **3.2** with $LiAlH_4$ gave diol **3.3** in 81% yield (Figure 3.8).[116,117] The ^1H NMR spectrum confirmed the synthesis of diol **3.3** had been achieved, by the disappearance of the ester group methyl resonances between 3.77–3.63 ppm.

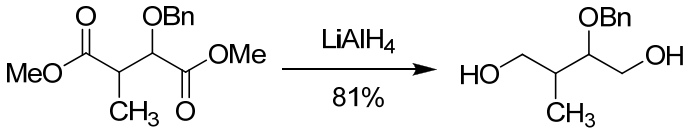

3.2 **3.3**

Figure 3.8: Reduction of benzyl ester 3.2 to give diol 3.3.

The phosphorylation of diol **3.3** can potentially give three compounds, the two monophosphorylated regioisomers **3.4**, **3.5** and the diphosphorylated compound **3.6** (Figure 3.9). The ratio of the phosphorylating reagent to the starting material was expected to be important in this reaction as too much could result in increased amounts of the diphosphorylated compound **3.6**, and too little may result in low yields of desired compound **3.4**.

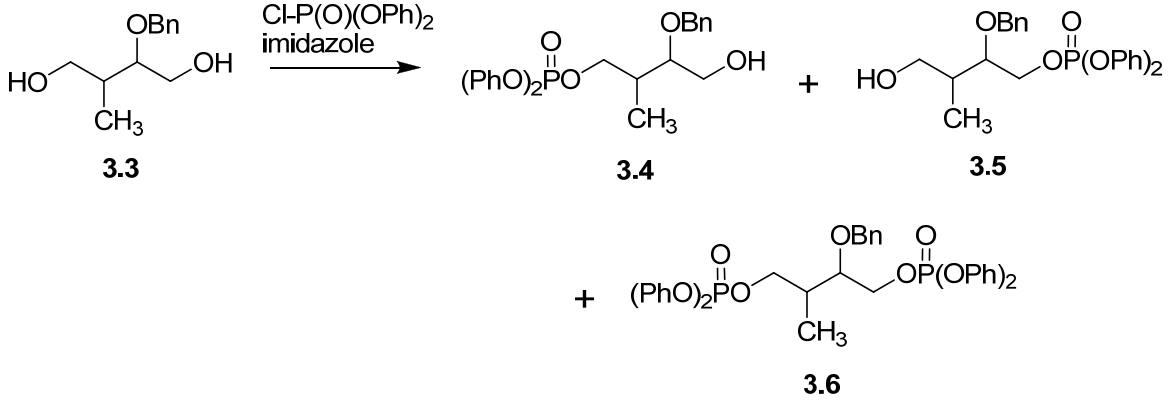

3.3 **3.4** **3.5** **3.6**

Figure 3.9: Possible compounds from phosphorylation of diol 3.3.

It was expected that the bulky benzyl group of diol **3.3** would have some sort of steric effect on the phosphorylation reaction, and the desired compound **3.4** was expected to be the major

isomer. This is due to the results seen with phosphorylating diol **2.3** in Chapter 2 to give desired phosphate **2.4**, the other monophosphorylated compound **2.5** and diphosphorylated compound **2.6** in a 3:1:1 ratio. In the hope of further increasing the yield of compound **3.4** over those of compounds **3.5** and **3.6**, the sterically bulky diphenyl chlorophosphate was chosen as the phosphorylating reagent.

Diol **3.3** was phosphorylated using diphenyl chlorophosphate and imidazole giving a mixture of compounds. TLC analysis of the crude mixture before separation by flash chromatography, showed four compounds with R_f values of 0.81, 0.57, 0.27 and 0.15 (1:1 EtOAc:Pet ether), corresponding to phosphorylating reagent, unknown compound 1, unknown compound 2, and starting material **3.3** respectively. The mixture was separated by flash chromatography and mass spectrometry was used to ascertain that unknown compound 1 (R_f = 0.57) was the diphosphorylated compound **3.6** (mass spectrometry determined a mass of 675.1913 (calc. for $C_{36}H_{36}O_9$ $[M+H]^+$: 675.1913)). Whereas, compound **3.4** and **3.5** would have a lower mass (calc. $C_{24}H_{28}O_6P$ $[M+H]^+$: 443.1624). Mass spectrometry also determined unknown compound 2 (R_f = 0.27) was monophosphorylated compound **3.4** or **3.5** (calc. $C_{24}H_{28}O_6P$ $[M+H]^+$: 443.1624; found: 443.1626).

To determine which monophosphorylated compound had been isolated, phosphates **3.4** or **3.5**, ^{13}C NMR spectroscopy was used. If compound **3.4** was isolated we would expect the resonance arising from C4 to have altered chemical shifts due to the attachment of a phosphorous group. We would also expect the resonance arising from C4 to spilt due to ^{31}P-^{13}C coupling ($^2J_{POC}$). The same would be true for the formation of compound **3.5** except the changes would be expected to be observed at C1 not C4. By comparing the two ^{13}C spectra of starting material diol **3.3** and unknown compound 2 (Figure 3.10), it was determined that unknown compound 2 was the desired monophosphorylated compound **3.4**. The resonance for C4 was observed further downfield relative to its position in the starting material (65.8 ppm to 71.5 ppm). This signal also was present as a doublet due to ^{31}P-^{13}C coupling ($^2J_{POC}$ = 6.6 Hz). 2D NMR spectroscopy, COSY and HSQC were used to fully assign the ^1H and ^{13}C NMR spectra of this compound.

Surprisingly, the ^{13}C NMR spectrum of diol **3.3** showed no minor peaks due to the minor diastereoisomer, with the exception of a very small peak at 36.9 ppm corresponding to the

resonance for C3 of the minor diastereoisomer (Figure 3.10). Phosphorylation of diol **3.3** results in the resolution of the two diastereoisomers.

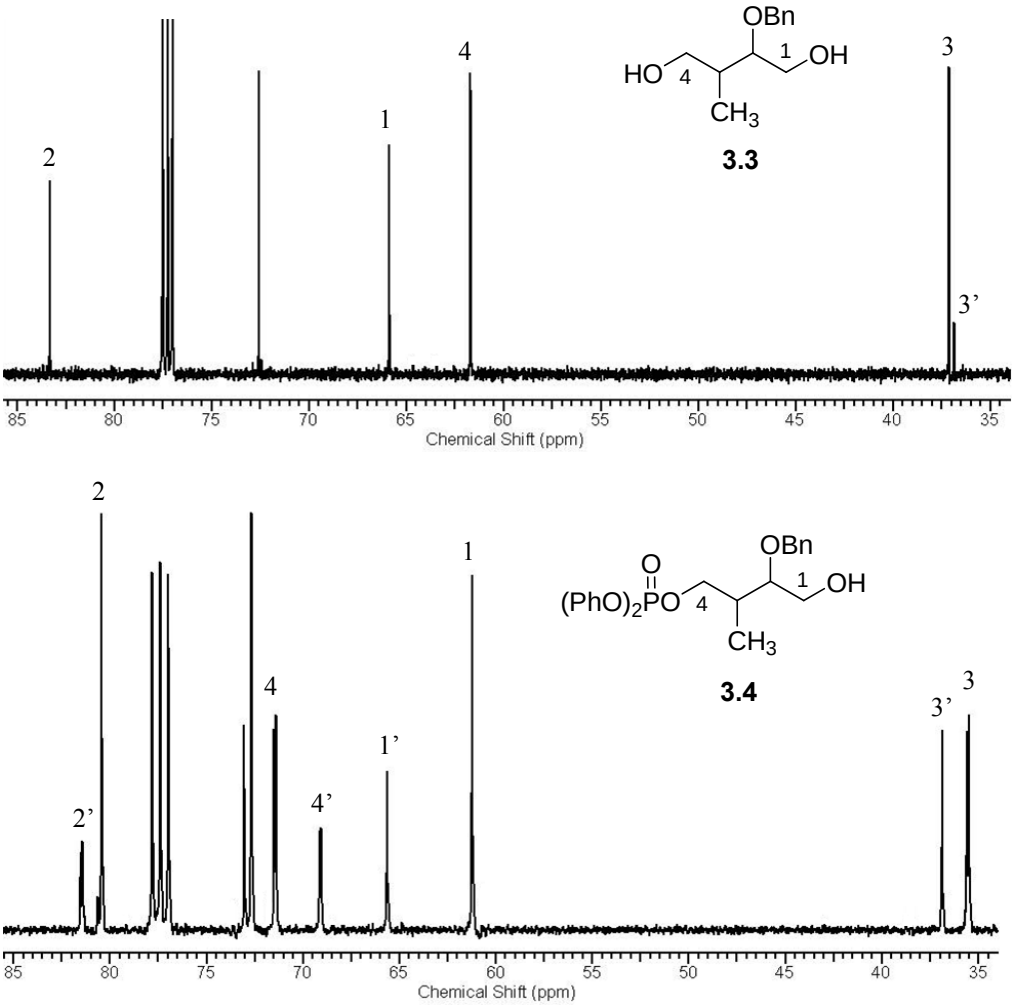

Figure 3.10: (Top) Partial ^{13}C NMR spectrum of diol 3.3. (Bottom) Partial ^{13}C NMR spectrum of compound 3.4 showing minor peaks due to diastereoisomers.

Overall, analysis of the separated components of the reaction mixture by mass spectrometry and NMR (particularly using ^{13}C NMR spectroscopy and ^{31}P-^{13}C coupling) showed only the desired monophosphorylated compound **3.4** and the diphosphorylated compound **3.6** had been formed in 22% and 21% yields, respectively. Unreacted starting material **3.3** was also recovered (30% recovered). Phosphate **3.4** was isolated as a pair of inseparable diastereoisomers (ratio 3:1). The best yields of the desired monophosphorylated compound **3.4** were obtained using 0.9 equivalents of the phosphorylating reagent. No monophosphorylated compound **3.5** was isolated or detected in the reaction. This compound could have been useful for the synthesis of the 2-methylE4P analogue.

DMP was chosen as the oxidising agent for the oxidation of compound **3.4** due to its milder reaction conditions (room temperature, neutral pH), shorter reaction times and higher yields compared to more traditional chromium- and DMSO-based oxidants.[118-122] This reagent is even preferred over the Swern oxidation[123,124] and is mainly due to the side-product dimethyl sulphide, one of the most foul odours known in organic chemistry, that is produced during the oxidation reaction.

The monophosphorylated compound **3.4** was oxidised using freshly prepared DMP to give aldehyde **3.7** in 81% yield (Figure 3.11).[125] The ratio of diastereoisomers also changed when phosphate **3.4** (ratio 3:1) was oxidised to give aldehyde **3.7** (ratio 2:1). This change is thought to be due to partial resolution of the diastereoisomers of aldehyde **3.7** during purification by flash chromatography. Aldehyde **3.7** was confirmed by a ^{1}H NMR spectrum showing the aldehyde resonances at 9.69 and 9.60 ppm, corresponding to the diastereoisomers of aldehyde **3.7**.

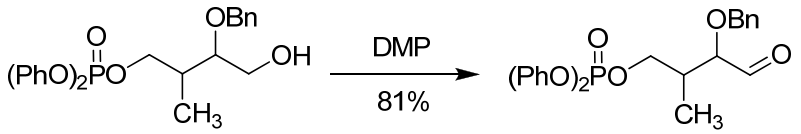

3.4 **3.7**

Figure 3.11: Oxidation of monophosphorylated compound 3.4 with DMP to give aldehyde 3.7.

Aldehyde **3.7** needed to be protected as its dimethyl acetal to prevent reduction from hydrogenation in the following deprotection step. Aldehyde **3.7** was protected as the dimethyl acetal giving the fully protected analogue **3.8** in 87% yield (Figure 3.12).[95] ^{1}H NMR spectroscopy confirmed the disappearance of the aldehyde resonances at 9.69 and 9.60 ppm in the spectrum. Additionally, formation of the diastereotopic methoxy group proton resonances at 3.44 and 3.40 ppm for the major diastereoisomer, and at 3.34 and 3.32 ppm for the minor diastereoisomer was also observed in the ^{1}H NMR spectrum (ratio 2:1).

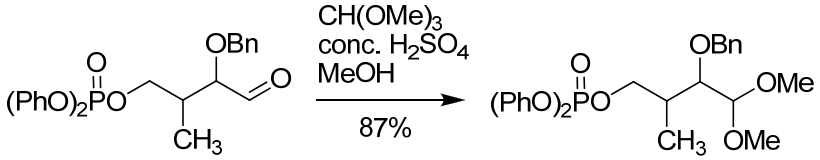

3.7 **3.8**

Figure 3.12: Acetal protection of aldehyde 3.7 to give the protected analogue 3.8.

The protected analogue **3.8** was treated by hydrogenolysis over PtO_2 in MeOH to give crude sugar **3.9** in 100% yield (Figure 3.13). The reaction mixture was checked by ^{1}H NMR spectroscopy to ensure complete loss of the aromatic proton resonances between 7.34–7.16 ppm was observed in the spectrum. The acetal protecting groups were then hydrolysed in water at 40°C, where the phosphoric acid group provided the acid catalyst, to give 3-methylE4P. ^{1}H NMR spectroscopy was used to confirm that the methoxy group proton resonances between 3.46–3.32 ppm had been cleaved. Additionally, 3-methylE4P was detected by mass spectrometry with a molecular mass of 197.0223 (calc. $C_5H_{10}O_6P$ $[M-H]^-$: 197.0215). 3-MethylE4P was used directly in enzyme assays without further purification.

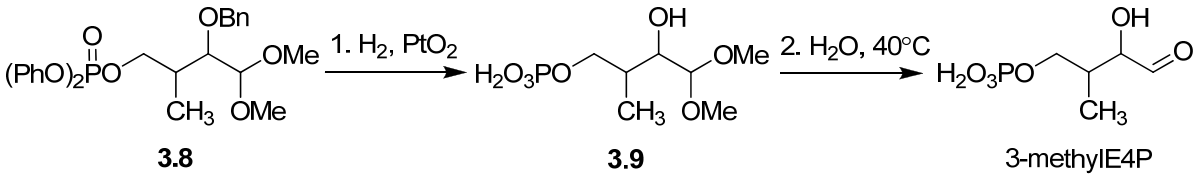

Figure 3.13: Synthesis of 3-methylE4P.

3.2.1.1 Stereochemistry of diester 3.1

Seebach *et al.*[107] have reported that methylation of compound (2*S*)-**2.1** gave diester **3.1** in 65% yield as a mixture of diastereoisomers (Figure 3.14). The diastereoisomer ratio of the major product ((2*S*, 3*R*)-**3.1**) to the minor product ((2*S*, 3*S*)-**3.1**) was 10:1 and was determined by capillary gas chromatography.

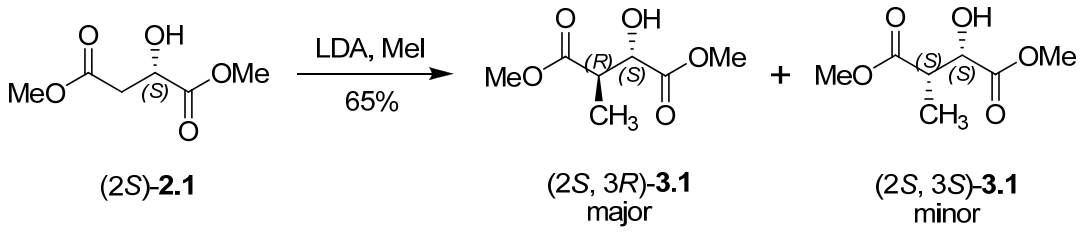

Figure 3.14: Synthesis of the diastereoisomers of diester 3.1 from (2*S*)-2.1 by Seebach *et al.*[107]

From these results by Seebach *et al.*, methylation of the racemic mixture of compound **2.1** (c.f. Figure 3.5, page 66) would be expected to result in a mixture of isomers with the major products of diester **3.1** having the (2*S*, 3*R*)- and (2*R*, 3*S*)-configurations and the minor products having the (2*S*, 3*S*)- and (2*R*, 3*R*)-configurations (ratio of 6:1 as determined by ^{1}H

NMR spectroscopy, Figure 3.15). Diester (2*R*, 3*S*)-**3.1** would have the correct stereochemistry with respect to E4P.

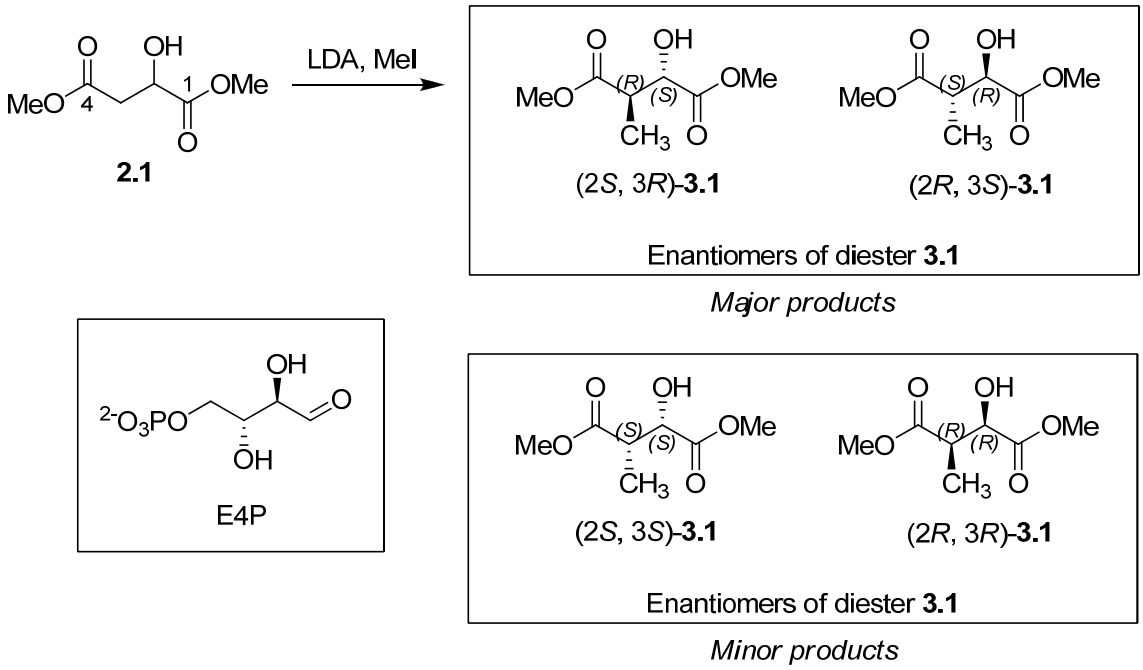

Figure 3.15: Stereoisomers of diester 3.1 from methylation of racemic diester 2.1. E4P is shown for comparison.

Although the ratio of diastereoisomers was not the same as that reported by Seebach *et al.*, this was probably due to different experimental conditions for the synthesis of the mixture of diastereoisomers of diester **3.1**, and that used for the synthesis of (2*S*, 3*R*)-**3.1** by Seebach *et al.* Only a general experimental procedure was reported by Seebach *et al*. Purification of the mixture of diastereoisomers of diester **3.1** could also account for the lower ratio seen, as the diastereoisomers of diester **3.1** may have been partially resolved during flash chromatography.

3.2.2 Initial enzyme assays with *E. coli* DAH7P synthase

Standard assay conditions were used to first determine whether 3-methylE4P was a substrate for the type Iα *E. coli* DAH7P synthase (phe) or not.

To determine whether 3-methylE4P was a substrate or not, reaction mixtures were setup that contained 3-methylE4P (5–50 μL, unknown concentration), $MnSO_4$ (100 μM) and PEP (150 μM) in 50 mM BTP buffer at pH 6.8. In each case, the reaction was initiated by the addition of purified *E. coli* DAH7P synthase (2–30 μL, 5.86 mg/mL). All assays were carried out at 25°C in a total volume of 1.0 mL and the loss of PEP was monitored at 232 nm. Initial readings showed that 3-methylE4P was not a substrate for *E. coli* DAH7P synthase, as no PEP loss was observed at 232 nm, even though high concentrations of enzyme were employed.

To confirm the enzyme was active under the assay conditions, selected reactions were spiked with the natural substrate E4P. Absorption loss of PEP was observed immediately indicating the enzyme was catalysing the reaction between E4P and PEP and not between 3-methylE4P and PEP. An analysis of why 3-methylE4P was not a substrate for *E. coli* DAH7P synthase can be found in Chapter 5.

3.3 Attempts to synthesise 2-methylE4P

3.3.1 Early approaches: Method 1

The first attempted synthesis of 2-methylE4P followed a similar route to that which was employed for the successful synthesis of 3-methylE4P and used the same starting material, DL-malic acid. Figure 3.16 shows the three general key chemical manipulations that are required to convert the acid into 2-methylE4P. These steps are alkylation at the α-position, phosphorylation at one end of the molecule and reduction at the other end to give the aldehyde functionality.

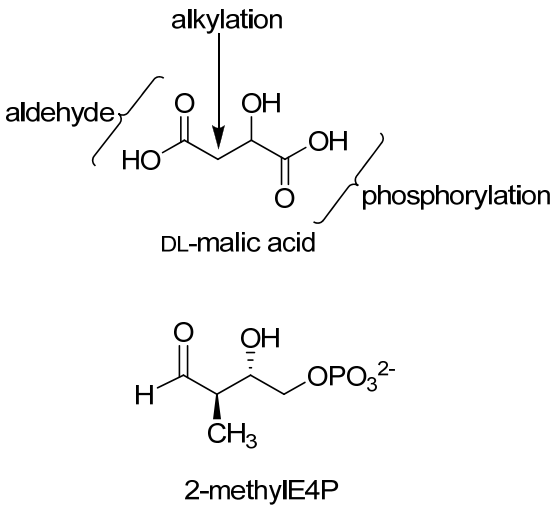

Figure 3.16: Analysis of DL-malic acid for the synthesis of 2-methylE4P.

Shown in Scheme 3.2 is the first synthetic scheme that was used to attempt to synthesise 2-methylE4P from DL-malic acid. The first two steps of the proposed scheme would require the orthogonal protection of each of the carboxylate ends of malic acid to give acid **3.11** and ester **3.12**. Ester **3.12** would then be alkylated to afford compound **3.13** followed by deprotection of the cyclohexylidene acetal protecting group to give acid **3.14**. Acid **3.14** would then be selectively reduced at the carboxylate end, followed by monophosphorylated at the primary alcohol position to give compounds **3.15** and **3.16** respectively. Selective reduction of the ester to an aldehyde would afford aldehyde **3.17**, followed by protection of the aldehyde group with dimethyl acetal to give the protected analogue **3.18**. Subsequent deprotection steps would give 2-methylE4P.

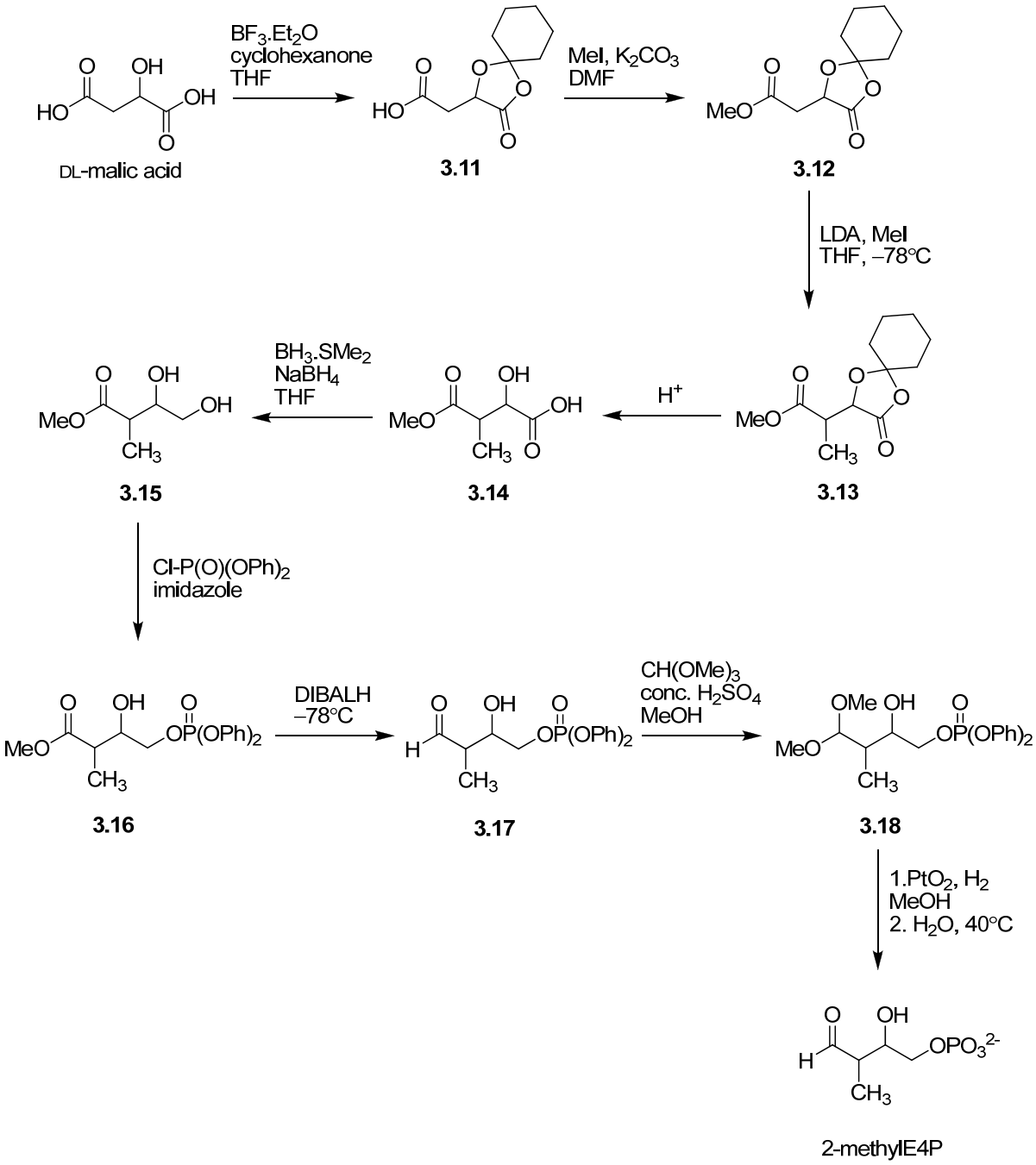

Scheme 3.2: Proposed synthetic scheme for the synthesis of 2-methylE4P. Method 1.

3.3.1.1 Implementation of Scheme 3.2

The first attempts to synthesise acid **3.11** followed the procedure of Monma *et al.*[126] and yielded acid **3.11** in a disappointingly low yield of 7–8%. The low yields were attributed to the reaction producing an equivalent of water which would be detrimental to the reaction. However, Monma *et al.* did not report the use of any dehydrating reagents in their procedure. The reaction was retried but this time with an added dehydrating reagent, 4Å sieves, to

remove water and drive the reaction to completion. The yield obtained for acid **3.11** was 66% (lit.[126] 67%) following purification by flash chromatography (Figure 3.17). The ^{1}H and ^{13}C NMR spectra of acid **3.11** matched those reported in literature.[126,127]

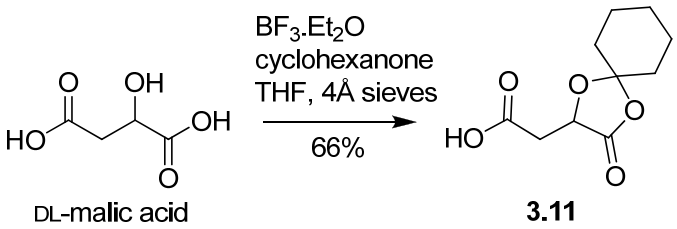

Figure 3.17: Synthesis of acid 3.11.

Esterification of acid **3.11** using a modified method by Karanewsky *et al.*[128] gave the ester **3.12** with a 95% yield after flash chromatography (Figure 3.18). Ester **3.12** was confirmed by a ^{1}H NMR spectrum showing the ester group methyl resonance at 3.71 ppm.

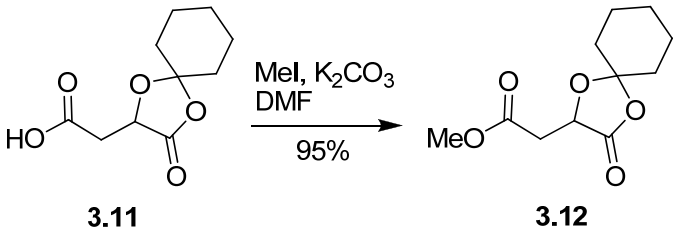

Figure 3.18: Synthesis of ester 3.12.

With the successful synthesis of ester **3.12**, attempts were made to alkylate the ester at the C3 position to give compound **3.13**. The first attempts involved using the base LDA and the electrophile MeI, but these were unsuccessful in alkylating the ester **3.12** (Figure 3.19). Several attempts were trialled using either 1.2 or 2.2 equivalents of LDA but with no success. TLC analysis of the reactions mixtures showed multiple unidentifiable side-products (most likely due to degradation of ester **3.12**), and only some starting material **3.12** could be recovered (16% recovered). Due to these problems, this reaction was not investigated further.

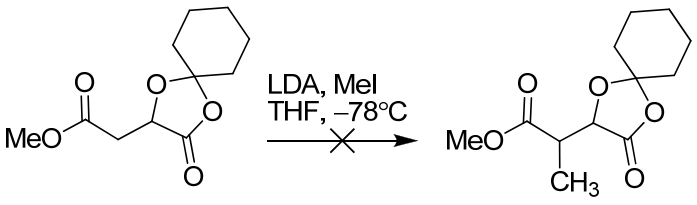

3.12 **3.13**

Figure 3.19: Attempts to alkylate ester 3.12 using LDA and MeI.

Following the unsuccessful synthesis of compound **3.13** using the LDA/MeI method, the procedure by Casper *et al.*[129] was also trialled. Casper *et al.* synthesised compound **3.21** using $TiCl_4$, Et_3N via the enolate **3.20** (Figure 3.20). This reaction is similar to the reaction described in Figure 3.19 using LDA. The procedure was trialled on ester **3.12**, but unfortunately only starting material could be detected by TLC during the reaction (Figure 3.21).

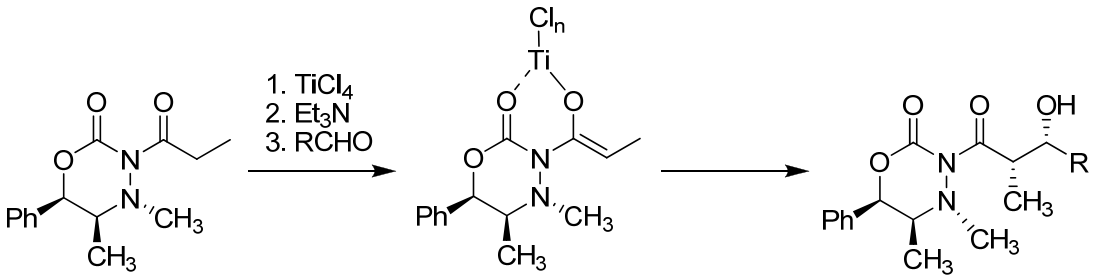

3.19 **3.20** **3.21**

Figure 3.20: Synthesis of compound 3.21 by Casper *et al.*[129]

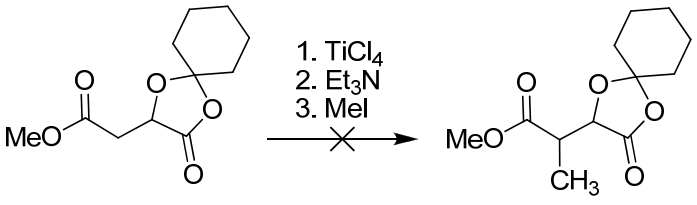

3.12 **3.13**

Figure 3.21: Attempts to alkylate ester 3.12 using $TiCl_4$, Et_3N and MeI.

The lack of success with this alkylation reaction may well be due to steric factors. The bulky cyclohexylidene protecting group could hinder access to the carbonyl group of ester **3.12** from coordinating with the large $TiCl_4$ Lewis acid, as seen in enolate **3.20**. Therefore, stabilisation of the enolate would not be possible and the reaction would not proceed. This was supported by a large amount of starting material being recovered following purification

by flash chromatography (75–100% recovered). In contrast, the reaction carried out by Casper *et al.*[129] worked because the large $TiCl_4$ Lewis acid was able to stabilise the enolate **3.20**, by coordinating to the two carbonyl groups.

Due to the failed attempts in alkylating ester **3.12** to give compound **3.13**, this cyclohexylidene protecting group method shown in Scheme 3.2 was abandoned and alternative schemes were investigated.

3.3.2 Selective reduction of dimethyl malate ester 2.1: Method 2

With the failed attempts in alkylating ester **3.12**, as described in the previous section, it was thought that the use of a protecting group at the start of the synthesis (i.e. the cyclohexylidene protecting group, Scheme 3.2) may not be necessary. A search of literature[110,130-133] revealed that diester **2.1** (a readily available starting material used for the synthesis of 3-methylE4P and 3-deoxyE4P) can be selectively reduced at the C1 ester end over the C4 end. By selectively reducing the C1 ester end of diester **2.1** over the C4 end, one could then alkylate the C3 position to give compound **3.23**. Phosphorylation at the primary hydroxyl, followed by selective reduction at the ester end of compound **3.23** would give the phosphate and aldehyde groups of 2-methylE4P, respectively (Figure 3.22). The proposed synthetic scheme for this route is shown in Scheme 3.3 and requires eight steps to reach the target compound.

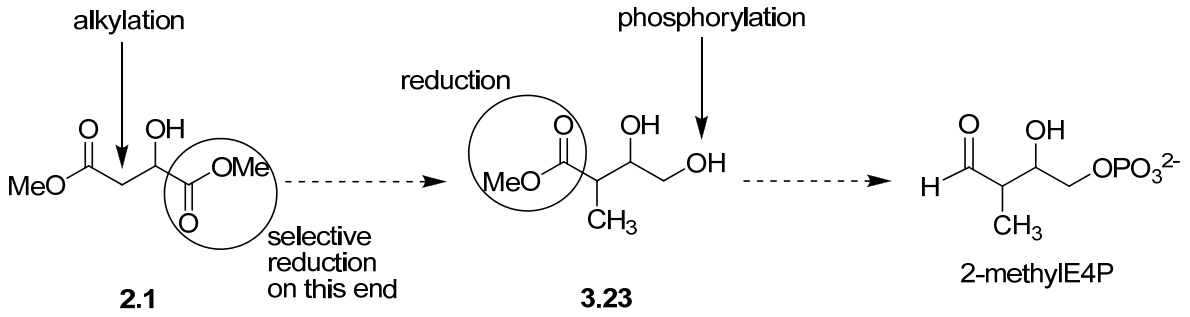

Figure 3.22: Analysis of DL-malic acid for selective reduction at only one of the carboxylate ends.

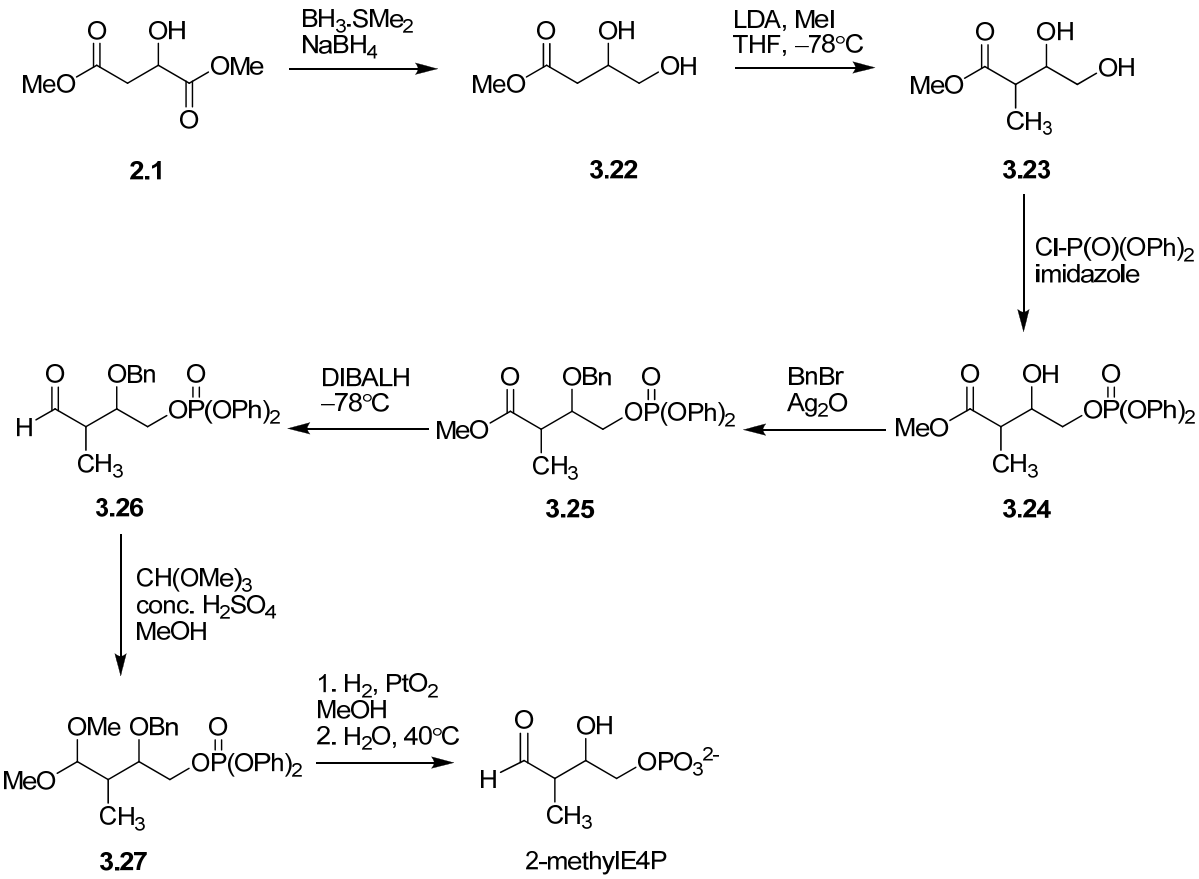

Scheme 3.3: Proposed synthetic scheme for the synthesis of 2-methylE4P. Method 2.

3.3.2.1 Implementation of Scheme 3.3

Initial attempts to selectively reduce diester **2.1** using borane-dimethyl sulphide complex and a catalytic amount of $NaBH_4$ (10 mol%), gave the diol **3.22** in 52% yield. By dropping the molar percentage of $NaBH_4$ to 3% and carefully monitoring the reaction by TLC, diol **3.22** was obtained in 94% yield (Figure 3.23). The NMR spectral data for diol **3.22** were in accordance with the literature report.[131]

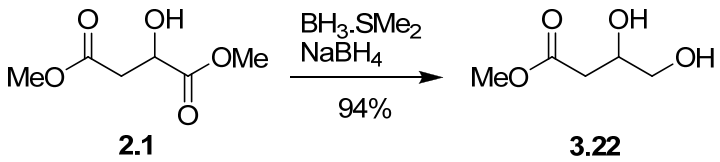

Figure 3.23: Selective reduction of diester 2.1 using $BH_3.SMe_2$ and $NaBH_4$ to give diol 3.22.

Unfortunately, attempts to alkylate **3.22** were unsuccessful (Figure 3.24). TLC analysis observed that starting material was being consumed to give a new compound but on closer

analysis with ^{1}H NMR spectroscopy it was determined this new compound was not compound **3.23**. Instead, the ^{1}H NMR spectrum of this compound showed that the peak at 3.70 ppm, corresponding to the ester group methyl resonance, had gone. One possible reason for the disappearance of the methyl resonance is that the reaction produced lactone **3.28** instead of the desired compound **3.23** (Figure 3.25). Analysis of this compound by mass spectrometry would confirm whether lactone **3.28** was being formed, but was not investigated as this method was subsequently abandoned. Although lactone **3.28** could still be alkylated itself, no alkylated product was detected in the ^{1}H NMR spectrum.

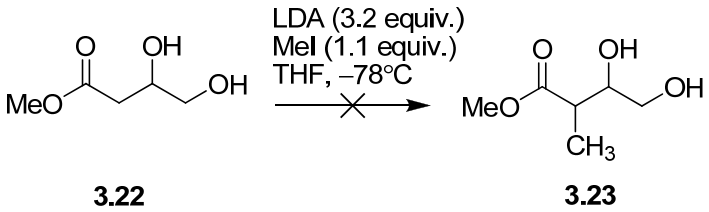

3.22 **3.23**

Figure 3.24: Attempts to alkylated diol 3.22.

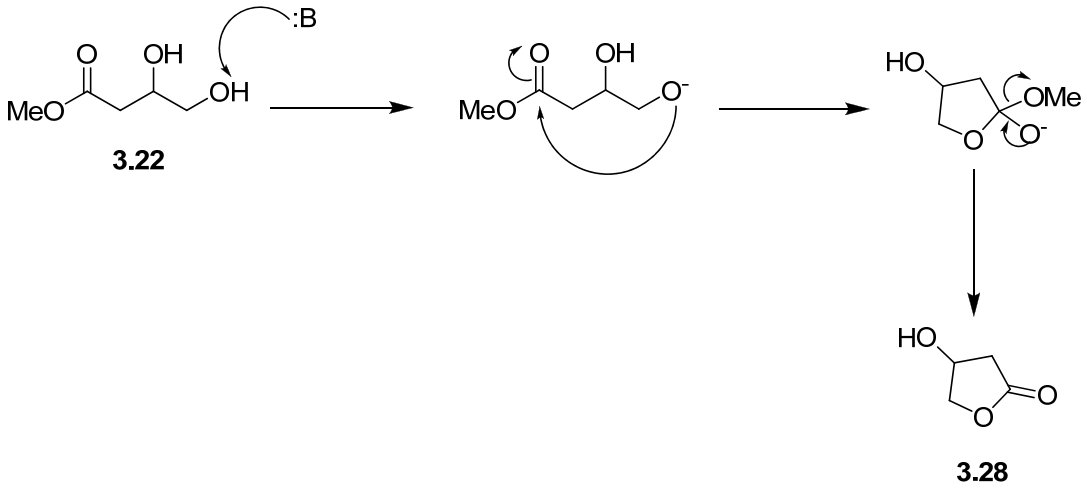

3.22 **3.28**

Figure 3.25: Possible cyclisation of diol 3.22 to lactone 3.28 mechanism.

In an attempt to prevent cyclisation of diol **3.22** to lactone **3.28**, the primary alcohol group on diol **3.22** was protected using a silyl ether protecting group, TBDPS, to give ester **3.29** with a 90% yield (Figure 3.26). Unfortunately, attempts to alkylate ester **3.29** using LDA and MeI resulted in multiple unidentifiable side-products (TLC analysis). These side-products were not isolated or investigated further.

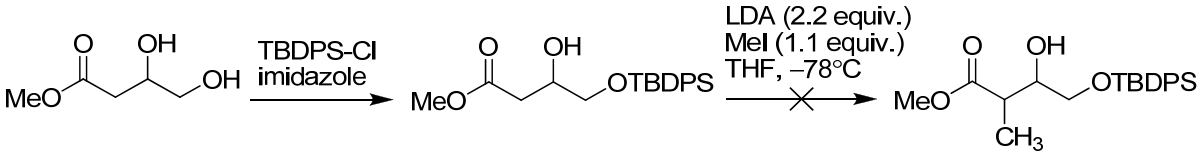

3.22 **3.29** **3.30**

Figure 3.26: Synthesis of ester 3.29 and attempts to synthesise compound 3.30.

With the unsuccessful synthesis of compounds **3.23** and **3.30** by alkylation using LDA/MeI, the method proposed in Scheme 3.3 was subsequently abandoned and another method to synthesise 2-methylE4P was investigated.

3.3.3 A modified method of the synthesis of 3-methylE4P: Method 3

Due to the difficulties encountered in alkylating derivatives of DL-malic acid in Scheme 3.2 and Scheme 3.3 (previous sections) it was decided to look back at the synthetic scheme for the synthesis of 3-methylE4P (Scheme 3.1), in particular the successful synthesis of diester **3.1** and diol **3.3** (Figure 3.27).

3.1 **3.3**

Figure 3.27: Compounds 3.1 and 3.3 from the synthesis of 3-methylE4P.

Diester **3.1** can be readily prepared from DL-malic acid as seen previously for the synthesis of 3-methylE4P. Furthermore, following two more steps, diester **3.1** can be converted to the diol **3.3**. The idea was to monoprotect diol **3.3** using a large protecting group at the less hindered primary alcohol, and follow this with phosphorylation on the other end. The large triisopropylsilane (TIPS) protecting group was chosen (Figure 3.28), due to its availability and use in our laboratory, steric bulk, and stability under a wide range of reaction conditions.[103,134]

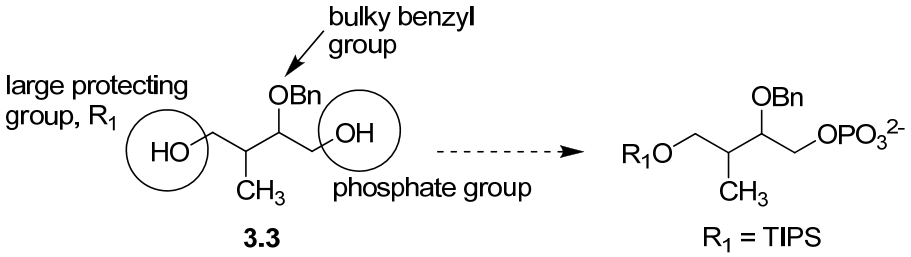

Figure 3.28: Analysis of diol 3.3 for the synthesis of 2-methylE4P. The less hindered alcohol end of diol 3.3 would be protected using a large TIPS group followed by phosphorylation at the other end.

The synthetic scheme proposed to synthesise 2-methylE4P from diol **3.3** is shown in Scheme 3.4. Diol **3.3** would be monoprotected using TIPSCl giving three possible products **3.31**–**3.33**. The major regioisomer **3.31** would then be isolated from the other compounds and phosphorylated, followed by deprotection of the TIPS group to give alcohol **3.35**. The exposed primary alcohol group on alcohol **3.35** would then be oxidised to give aldehyde **3.36**. Subsequent reactions of protection of the aldehyde group on aldehyde **3.36**, followed by deprotection steps would give 2-methylE4P.

In addition, it was thought that the diphenyl chlorophosphate reagent used for the synthesis of 3-methylE4P may be too bulky to give the phosphorylated compound **3.31**. This is because no regioisomer **3.5** (Figure 3.9, page 67) was detected or isolated during the monophosphorylation reaction of diol **3.3**. Therefore, the less bulky phosphorylating reagent, diethyl chlorophosphate, was chosen instead (Scheme 3.4).

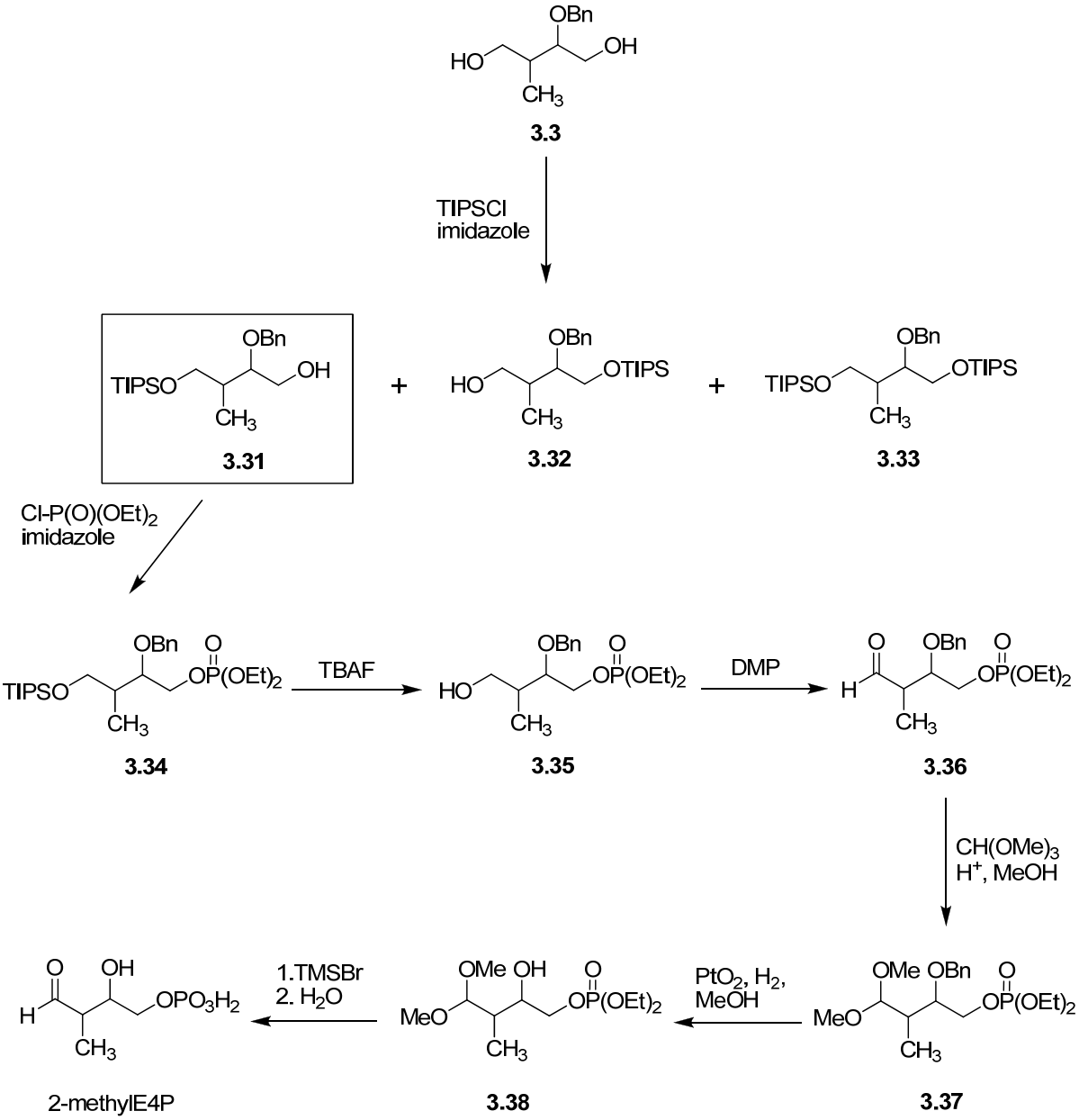

Scheme 3.4: The proposed synthetic scheme for the synthesis of 2-methylE4P. Method 3.

3.3.3.1 Implementation of Scheme 3.4

Following the successful synthesis of diol **3.3** using the method shown in Scheme 3.1, diol **3.3** was monoprotected using TIPSCl (1.1 equiv.) and imidazole to give a mixture of three compounds, as indicated by TLC analysis. These compounds could potentially be the three products **3.31**–**3.33** (Figure 3.29).

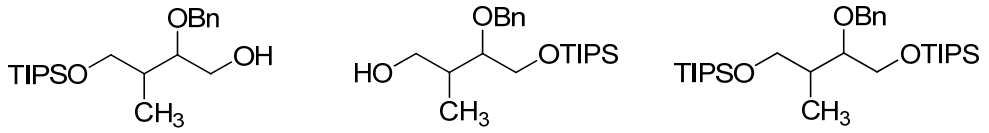

3.31 **3.32** **3.33**

Figure 3.29: Monoprotection of diol 3.3 using TIPS giving potentially three regioisomers 3.31–3.33.

The three unknown compounds with R_f (1:9 EtOAc:Pet ether) values of 0.58, 0.13 and 0.04 were separated by flash chromatography and TLC analysis indicated the most polar compound, R_f = 0.04, was starting material **3.3** (28% recovered). ^{1}H NMR analysis confirmed that this lowest R_f spot was indeed starting material **3.3**. It was assumed that the less polar compound, R_f = 0.58, was the disilylated compound **3.33** as this compound would be the less polar compared to compounds **3.3**, **3.31** and **3.32**. Analysis of this compound by mass spectrometry determined a mass of 523.3945 (calc. $C_{30}H_{59}O_3Si_2$ $[M+H]^+$: 523.3940), which corresponds to the disilylated compound **3.33** (20% yield). The mass determined for the compound with R_f = 0.13, was 367.2655 (calc. $C_{21}H_{39}O_3Si$ $[M+H]^+$: 367.2668). This mass corresponds to either monosilylated compound **3.31** or **3.32**. Interpretation of the ^{1}H and ^{13}C NMR spectrums, with the aid of 2D NMR spectroscopy (HSQC, HMBC and COSY), confirmed that this compound was the desired regioisomer **3.31** (51% yield).

The overall yield for the monoprotection reaction of diol **3.3** using TIPS to give monosilylated compound **3.31** (51% yield, Figure 3.30), was better than expected in comparison to the synthesis of compound **3.4** (22% yield) from the monophosphorylation of diol **3.3**. The ratio of the reagent TIPSCl used in this reaction, compared to the starting material diol **3.3**, also seemed to matter in the synthesis of alcohol **3.31**. When 0.9 equivalents of TIPSCl was used instead of 1.1 equivalent, compound **3.31** was synthesised in 32% yield i.e. fewer equivalents decreased the yield. This was the opposite observation to that which was made with the monophosphorylation of diol **3.3**, as more equivalents of the phosphorylating reagent resulted in a decrease in yield of compound **3.4**. Optimisation studies, where the amount of silyating reagent is varied, could be done in the future to obtain the maximum yield for alcohol **3.31**.

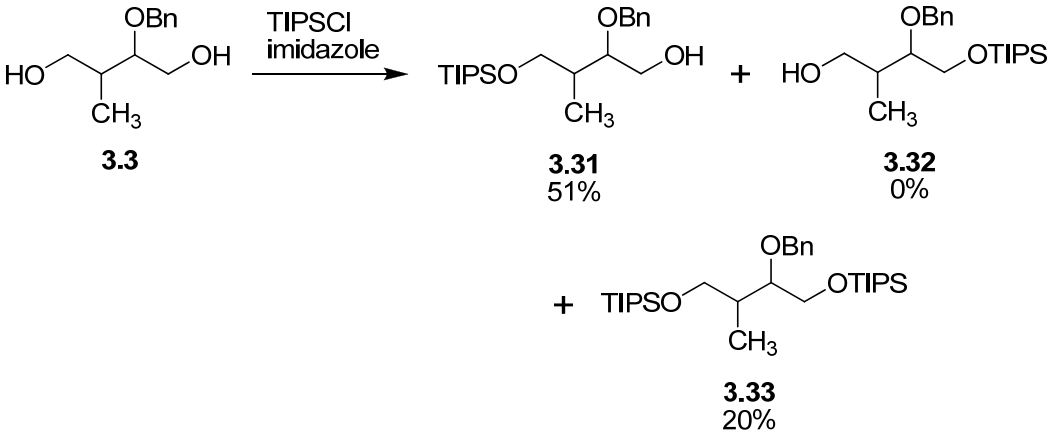

Figure 3.30: Monoprotection of diol 3.3 using the TIPS protecting group.

No minor regioisomer **3.32** could be isolated or detected in the reaction (Figure 3.30), and this observation was similar to that made in the monophosphorylation reaction for the synthesis of 3-methylE4P where no minor regioisomer **3.5** could be detected in the reaction as well (Figure 3.9, page 67). The minor regioisomer **3.32** could have also been useful for the synthesis of 3-methylE4P analogue.

Alcohol **3.31** was then phosphorylated using diethyl chlorophosphate and imidazole to give phosphate **3.34** in 72% yield (Figure 3.31 and Figure 3.32). ^{31}P NMR spectroscopy confirmed the presence of the phosphate ester resonance at −0.33 ppm in the spectrum. Additionally, phosphate **3.34** was detected by mass spectrometry as the protonated compound, with a molecular mass of 503.2937 (calc. $C_{25}H_{48}O_6SiP$ $[M+H]^+$: 503.2958).

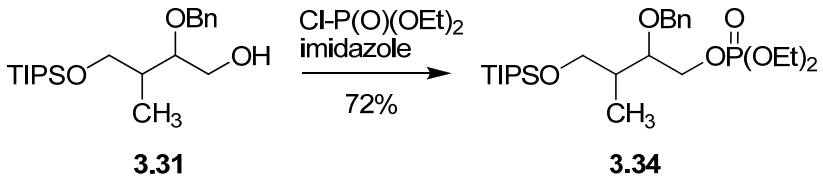

Figure 3.31: Synthesis of phosphate 3.34.

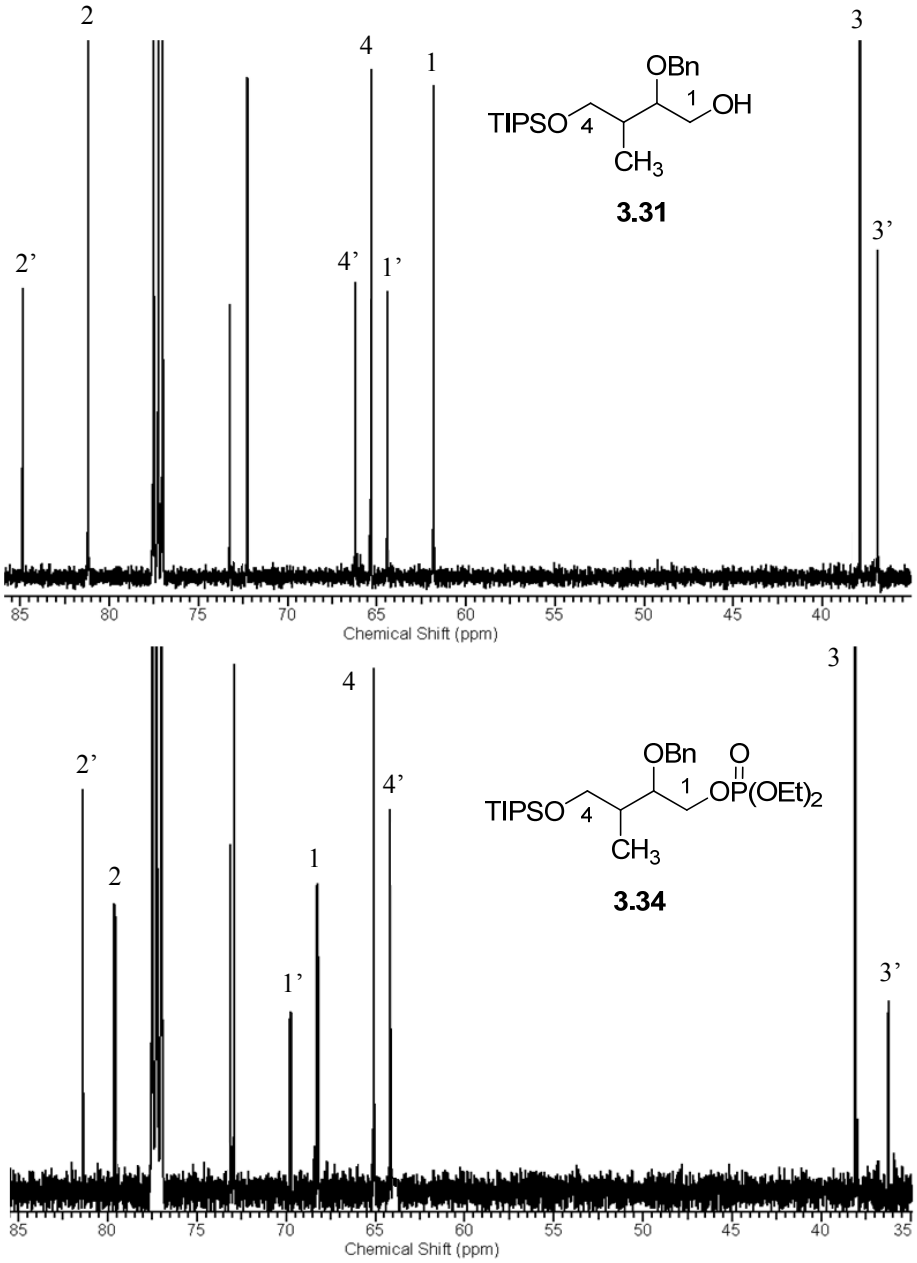

Figure 3.32: Comparison of the partial ^{13}C NMR spectra of compounds 3.31 and 3.34. Peaks were assigned using HSQC and COSY spectra.

Deprotection of phosphate **3.34** using TBAF at room temperature gave alcohol **3.35** in 90% yield (Figure 3.33). ^{1}H NMR spectroscopy confirmed that the deprotection had occurred, with the disappearance of the peaks arising from the isopropyl group resonances between 1.09–0.98 ppm in the spectrum.

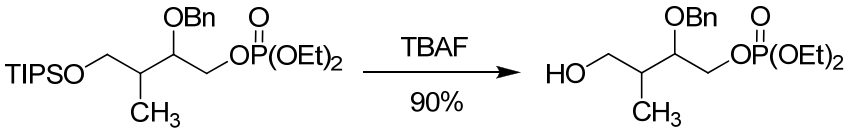

3.34 **3.35**

Figure 3.33: Synthesis of alcohol 3.35.

Alcohol **3.35** was initially oxidised using DMP that had been prepared a month earlier to give aldehyde **3.36** in 56%. By using freshly prepared DMP, which had been prepared the day before, the yield for aldehyde **3.36** was increased to 72% (Figure 3.34). The presence of the product was confirmed by a ^{1}H NMR spectrum showing the aldehyde resonances at 9.74 and 9.70 ppm, corresponding to the diastereoisomers of aldehyde **3.36** (ratio 2:1).

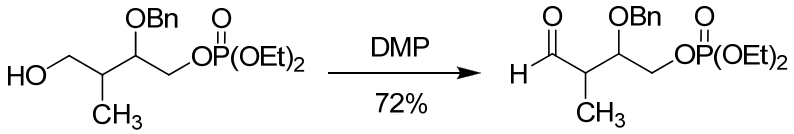

3.35 **3.36**

Figure 3.34: Oxidation of alcohol 3.35 using DMP to give aldehyde 3.36.

The aldehyde group on aldehyde **3.36** needed to be protected as its dimethyl acetal to prevent reduction from hydrogenation in the following deprotection steps. Protection of aldehyde **3.36** was accomplished using MeOH and concentrated H_2SO_4 to give acetal **3.37** in 77% yield (Figure 3.35). The presence of the product was confirmed by a ^{1}H NMR spectrum showing the aldehyde resonances at 9.74 and 9.70 ppm had disappeared. Additionally, the formation of the diastereotopic methoxy group proton resonances at 3.36 and 3.33 ppm for the major diastereoisomer, and at 3.47 and 3.43 ppm for the minor diastereoisomer were also observed in the spectrum (ratio 2:1).

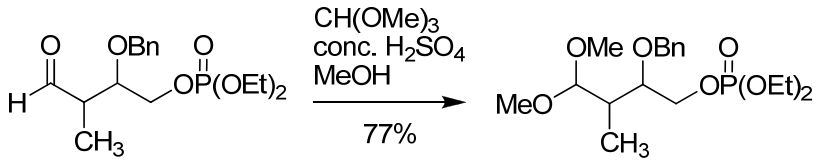

3.36 **3.37**

Figure 3.35: Synthesis of acetal 3.37.

Hydrogenation of acetal **3.37** using a platinum catalyst on carbon gave compound **3.38** in 95% yield (Figure 3.36). ^{1}H NMR spectroscopy confirmed that all aromatic proton

resonances had been lost with the disappearance of the peaks between 7.37–7.26 ppm in the spectrum.

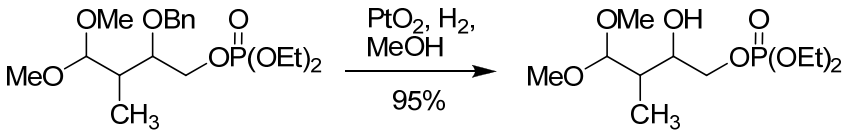

3.37 **3.38**

Figure 3.36: Synthesis of compound 3.38.

Unfortunately, treatment of compound **3.38** with TMSBr (2.2 equiv.) did not result in the synthesis of 2-methylE4P (Figure 3.37). During the reaction, TLC analysis indicated the loss of the starting material **3.38** and the development of a new compound producing a spot on the baseline. It was thought that the phosphate ester ethyl groups had been hydrolysed off forming the polar phosphate acid that would appear on the baseline. The ^{1}H NMR spectrum of the crude sample after work up (concentrated *in vacuo* to remove volatiles) showed that the phosphate ester group ethyl resonances at 4.11 and 1.73 ppm had not been cleaved by TMSBr. The dimethyl acetal protection group had however been removed to give the aldehyde functionality. This was indicated by the disappearance of the methoxy group proton resonances at around 3.40 ppm and the appearance of the aldehyde group at 9.20 ppm in the ^{1}H NMR spectrum. It appears the acidity of the reaction mixture (pH 1–2, by pH paper) resulted in the hydrolysis of the dimethyl acetal protection group rather than the ester groups. Unfortunately, at this point of the synthesis all of compound **3.38** had been used up.

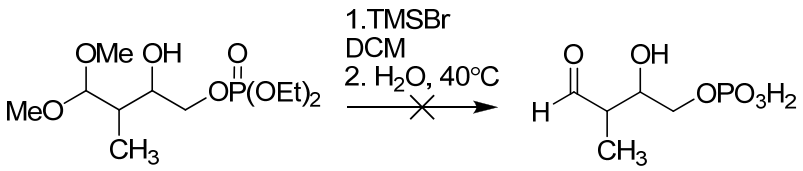

3.38 2-methylE4P

Figure 3.37: Attempts to synthesise 2-methylE4P.

Chouinard *et al.*[135] also observed that the cleavage of alkyl phosphate esters was extremely difficult using TMSBr. The authors reported deprotection of compound **3.41** using TMSBr resulted in dephosphorylation and the cleavage of the allylic C-O bond of compound **3.41** (Figure 3.38). Although some product **3.43** was formed, the reaction was not reproducible. The authors eventually directed their efforts to phosphate esters that were more readily

cleaved, and used compound **3.42** for the synthesis of compound **3.43**. It was also noted that Chouinard *et al.* added pyridine in their reaction to reduce the acidity of the reaction mixture. Although no basic reagents were added during the attempted deprotection of compound **3.38** with TMSBr, this could be trialled in the future to prevent cleavage of the acetal protection group. Investigations into using the benzyl phosphate for phosphorylating compound **3.31** could also be trialled, as Chouinard *et al.* found that cleavage of phosphate **3.42** was easier than when alkyl phosphates were used. Additionally, research into the use of a more robust aldehyde protecting group (e.g. cyclic acetals)[103] for compound **3.36** may aid in the survivability of the compound during the TMSBr deprotection step.

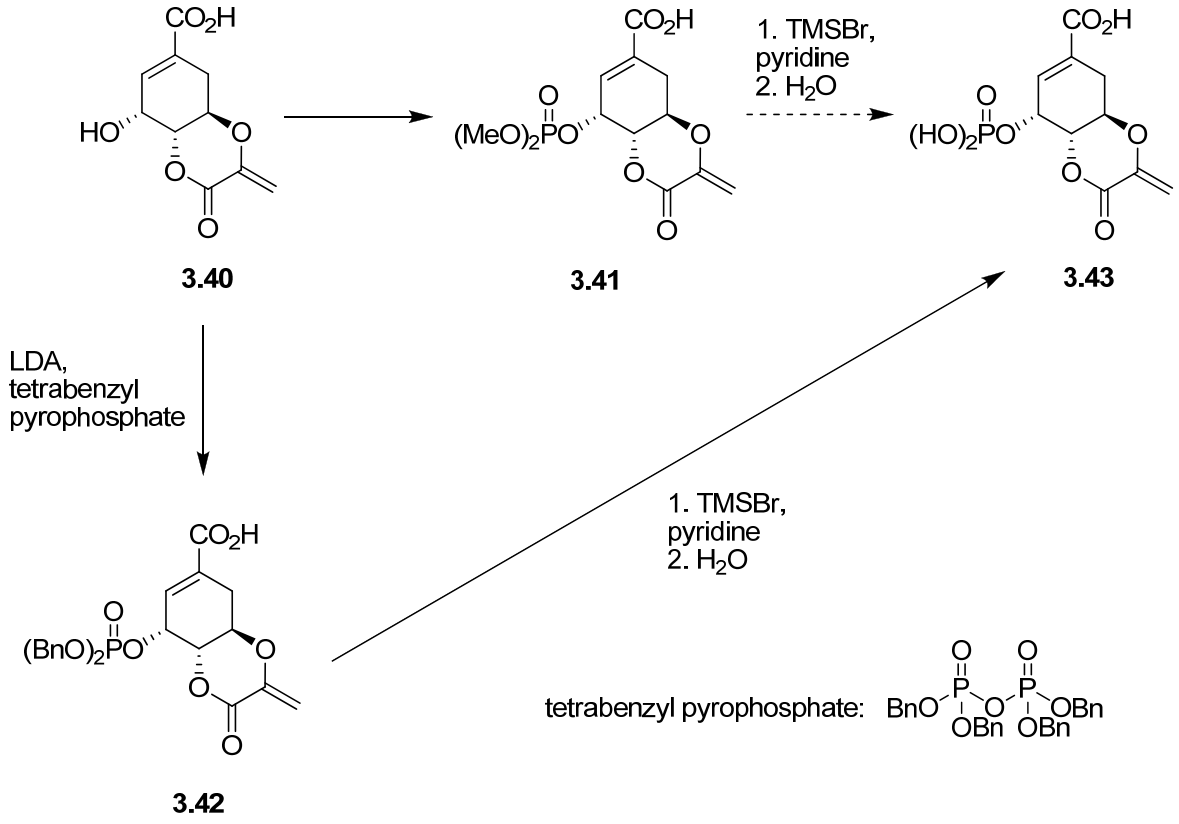

Figure 3.38: Deprotection of compound 3.41 and 3.42 to give compound 3.43 by Chouinard *et al.*[135]

3.4 Summary

3-MethylE4P was successfully synthesised in nine steps via DL-malic acid as seen in Scheme 3.1, and summarised in Figure 3.39 below. The yields for each step were generally moderate to high yielding, with only the monophosphorylation of diol **3.3** step being low yielding (22%).

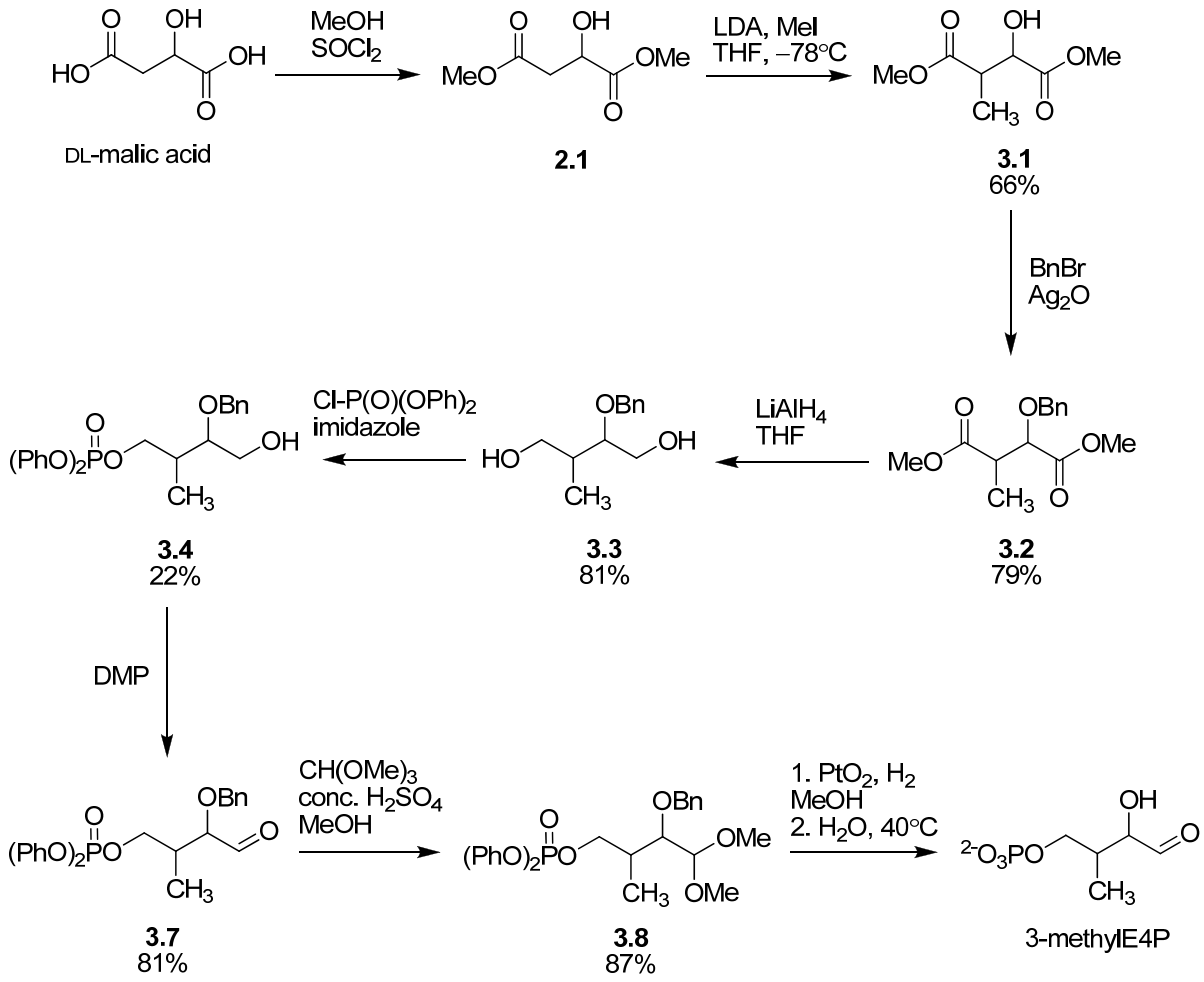

Figure 3.39: Overall synthetic scheme used to synthesis 3-methylE4P from DL-malic acid.

Standard enzyme assays showed that 3-methylE4P was not a substrate for *E. coli* DAH7P synthase (phe), although substrate specificity tests with D/L-T4P and 2/3-deoxyE4P indicated that the C2 and C3 hydroxyls of E4P and the active site residues they interact with have a limited role to play in substrate selection by the enzyme. This suggests that the active site of *E. coli* DAH7P synthase (phe) cannot accommodate the bulk of a methyl group in the C3 position of E4P.

The summary for the attempted synthesis of 2-methylE4P starting from DL-malic acid is shown below (Figure 3.40). Although the synthesis of this compound was not completed due to the difficulties in the deprotection of compound **3.38** the characterisation and methodology for the synthesis of compounds **3.3**, **3.31**, **3.32** and **3.34**–**3.38** have been well documented in this thesis. Future synthesis of 2-methylE4P could re-use this synthetic route but use a different phosphorylating method or a more robust aldehyde protecting group to facilitate the deprotection method.

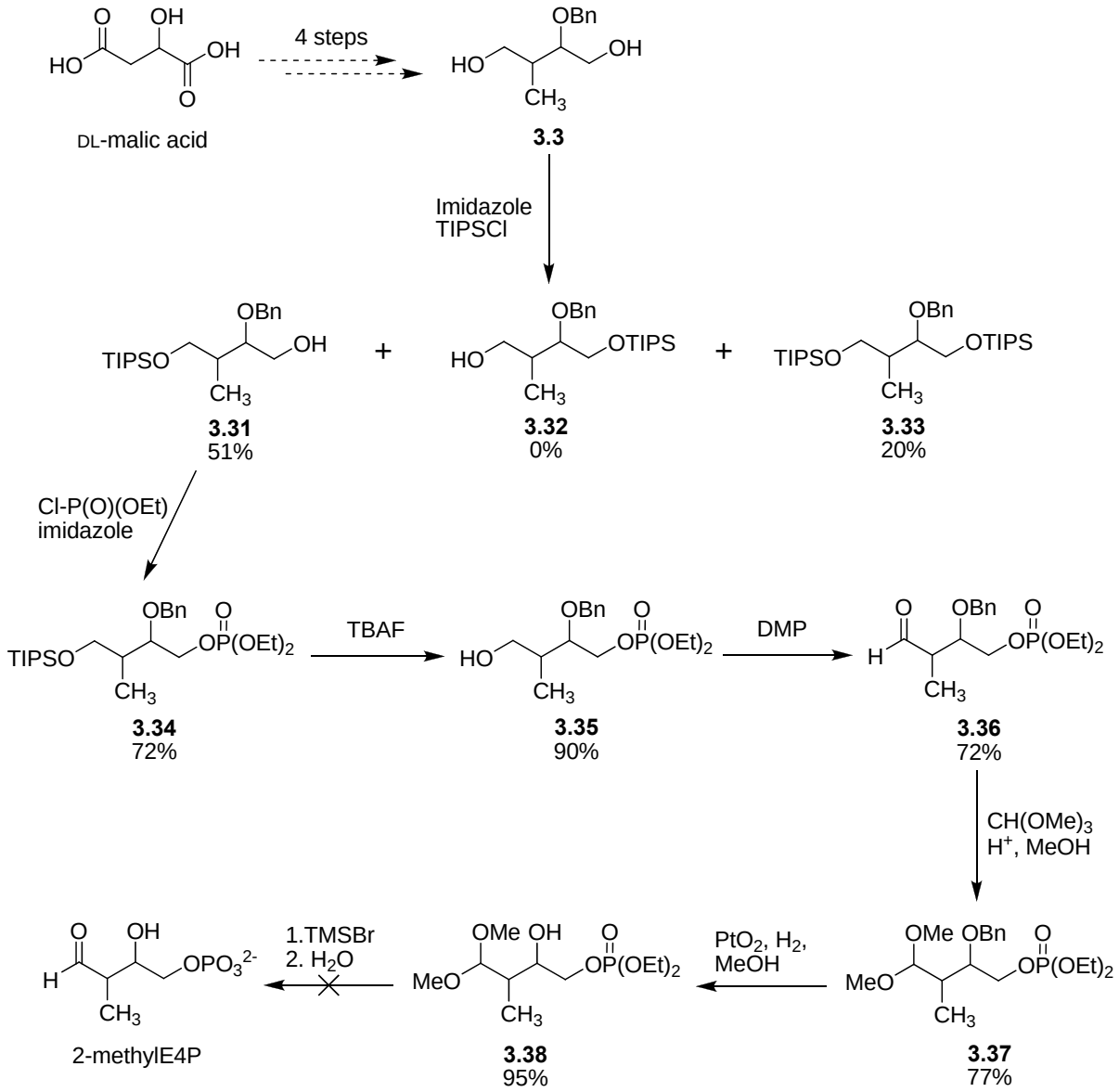

Figure 3.40: Overall synthetic scheme used for the attempted synthesis of 2-methylE4P.

A discussion on why 3-methylE4P was not a substrate for DAH7P synthase, and the predicted outcome for 2-methylE4P can be found in Chapter 5.

Chapter 4: Phosphonate analogues of E4P

4.1 Introduction

Phosphonic acids often exhibit important biological properties because of their similarity to phosphates, and the preparation and investigation of phosphonic acid analogues of natural substrates has been of particular interest in the literature.[136-139] For example, the phosphonate analogue of adenosine triphosphate (ATP), adenosine 5'-[β,γ-methylene] triphosphate (Figure 4.1), has been found to be an inhibitor of polynucleotide phosphorylase (involved in mRNA processing) and is capable of replacing ATP as a substrate in RNA polymerase.[136,140] Phosphonate analogues of natural substrates also have the advantage of being more stable to hydrolysis as the C-P bond in phosphonates, unlike the O-P bonds of phosphates or phosphate esters, is resistant towards chemical and enzymatic hydrolysis. This resistance to hydrolysis by enzymes is advantageous in drug design as most biological fluids contain phosphatases that cleave phosphate containing drugs before they are able to reach their intracellular targets.[138,139]

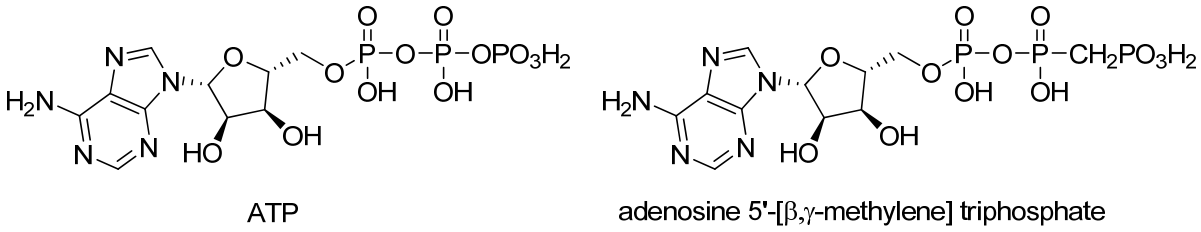

Figure 4.1: The isosteric phosphonate analogue of ATP.

Analogues of E4P in which the phosphate group C-O-P is replaced by a C-P group (non-isosteric phosphonate analogue) or by a C-CH_2-P group (isosteric or homophosphonate analogue) have been synthesised in the past by Le Marechal *et al.*[141], and substrate specificity studies were conducted on transaldolase and transketolase (both involved in the pentose phosphate pathway for the biosynthesis of nucleic acids). Although no kinetic data was given by Le Marechal *et al.*, it was reported that the homophosphonate analogue was a substrate for both these enzymes and the phosphonate analogue was a substrate for transaldolase.

The substitution of a phosphonate moiety for the phosphate moiety on E4P could have interesting effects on the way the substrate interacts with enzymes. For example, the phosphonate analogue of E4P would be shorter in length compared to E4P due to the deletion of the oxygen, whereas the homophosphonate analogue would be more similar in length. This could alter the way that the substrate binds to the active sites of enzymes.

Phosphonate analogues of E4P have been of particular interest in our research group and it would be interesting to see how sensitive DAH7P synthases are to substitution of the phosphate moiety of E4P for a phosphonate group. The phosphonate group would be particularly important for the development of inhibitors because of the stability of the phosphonate group to resist cleavage by phosphatases in biological fluids. This chapter describes the attempts at synthesising the phosphonate analogue of E4P, D-erythrose 4-phosphonate, and the synthesis of the analogue 2,3-dideoxy erythrose 4-phosphonate **4.38** (Figure 4.2).

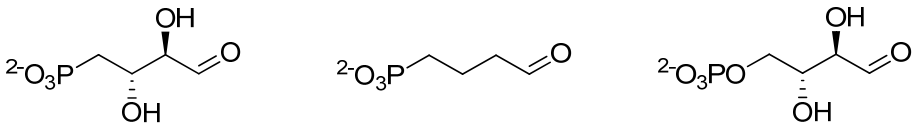

Figure 4.2: D-Erythrose 4-phosphonate and 2,3-dideoxy erythrose 4-phosphonate 4.38.

4.2 Attempts to synthesise D-erythrose 4-phosphonate

D-Erythrose 4-phosphonate was first synthesised by Le Marechal *et al.*[141] in 1980 by the oxidative cleavage of D-glucose 6-phosphonate **4.14** using lead tetraacetate. This procedure is similar to the lead tetraacetate oxidative cleavage of D-glucose 6-phosphate for the preparation of E4P (Figure 4.3).[89,90] Although the authors reported the synthesis of D-erythrose 4-phosphonate, there was no experimental or spectroscopic data given in the paper for D-erythrose 4-phosphonate. Interestingly, the authors for the preparation of E4P from D-glucose 6-phosphate using lead tetraacetate also did not give any form of data to confirm the synthesis of E4P.

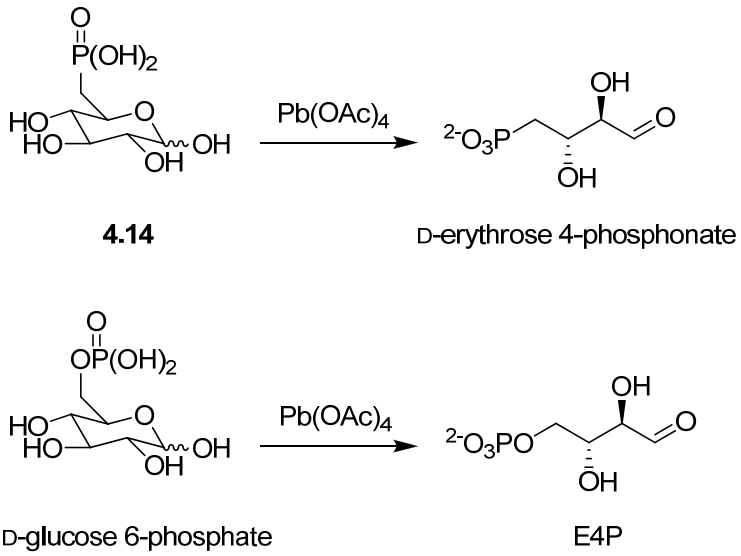

Figure 4.3: Lead tetraacetate oxidative cleavage of D-glucose 6-phosphonate 4.14 and D-glucose 6-phosphate.

There are several disadvantages of synthesising D-erythrose 4-phosphonate using the lead tetraacetate procedure described by Le Marechal *et al*. and these disadvantages are analogous to the ones mentioned in Chapter 1 for the synthesis of E4P from D-glucose 6-phosphate. For example, Le Marechal *et al.* reported over and under oxidation of **4.14** producing the three carbon and five carbon phosphonate side-products glyceraldehyde 3-phosphonate and arabinose 5-phosphonate, respectively.

Although no experimental data was given for the synthesis of compound **4.14** by Le Marechal *et al.*, a reference for the synthesis of this compound was given to a report by Griffin *et al.*[142] The synthesis of compound **4.14** by Griffin *et al.* is shown in Figure 4.4 and

starts with the compound **4.6**. Unfortunately, there was hardly any spectroscopic data to confirm the synthesis of these compounds (Figure 4.4), only optical rotation and melting point data was presented.[142] At this point a retrosynthetic analysis of compound **4.14** was carried out in order to develop a scheme for the synthesis of this compound.

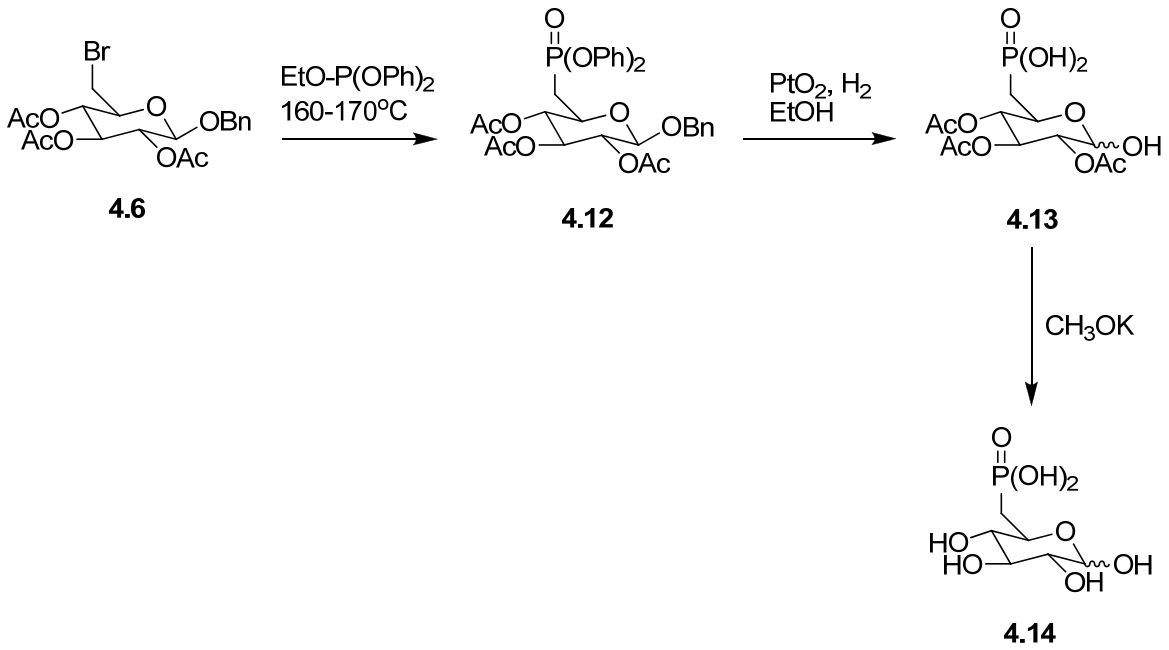

Figure 4.4: Synthetic scheme used by Griffin *et al.* to synthesise D-glucose 6-phosphonate 4.14.

Shown in Figure 4.5 is the retrosynthetic analysis for the synthesis of compound **4.14**. The retrosynthetic analysis shows that the C1–C4 secondary hydroxyls of D-glucose have to be protected first, whilst leaving the C6 hydroxyl of D-glucose available for chemical manipulation. This C6 hydroxyl is versatile and can be interconverted into many other functional groups, and in this case a halide. The halide can then be phosphonylated to give a phosphonate followed by deprotection steps of the protecting groups to give compound **4.14**.

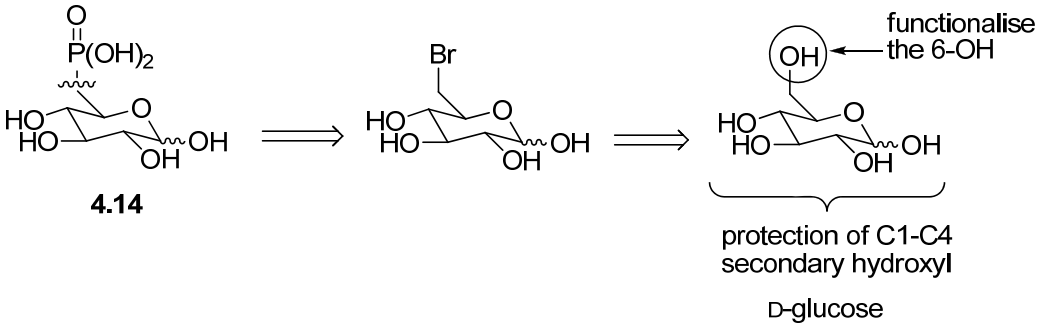

Figure 4.5: Retrosynthetic analysis of D-glucose 6-phosphonate 4.14.

The conversion of the C6 halide group of glucose into a phosphonic acid moiety could be achieved by using the Arbuzov[143,144] reaction (Figure 4.6). The first step in the Arbuzov reaction involves nucleophilic attack of the phosphorus on the alkyl halide, followed by dealkylation of resulting trialkoxyphosphonium salt to give a phosphonate. The Arbuzov reaction was also used for the synthesis of phosphonate **4.12** by Griffin *et al.*[142] (Figure 4.4).

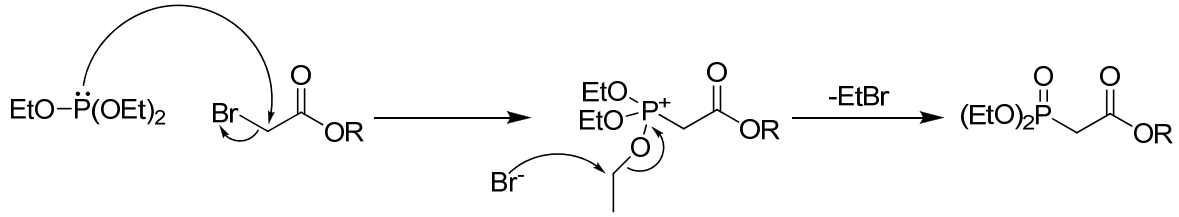

Figure 4.6: The mechanism of the Arbuzov reaction.[144]

4.2.1 Early approaches to the synthesis of D-glucose 6-phosphonate 4.14

To synthesise D-erythrose 4-phosphonate an overall synthetic scheme was devised for the synthesis of the precursor **4.14** (Scheme 4.1). Scheme 4.1 was developed from the retrosynthetic analysis in Figure 4.5, with the incorporation of the synthetic scheme used by Griffin *et al.*[142] for the synthesis of compounds **4.6**, **4.12**–**4.14**. Additionally, this synthetic scheme starts with the commercially available and cheap starting material D-glucose. By chemically manipulating the C6 hydroxyl group of D-glucose it was hoped that compound **4.14** could be synthesised in nine steps.

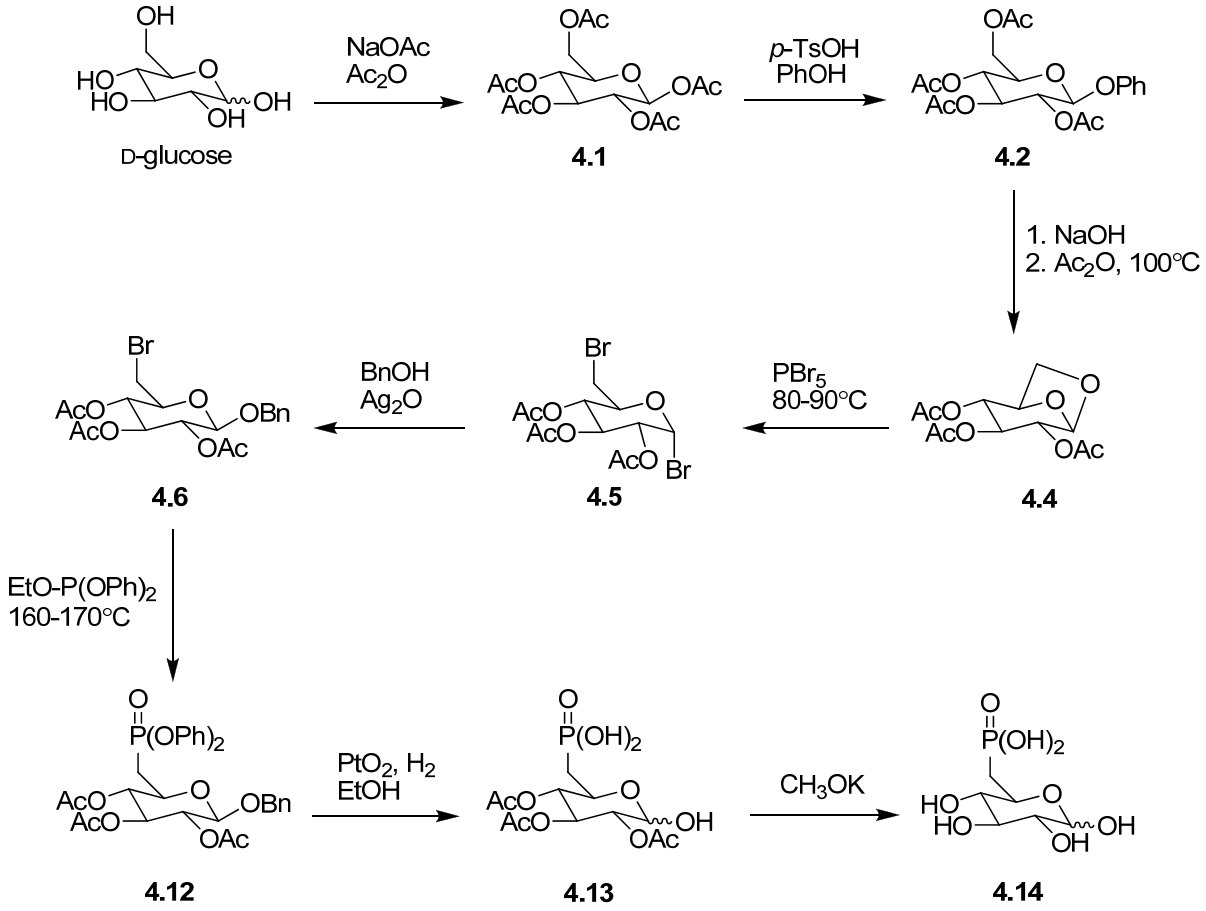

Scheme 4.1: First attempts to synthesise D-glucose 6-phosphonate. Method 1. No modifications were made for the synthesis of compounds 4.6, 4.12–4.14 as described by Griffin *et al.*[142]

Shown in Scheme 4.1 is the synthetic scheme that was devised to attempt to synthesise compound **4.14**. The first two steps involve protecting the hydroxyl groups on D-glucose using acetyl groups followed by a base-assisted intramolecular displacement of the leaving group at the anomeric position to form the sugar **4.4**. Sugar **4.4** is then treated with PBr_5 to give the dibromo-derivative **4.5**, which then undergoes a Koenigs-Knorr[145-147] reaction to give bromide **4.6**. Ethyl diphenyl phosphite is then reacted with bromide **4.6** to give the phosphonate **4.12** followed by two deprotection steps to give D-glucose 6-phosphonate **4.14**.

The first step of Scheme 4.1 was carried out following the literature procedure by Tsuji *et al.*[148] The reaction was performed by refluxing D-glucose, Ac_2O and NaOAc in benzene to give crude acetate **4.1**. Purification of crude acetate **4.1** by recrystallisation from EtOH gave acetate **4.1** in 16% yield (lit.[148] 73%). The product was characterised by the ^{1}H NMR spectrum showing five acetyl group methyl resonances between 2.10–2.00 ppm. The experimental data for acetate **4.1** also matched those reported by Tsuji *et al.*[148] Attempts were

made to improve the yield of acetate **4.1** and the reaction was repeated, but the solvent was switched to toluene. By doing this, the yield of acetate **4.1** was increased to 44% (Figure 4.7). Although the yields of this reaction were low, D-glucose is a readily available and cheap starting material, and the low yield was not considered to be a major drawback in the synthesis of acetate **4.1**.

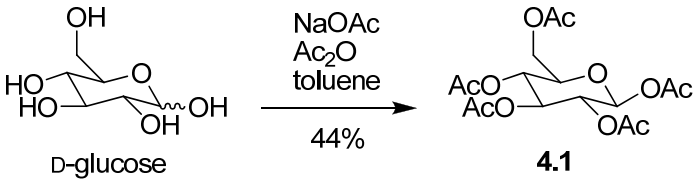

Figure 4.7: Synthesis of acetate 4.1.

Following the procedure by Montgomery *et al.*[149], acetate **4.1** was treated with *p*-TsOH and phenol. The homogenous melt that formed was heated *in vacuo* at 100°C for 1 hour. The mixture was worked up, and purified by recrystallisation from EtOH to give the β-phenylglycoside **4.2** in 32% yield (lit.[149] 64%) (Figure 4.8). The spectroscopic data for the β-phenylglycoside **4.2** were identical to those reported by Montgomery *et al.*, with signals corresponding to the phenyl proton resonances between 7.34–7.25 ppm in the ^{1}H NMR spectrum.

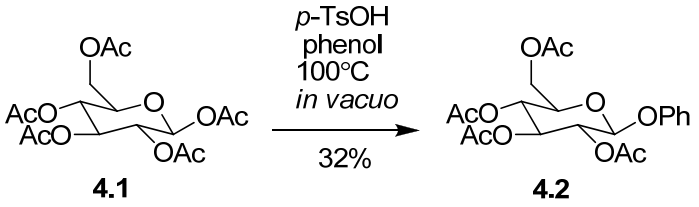

Figure 4.8: Synthesis of β-phenylglycoside 4.2.

In an attempt to increase the yield of β-phenylglycoside **4.2** the reaction was repeated but the heating time was varied (2 hours). Unfortunately, during this time a black tar mixture had formed that was hard to stir and after purification only a 28% yield of β-phenylglycoside **4.2** was obtained. This indicated that the reaction time and maybe even the temperature had to be optimised in the future if a better yield was to be obtained. With the combined yields of both reactions it was decided to carry on investigating the overall synthetic scheme despite the low yields for the synthesis of β-phenylglycoside **4.2**.

The β-phenylglycoside **4.2** was subjected to a base-assisted intramolecular displacement reaction of the anomeric phenyl group following the procedure by Lu *et al.*[150] (Figure 4.9) to give the sugar **4.4** as a white solid. The ^{1}H NMR spectrum obtained for sugar **4.4** matched that reported in literature.[151] Numerous attempts were made to synthesise the sugar **4.4** with varying results. In some attempts the reaction would proceed smoothly producing sugar **4.4** in 11–39% yield. In subsequent reactions, under exactly the same reaction conditions, the reaction would produce a black tar-like mixture with multiple unidentifiable products, as indicated by TLC analysis. No product or starting material could be recovered from this black mixture. The varying result made the synthesis of sugar **4.4** extremely difficult and the maximum yield obtain from these trials was 39% (lit.[150] 73%).

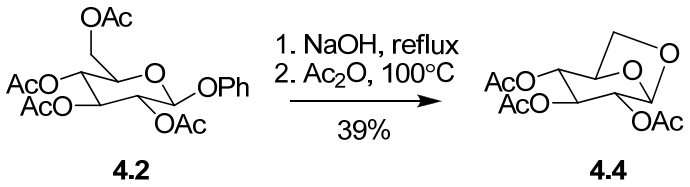

4.2 **4.4**

Figure 4.9: Synthesis of sugar 4.4.

The synthesis of the dibromo-derivative **4.5** was accomplished by heating sugar **4.4** with PBr_5 at 80–90°C under solvent-free and anhydrous conditions as described by Irvine *et al.*[152] Care has to be taken when handling phosphorous pentabromide as it is highly corrosive and reacts violently with water. The synthesis was carried out and the dibromo-derivative **4.5** was synthesised in 34% yield (Figure 4.10). Mass spectrometry detected the sodiated dibromo-derivative **4.5** as a compound with a monoisotopic mass of 452.9158 (calc. $C_{12}H_{16}Br_2NaO_7$ $[M+Na]^+$: 452.9155).

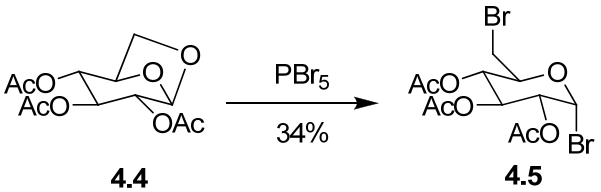

4.4 **4.5**

Figure 4.10: Synthesis of the dibromo-derivative 4.6.

Although the yield was low, Irvine *et al.* only reported a 50% maximum yield for the dibromo-derivative **4.5**. No attempts were made at this stage to increase this yield.

Benzylation of the anomeric position of dibromo-derivative **4.5** gave bromide **4.6** in 18% yield (Figure 4.11). ^{1}H NMR spectroscopy detected the presence of the aromatic proton resonance between 7.39–7.29 ppm in the spectrum. Additionally, mass spectrometry detected the sodiated bromide **4.6** as a compound with a monoisotopic mass of 481.0478 (calc. $C_{19}H_{23}BrNaO_6$ $[M+Na]^+$: 481.0469).

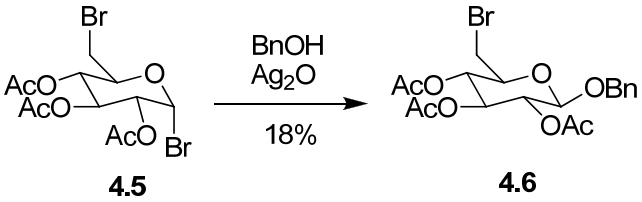

4.5 **4.6**

Figure 4.11: Synthesis of bromide 4.6.

The reaction shown in Figure 4.11 is a Koenigs-Knorr reaction which favours nucleophilic attack of the alkoxide ion at the anomeric position. The Koenigs-Knorr reaction (Scheme 4.2) can be understood by assuming that the dibromo-derivative **4.5** undergoes a spontaneous loss of Br^- forming an oxocarbenium ion (that is stabilised by the lone pair of electrons on oxygen) to give the intermediate **4.7**. Intermediate **4.7** then undergoes an internal reaction with the ester group at C2 to form an oxonium ion intermediate **4.8**. Back-side attack by the alcohol at C1 gives bromide **4.9** and regenerates the acetate at C2.

Although the Koenigs-Knorr reaction is favoured, two possible reasons for the low yielding reaction are shown in Scheme 4.2. Side-product **4.10** is formed by the alcohol attacking at the C6 position and not the anomeric position. Side-product **4.11** would result from the hydrolysis of the dibromo-derivative **4.5**. Although the reaction was carried out under anhydrous conditions, even small amounts of water will lead to side-product **4.11**.[153] TLC analysis of the reaction mixture after work-up, showed multiple compounds indicating other products aside from bromide **4.6** had been formed. These other products could possibly be the side-products **4.10** and **4.11** but were not isolated or investigated.

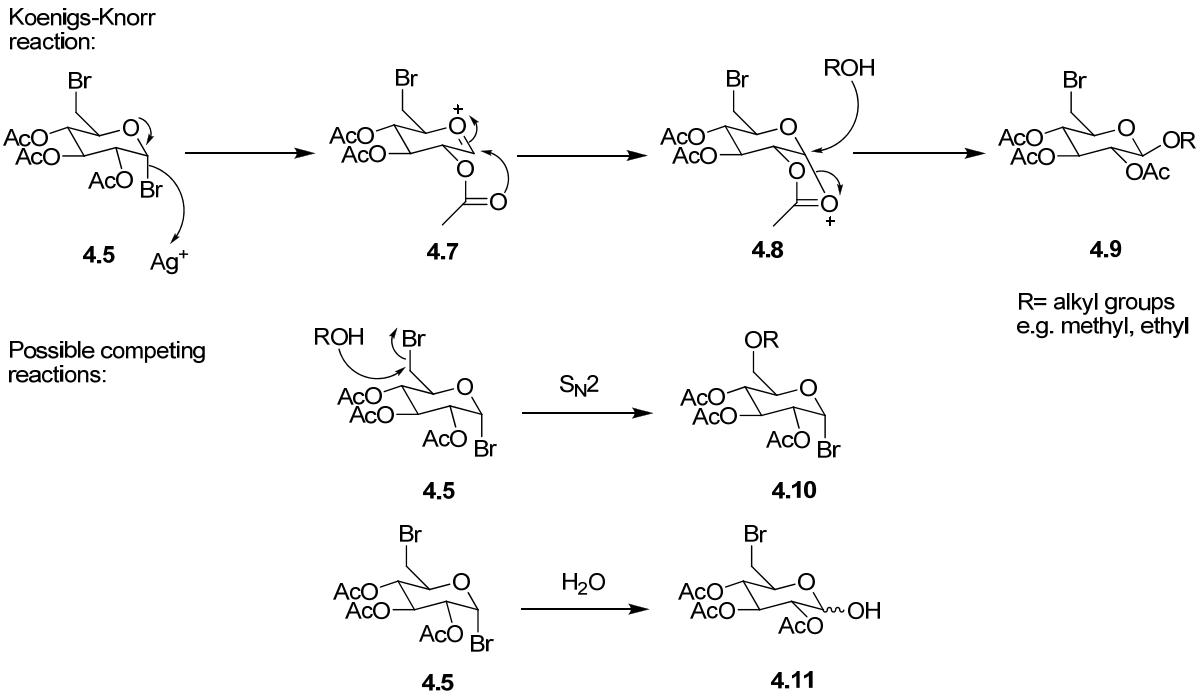

Scheme 4.2: Proposed side-products for the benzylation of dibromo-derivative 4.5.

The phosphonylating reagent, ethyl diphenylphosphate (EDPP), required for the phosphonylation of bromide **4.6** was synthesised from the precursor ethyl dichlorophosphite (EDCP).[154,155] EDCP was synthesised by reacting ethanol with phosphorous trichloride at −20°C to give EDCP in 14–19% yield after purification by distillation (lit.[155] 42%). EDCP was then reacted with phenol and triethylamine to afford EDPP in 73% yield (lit.[156] 85%). The NMR spectral data for EDCP and EDPP were in accordance with the literature reports.[154-156]

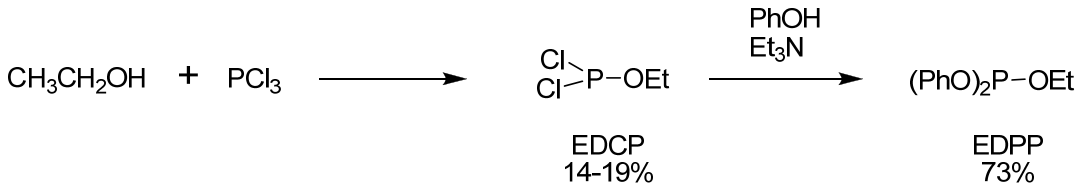

Figure 4.12: Synthesis of EDCP and EDPP.

Due to the limited amounts of bromide **4.6**, a small scale trial reaction of the phosphonylating reagent EDPP with ethyl bromoacetate was setup to ascertain the viability of the reagent and to test the Arbuzov method for synthesising phosphonates. The small scale test was successful and produced ethyl diphenylphosphonoacetate (Figure 4.13) with a ^{1}H NMR spectrum in accordance with that reported in the literature.[157]

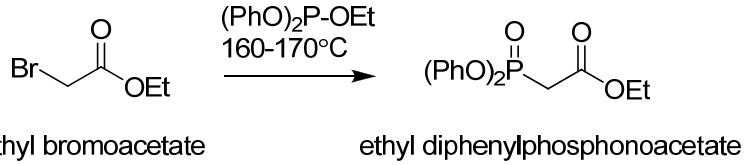

Figure 4.13: Synthesis of ethyl diphenylphosphonoacetate using the phosphonylating reagent EDPP.

When EDPP was reacted with bromide **4.6**, no phosphonate **4.12** could be detected by TLC and only starting material and reagent could be observed (Figure 4.14). This was contrary to what Griffin *et al.*[142] had reported when they had reacted EDPP with bromide **4.6**. Unfortunately, at this point of the synthesis all of the bromide **4.6** (Figure 4.14) had been used up and due to the difficulties in synthesising sugar **4.4**, coupled with the low yields of compounds **4.1**, **4.2**, **4.4**–**4.6** in Scheme 4.1, this synthetic scheme was not investigated further and abandoned. Other methods for the preparation of D-glucose 6-phosphonate **4.14** were investigated.

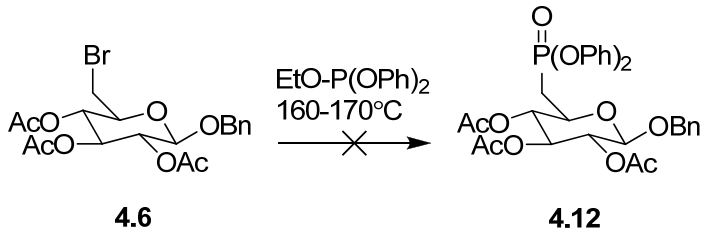

Figure 4.14: Attempt at synthesising phosphonate 4.12.

4.2.2 Synthesis of precursor phenylmethyl 6-bromo-6-deoxy-2,3,4-tris-*O*-(phenylmethyl)-β-D-glucopyranoside 4.18

Due to the failed attempts to phosphonylated bromide **4.6** (Scheme 4.1 and Figure 4.14) alternative methods for the synthesis of precursor **4.14** were investigated. The retrosynthetic analysis in the previous section (Figure 4.5) contains three key steps for the synthesis of the precursor **4.14**: protection of the C1–C4 secondary hydroxyl groups of D-glucose, chemically manipulate the C6 hydroxyl group to give a halide, and phosphonylation of this halide (Figure 4.15). With these three key steps in mind, and after an extensive review of the literature, the synthetic scheme used by Lu *et al.*[158] was employed to synthesise the alcohol **4.17** (Figure 4.16). Alcohol **4.17** meets the criteria mentioned before. The C1–C4 secondary hydroxyl groups of D-glucose are protected as the benzyl ethers leaving the C6 hydroxyl

group free to be chemically manipulated into the halide. Phosphonylation of this halide would give the phosphonate moiety.

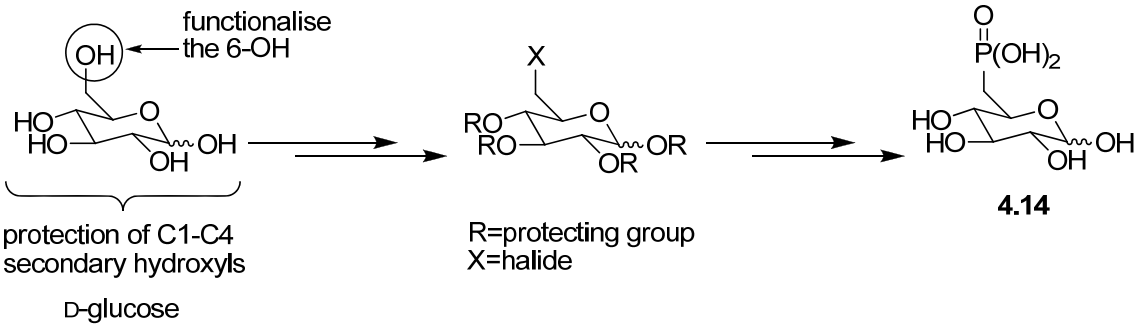

Figure 4.15: Key steps for the synthesis of precursor 4.14.

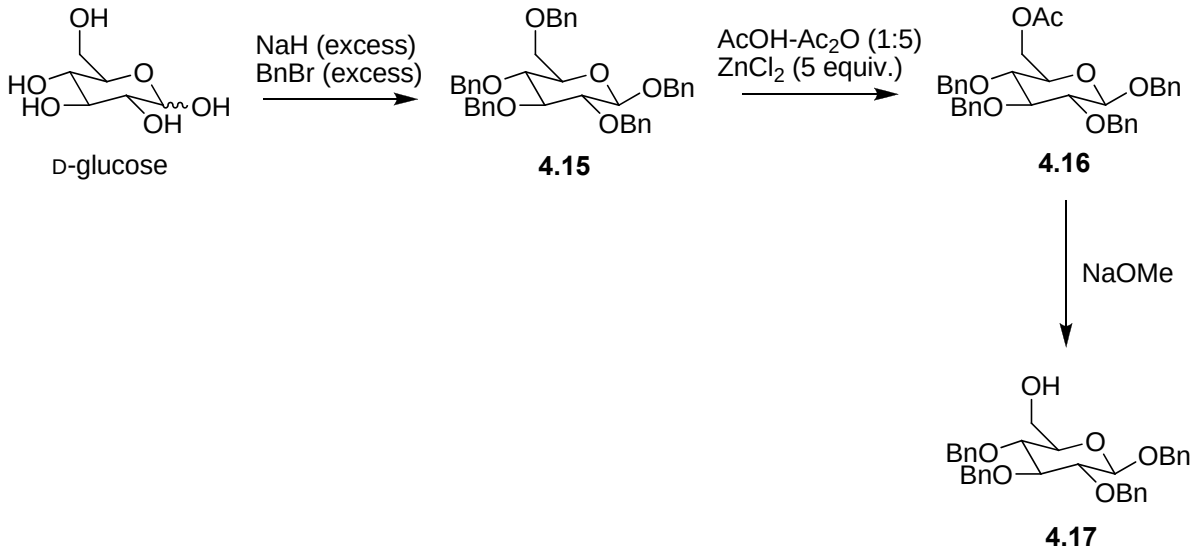

Figure 4.16: Synthetic scheme used by Lu *et al.* to synthesise the alcohol 4.17.

The approach used by Lu *et al.*[158] to synthesise alcohol **4.17** involved the selective debenzylation-acetolysis of the β-perbenzylated glucose **4.15** to give acetate **4.16**. Acetate **4.16** is then deprotected under Zemplen conditions[159,160] to give alcohol **4.17** (Figure 4.16).

D-Glucose was benzylated using NaH and BnBr. After 24 hours the reaction was quenched carefully with MeOH. Purification by flash chromatography followed by recrystallisation from EtOH gave β-perbenzylated glucose **4.15** in 32% yield. The ^{1}H NMR spectrum detected a doublet at 4.54 ppm, corresponding to the anomeric proton resonance with a large coupling constant (^{3}J = 7.7 Hz). This large coupling constant corresponded to the β-isomer of compound **4.15**, and was consistent with the data reported by Lu *et al.*[158]

Although the yield of 32% was consistent with the initial findings of Lu *et al.*[158] (25–30% yield), it was also reported that by adding the reagents NaH and BnBr portionwise over several hours gave β-perbenzylated glucose **4.15** in 60–66%. Unfortunately, when the exact method described by Lu *et al.*[158] was carried out and repeated several times in our laboratory, the yields for the synthesis of β-perbenzylated glucose **4.15** were only 13–32% (Figure 4.17).

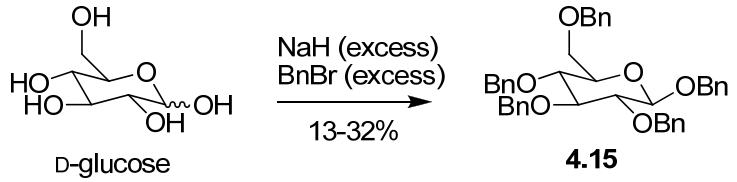

Figure 4.17: Synthesis of β-perbenzylated glucose 4.15.

The selective C6 debenzylation and acetolysis of β-perbenzylated glucose **4.15** was carried out using $ZnCl_2$ in a solution of AcOH-Ac_2O (1:5).[158,161,162] Purification by flash chromatography gave acetate **4.16** in 64% yield (lit.[158] 78%) (Figure 4.18). ^{1}H NMR spectroscopy detected the presence of the acetyl group methyl resonance at 2.07 ppm in the spectrum.

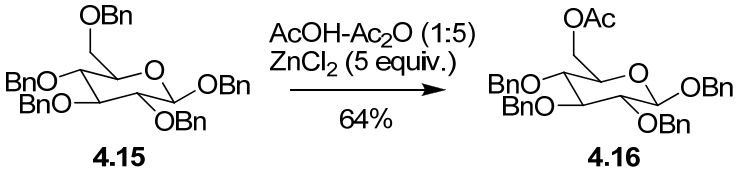

Figure 4.18: Selective debenzylation and acetolysis of 4.15.

Deprotection of acetate **4.16** under Zemplen conditions gave the alcohol **4.17** in 96% yield (lit.[158] 97%) (Figure 4.19). ^{1}H NMR spectroscopy showed that deprotection had occurred, with the disappearance of the acetyl group methyl resonance at 2.07 ppm in the spectrum. Alternatively, alcohol **4.17** was also prepared by subjecting crude **4.16** (after precipitation and drying) to NaOMe. Using this approach pure **4.17** was obtained in 50–70% yield following flash chromatography.

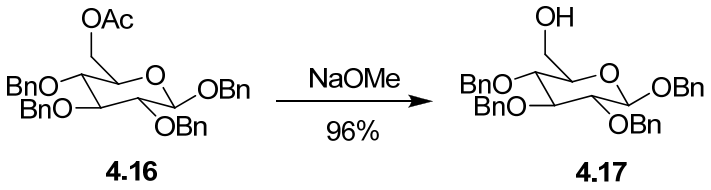

4.16 **4.17**

Figure 4.19: Deprotection of acetate 4.16 under Zemplen conditions.

With the successful synthesis of alcohol **4.17** the C6 hydroxyl group could now be converted into a halide. Several attempts at brominating alcohol **4.17** were employed and the successes and failures of these methods are described below. A summary of these results can be found in Table 4.1.

The first attempt to brominate alcohol **4.17** involved using the method by Ruiz *et al.*[163] Alcohol **4.17** was stirred with PBr_3 for 16 hours at room temperature and monitored periodically using TLC analysis. Unfortunately, only starting material was detectable by TLC (Figure 4.20).

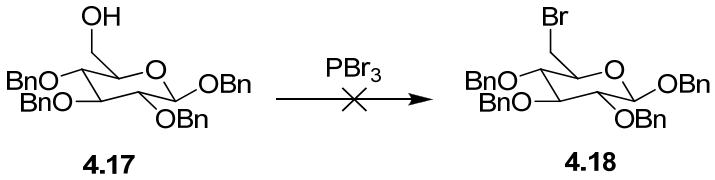

4.17 **4.18**

Figure 4.20: Attempts to brominated alcohol 4.17 using PBr_3.

The second attempt used a method employed by Vidal *et al.*[164] where the primary hydroxyl group of the alcohol **4.17** is first tosylated (to form a better leaving group) followed by bromination using LiBr. The reaction was carried out on a small scale, and the reaction mixture was monitored by TLC. Initial TLC analysis after an hour indicated a new compound, presumably the tosylated compound, had formed along with residual starting material. At this point the reaction was worked up and LiBr was added to this crude mixture. The reaction was stirred for a further 24 hours at room temperature and monitored by TLC. Unfortunately, there was no indication of any halide **4.18** being formed by TLC (Figure 4.21) and this method was not investigated further.

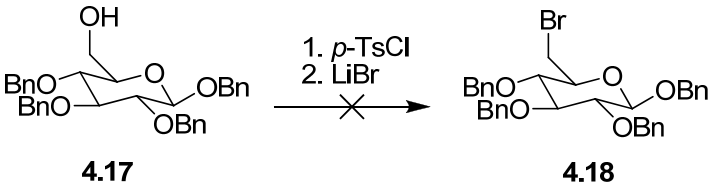

4.17 **4.18**

Figure 4.21: Attempts to brominated alcohol 4.17 using LiBr.

The third attempt proved to be successful in brominating alcohol **4.17** and involved bromine.[165] Although this reaction worked the yield of halide **4.18** was only 9% after purification by flash chromatography.

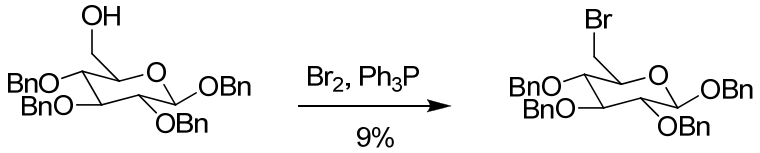

4.17 **4.18**

Figure 4.22: Bromination of alcohol 4.17 using bromine.

The method used by Berkowitz *et al.*[166] was also used for the synthesis of halide **4.18** and involved the reagents NBS and Ph_3P. The method was conducted and halide **4.18** was obtained in 27% yield which was considerably better than the 9% yield obtained in the reaction using bromine (Figure 4.22). Mass spectrometry detected the sodiated halide **4.18** as a compound with a monoisotopic mass of 625.1573 (calc. $C_{34}H_{35}NaO_5Br$ $[M+Na]^+$: 625.1566). By increasing the amount of NBS and Ph_3P used in the reaction to three equivalents each, halide **4.18** was obtained in 87–92% yield (Figure 4.23).

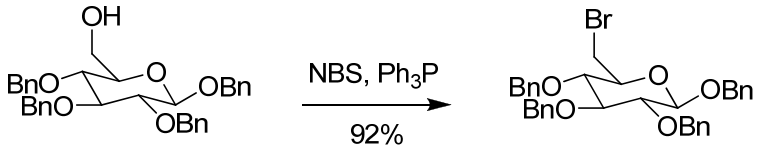

4.17 **4.18**

Figure 4.23: Bromination of alcohol 4.17 using NBS.

Care had to be taken when performing the reaction shown in Figure 4.23 on a large scale as the reaction becomes highly exothermic on the addition of NBS to a solution of Ph_3P in CH_2Cl_2. The addition of NBS to the solution was done slowly, portionwise and at 0°C in order to maintain control of the reaction.

Reaction	Bromination method	Results
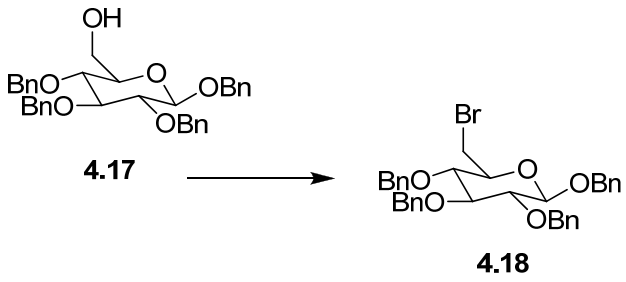 **4.17** **4.18**	PBr_3, DCM	NR
	p-TsCl, LiBr	NR
	Br_2, Ph_3P	9% yield
	NBS, Ph_3P	92% yield

Table 4.1: Summary of the bromination methods used to synthesise halide 4.18. NR = no reaction.

With the successful synthesis of halide **4.18**, halide **4.18** now needed to phosphonylated to form the phosphonate ester. Two methods were employed, the Cs_2CO_3 method by Cohen *et al.*[167] and the Arbuzov method. Due to the limited amounts of the starting material, small scale tests of each method were trialled on the precursor **4.18** to ascertain the viability of each method and the results of these small scale trial reactions are discussed in the next two sections.

4.2.2.1 The Cohen method

Shown in Figure 4.24 is the general method used by Cohen *et al.*[167] to synthesise phosphonate analogues. A dialkyl phosphite ester **4.19** is deprotonated using cesium carbonate to generate the phosphonate anion **4.20** *in situ*. Subsequent alkylation of anion **4.20** with an alkyl halide produces the corresponding phosphonate **4.21**.

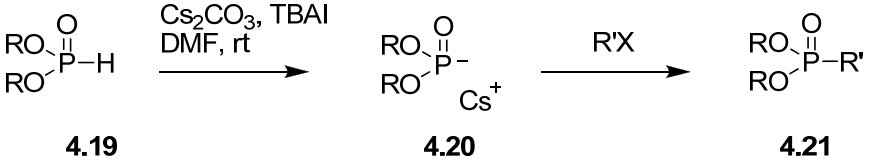

Figure 4.24: General reaction scheme by Cohen *et al.*

Two different phosphite ester reagents were chosen to phosphonylate halide **4.18**: diethyl phosphite and dibenzyl phosphite (Figure 4.25).

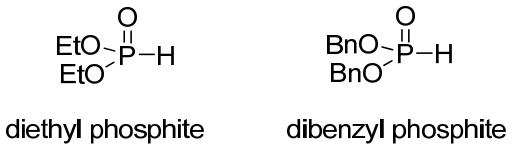

diethyl phosphite dibenzyl phosphite

Figure 4.25: Phosphonylation reagents: diethyl phosphite and dibenzyl phosphite.

Diethyl phosphite was reacted with halide **4.18** under similar conditions described by Cohen *et al.*[167] and phosphonate **4.22** was obtained in 41% after stirring for three days at room temperature and purification by flash chromatography (Figure 4.26). ^{31}P-^{13}C coupling on the resonance of C6 was observed in the ^{13}C NMR spectrum of phosphonate **4.22**, with a large $^{1}J_{PC}$ coupling of 143 Hz at 28.4 ppm.

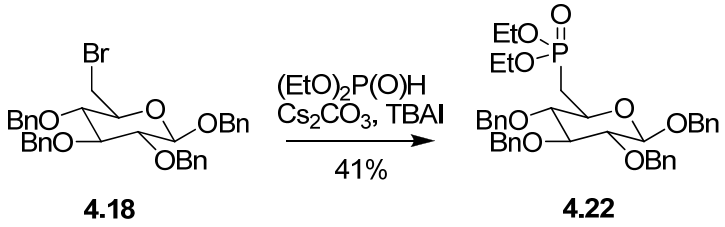

4.18 **4.22**

Figure 4.26: Synthesis of phosphonate 4.22.

Phosphonate **4.23** was synthesised using dibenzyl phosphite under similar conditions described by Cohen *et al.* (Figure 4.27). The reaction was periodically monitored by TLC, and after five days, it was decided to stop the reaction even though not all the starting material had been consumed. Following purification by flash chromatography the yield for phosphonate **4.23** was 36%. A large amount of starting material **4.18** was also recovered (56% recovered). ^{31}P-^{13}C coupling on the resonance of C6 was observed in the ^{13}C NMR spectrum of phosphonate **4.23**, with a large $^{1}J_{PC}$ coupling of 143 Hz at 29.1 ppm.

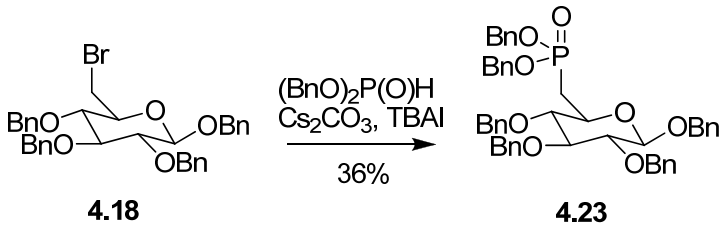

4.18 **4.23**

Figure 4.27: Synthesis of phosphonate 4.23.

The diethyl phosphite route had the advantage of being slightly better yielding, 41%, compared to the dibenzyl phosphite route of 36% (Figure 4.28). This better yield may be due

to steric factors with the ethyl ester groups being smaller and less cumbersome than the bulky benzyl groups, whereas diethyl phosphite would have easier access to the C6-Br on halide **4.18**. Reaction conditions, such as heating the reaction, could be investigated in the future to optimise the yields for the synthesis of phosphonate **4.22** or **4.23**.

The disadvantage of the diethyl phosphite route is that there would be three overall steps to synthesise compound **4.14** from halide **4.18**. The dibenzyl phosphite route would take only two steps, avoiding the extra deprotection step of the ethyl ester groups on phosphonate **4.22** (Figure 4.28). Both reagents were chosen due to their availability in our laboratory, and for the ease of deprotection of the phosphonate esters later on in the synthesis. Overall, phosphonylation reactions of halide **4.18** using either diethyl or dibenzyl phosphite were successful.

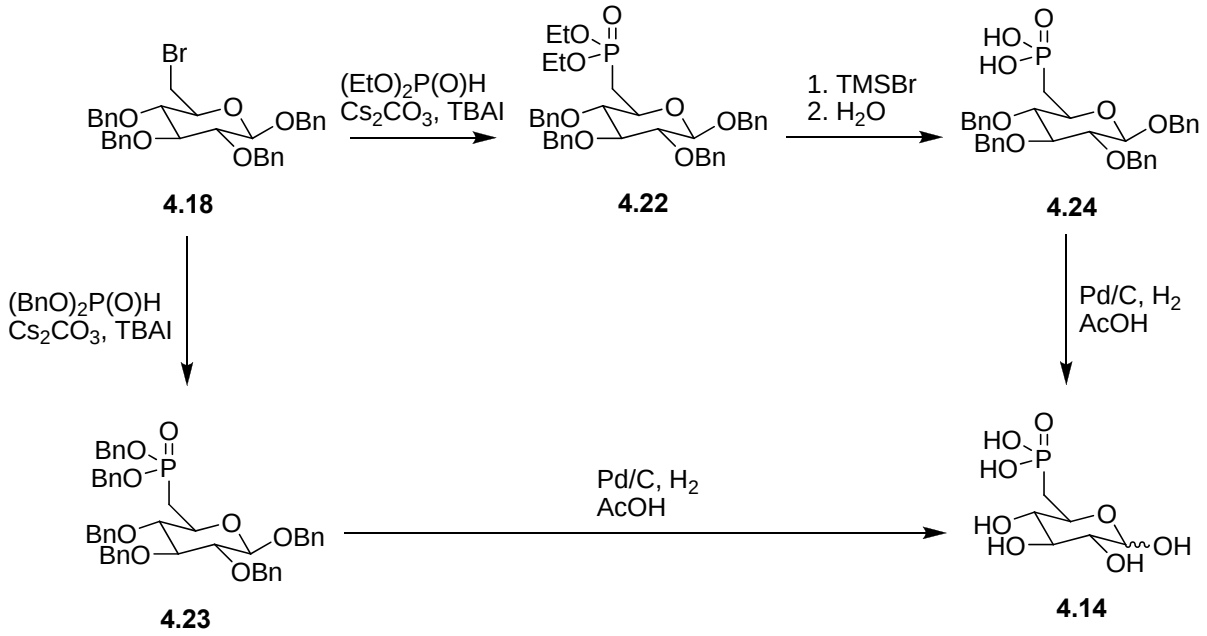

Figure 4.28: Summary for the synthesis of phosphonates 4.23 and 4.24 using two different phosphonylating reagents.

4.2.2.2 The Arbuzov method

Halide **4.18** was reacted with a large excess of triethyl phosphite (50 equiv.), stirred and heated to 140°C on an oil bath. The reaction was monitored by TLC and after three days the reaction was worked up and purified by flash chromatography to give 69% yield of phosphonate **4.22** (Figure 4.29). This yield for phosphonate **4.22** was better than that

achieved using the diethyl phosphite method employed by Cohen *et al.*[167] (c.f. 41%, Figure 4.26).

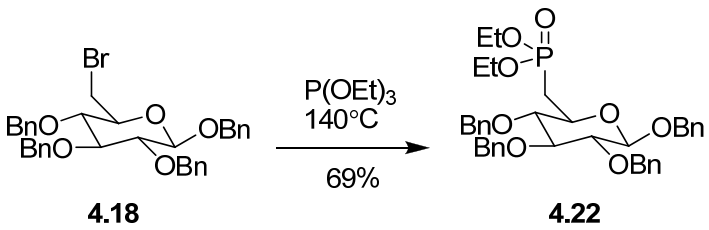

4.18 **4.22**

Figure 4.29: Synthesis of phosphonate 4.22 via the Arbuzov method.

4.2.2.3 Summary

Both methods employed for the phosphonylation of the halide **4.18** were successful in synthesising the phosphonates **4.22** and **4.23**, depending on the phosphite reagent used, and a summary of these results can be found in Table 4.2 below.

Entry	Phosphite Reagent	Method used	Conditions	Time (days)	Yield of phosphonate
1	$(BnO)_2P(O)H$	Cohen	Room temp.	5	36% (**4.23**)
2	$(EtO)_2P(O)H$	Cohen	Room temp.	3	41% (**4.22**)
3	$P(OEt)_3$	Arbuzov	Heat 140°C	3	69% (**4.22**)

Table 4.2: Summary of the Cohen and Arbuzov methods for phosphonylation of halide 4.18.

The use of both methods to synthesise the phosphonate analogues **4.22** and **4.23** had their advantages and disadvantages. The reaction in Table 4.2, entry 1, has the advantage of having one less step in the overall synthesis of compound **4.14** (Figure 4.28), but this reaction was lower yielding compared to those depicted in entries 2 and 3. This is probably due to the fact that the dibenzyl phosphite reagent is sterically bulky making it difficult to displace the C6-Br group on halide **4.18**. This was also indicated by the recovery of a large amount of starting material after purification (56% recovered).

In summary, although the Cohen method is carried out under very mild conditions making it a suitable method for substrates that could thermally degrade under Arbuzov conditions, the Arbuzov method was deemed the most successful for the synthesis of phosphonate **4.22** due

to the higher yield. Subsequently, this method was chosen for repeating this synthesis of phosphonate **4.22** from halide **4.18**.

4.2.3 Synthesis of D-glucose 6-phosphonate 4.14

With the successful synthesis of the phosphonate **4.22**, the final steps to synthesise the precursor **4.14** was carried out and the synthetic scheme used is shown in Scheme 4.3.

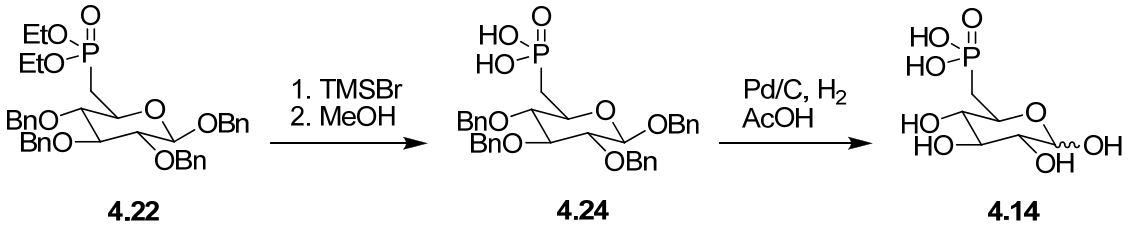

Scheme 4.3: Synthesis of D-glucose 6-phosphonate 4.14.

Phosphonate **4.22** was deprotected using TMSBr followed by hydrolysis to give the phosphonic acid **4.24** in 98% yield (Figure 4.30). ^{1}H NMR spectroscopy showed that the phosphonate ester group had been cleaved, due to the disappearance of the ethyl resonances at 4.13 and 1.34 ppm in the spectrum.

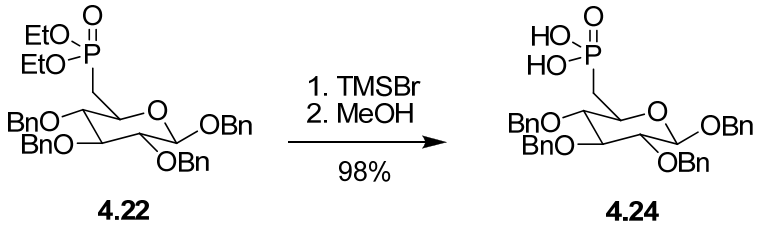

Figure 4.30: Synthesis of phosphonic acid 4.24.

The benzyl ethers were removed from the phosphonic acid **4.24** by hydrogenation using a palladium on carbon catalyst. When the conventional solvent MeOH was used for hydrogenation the reaction was completed in 4 days (100% yield). ^{1}H NMR spectroscopy showed the disappearance of all aromatic proton resonances between 7.43–7.03 ppm in the spectrum. By switching from the conventional solvent MeOH to AcOH, the hydrogenation reaction was completed in 2 days (Figure 4.31). This is due to the fact that polar protic solvents such as AcOH help to facilitate the reaction by protonating the oxygen on the benzyl ether.[103]

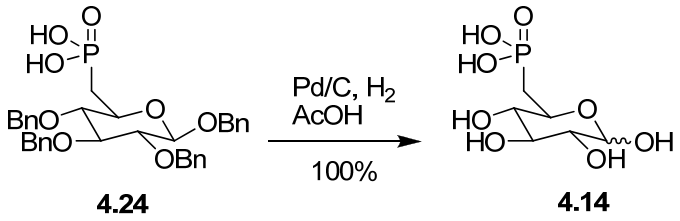

Figure 4.31: Hydrogenation of phosphonic acid 4.24 in acetic acid.

The hydrogenation reaction product mixture was then purified using a reverse phase C18 silica column to give compound **4.14** as a sugary semi-solid (100% yield). Both α- and β-anomers were present in a 1:1.3 ratio respectively, and were assigned by their coupling constants (α-anomer: 5.07 ppm, d, ^3J = 3.3 Hz; β-anomer: 4.53 ppm, d, ^3J = 7.7 Hz).

4.2.4 Attempts to synthesise D-erythrose 4-phosphonate

With the successful synthesis of the D-glucose 6-phosphonate **4.14**, this compound was then subjected to oxidative cleavage by lead tetraacetate in the hopes of affording D-erythrose 4-phosphonate. This method is similar to the method used by Simpson *et al.*[90] and Sieben *et al.*[89] to synthesise E4P from D-glucose 6-phosphate, although no NMR or mass spectrometry data was given for E4P by either author. The reaction was carried out, worked up by filtering through celite and continuously extracted with ether to remove solid impurities and acetic acid, respectively. The aqueous layer after the ether extraction was then analysed without further purification. Unfortunately, when the reaction was carried out there was no indication of D-erythrose 4-phosphonate being formed (Figure 4.32), and by this stage of the synthesis all of precursor **4.14** had been used up.

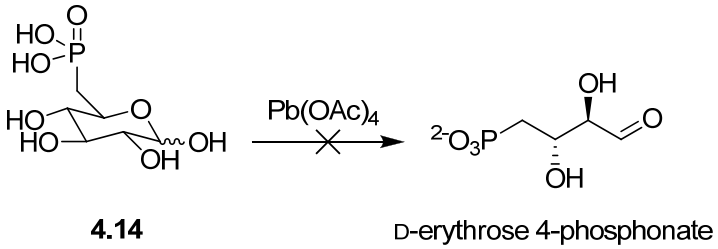

Figure 4.32: Lead tetraacetate oxidative cleavage of D-glucose 6-phosphonate 4.14. Attempt to synthesise D-erythrose 4-phosphonate.

The reaction with $Pb(OAc)_4$ is a long and laborious experimental procedure with difficulties in monitoring the reaction as it progresses. ^{1}H NMR spectroscopy was used in an attempt to

monitor the reaction periodically, from start to work-up, but peaks in the spectrum were extremely broad and overlapping peaks made interpretation of the spectrum impossible. Overlapping of peaks in the ^{1}H NMR spectrum were probably due to the side-products glyceraldehyde 3-phosphonate (from over oxidation) and arabinose 5-phosphonate (from under oxidation). Standard TLC monitoring techniques could not be used to monitor the reaction as the compounds were extremely polar and remained on the baseline. Highly polar solvent systems for TLC analysis such as 10% MeOH:DCM, 1:6:3:0.2 water:isopropanol:ethyl acetate: acetic acid and 80:60:30:3:5 chloroform:methanol:acetic acid:water were also used to visualise the reaction but with no success. The authors Simpson *et al.*[90] and Sieben *et al.*[89] did not mention how they monitored their reactions either. Attempts to find the mass of D-erythrose 4-phosphonate using mass spectrometry were unsuccessful. The mass for the side-product arabinose 5-phosphonate was detected as its dimethyl acetal (calc. $C_7H_{16}O_{8P}$ $[M-H]^-$: 259.0583; found: 259.0579, sample was run in MeOH), indicating that under oxidation had occurred.

As stated earlier in the introduction of this chapter, D-erythrose 4-phosphonate was first synthesised by Le Marechal *et al.*[141] but no experimental procedure and spectroscopic data was given for this compound. The compound was however tested as a substrate on transaldolase and found to be a substrate for this enzyme. With this in mind, it was decided to do a quick test on two enzymes, *E. coli* (phe) and *N. meningitidis* DAH7P synthase, to see if the crude mixture contained a substrate. Unfortunately, it was found that the crude mixture was not a substrate for either synthase. Had the crude mixture been found to contain substrate, this would suggest that D-erythrose 4-phosphonate had been synthesised, although it is also possible it is not a substrate, or was not synthesised at all. The thiobarbituric acid assay could also be used to provide evidence for the synthesis of D-erythrose 4-phosphonate. This assay provided evidence for the synthesis of 6-deoxyDAH7P from the reaction between PEP and 3-deoxyE4P catalysed by *M. tuberculosis* DAH7P synthase in Chapter 2.

4.3 2,3-Dideoxy erythrose 4-phosphonate

The synthesis of 2,3-dideoxy erythrose 4-phosphonate **4.38** was investigated primarily for method development. It was also predicted that this analogue would not be a substrate for DAH7P synthase due to past substrate experiments on 2,3-dideoxy erythrose 4-phosphate.[65,168]

Past substrate studies on 2,3-dideoxy erythrose 4-phosphate found that this analogue was not a substrate for *E. coli* DAH7P synthase (phe), as at least one hydroxyl group on E4P is required to bind E4P to the enzyme and orientate it in the active site for catalysis c.f. 2- and 3-deoxyE4P results (Chapter 2). However, the synthesis of this compound was expected to be more straightforward than for the synthesis of the full E4P analogue.

Shown in Figure 4.33 is the retrosynthetic analysis for compound **4.38**. Compound **4.38** can be synthesised from the very cheap and commercially available starting material butan-1,4-diol. This diol can then be converted into compound **4.38** by first orthogonally protecting one end of the diol, followed by three key chemical manipulation steps of bromination, phosphonylation and oxidation.

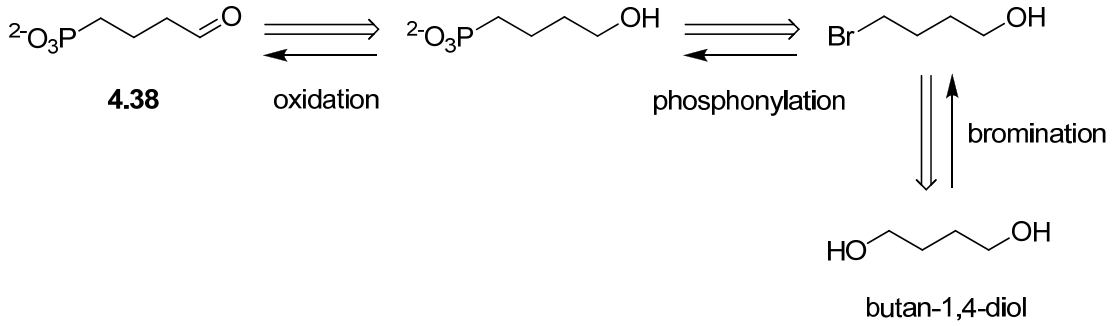

Figure 4.33: The retrosynthetic analysis of 2,3-dideoxy erythrose 4-phosphonate 4.38.

Two protecting groups were chosen to monoprotect butan-1,4-diol, the benzyl ether protecting group (Bn) and the *tert*-butyldimethylsilyl ether (TBDMS) group. Both groups were used in parallel in an attempt to synthesise target compound **4.38**. The synthetic scheme used to synthesise compound **4.38** is shown in Scheme 4.4.

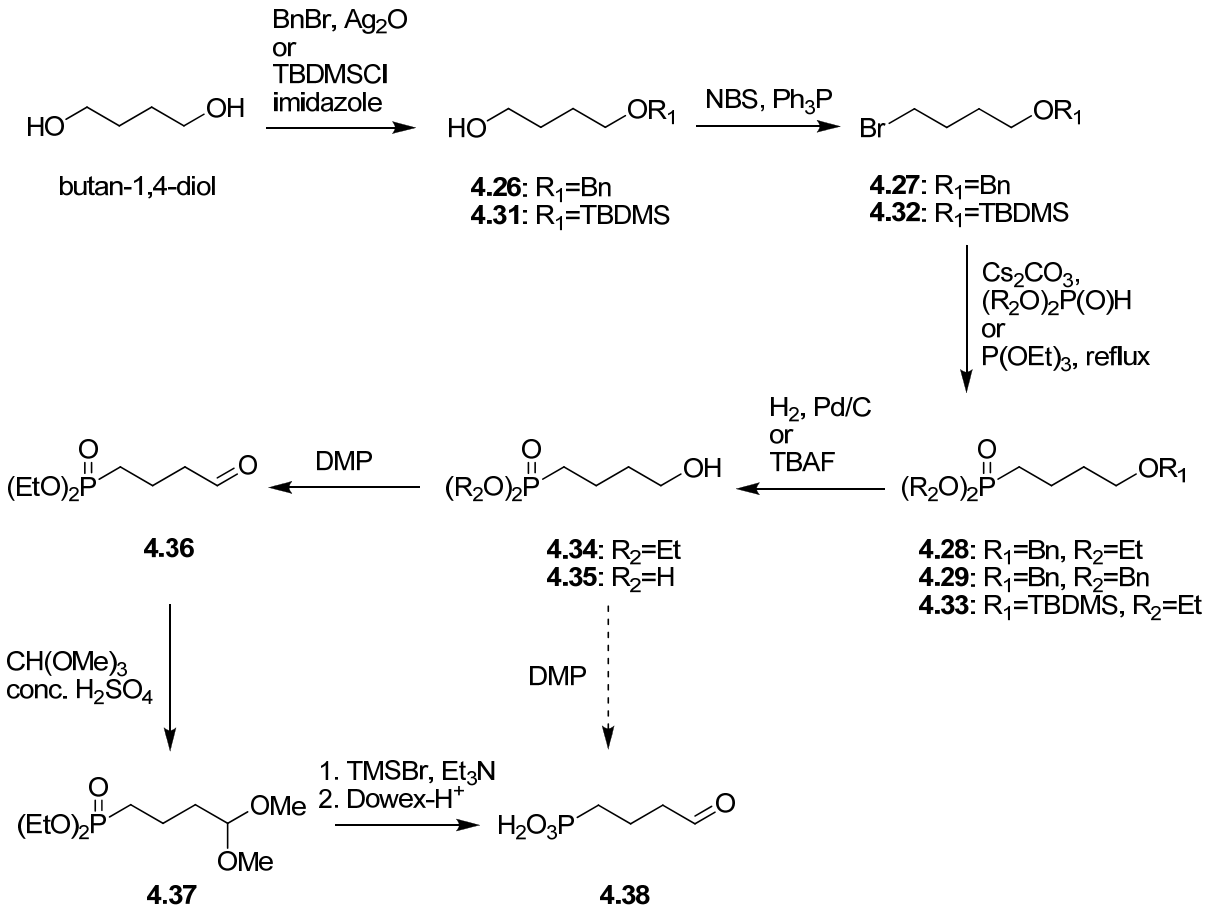

Scheme 4.4: The synthetic route used to synthesise compound 4.38. Both Bn and TBDMS protecting groups were used in parallel to synthesise compound 4.38.

Monoprotection of butan-1,4-diol using the benzyl ether protection groups afforded compound **4.26** in 75% yield following purification by flash chromatography (Figure 4.34). The ^{1}H and ^{13}C NMR spectra of compound **4.26** matched those reported in the literature.[169]

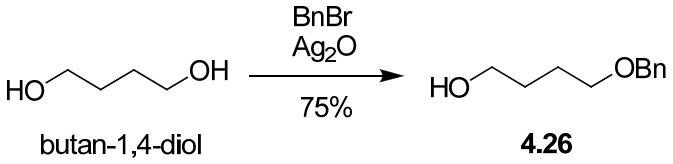

Figure 4.34: Monoprotection of butan-1,4-diol using the Bn group.

The TBDMS protecting group was also used to monoprotect butan-1,4-diol giving compound **4.31** in 70% yield (Figure 4.35). The ^{1}H and ^{13}C spectra of compound **4.31** were in accordance with those reported in literature.[170-172] Small scale trials using DMF, THF and DCM as the solvents were investigated with the yields of compound **4.31** varying depending on the solvent used. When DMF was chosen as the solvent for the monoprotection of butan-

1,4-diol a 33% yield was obtained for compound **4.31**, THF gave a 56% yield and DCM gave the highest yield of 70%. Contamination of the solvents due to water was probably a factor for these yields as THF and DCM were freshly distilled before use, whereas DMF was used from a bottle that had been prepared a few weeks prior. With the success of the high yielding DCM trial, the DMF and THF trials were not investigated further.

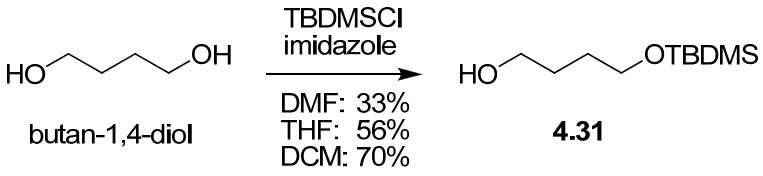

Figure 4.35: Monoprotection of butan-1,4-diol using the TBDPS group.

Bromination of both monoprotected compounds **4.26** and **4.31** using *N*-bromosuccinimide (NBS) and triphenylphosphine, gave halide **4.27** in 86% and halide **4.32** in 31% yield respectively (Figure 4.36). The ^{1}H and ^{13}C NMR spectra of halides **4.27**[173] and **4.32**[172,174] were in accordance with those reported in the literature.

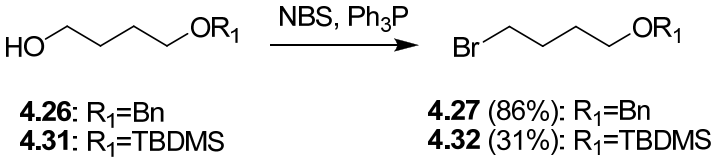

Figure 4.36: Synthesis of halides 4.27 and 4.32.

Several brominating reagents were also trialled to increase the yield of halide **4.32**. These reagents included oxalyl bromide, NBS and dimethyl sulphide, and phosphorus tribromide but unfortunately the use of these conditions resulted in the degradation of the starting material **4.31** as observed by TLC. TLC analysis showed that after 30 minutes of stirring the reaction (using any of the brominating methods mentioned before) at 0°C the starting material starts to degrade with the formation of a compound at the baseline (30% EtOAc:Pet ether, $KMnO_4$ stain). Testing each reaction with pH paper showed that the pH of the solutions were between 1 and 2. The solutions of each bromination reaction were probably too acidic and this acidity was able to hydrolysis the TBDMS protecting group giving butan-1,4-diol which would remain on the baseline of the TLC plate. The use of a more bulky silyl protecting group such as TBDPS or TIPS could possibly increase the yield, as the bulkier the substituent on the silicon the more stable it is towards acid or base hydrolysis.[103]

Phosphonylation of the halides **4.27** and **4.32** was carried out using the method employed by Cohen *et al.*[167] to produce **4.28**, **4.29** and **4.33**. The Arbuzov reaction was also employed as an alternate method to produce **4.28**.

Two different phosphite ester reagents were chosen to phosphonylate halide **4.27** using the method employed by Cohen *et al.*, diethyl phosphite and dibenzyl phosphite, producing the phosphonates **4.28** and **4.29** in 83% and 49% yields, respectively (Figure 4.37). NMR spectroscopy detected phosphonate **4.28** and **4.29** with the formation of the phosphonate ester group ethyl resonances at 4.09 and 1.32 ppm and the aromatic proton resonances between 7.47–7.20 ppm in the ^{1}H NMR spectrum respectively. A large $^{1}J_{PC}$ coupling of 141 and 140 Hz in the ^{13}C NMR spectrum was also observed, due to ^{31}P-^{13}C coupling on the resonance of C4, for phosphonates **4.28** and **4.29** respectively.

Phosphonylation of halide **4.32** was carried out using the method employed by Cohen *et al.* Halide **4.32** was phosphonylated to give the phosphonate **4.33** in 49% yield following flash chromatography (Figure 4.37). ^{31}P-^{13}C coupling was observed for the signal corresponding to the C4 secondary carbon resonance of phosphonate **4.33**, with a large $^{1}J_{PC}$ coupling of 141 Hz in the ^{13}C NMR spectrum. The Arbuzov method was not trialled as it was thought the reaction conditions would be too harsh for the TBDMS protecting group to survive.

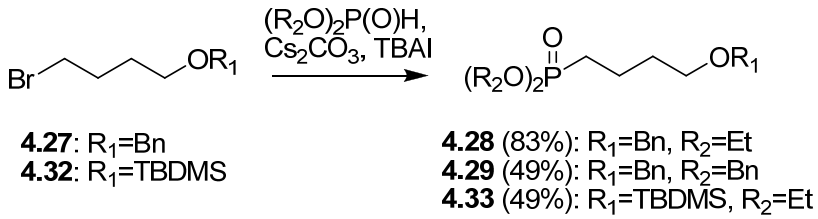

Figure 4.37: Synthesis of phosphonates 4.28 , 4.29 and 4.33 via the method employed by Cohen *et al.*

When halide **4.27** was phosphonylated using the Arbuzov method the reaction produced a persistent side-product **4.30** that was inseparable from phosphonate **4.28** (Figure 4.38). The ^{31}P NMR spectrum showed two peaks at 32 ppm and 34 ppm corresponding to phosphonate **4.28** and side-product **4.30**[175,176] respectively. Side-product **4.30** would form by the reaction of ethyl bromide (a side-product of the Arbuzov reaction, Figure 4.6) with $P(OEt)_3$. Although the two compounds were inseparable by flash chromatography it was decided to carry through to the next step in hope that the mixture could be separate after hydrogenation. This is because the product, alcohol **4.34**, would be more polar than the side-product **4.30** after

hydrogenation of the mixture. The mixture of compounds **4.28** and **4.30** were hydrogenated using hydrogen and Pd/C to give alcohol **4.34** (two steps, 20% yield) and side-product **4.30**, both compounds were separated following flash chromatography (Figure 4.37). ^{1}H NMR spectroscopy showed that deprotection of phosphonate **4.28** had taken place, due to the disappearance of the aromatic proton resonances between 7.37–7.26 ppm in the spectrum. The NMR spectral data for side-product **4.30** matched those reported in literature.[175,176] Due to the low yield for this reaction, formation of side-product **4.30** and the success of synthesising phosphonate **4.28** using the method employed by Cohen *et al.*, this method was not investigated further.

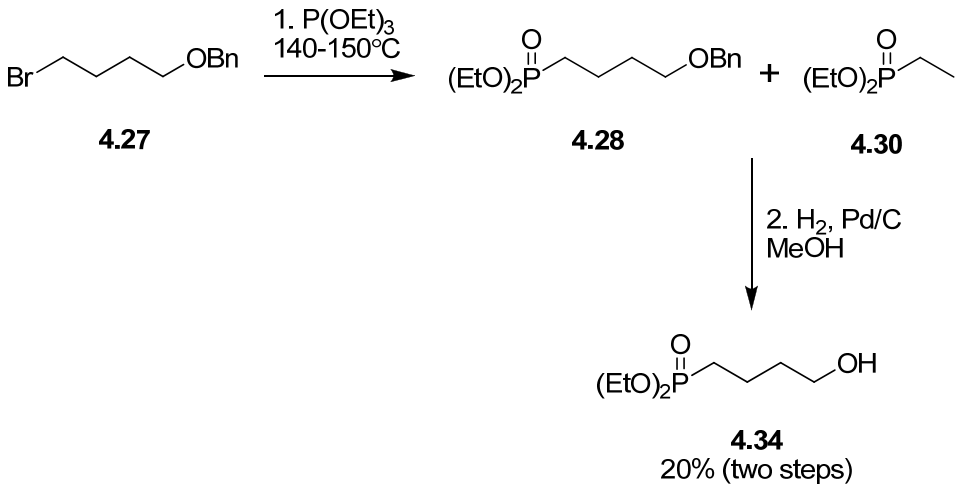

Figure 4.38: Synthesis of alcohol 4.34 via the hydrogenation of a mixture of phosphonate 4.28 and side-product 4.30.

Deprotection of phosphonates **4.28** and **4.33** by hydrogenation or TBAF (respectively) gave alcohol **4.34** in 24% (from **4.28**) and 52% (from **4.33**) (Figure 4.39). Although the yield for the deprotection of phosphonate **4.33** using TBAF is a modest yield, it was an improvement on synthesising **4.34** using the benzyl ether route. ^{1}H NMR spectroscopy confirmed the deprotection had occurred with the disappearance of the silyl methyl resonances at 0.89 and 0.04 ppm in the spectrum for phosphonate **4.33**. ^{1}H NMR spectroscopy confirmed the deprotection of phosphonate **4.28** with the disappearance of the aromatic proton resonances between 7.37–7.26 ppm in the spectrum. No attempts were made to optimise the yields of these two reactions.

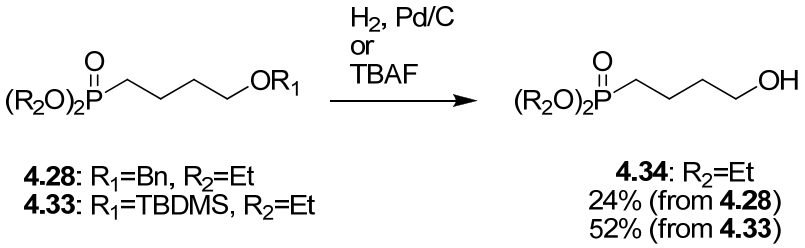

Figure 4.39: Synthesis of compound 4.34.

Alcohol **4.34** was subsequently oxidised using DMP to give aldehyde **4.36** in 73% yield following flash chromatography (Figure 4.40). The presence of the product was confirmed by a ^{1}H NMR spectrum showing the aldehyde resonance at 9.79 ppm.

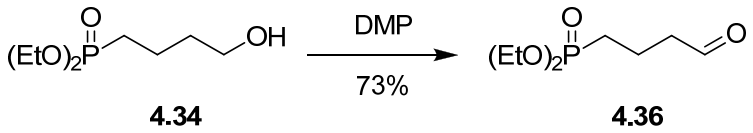

Figure 4.40: Synthesis of aldehyde 4.36.

The aldehyde group on aldehyde **4.36** was protected as its dimethyl acetal to prevent any side reactions as aldehyde groups are highly reactive.[103] Aldehyde **4.36** was protected using trimethyl orthoformate and concentrated H_2SO_4 to give acetal **4.37** in 72% yield (Figure 4.41). ^{1}H NMR spectroscopy confirmed the disappearance of the aldehyde resonance at 9.79 ppm in the spectrum.

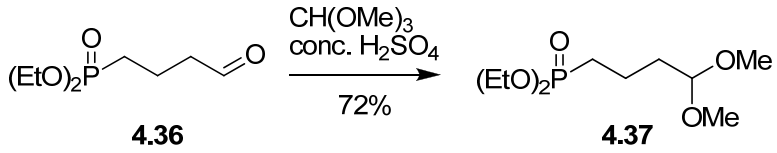

Figure 4.41: Synthesis of acetal 4.37.

Treatment of acetal **4.37** with TMSBr was used to cleave off the ester groups followed by hydrolysis using Dowex-H^+ resin to remove the dimethyl acetal groups, afforded the target compound **4.38** (Figure 4.42). The solution was evaporated to dryness and then made up to 1.0 mL in H_2O and used without further purification for enzyme assays. In contrast to the attempted synthesis of 2-methylE4P (Chapter 3), deprotection of the phosphonate group esters was successful here because the deprotection was of a stable phosphonate group and not a phosphate group. Phosphonate groups are more stable towards hydrolysis than phosphate groups as mentioned in the introduction of this chapter. In addition, the base Et_3N

was added to neutralise the acidic conditions generated by the TMSBr in the reaction. ^{1}H NMR spectroscopy detected the formation of the aldehyde resonance at 9.60 ppm in the spectrum. Additionally, compound **4.38** was detected by mass spectrometry as the protonated compound with a molecular mass of 153.0311 (calc. $C_4H_9O_4P$ $[M+H]^+$: 153.0311).

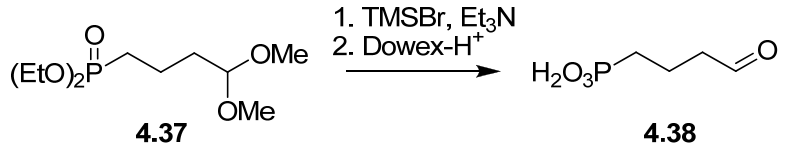

Figure 4.42: Synthesis of 2,3-dideoxy erythrose 4-phosphonate 4.38.

An alternative route to compound **4.38** was also trialled. Phosphonate **4.29** was deprotected by hydrogenation to afford the phosphonic acid **4.35** in 100% yield (Figure 4.43). ^{1}H NMR spectroscopy showed that deprotection had occurred, with the disappearance of the aromatic proton resonances between 7.47–7.20 ppm in the spectrum. Unfortunately, all attempts to oxidise compound **4.35** directly to compound **4.38** using DMP failed, and was probably due to solubility issues of **4.35**.

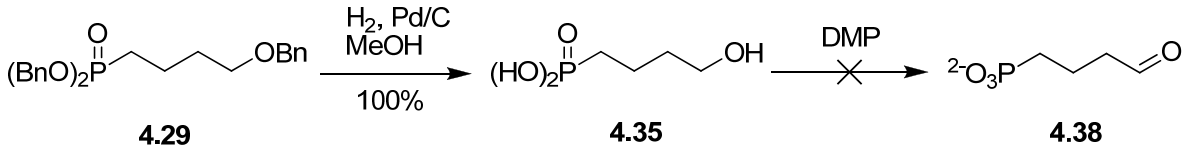

Figure 4.43: Synthesis of compound 4.35 and attempts to synthesis 4.38.

Due to the highly polar nature of compound **4.35**, this compound did not dissolve in the solvents $CHCl_3$, DCM, acetone or CH_3CN. Although it was not soluble in any of these solvents, it was thought that maybe the suspension of compound **4.35** and DMP in each solvent could still work and small scale reactions were trialled (Table 4.3). ^{1}H NMR spectroscopy was used to monitor the reactions. Crude samples were taken periodically, worked up (filtered and evaporated to dryness) and dissolved in CD_3OD, then scanned for any formation of an aldehyde resonance at around 9.70–9.40 ppm in the ^{1}H spectra (as previously synthesised analogues, such as the 2- and 3-deoxyE4P substrates, had aldehyde groups at around this range). Unfortunately, there was no indication of any aldehyde functionality being formed.

Reagent 1	Reagent 2	Solvent	Dielectric constant (ε)[177]	Time (hours)	Reaction conditions	Analysis of crude samples by ^{1}H NMR for aldehyde group signal
4.35	DMP	$CHCl_3$	4.7	72	RT	×
		DCM	8.9	72	RT	×
		Acetone	20.7	72	RT	×
		Acetone	20.7	7	reflux	×
		CH_3CN	36.2	108	RT	×

Table 4.3: Solvent trials on the oxidation of phosphonate 4.35 with DMP. RT = room temperature. Samples were made up in CD_3OD before analysis by NMR.

4.3.1 Initial enzyme assays with *E. coli* DAH7P synthase (phe)

Standard assay conditions were used to first determine whether 2,3-dideoxy erythrose 4-phosphonate **4.38** was a substrate for *E. coli* DAH7P synthase or not.

To determine whether compound **4.38** was a substrate or not, reaction mixtures contained compound **4.38** (2–150 μL, unknown concentration), $MnSO_4$ (100 μM) and PEP (150 μM) in 50 mM BTP buffer at pH 6.8. In each case, the reaction was initiated by the addition of purified *E. coli* DAH7P synthase (3–30 μL, 5.86 mg/mL). All assays were carried out at 25°C in a total volume of 1.0 mL and the loss of PEP was monitored at 232 nm. Initial readings showed that compound **4.38** was not a substrate for *E. coli* DAH7P synthase, as no PEP loss was observed at 232 nm.

To confirm the enzyme was capable of catalysing the reaction between PEP and the substrate, selected samples were spiked with the natural substrate E4P. Absorption loss of PEP was observed immediately indicating the enzyme was catalysing the reaction between E4P and PEP and not between compound **4.38** and PEP.

Preliminary studies also indicated that compound **4.38** was not an inhibitor of *E. coli* DAH7P synthase. Standard enzyme conditions with compound **4.38** (5–100 μL, unknown concentration), E4P (150 μM) and PEP (150 μM) were initiated with *E. coli* DAH7P

synthase (5 μL, 5.86 mg/mL) and the initial rate of PEP loss was measured. The initial rate of PEP loss was also measured for a second sample that contained only E4P and PEP. The rates were found to be the same (within 10% error), indicating that compound **4.38** was not an inhibitor of *E. coli* DAH7P synthase at the concentrations tested, although as the precise concentration was unknown, the detection limit could not be determined. A discussion on why compound **4.38** was not a substrate for *E. coli* DAH7P synthase can be found in Chapter 5.

4.4 Summary

The summary for the attempted synthesis of D-erythrose 4-phosphonate starting from D-glucose is shown below (Figure 4.44).

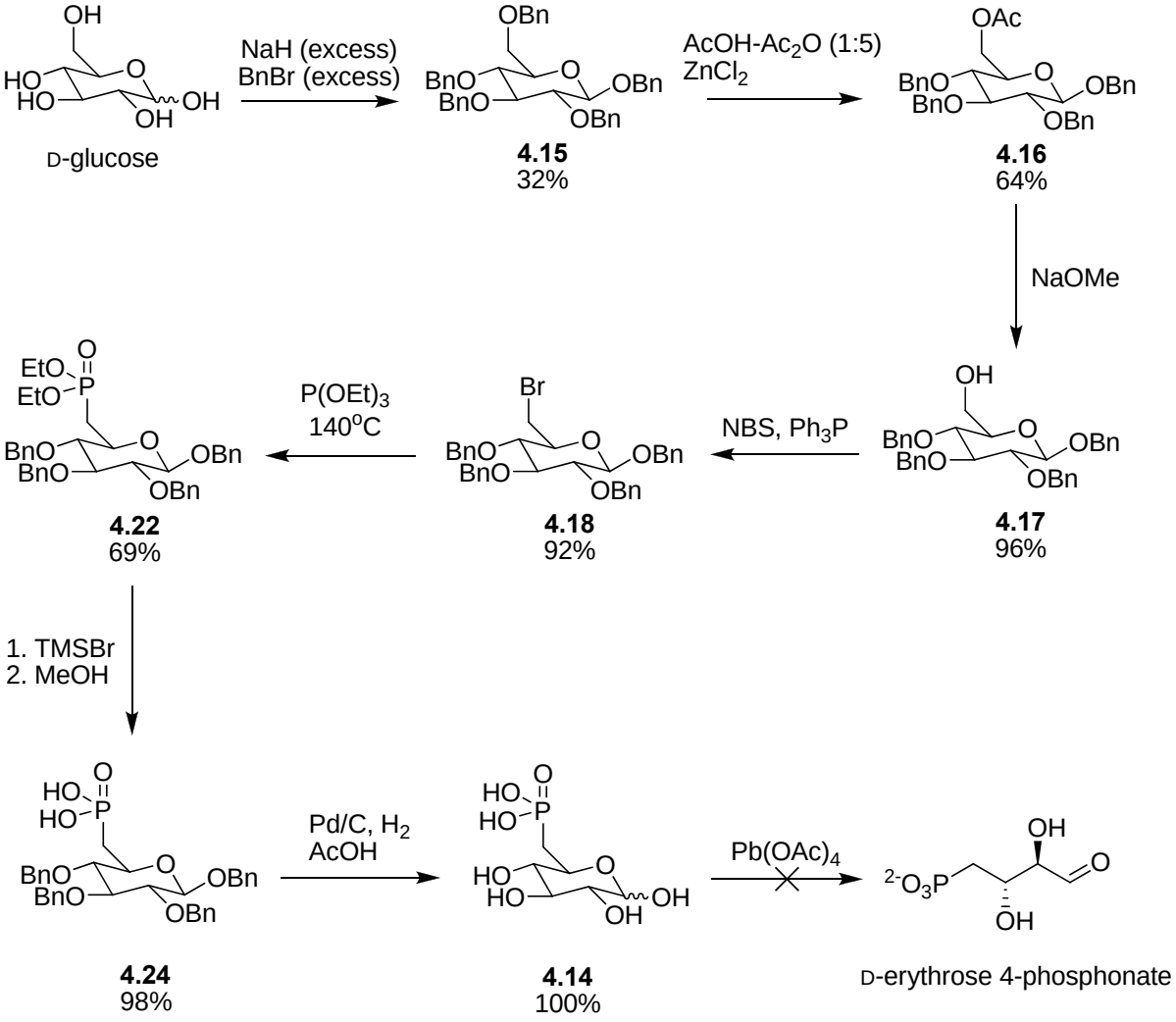

Figure 4.44: Attempts at synthesising D-erythrose 4-phosphonate.

Although the synthesis of D-erythrose 4-phosphonate was not completed, due to the difficult chemistry involved, the characterisation and methodology for the syntheses of compounds **4.14**, **4.15**–**4.18**, **4.22** and **4.24** have been well documented in this thesis. This synthetic route could be used in the future for the synthesis of D-erythrose 4-phosphonate if an alternative method (other than $Pb(OAc)_4$) for the cleavage of two carbon atoms in compound **4.14** can be found, or if a method for monitoring the reaction can be developed. Additionally, future attempts to synthesise D-erythrose 4-phosphonate could involve starting with the compound *meso*-tartaric acid (Figure 4.45). The structure of *meso*-tartaric acid has certain advantages for the synthesis of D-erythrose 4-phosphonate over the D-glucose method. These include starting with the right number of carbons (therefore avoiding the $Pb(OAc)_4$ procedure) and having a very similar structure to the target compound (see Chapter 5 for further discussion).

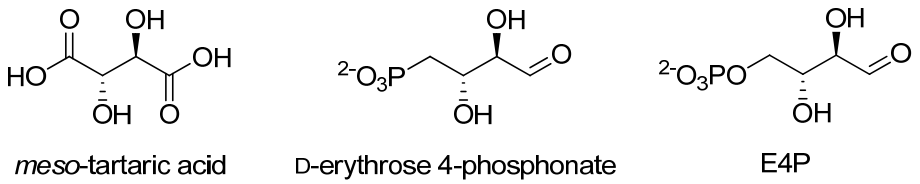

meso-tartaric acid D-erythrose 4-phosphonate E4P

Figure 4.45: Structures of *meso*-tartaric acid compared to D-erythrose 4-phosphonate and E4P.

The synthesis of 2,3-dideoxy erythrose 4-phosphonate **4.38** was synthesised primarily for method development and was predicted not to be a substrate for *E. coli* DAH7P synthase (phe) due to previous substrate studies on 2,3 dideoxy erythrose 4-phosphate.[65,168] Synthesis of compound **4.38** was achieved in overall eight steps using two different protection groups (Bn and TBDMS) concurrently (Figure 4.46). All steps were moderate to high yielding with the exception of compound **4.32** with a low 31% yield. The low yield of compound **4.32** was due to the desilylation of the silyl group owing to the highly acidic reaction conditions. The use of a more robust silyl protecting group such as the TBDPS or TIPS group, or even the addition of a mild base (e.g. Et_3N) to counteract the acidity of the reaction conditions could help increase the yield in future. Standard enzyme assays showed that compound **4.38** was not a substrate for *E. coli* DAH7P synthase (phe), as was predicted.

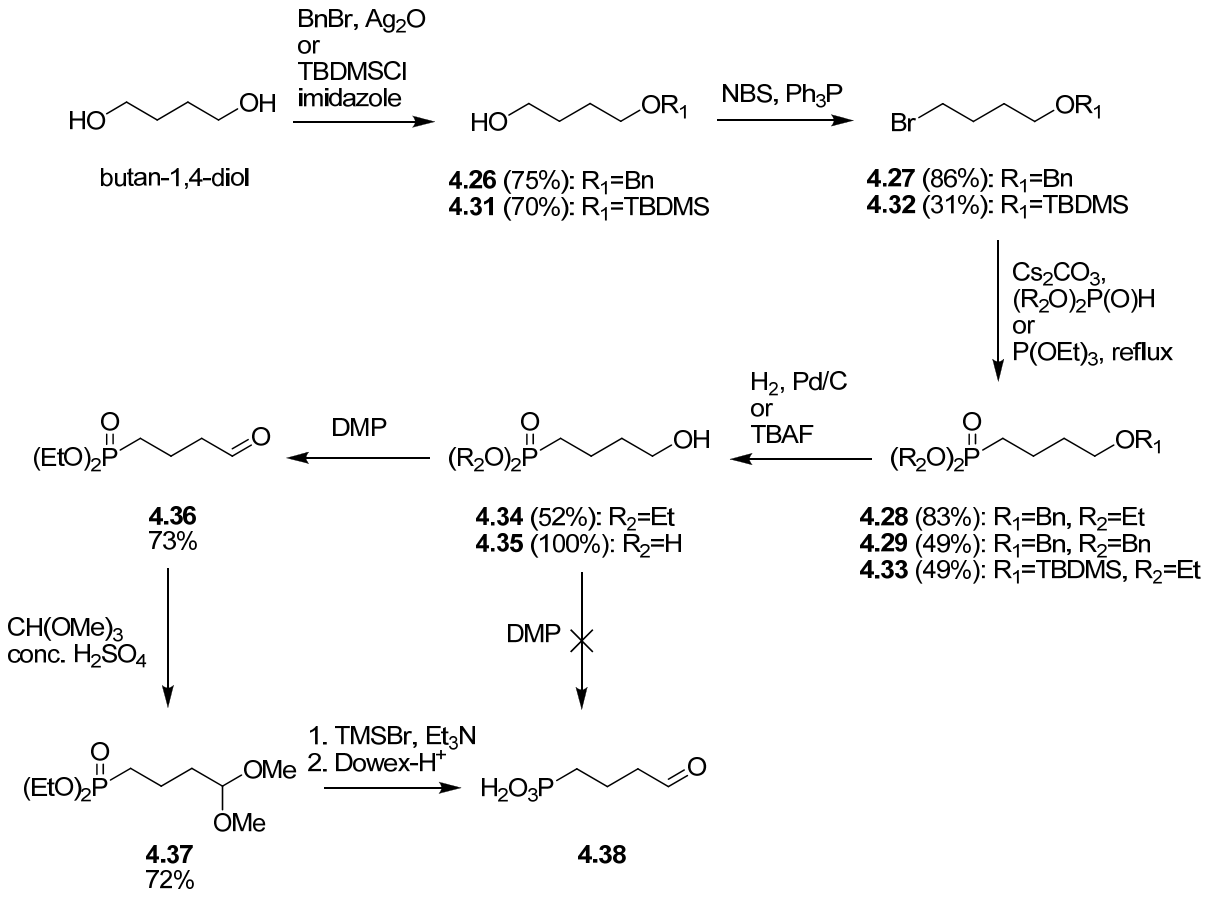

Figure 4.46: Overall synthetic scheme for the synthesis of compound 4.38.

A discussion on why compound **4.38** was not a substrate for DAH7P synthase and the predicted outcome for D-erythrose 4-phosphonate can be found in Chapter 5.

Chapter 5: Discussion, conclusions and future directions

The aim of this project was to synthesise a range of alternative non-natural four carbon analogues of E4P to help to probe the substrate specificity of the different types of DAH7P synthases. This aim has been achieved, with a number of new analogues being designed, synthesised and evaluated as alternative substrates for DAH7P synthases during the course of this project (Figure 5.1). From comparison of these molecules (2-deoxyE4P, 3-deoxyE4P, 3-methylE4P and compound **4.38**), new insights into the substrate specificity of DAH7P synthase can be obtained.

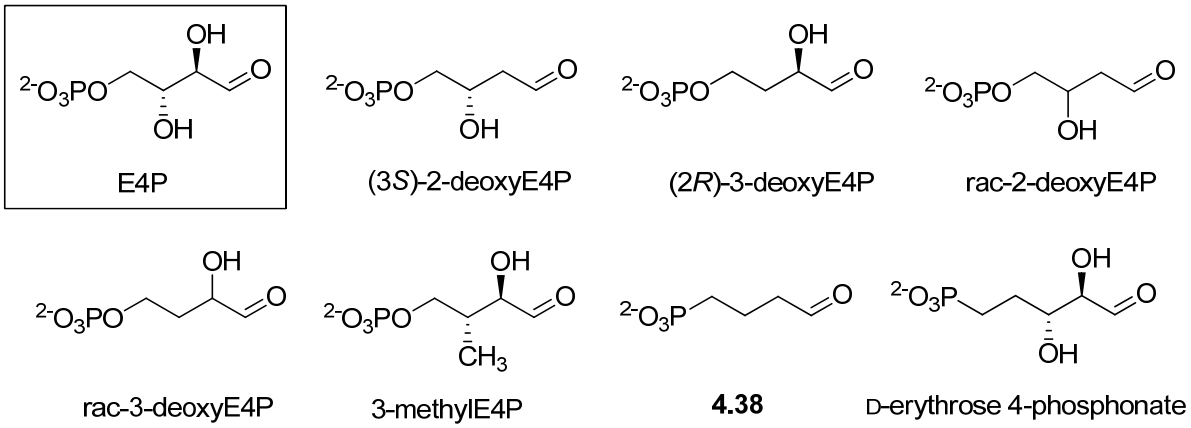

Figure 5.1: A summary of E4P analogues synthesised for evaluation on DAH7P synthase and the structure of E4P for comparison.

As was discussed in Chapter 2, both (3*S*)-2-deoxyE4P and (2*R*)-3-deoxyE4P were found to be substrates for the type II DAH7P synthase from *M. tuberculosis*. These results indicate that removal of either the C2 or C3 hydroxyl groups of E4P does not completely disrupt catalysis, and that the presence of the C3 hydroxyl group appears to be more important for efficient catalysis than the C2 hydroxyl group. In addition, the studies carried out on rac-2-deoxyE4P showed that only the (3*S*)-enantiomer is utilised by this type II enzyme; with the presence of (3*R*)-enantiomer having no effect on the kinetic parameters of the enzyme. Furthermore, studies on rac-3-deoxyE4P showed that the (2*R*)-enantiomer was utilised but the (2*S*)-enantiomer was likely to be acting as a competitive inhibitor.

Chapter 3 describes the attempts to synthesise 2-methylE4P, and the successful synthesis and evaluation of 3-methylE4P as a substrate for type Iα *E. coli* DAH7P synthase (phe). This compound was found not to be a substrate for this enzyme.

The synthesis and evaluation of 2,3-dideoxy erythrose 4-phosphonate **4.38** on the type Iα *E. coli* DAH7P synthase (phe), and the attempts to synthesise D-erythrose 4-phosphonate are described in Chapter 4. The synthesis of compound **4.38** was relatively straightforward, and no evidence was found that this compound could act as a substrate for the enzyme. In contrast, the attempts to synthesise D-erythrose 4-phosphonate from D-glucose were fraught with challenges, and ended in this analogue not being synthesised during this project.

5.1 Role of the E4P hydroxyl groups in DAH7P synthase

A summary of available kinetic data for E4P substrate analogues with various DAH7P synthases is presented in Table 5.1 (page 127). The data presented in Table 5.1 indicate that the C2 and C3 hydroxyl groups of E4P are not essential for binding of the aldehydic substrate or catalysis for type Iα, Iβ and II DAH7P synthase from *E. coli*, *P. furiosus* and *M. tuberculosis* respectively.

Although there have been no structures solved of DAH7P synthase with E4P bound in the active site in a catalytically competent manner, modelling studies that shall be detailed in this section shed some light on the way in which E4P hydroxyl groups interact with the enzyme.

Substrate	DAH7P synthase source								
	***E. coli* (phe) (type Iα)**			***P. furiosus* (type Iβ)**			***M. tuberculosis* (type II)**		
	K_M (μM)	k_{cat} (s^{-1})	k_{cat}/K_M ($s^{-1}\mu M^{-1}$)	K_M (μM)	k_{cat} (s^{-1})	k_{cat}/K_M ($s^{-1}\mu M^{-1}$)	K_M (μM)	k_{cat} (s^{-1})	k_{cat}/K_M ($s^{-1}\mu M^{-1}$)
E4P 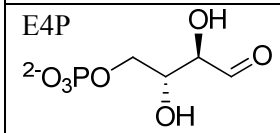	39±4	26±2	0.67	9±1	1.4±0.1	0.16	37±2	5.4±0.1	0.15
(3*S*)-2-deoxyE4P 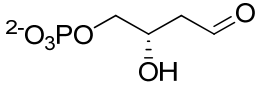	410±40	19±1	0.05	6±1	3.0±0.1	0.49	46±5	4.9±0.2	0.11
(2*R*)-3-deoxyE4P 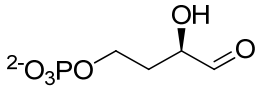	2700±140	4.5±0.1	0.002	200±30	2.1±0.1	0.01	77±9	2.4±0.1	0.031
3-methylE4P 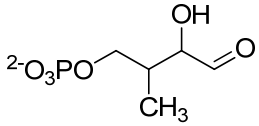	NS			ND			ND		
4.38 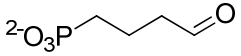	NS			ND			ND		

Table 5.1: Kinetic parameters of type Iα, Iβ and II DAH7P synthases with four carbon sugar analogues of E4P. Kinetic data for (3*S*)-2-deoxy and (2*R*)-3-deoxyE4P with *E. coli* DAH7P synthase (phe) were determined by Dr Pietersma[66]; *P. furiosus* DAH7P synthase kinetic data were determined by Dr Schofield.[32] ND = not determined. NS = not a substrate.

The kinetic data for the type Iβ DAH7P synthase from *P. furiosus* indicate that the C3 hydroxyl group of E4P is significant for binding and catalysis, while the C2 hydroxyl has no major effect. The crystal structure of *P. furiosus* DAH7P synthase with E4P modelled into the active site may provide clues about these observations (Figure 5.2).[32]

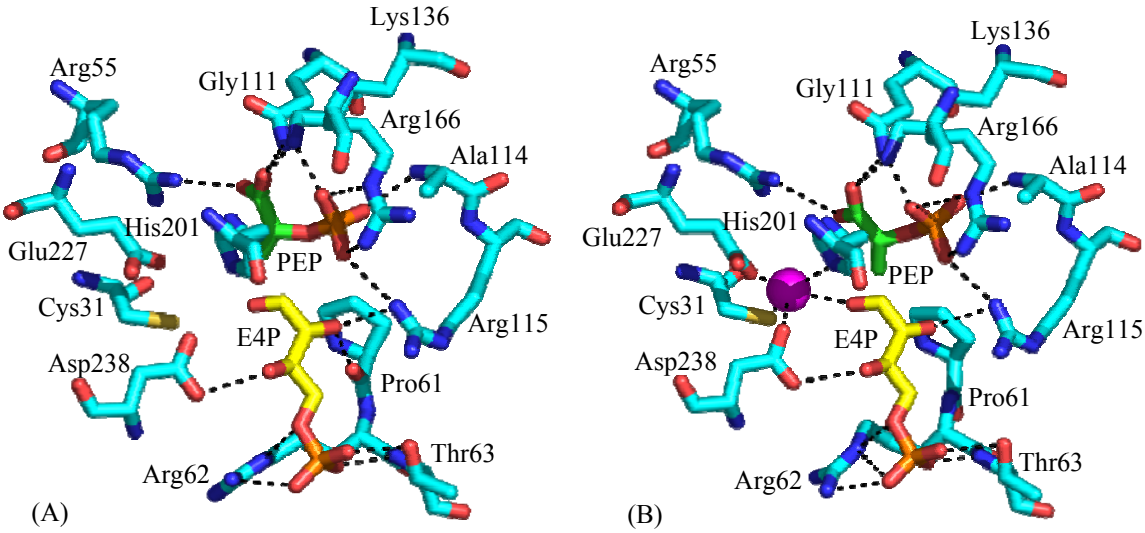

Figure 5.2: Active site of *P. furiosus* DAH7P synthase (PDB code 1ZCO).[32] E4P (yellow/orange/pink) has been modelled into the structure on the basis of E4P binding to *T. maritima*[62] DAH7P synthase and D-glycerol 3-phosphate to *S. cerevisiae*[61] DAH7P synthase. (A) Pro61 carbonyl group pointing towards the modelled E4P as found in subunit A of *P. furiosus* DAH7P synthase. (B) Pro61 carbonyl group pointing away from the modelled E4P as found in subunit B of *P. furiosus* DAH7P synthase. Mn^{2+} metal (magenta sphere) is present in subunit B, but not subunit A.

Modelling studies of E4P in the active site of *P. furiosus* DAH7P synthase have indicated that the C3 hydroxyl group of E4P interacts with the conserved Asp residue (Asp238) that binds the metal ion (Figure 5.2). The activation of the E4P carbonyl by this metal ion appears to be a key step in the condensation reaction. The hydrogen bonding interaction of the C3 hydroxyl group with the metal-binding Asp residue is likely to activate the metal by making it a stronger Lewis acid, further activating the C1 of E4P for attack by PEP. Therefore, when the C3 hydroxyl group is missing, the binding is reduced, as indicated by the higher K_M value seen for 3-deoxyE4P compared to E4P.

The modelling studies also indicate that the C2 hydroxyl group of E4P interacts with Arg115 and the carbonyl group of Pro61. Additionally, this Pro residue is part of the absolutely conserved LysProArgThr motif found on the β2–α2 loop in all DAH7P synthases (Figure 5.3). However, the crystal structure of *P. furiosus* DAH7P synthase shows that Pro61 exists in two different conformations: in one subunit of the asymmetric unit (Figure 5.2A), the

Pro61 carbonyl group is pointing towards the modelled E4P, but in the other subunit (Figure 5.2B) it is pointing away, which indicates this part of the protein is flexible.[32] This loop does not appear to be as flexible for the Iα enzymes where it is buttressed by intersubunit contacts.[21] The flexibility in the active site may make binding to the substrate less entropically favourable, weakening the interaction and making the C2 hydroxyl group less important for substrate binding. This is indicated by the very similar K_M and k_{cat} values of 2-deoxyE4P compared to E4P with *P. furiosus* DAH7P synthase.

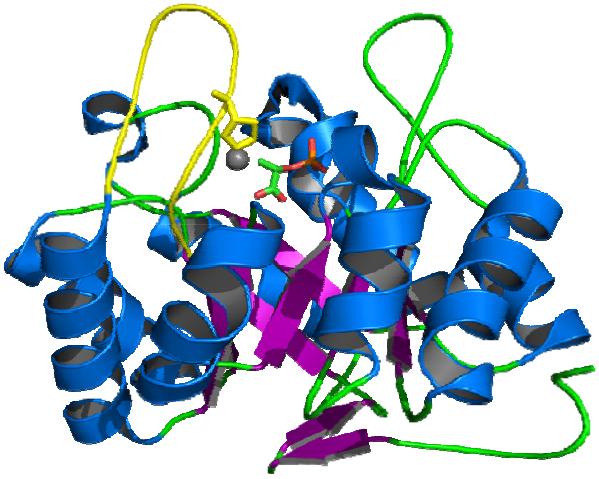

Figure 5.3: *P. furiosus* DAH7P synthase monomer structure showing the α-helices (blue) and β-sheets (red) of the basic $(\beta/\alpha)_8$ TIM barrel (PDB code 1ZCO). The β2–α2 loop is coloured yellow, with the Pro residue on the loop shown as a stick model. PEP stick model (green/orange/pink), metal ion sphere (grey).

The kinetic data for the type Iα DAH7P synthase from *E. coli* show that removing either the C2 or C3 hydroxyl group of E4P has significant impact on catalysis and binding of the substrate. This is in contrast to what is observed with the type Iβ enzyme, where only removal of the C3 hydroxyl group of E4P affected the activity.

The same argument previously used to explain the high K_M values for 3-deoxyE4P with the type Iβ enzyme can also explain the kinetic data for 3-deoxyE4P with the type Iα DAH7P synthase from *E. coli*: as there is no interaction between the C3 hydroxyl group of 3-deoxyE4P with the metal-binding Asp residue, this causes a weakened contact between the metal-E4P aldehyde interaction and results in a decrease in catalytic efficiency and severely compromised binding.

The same Pro residue (of the LysProArgThr motif) is implicated in E4P binding in both type Iα and Iβ DAH7P synthases from *E. coli* and *P. furiosus* respectively. It is located on the β2−α2 loop and in the Iα enzyme this loop is constrained by the interface with the adjacent monomer that is located close to the active site (Figure 5.4).[21] These β2–α2 dimer interactions seen in the type Iα enzyme from *E. coli* are not seen in the type Iβ *P. furiosus* DAH7P synthase in solution, resulting in an active site with less flexibility compared to the Iβ enzyme.[32] The more rigid conformation of this loop containing the conserved Pro residue that interacts with the C2 hydroxyl group of E4P may explain why a higher K_M and a lower k_{cat} is observed for 2-deoxyE4P, as the interaction between the C2 hydroxyl group of E4P with the Pro residue is more important for catalysis and binding in this type Iα enzyme.

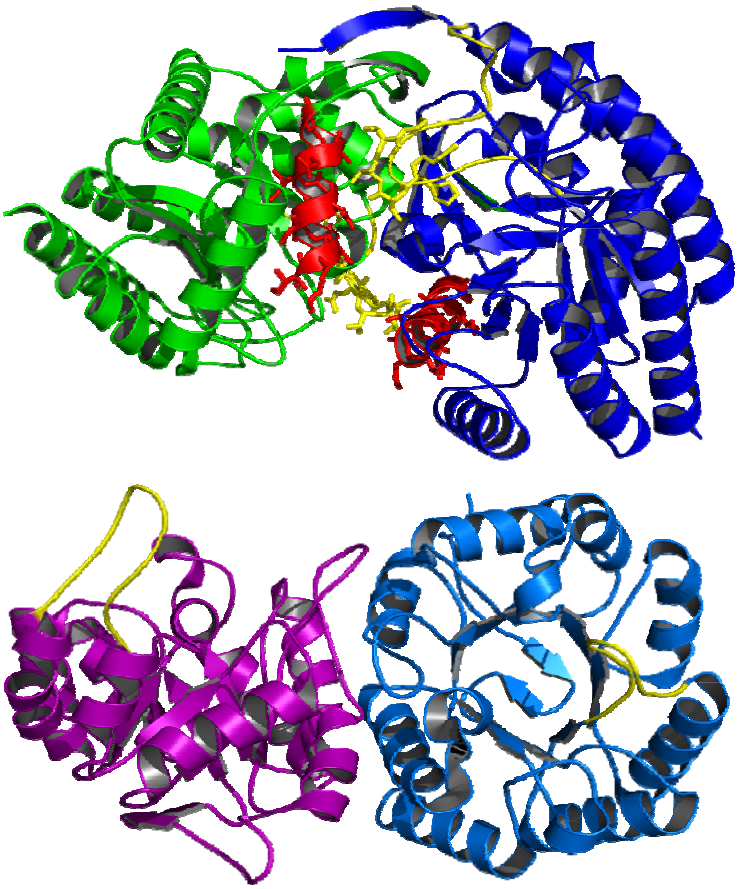

Figure 5.4: (Top) Type Iα *E. coli* DAH7P synthase (phe) dimer (PDB code 1QR7). Intersubunit interactions between the β2−α2 loop (yellow) of one monomer (green) with the α5 helix (red) in the other (blue), are involved in dimer formation in type Iα enzymes.[21] (Bottom) Type Iβ *P. furiosus* DAH7P synthase dimer (PDB code 1ZCO). The β2−α2 loop (yellow) is not involved in dimer formation in *P. furiosus* DAH7P synthase.

Models of E4P bound in the active site of type II *M. tuberculosis* DAH7P synthase (Figure 5.5) can be used to explain the similar kinetic data obtained for E4P, 2-deoxyE4P and 3-deoxyE4P with this enzyme.[38,178]

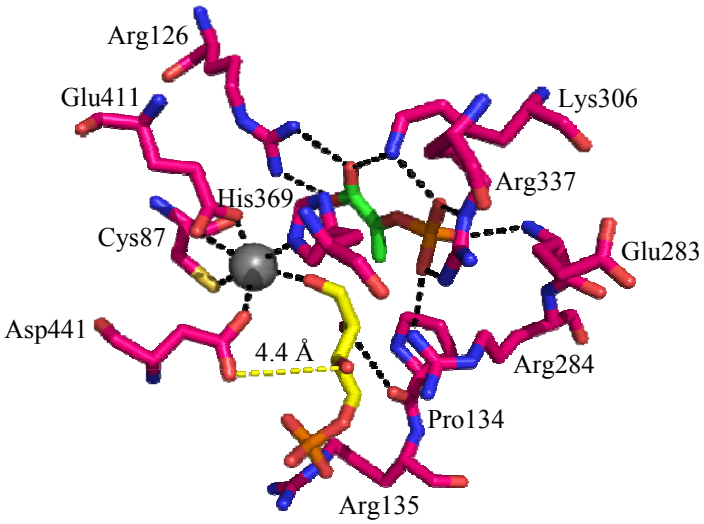

Figure 5.5: Diagram of the metal-PEP-E4P-binding ligands in the *M. tuberculosis* active site.[32] The distance between the C3 hydroxyl of E4P (yellow/orange/pink) and Asp441 is 4.4 Å. E4P was docked into the active site of the enzyme with positional constraints between C1 of E4P and C3 of PEP, and between the aldehyde oxygen of E4P and the metal ion. Modelling was performed by Dr Wanting Jiao.

The model of E4P in the active site of the type II enzyme from *M. tuberculosis* shows the distance between the C3 hydroxyl group of E4P and the conserved metal-binding Asp441 is 4.4 Å (compared to a distance of 3.3 Å in the type Iβ enzyme from *P. furiosus*). As this distance is too long to constitute a hydrogen bond, the E4P modelled structure suggests that there is little binding interaction between the two. This model could explain why removal of the C3 hydroxyl group of E4P has a less effect on the binding to the type II enzyme when compared to the effect that loss of this hydroxyl group has on the type Iβ enzyme from *P. furiosus*.

Although both enzymes are tetrameric, the quaternary structure of the type II enzyme from *M. tuberculosis* is quite distinct from that of the Iα enzyme from *E. coli*. The β2–α2 loop is therefore not buttressed by a neighbouring subunit (Figure 5.6). The increased flexibility in the active site could explain why 2-deoxyE4P is a relatively good substrate for the enzyme. This may be due to the interaction between the conserved Pro residue and the C2 hydroxyl group of E4P being less important for binding and catalysis in this type II enzyme. Similar results were also observed with the type Iβ DAH7P synthase from *P. furiosus*.

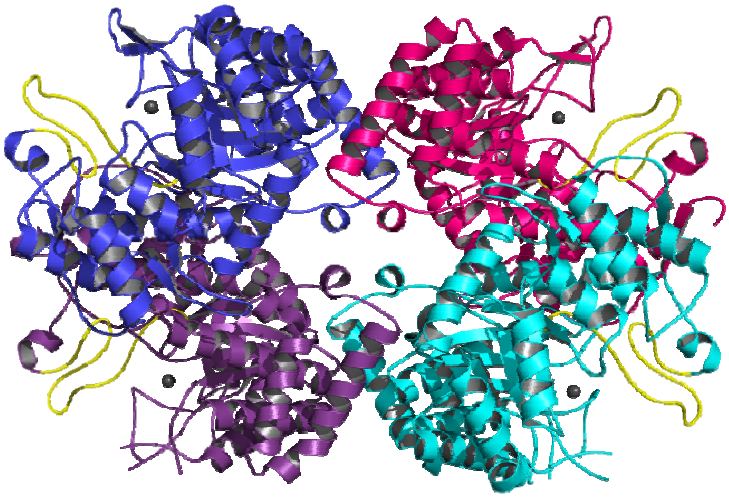

Figure 5.6: Type II *M. tuberculosis* DAH7P synthase tetramer (PDB code 2B7O). The β2–α2 loops are coloured yellow, Mn^{2+} ion sphere (grey).

5.1.1 Mechanistic insights

An early proposal for the mechanism of DAH7P synthase suggested that the C3 hydroxyl group of E4P played a vital role in the reaction mechanism (Figure 5.7). In this proposed mechanism, the C3 of PEP attacks the carbonyl group of E4P to form the oxocarbenium ion intermediate **1.1** which then cyclises to give the cyclic hemiketal biphosphate compound **1.2**. Cyclisation of the oxocarbenium ion intermediate **1.1** is achieved by the hydroxyl group on C3 of E4P attacking the carbocation formed at C2 of PEP. This mechanism has been discredited as 3-deoxyE4P was found to be a substrate for type Iα and Iβ DAH7P synthases. Furthermore, structural studies on *E. coli* (type Iα), *P. furiosus* (type Iβ) and *M. tuberculosis* (type II) DAH7P synthases have shown the active site to be a long linear pocket in which there is unlikely to be sufficient room for intramolecular cyclisation making this cyclic mechanism implausible.[21,32,38,63]

However, the cyclic mechanism had never been disproved for type II DAH7P synthases. The results presented in this thesis show that 3-deoxyE4P is a substrate for type II DAH7P synthase from *M. tuberculosis*, showing that the C3 hydroxyl group is not essential for catalysis, and suggests that type II DAH7P synthases is unlikely to proceed by the cyclic mechanism.

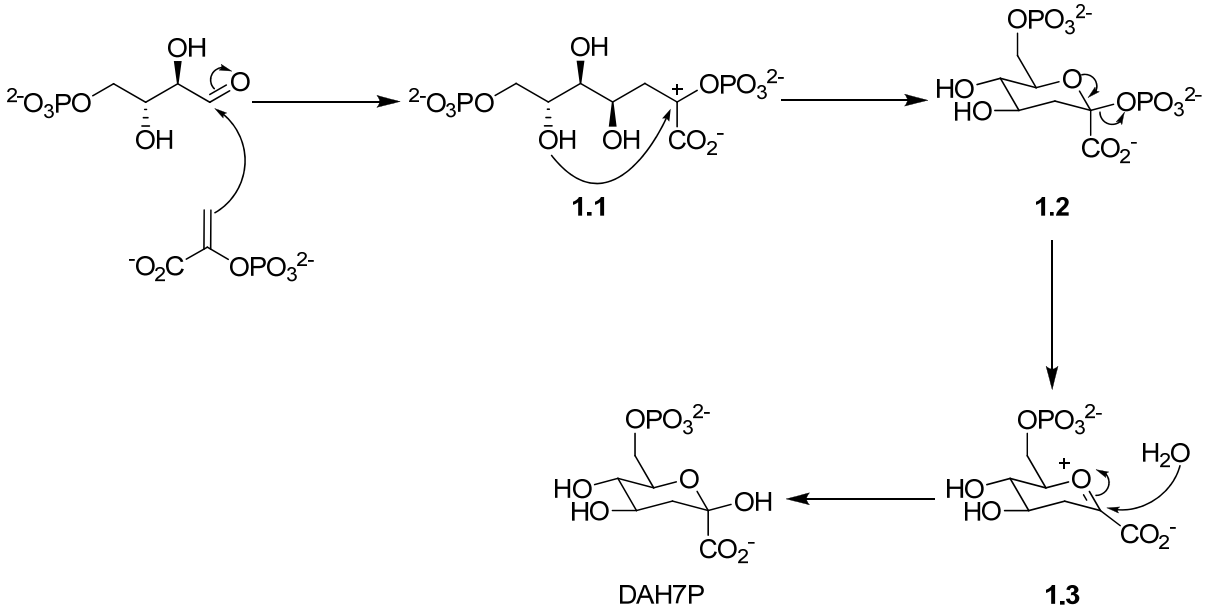

Figure 5.7: Proposed cyclic mechanism of DAH7P synthase.

5.2 Methyl analogues of E4P

5.2.1 3-MethylE4P

Modelling studies with E4P bound in the active site of *P. furiosus* DAH7P synthase can be used to rationalise why 3-methylE4P is not a substrate for *E. coli* DAH7P synthase (phe) (Figure 5.2). As mentioned previously, the C3 hydroxyl group on E4P binds to an Asp residue and removal of this interaction as in 3-deoxyE4P causes a large decrease in affinity of the substrate. However, 3-deoxyE4P is still a substrate, although a poor one, so loss of this hydrogen bond alone cannot explain why 3-methylE4P is not a substrate.

Not only is hydrogen bonding at the C3 position not possible, the structure of 3-methylE4P is more hydrophobic compared to E4P making it more difficult for 3-methylE4P to bind in the hydrophilic active site. The C3 methyl group of 3-methylE4P is also sterically bulkier compared to the C3 hydroxyl group of E4P. This increase in size on the C3 position could have adverse consequences in the active site, as the C3 methyl group would sterically clash with the Asp residue that binds the C3 hydroxyl group of E4P. Overall, it is not surprising that the sterically bulky and hydrophobic methyl group may seriously disrupt binding of the aldehydic substrate.

Future work that could be investigated on 3-methylE4P would involve testing the analogue on the type Iβ and II DAH7P synthases from *P. furiosus* and *M. tuberculosis*. This is because these enzymes have been shown to be more promiscuous than the type Iα enzyme from *E. coli*, and therefore 3-methylE4P might be utilised as a substrate. Inhibitor studies on 3-methylE4P could also be investigated in the future on *E. coli* DAH7P synthase (phe) to determine whether 3-methylE4P is acting as an inhibitor on this enzyme.

5.2.2 2-MethylE4P

Although 2-methylE4P was not synthesised during this project, the results obtained from the studies with 2-deoxyE4P, 3-deoxyE4P and 3-methylE4P could be used to predict whether 2-methylE4P would be a substrate for DAH7P synthase or not.

Generally, DAH7P synthases has been observed to be more tolerant to changes in the C2 position of E4P than the C3 position. These observations can be used to predict that 2-methylE4P might be a substrate for DAH7P synthase, as changes made on the C2 position of E4P has a significantly less detrimental effect on binding and catalysis in the enzyme. This is particularly true of the type Iβ and II DAH7P synthases that can accept 2-deoxyE4P, but for the more C2 specific type Iα enzyme, 2-methylE4P would be predicted to be a much poorer substrate, if at all.

A future synthesis of 2-methylE4P could involve using a more robust protecting group for the aldehyde functionality (Figure 5.8). This is because deprotection of compound **3.38** using TMSBr results in the loss of the acyclic aldehyde protecting group, due to the acidic reaction conditions (described in Chapter 3). The cyclic acetal protecting group seen in compound **5.1** could be employed, as this protecting group is more robust and resistant to hydrolysis than the acyclic acetal protecting group on compound **3.38**, therefore increasing the resistance of compound **5.1** to hydrolysis during the TMSBr deprotection step.[103] Additionally, the base Et_3N could also be added to decrease the acidity of the reaction. This would aid in preventing the unwanted hydrolysis of the cyclic acetal protecting group in compound **5.1** during the TMSBr step.

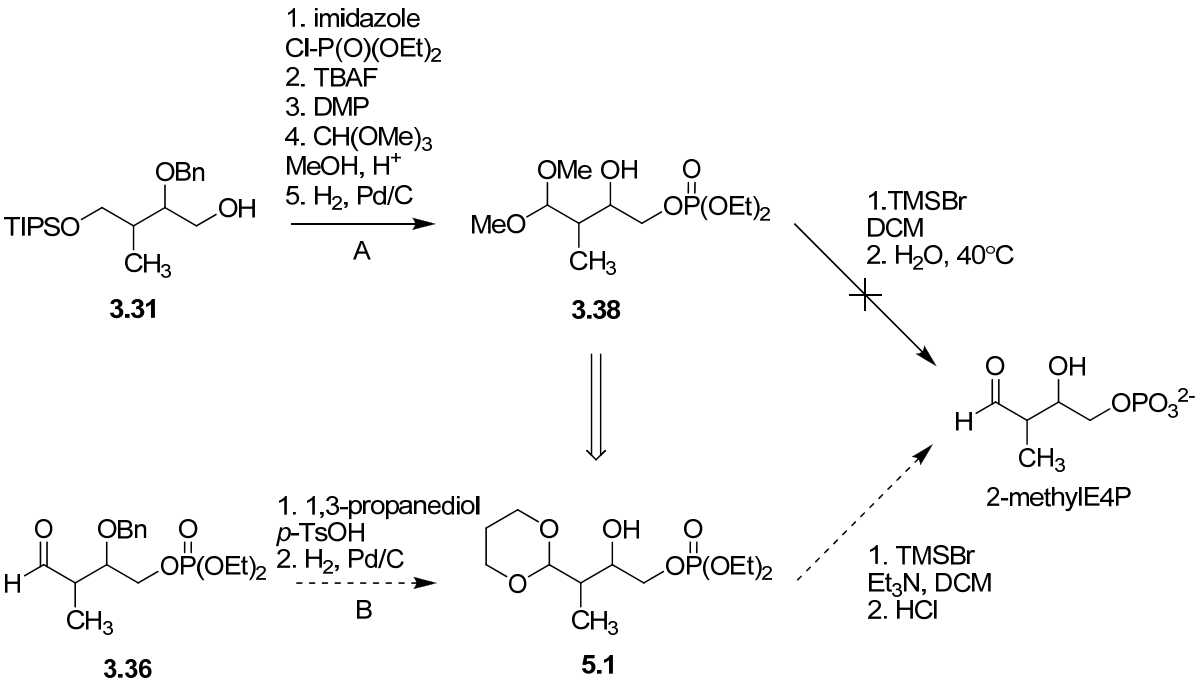

Figure 5.8: (A) The original route, from Chapter 3, used to attempt to synthesise 2-methylE4P. This route utilised the acyclic acetal protecting group (compound 3.38). (B) Proposed synthesis of 2-methylE4P from compound 5.1.

5.3 Phosphonate analogues of E4P

5.3.1 D-Erythrose 4-phosphonate

The synthesis of the phosphonate analogue of E4P was primarily done for method development and to pave the way for the synthesis of the homophosphonate analogue of E4P, as previous substrate specificity studies reported that DAH7P synthase only accepted four carbon and five carbon sugar analogues of E4P (Chapter 1).[24,32,47] Therefore it was decided to attempt to synthesise the phosphonate analogue of E4P to begin with, and examine this compound on DAH7P synthase, before investigating the homophosphonate analogue of E4P. Unfortunately, due to unforeseeable difficulties in the synthesis of the phosphonate analogue of E4P, the synthesis of the homophosphonate analogue of E4P was not investigated.

Although D-erythrose 4-phosphonate was not synthesised during this project, prior studies using D-glyceraldehyde 3-phosphate **1.24** (Figure 5.9) can be used to predict whether this analogue would be a substrate for DAH7P synthase or not.[24,32,47]

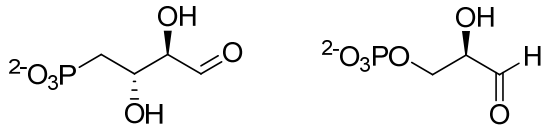

D-erythrose 4-phosphonate **1.24**

Figure 5.9: Structures of D-erythrose 4-phosphonate and D-glyceraldehyde 3-phosphate 1.24

Studies carried out on compound **1.24**, a substrate that is one carbon shorter than E4P, has shown that it is not a substrate for the type Iα *E. coli* DAH7P synthase (phe) and was due to the molecule being too short. The contracted chain of compound **1.24** would not allow the C1 carbonyl to be sufficiently close enough to interact with the metal atom (which activates the E4P for attack by PEP) and PEP in the active site resulting in catalysis not occurring. These results suggest that D-erythrose 4-phosphonate would not be a substrate for the enzyme as substitution of a phosphate moiety in E4P for a phosphonate would shorten the structure due to the loss of a bridging oxygen atom. The synthesis and testing of the homophosphonate analogue may help resolve whether chain length or phosphonate moiety is responsible for a lack of reactivity in DAH7P synthases.

For future investigations where D-erythrose 4-phosphonate is required, D-erythrose 4-phosphonate could be synthesised from the commercially available sugar: *meso*-tartaric acid (Figure 5.10). The structure of *meso*-tartaric acid is very similar to that of the target compound. It has the right number of carbons and the synthesis would not involve the cleavage of any carbons (c.f. the synthesis from D-glucose 6-phosphonate **4.14**), making it an ideal starting material. The conversion of *meso*-tartaric acid to D-erythrose 4-phosphonate would involve four key chemical manipulation steps of reduction, oxidation, bromination and phosphonylation.

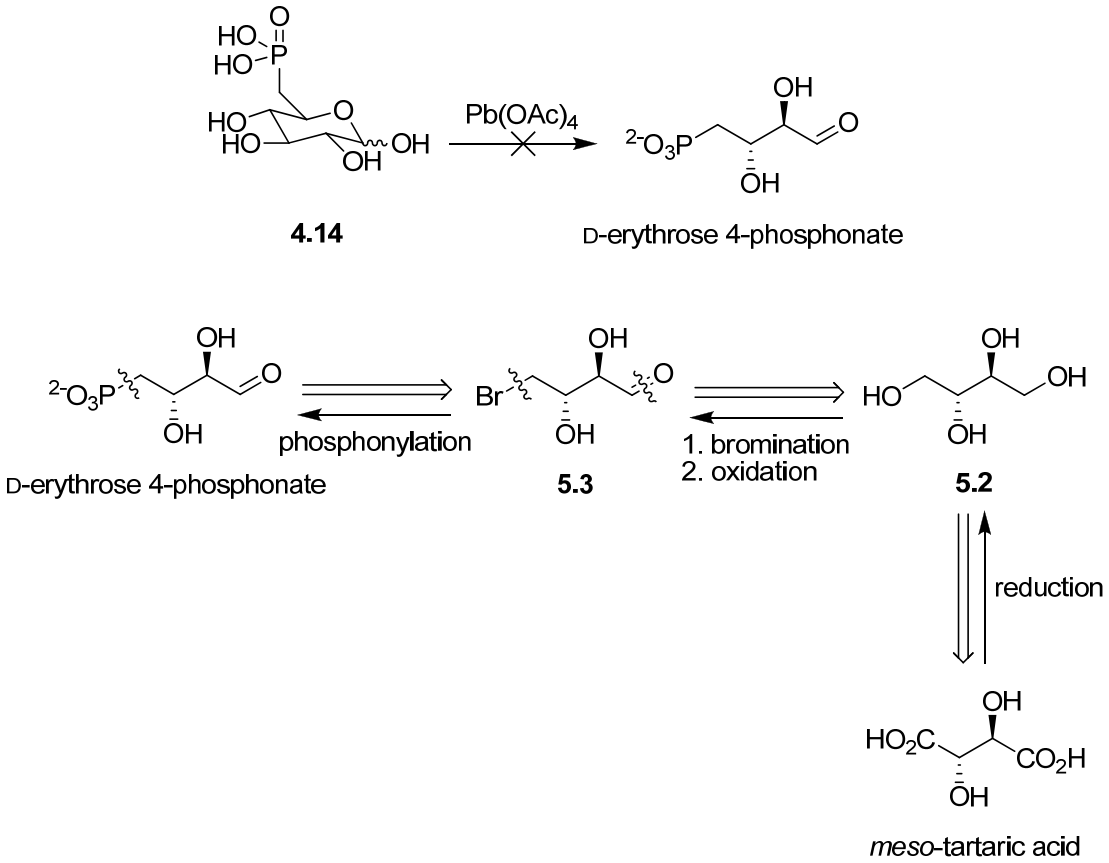

Figure 5.10: Attempts to synthesis D-erythrose 4-phosphonate from D-glucose 6-phosphonate 4.14 (Chapter 4), and the retrosynthetic analysis of D-erythrose 4-phosphonate to give *meso*-tartaric acid.

5.3.2 2,3-Dideoxy erythrose 4-phosphonate 4.38

Structures of DAH7P synthase with E4P modelled into the active site was used to infer information about why phosphonate **4.38** was not a substrate for the *E. coli* DAH7P synthase (phe) (Figure 5.2).[32,61] As mentioned previously, each hydroxyl group on E4P, either on C2 or C3, is not essential for binding and catalysis in the enzyme, and that the C3 hydroxyl group is more important than the C2 hydroxyl group. The hydroxyl groups however, seem to be required for the orientation and the positioning of E4P in a catalytically competent manner to allow E4P to be close enough to PEP and the metal ion. By removing both hydroxyls of E4P, the substrate would not be positioned and orientated in a competent manner, and compound **4.38** would not be utilised by DAH7P synthase. These results were parallel with the results reported for 2,3-dideoxy erythrose 4-phosphate, as this substrate was also found not to be a substrate for *E. coli* DAH7P synthase (phe) (Figure 5.11).[65,168] Although it should be noted that compound 4.38 is not really a particularly good test of the ability of

phosphonate groups to be incorporated in aldehydic substrates and was primarily synthesised for method development.

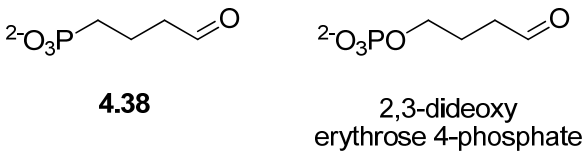

4.38 2,3-dideoxy erythrose 4-phosphate

Figure 5.11: Compound 4.38 and 2,3-dideoxy erythrose 4-phosphate.

5.4 Future directions

The investigations into the substrate specificity of DAH7P synthase has revealed a number of interesting insights which could now be used in the proposal of future studies in order to complete and advance the research presented here.

5.4.1 Isosteric phosphonates

The unique properties of phosphonate analogues of the natural phosphoric acid esters make them suitable for use in a continuously increasing variety of applications.[179] Replacement of a C-O-P moiety by a C-P group (non-isosteric phosphonates) or a C-CH_2-P group (homophosphonates) in a biologically-active molecule might be expected to have interesting biological effects.[139] This modification can confer greater stability on these analogues as the C-P bond that replaces the C-O-P bond is resistant to degradation by phosphatase enzymes and could aid in the development of prodrugs.[138]

Work conducted by Kabak *et al.*[180] and Shopsis *et al.*[181] demonstrated that the homophosphonate analogue of D-glycerol 3-phosphate (G3P) was a substrate for glycerol 3-phosphate dehydrogenase from *E. coli*, but the phosphonate analogue **5.4** was not (Figure 5.12). These studies concluded that the corresponding size of the analogue to the natural substrate was the deciding factor for activity i.e. compound **5.5** has a similar chain length to G3P.[136]

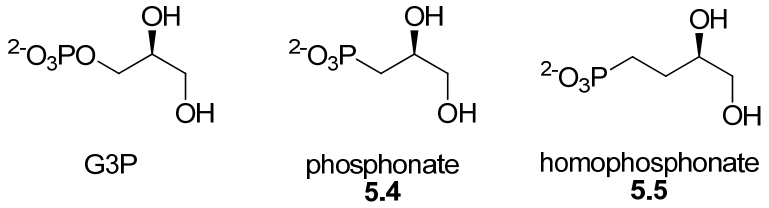

Figure 5.12: Phosphonate analogues of G3P.

To resolve whether chain length or phosphonate moiety is responsible for a lack of reactivity in DAH7P synthase, the homophosphonate analogue of E4P could be synthesised (Figure 5.13). The homophosphonate analogue of E4P would have a similar chain length to E4P, unlike the phosphonate analogue where the oxygen group is not present, as the oxygen group is replaced with a CH_2 group.

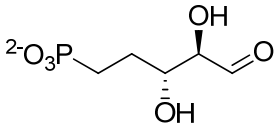

Figure 5.13: Homophosphonate analogue of E4P.

The retrosynthetic analysis of the homophosphonate analogue E4P is shown below (Figure 5.14). This analogue of E4P could be synthesised starting from *meso*-tartaric acid. The hydroxyl groups on tartaric acid would have to be protected, followed by reduction to give compound **5.2**, similar to the retrosynthetic analysis for the future synthesis of 2-methylE4P (Figure 5.10). One of the two primary hydroxyl groups on compound **5.2** would then undergo a homologation reaction, to extend the carbon chain length by one carbon. This homologation reaction can be achieved by first oxidising the primary hydroxyl group to give an aldehyde group followed by a Wittig reaction using the reagent $(PhO)_2P(O)CH{=}PPh_3$.[182-184] The other primary hydroxyl group would then be oxidised to give the aldehyde functionality.

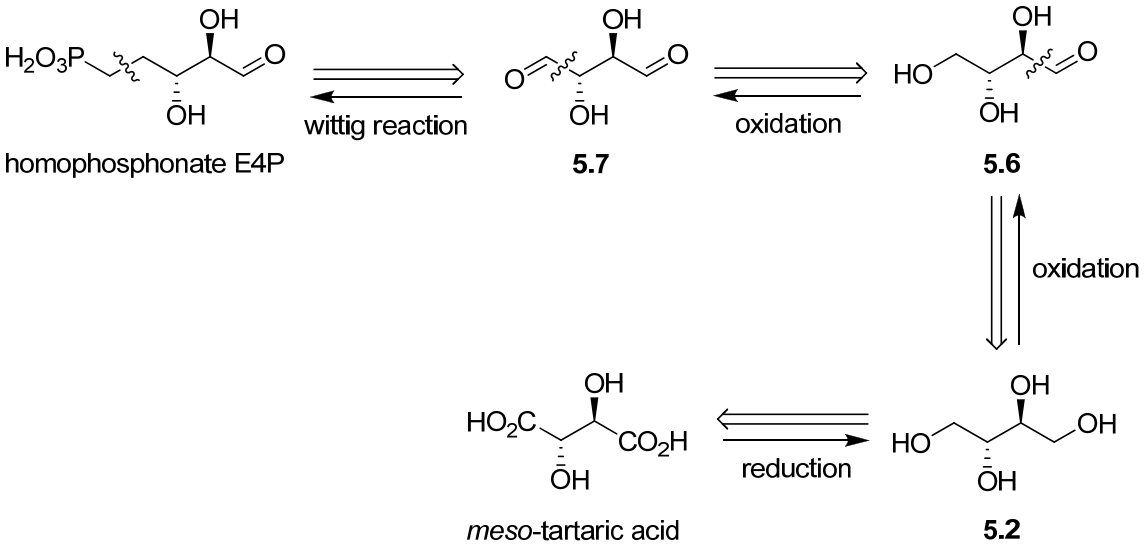

Figure 5.14: Retrosynthetic analysis of the homophosphonate analogue of E4P.

Other isosteric phosphonates could also be synthesised to probe the substrate specificity of DAH7P synthases and include the (3*S*)-2- and (2*R*)-3-deoxy erythrose 4-homophosphonates (Figure 5.15). This would allow further investigation into the requirements for E4P for catalysis and binding in DAH7P synthase. As we have seen both compound **4.38** and 2,3-dideoxy erythrose 4-phosphate were not substrates for DAH7P synthase, but the 2- and 3-deoxyE4P were, indicating removal of both hydroxyl groups of E4P stops binding and catalysis in DAH7P synthase, but removal of only one of the hydroxyl groups of E4P does not. Therefore, it would be interesting to see how DAH7P synthases would react to the homophosphonate analogues of 2- and 3-deoxyE4P.

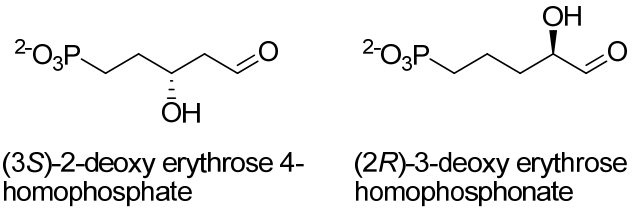

Figure 5.15: Homophosphonate analogues of 2- and 3-deoxyE4P.

The potential synthesis of (3*S*)-2-deoxy erythrose 4-homophosphonate could start with compound **2.14** that was used for the synthesis of (3*S*)-2-deoxyE4P in Chapter 2. The proposed synthetic scheme for the synthesis of the target compound (Figure 5.16) would require first synthesising compound **2.14** starting from β-hydroxy-γ-butyrolactone, followed by oxidation of the primary hydroxyl to give aldehyde **5.8**. A subsequent homologation

reaction of aldehyde **5.8** using a Wittig reaction, followed by deprotection steps would give (3*S*)-2-deoxy erythrose 4-homophosphonate.

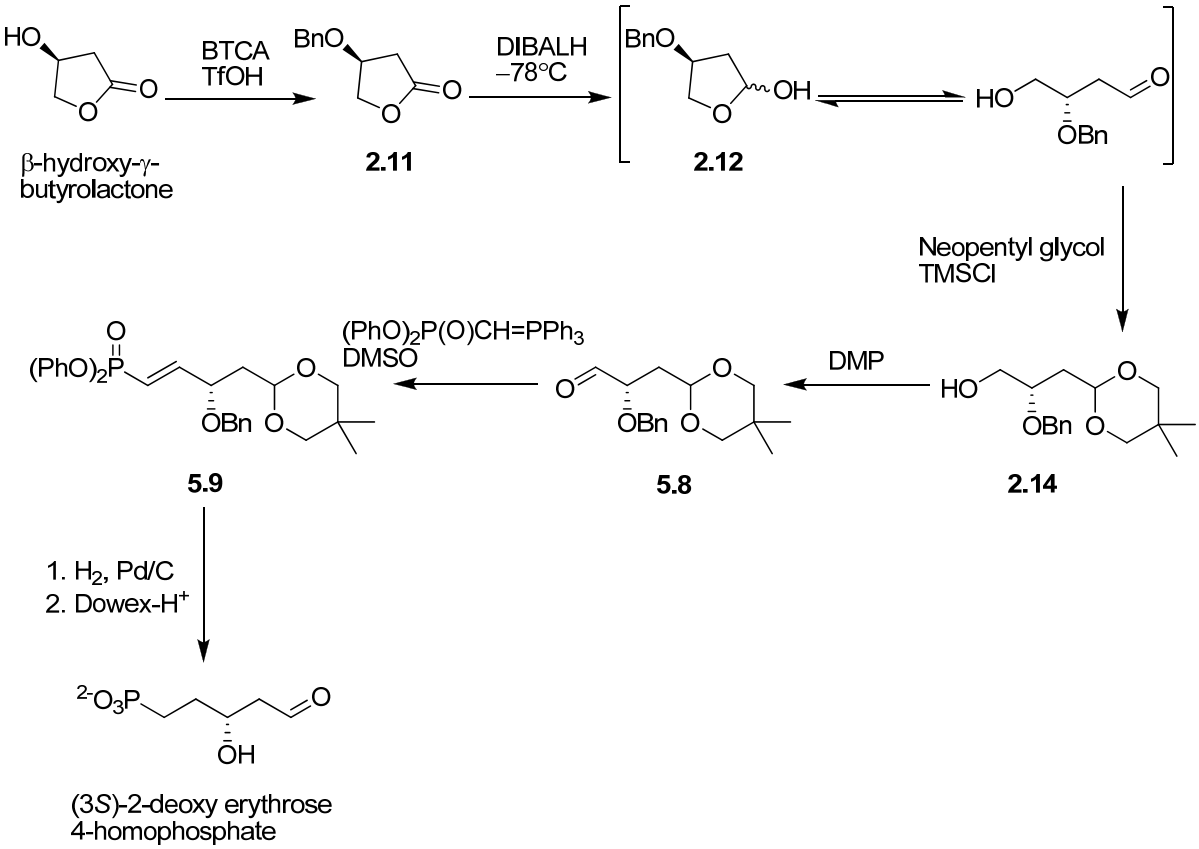

Figure 5.16: Proposed synthetic scheme for the synthesis of (3*S*)-2-deoxy erythrose 4-homophosphonate.

5.4.2 Fluorinated E4P analogues

Introduction of fluorine into a certain position of a bioactive compound can have strong influence on its activity[185], often caused by mimicking and blocking effects.[186] Because of the similarity in size of fluorine (van der Waals radius = 1.47 Å) to oxygen (van der Waals radius = 1.52 Å) and even hydrogen (van der Waals radius = 1.20 Å), it has been shown that microorganisms and enzymes often do not recognise the difference between a natural substrate and its analogue wherein a C-O or C-H bond of the substrate has been replaced with a C-F bond. This observation is the basis of what is regarded as the *mimic effect* of fluorine.[186,187] The blocking effect is the phenomenon that where the high electronegativity of a fluorine atom lowers the surrounding electron density, which prevents certain reactions, such as oxidation of hydroxyl or amino groups, from occurring. For example, fluticasone propionate (Flixotide™), an anti-inflammatory steroid for the treatment of asthma contains

fluorine at the 9α position. The role of the 9α-fluorine is to increase the acidity of the hydroxyl group at the 11 position, which promotes better binding to the enzyme active site and inhibits undesirable oxidation (Figure 5.17).[186]

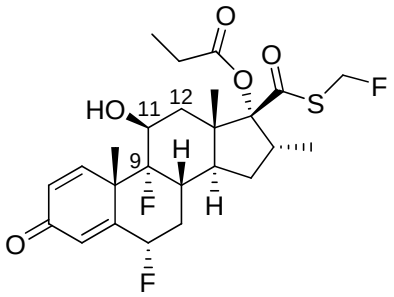

Figure 5.17: Fluticasone propionate (Flixotide™).

The synthesis of fluorinated analogues of E4P, 2- and 3-deoxyfluoroE4P, could prove to be very useful in probing the substrate specificity of DAH7P synthase. This is because fluorine has a similar electronegativity as a hydroxyl group, without the ability to be a hydrogen-bond donor, and is a similar size. The replacement of the C2 or C3 hydroxyl group of E4P with a fluorine would increase the acidity of the adjacent hydroxyl (blocking effect), potentially promoting better binding in the active site. Additionally, the increased electronic effects due to the incorporation of fluorine would draw electron density away from the carbonyl group of 2- or 3-deoxyfluoroE4P, further activating the carbonyl group for attack by PEP during the aldol reaction. This could potentially increase the catalytic efficiency of the enzyme catalysed reaction and would be more prevalent for 2-deoxyfluoroE4P due to the proximity of the fluorine group to the carbonyl group.

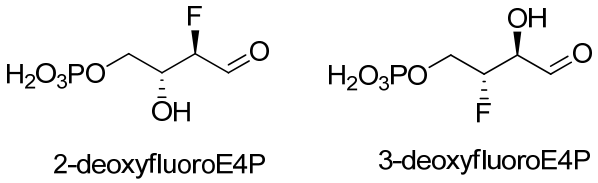

Figure 5.18: 2- and 3-DeoxyfluoroE4P analogues.

The retrosynthetic analysis of 2-deoxyfluoroE4P is shown in Figure 5.19. Both 2- and 3-deoxyfluoroE4P can both be synthesised from malic acid. The key step is the electrophilic fluorination of malic acid and could be achieved via a number of commercially available fluorinating reagents such *N*-fluorobenzenesulfonimide (NFSI) and Selectfluor® (Figure

5.20).[188-190] Methods for controlling the stereochemistry of this key step would have to be investigated, if enantiopure fluorinated analogues of E4P are required.

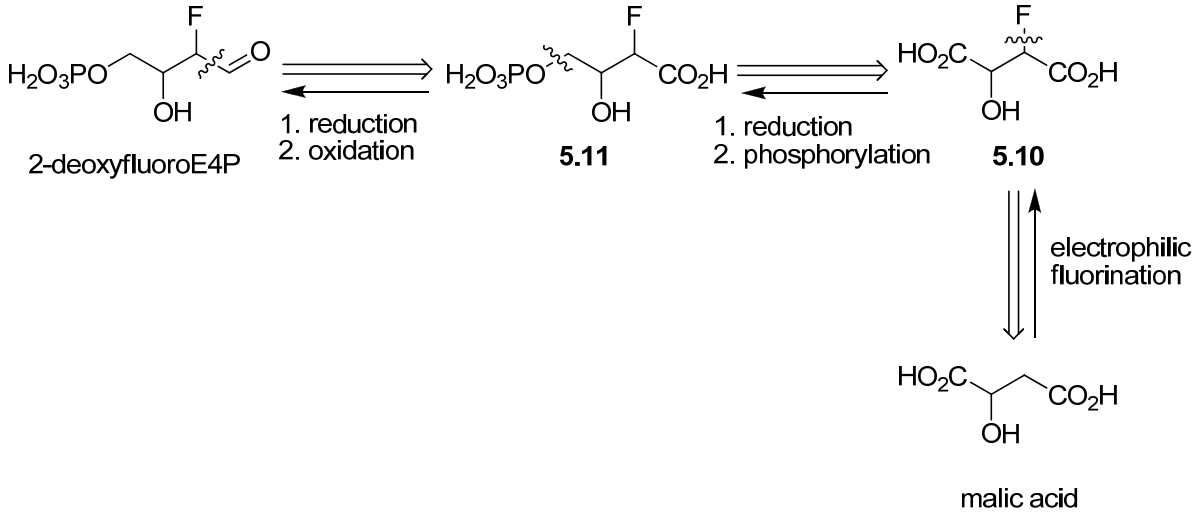

Figure 5.19: Retrosynthetic analysis of 2-deoxyfluoroE4P.

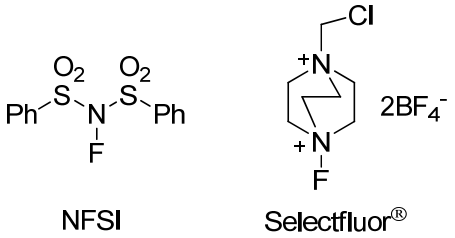

Figure 5.20: Electrophilic fluorinating regents.

5.5 Conclusions

This project describes the synthesis of a number of E4P analogues (2- and 3-deoxyE4P, 3-methylE4P and 2,3-dideoxy erythrose 4-phosphonate **4.38**) and the attempts to synthesise 2-methylE4P and D-erythrose 4-phosphate. The substrate specificity investigations of 2- and 3-deoxyE4P, 3-methylE4P and compound **4.38** on DAH7P synthases were also evaluated.

Chapter 6: Experimental

6.1 General chemical procedures

6.1.1 Reaction conditions and work up

All reactions were performed under an inert atmosphere of dry nitrogen (N_2), argon (Ar) or hydrogen (H_2) and were performed in oven- or flame-dried glassware unless otherwise stated. Crude organic extracts were dried with magnesium sulfate or sodium sulfate unless otherwise stated. Evaporations were performed on a rotary evaporator with the water bath temperature not exceeding 40°C unless otherwise stated. When necessary, a high vacuum pump (~0.1 mmHg) was used to remove the last traces of solvent from purified compounds. −78, −20 and −10°C cold baths were made using carbon dioxide/acetone, ice/salt and methanol/ice mixtures respectively.

6.1.2 Solvents and reagents

All chemical reagents and solvents used for experiments were purchased from commercially available sources and used as supplied unless otherwise noted.

Solvents were dried by standard methods prior to use.[177,191] Dimethylformamide (DMF) was sequentially dried over three batches of 3 Å molecular sieves (5% w/v, 12 hrs). Dichloromethane (DCM), toluene and diisopropylamine was distilled from CaH_2. Petroleum ether (pet ether) was distilled and the fraction at 40–60°C was collected for use. Ethyl acetate was distilled from CaH_2. Tetrahydrofuran and diethyl ether were freshly distilled from sodium wire/benzophenone. Pyridine was distilled from CaH_2 and stored over 4 Å molecular sieves. Cyclohexane was distilled, discarding the forerun, and stored over 4 Å molecular sieves. Analytical grade and HPLC grade acetone, methanol, and ethanol were used as supplied from commercial sources.

Silver oxide (Ag_2O) was freshly prepared using the published procedure[94]: A solution of 6.90 g (0.172 mol) of sodium hydroxide in 200 mL of water was heated to 80–90°C and added to a

solution of 30 g (0.177 mol) of silver nitrate in 200 mL of water, also heated to 80–90°C. The resulting hot suspension was quickly filtered, and the filter cake was washed with 200 mL of hot water and 200 mL of absolute ethanol (2x). The Ag_2O was dried under high vacuum overnight, weighed to give 17.8–18.3 g of Ag_2O (87–89%). Drying of Ag_2O was achieved by heating the wet Ag_2O at 45°C under high vacuum overnight before use.

2-Iodoxybenzoic acid (IBX) was prepared by oxidation of 2-iodobenzoic acid with Oxone® as previously described.[121] Dess-Martin periodinane was prepared by acetylation of IBX with hot Ac_2O and *p*-toluenesulfonic acid as previously described.[120] Cyclohexanone was dried over magnesium sulfate, filtered and distilled. Methyl iodide was poured through a short column of alumina to remove iodine then dried over calcium chloride before distillation. Benzyl alcohol was fractionally distilled under reduced pressure. Benzyl 2,2,2-trichloroacetimidate (BTCA) was freshly prepared using published procedures.[111,192] Butan-1,4-diol was distilled and stored over 4 Å molecular sieves. *N*-bromosuccinimide (NBS) was recrystallised from water, dried under high vacuum overnight and stored in the dark. Triethyl phosphite was distilled from sodium and stored over 3 Å or 4 Å molecular sieves. Lead tetraacetate ($Pb(OAc)_4$) was recrystallised using hot glacial acetic acid, any lead oxide was removed by filtration, and the white crystals of $Pb(OAc)_4$ was stored in a vacuum desiccator containing P_2O_5 overnight prior to use. Acetic acid was dried using Ac_2O (5% v/v) and distilled. Zinc chloride was subjected to high vacuum for 24 hrs prior to use. Lithium diisopropylamine (LDA) was prepared *in situ* according to the procedure by Seebach *et al.*[107] pH measurements were made using Whatman's full range pH paper.

Molecular sieves, 3 Å and 4 Å, were activated by heating under high vacuum using a hot air gun for 5–10 minutes, allowed to cool ~10 minutes (whilst still under high vacuum) and then repeated two more times. Rapid activation of molecular sieves was alternatively achieved by microwave irradiation (see Microwave); molecular sieves were subjected to microwave irradiation, on high for 30 sec, transferred to a dry glass container and then this process was repeated three to four times or till no condensation was seen forming on the glass container.

To prepare Dowex resin in its acidic form (Dowex-H^+), dowex resin was stirred in H_2O for 15 minutes then filtered and washed with H_2O. The resin was then stirred in 1.2 M HCl for 15 minutes and then filtered and washed with 1.2 M HCl. The resin was then washed with H_2O until the filtrate ran neutral to pH paper, then air-dried before use. Dowex resin in their

potassium form were prepared by washing the acidic resin well with 10% w/v KOH, then with H_2O until the filtrate ran neutral to pH paper, then air-dried.

Commercial solutions of *n*-butyllithium (*n*-BuLi) were quantified as required by a modification of a literature procedure[193]: titration of *n*-BuLi using a known quantity of diphenylacetic acid (~0.50 g) dissolved in 10 mL of dry THF, using an accurate syringe. The solution went from colourless to pale yellow at the end point of titration. A white precipitate sometimes formed as the end point approached. Titrations were performed at room temperature, under nitrogen with vigorous stirring and the concentration was taken from a mean of two concordant results.

6.1.3 Chromatography

Thin layer chromatography (TLC) was performed on Merck Kieselgel 60F254 pre-coated aluminium-backed plates. Visualisation of the plates was achieved using a UV lamp (254 nm), followed routinely by staining with basic aqueous potassium permanganate dip and heating with a hot air gun. Other visualisation dips included acidified ethanolic vanillin, ethanolic phosphomolybdic acid (PMA), acidified aqueous ammonium molybdate and 50% ethanolic H_2SO_4.[177,191]

Flash column chromatography was performed using Silica 60 230-400 mesh. Chromatographic EtOAc was distilled prior to use from CaH_2; Pet ether was distilled; analytical grade $CHCl_3$ and MeOH was used as supplied.

For acid sensitive compounds the silica was deactivated (reducing its acidity) before the sample was loaded. A solvent system containing 1-3% triethylamine was prepared. The column was packed using this system and flushed with solvent equal to the volume of the silica, and the eluant was discarded.

Reverse phase C18 column chromatography were carried out on reverse phase C18 silica, kindly donated by Professor Murray Munro of the Marine group at the University of Canterbury. C18 silica was loaded into a column using a MeOH slurry, followed by washing the column through with (1) 50% MeOH:H_2O; (2) 30% MeOH:H_2O and finally with 10%

MeOH:H_2O. Samples dissolved in water or MeOH was loaded onto the column. Gradient elution, usually 10% MeOH:H_2O to 100% methanol, was used to elute samples. Reverse phase C18 TLC plates were used to monitor the fractions unless otherwise stated. Regeneration of reverse phase C18 silica was accomplished by flushing the column with CH_3CN followed by several flushes with MeOH. The reverse phase C18 silica can be air dried or can be dried by careful use of a rotary evaporator. All solvents were HPLC grade; water was distilled.

6.1.4 Microwave

Microwave irradiations were performed in a domestic 1100 W microwave oven, modified to include a reflux condenser and inert gas source.

6.1.5 Hydrogenator

Hydrogenation reactions that require high pressures were carried out in a Parr series 4842 hydrogenator.

6.1.6 NMR spectroscopy

Proton (^1H) nuclear magnetic resonance spectra (δH) were recorded on a Varian INOVA 300 (300 MHz) or a Varian VNMR 500 (500 MHz) spectrometer and were calibrated according to the chemical shift of residual protons in the deuterated solvent stated. ^{13}C NMR spectra (δC) were recorded on a Varian INOVA 300 (75 MHz) or a Varian VNMR 500 (125 MHz) spectrometer and were calibrated according to the chemical shift of the deuterated solvent stated. ^{31}P NMR spectra (δP) were recorded on a Varian INOVA 300 (121 MHz) spectrometer and were calibrated to 85% phosphoric acid in the deuterated solvent stated. 2D NMR experiments were carried out on a Varian VNMR 500 (500 MHz) spectrometer. Assignment of ^1H and ^{13}C NMR signals were determined by COSY, HSQC and HMBC. All chemical shifts are quoted in parts per million (ppm) and coupling constants (*J*) in hertz (Hz). For acid sensitive compounds, 0.1% (v/v) of C_5D_5N (deuteropyridine) was added to the $CDCl_3$ solvent.

6.1.7 Mass spectrometry

High-resolution mass spectra were recorded on a Bruker maXis 3G with electrospray ionisation (positive or negative ion electrospray ionisation (ESI) techniques) or a Micromass LCT spectrometer (ESI^+ or ESI^-), both at the University of Canterbury.

6.1.8 Melting points

Melting points (mp) were recorded on an Electrothermal IA6304 melting point block and are uncorrected.

6.1.9 Freeze drying/lyophilisation

Samples to be freeze dried were frozen using liquid nitrogen and placed for 1–2 days on a Christ® freeze dryer, model Alpha I/5.

6.2 General biochemical procedures

6.2.1 UV-Visible spectrometry

UV-Visible spectrophotometry was carried out on a Varian Cary® One UV-Visible spectrophotometer at 25 or 30°C (as indicated) in a stoppered quartz cell. The temperature was continuously controlled using a jacketed multicell holder, connected to an external Varian Peltier temperature controller filled with water or ethylene glycol.

6.2.2 Buffers

Chemicals used for buffer preparation were purchased from commercially available sources.

MilliQ H_2O used to make aqueous buffers was treated with Chelex® resin for one hour then filtered through a 0.2 μm membrane before use.

BTP (bis-tris propane) buffers were prepared by dissolving sufficient BTP in MilliQ water to give a 50 mM solution and the solution was adjusted to the appropriate pH using HCl or NaOH solutions. The resulting mixture was treated with Chelex® resin for two hours, filtered through a 0.2 μm membrane, snap frozen using liquid nitrogen and stored at −20°C till required. The following buffers were used in standard assays for the following enzymes:

E. coli DAH7P synthase (phe) – 50 mM BTP, pH 6.8 at 25°C
M. tuberculosis DAH7P synthase – 50 mM BTP, 1 mM TCEP, pH 7.5 at 30°C
N. meningitidis DAH7P synthase – 50 mM BTP, pH 6.8 at 25°C

Stock solutions of PEP and E4P were prepared from monopotassium-PEP (Sigma) and sodium-E4P (Sigma) respectively, in BTP buffers. The stock solutions were filtered through a 0.2 μm membrane. Both PEP and E4P solutions were frozen and stored at −20°C. Stock solutions of manganese (II) sulfate were prepared in MilliQ H_2O at 10 mM and were filtered through a 0.2 μM membrane and stored frozen at −20°C.

6.2.3 Enzymes

Purified *E. coli* DAH7P synthase were kindly supplied by Penelope Cross, Dmitri Joseph and Dr Steve McNabb. Purified *M. tuberculosis* DAH7P synthase was kindly supplied by Dr Richard Hutton. *N. meningitidis* DAH7P synthase was kindly supplied by Penelope Cross. These enzymes were kept in aliquots by flash freezing in liquid nitrogen and stored at −80°C.

6.2.4 pH measurements

The pH of buffers used in this project were measured using a UB10 Ultrabasic Benchtop pH meter from Denver Instrument Company. For pH measurements in narrow containers e.g. test tubes, 1 mL eppendorf tubes; a pH micro glass-body combination pH electrode was used (Denver Instrument Company). The pH of solutions was adjusted using 1–10 M NaOH or 1–12 M HCl. pH probes were calibrated before use.

6.2.5 Standard enzyme assays

All standard enzyme assays were performed in a total volume of 1 mL, in 1 cm path length quartz cuvettes. Enzyme activity was monitored by UV-Visible spectrophotometry, following the decrease in absorbance at 232 nm as the enol alkene of PEP is consumed (ε = 2.8 x 103 $M^{-1}cm^{-1}$ at 25°C). Standard reaction mixtures contained PEP, E4P (or alternative substrate), metal and buffer in the cuvette. Cuvettes were mixed by inverting the stoppered cuvette three times and then incubated in the spectrophotometer for five minutes before initiation with enzyme. Assays were carried at 25°C for *E. coli*, *N. meningitidis* and 30°C for *M. tuberculosis*. One unit (1 U) of activity is defined as the loss of 1 μmol of PEP per minute at the stated temperature. Specific activity (U/mg) is defined as the loss of 1 μmol of PEP per minute at the stated temperature per mg of protein. K_M and k_{cat} values were determined by fitting the data to the Michaelis–Menten equation using GraFit (Erithacus Software). Allowance was made for the change in absorbance due to initiation by addition of the enzyme.

6.2.6 Determination of substrate concentrations

2-DeoxyE4P, 3-deoxyE4P and E4P substrate concentrations were determined using standard enzyme assays. For example, to determine the concentration of 2-deoxyE4P a reaction mixture consisting of <100 μM PEP, ~100 μM $MnSO_4$ and ~5 μL 2-deoxyE4P solution (of unknown concentration) is made up in BTP buffer and initiated with enzyme to give a final volume of 1 mL. The reaction is allowed to go to completion and the difference between the absorbance before initiation and the absorbance after completion (ΔA1) is measured. An identical reaction is set up in the absence of 2-deoxyE4P to determine how much change in absorbance is due to the addition of the enzyme (ΔA2). The correct change in absorbance is given by ΔA1 + ΔA2. To convert absorbance into concentration Beer's Law is applied (A = ε.c.l. where l = 1 cm and ε_{PEP} = 2.8 x 10^3 $M^{-1}cm^{-1}$).

6.2.7 Lanzetta assay for the detection of phosphates

The Lanzetta reagent was prepared fresh prior to use by the following preparations[93]:

3 parts 0.045% w/v malachite green oxalate in H_2O
1 part 4.2% w/v ammonium molybdate in 4 M HCl
0.1 parts 1.5% v/v Triton X-100

The components were mixed in the dark and stirred for 30 minutes before filtering through a 0.45 μM filter before use (pale yellow solution). For qualitative detection of products, 25 μL of Lanzetta reagent was added to 150 μL of sample and incubated for 30 minutes. The change in absorbance due to organic phosphate cleavage in an acidic environment was detected visually over a white surface (green for positive test). For quantitative analysis of substrate solutions, 300 μL of sample is mixed with 10 μL of calf alkaline phosphatase solution (10 units/mL, in 4 mM $MgCl_2$) and incubated for at least three hours. A 100 μL digest sample was then mixed with 700 μL of Lanzetta reagent, mixed and left at room temperature for 20 minutes before the absorbance was determined at 630 nm. A calibration curve for the determination of phosphate concentration was obtained from analogous analysis using samples of appropriate concentrations (5–150 μM) of KH_2PO_4 which had been dried in high vacuum for at least three hours before use. As a control, a glucose 6-phosphate (G6P) solution of known concentration was also digested with calf alkaline phosphatase and analysed.

6.2.8 Determination of the utilisation of racemic substrates by *M. tuberculosis* and *E. coli* DAH7P synthase

Rac-3-deoxyE4P

A solution containing G6P (mono-sodium salt) (25μL, ~4 mM in D_2O), rac-3-deoxyE4P (25 μL from a 6-fold diluted solution in H_2O, pH = 7.5, unknown concentration) and 200 μL of D_2O was added to a 3 mm NMR tube. A standard ^{31}P NMR (^{1}H-decoupled, 202 MHz, relaxation delay (d1) = 1 s, acquisition time = ~19 hours) spectrum was collected and the peaks due to rac-3-deoxyE4P (3.35 ppm) and G6P (1.73 ppm) were integrated to give a relative concentration of 1(G6P):1.56(rac-3-deoxyE4P).

G6P (above solution, ~4 mM in D_2O) was diluted 4-fold with H_2O (~1 mM) and its pH adjusted to 7–8 using $NaOH_{(aq)}$. A Lanzetta assay was run on this sample to determine an accurate concentration of G6P.

The amount of 3-deoxyE4P can be calculated using the concentration of G6P and the relative concentration of 3-deoxyE4P to G6P in the ^{31}P NMR spectrum and accounting for all dilutions: 1.56 x 4.29 x 6 = 40.15 mM. This is the concentration of both enantiomers of rac-3-deoxyE4P in solution.

Assays with *M. tuberculosis* DAH7P synthase contained an unknown concentration of rac-3-deoxyE4P (5 μL of the original undiluted solution), PEP (300 μM) and $MnSO_4$ (100 μM) in 50 mM BTP buffer containing 1 mM TCEP at pH 7.5. Reactions were initiated by the addition of *M. tuberculosis* DAH7P synthase (3 μL, 1.4 mg/mL) to give a final volume of 1 mL. Assays were carried out at 30°C. The control assays used to determine the absorbance increase due to the addition of enzyme used 5 μL of buffer in the place of the 5 μL of rac-3-deoxyE4P but were otherwise identical to the experimental assays. The decrease in absorbance due to the loss of PEP was monitored at 232 nm ($\varepsilon = 2.8 \times 10^3$ $M^{-1}cm^{-1}$ at 25°C) to completion and the concentration of rac-3-deoxyE4P consumed by the enzyme calculated from the change in absorbance observed after correction for the blank assay containing no rac-3-deoxyE4P. Assays were carried out in duplicate and averaged.

Results:

[G6P] determined from Lanzetta assay = 4.29 mM

Average [rac-3-deoxyE4P] determined from enzyme assay = 22.86 mM

[rac-3-deoxyE4P] determined from ^{31}P NMR experiment = 40.15 mM

From these results we can see that the concentration determined from the use of 3-deoxyE4P in solution is approximately half (0.57) that of the total concentration, consistent with the enzyme (*M. tuberculosis* DAH7P synthase) only using one enantiomer.

Determination of the utilisation of racemic substrates by *E. coli* DAH7P synthase

Assays with DAH7P synthase contained an unknown concentration of rac-3-deoxyE4P (5 μL), PEP (300 μM) and $MnSO_4$ (100 μM) in 50 mM BTP buffer at pH 6.8. Reactions were initiated by the addition of *E. coli* DAH7P synthase (3 μL, 5.86 mg/mL) to give a final volume of 1 mL. Assays were carried out at 25°C. The decrease in absorbance due to the loss of PEP was monitored at 232 nm ($\varepsilon = 2.8 \times 10^3$ $M^{-1}cm^{-1}$ at 25°C) to completion. The change in absorbance ($\Delta A1 = 0.74$) was recorded. A similar assay was carried out on rac-3-deoxyE4P (5 μL, unknown concentration), PEP (300 μM) and $MnSO_4$ (100 μM) in 50 mM BTP buffer containing 1 mM TCEP at pH 7.5, 30°C), but initiated with *M. tuberculosis* DAH7P synthase (3 μL, 1.4 mg/mL) and the change in absorbance ($\Delta A2 = 0.34$) was recorded. The absorbance loss using the same amount of rac-3-deoxyE4P with *E. coli* DAH7P synthase was 2.2 times higher than that observed when the *M. tuberculosis* enzyme was employed, indicating that in contrast to *M. tuberculosis* DAH7P synthase, *E. coli* DAH7P synthase utilises both enantiomers of the racemic mixture.

Rac-2-deoxyE4P

Rac-2-deoxyE4P was diluted 4-fold with H_2O and its pH adjusted to 7–8 using $NaOH_{(aq)}$. A Lanzetta assay was run on this sample.

Assays with DAH7P synthase contained an unknown concentration of rac-2-deoxyE4P (10 μL of the original solution), PEP (300 μM) and $MnSO_4$ (100 μM) in 50 mM BTP buffer containing 1 mM TCEP at pH 7.5. Reactions were initiated by the addition of *M. tuberculosis*

DAH7P synthase (3 μL, 1.4 mg/mL) to give a final volume of 1 mL. Assays were carried out at 30°C. The control assays used to determine the absorbance increase due to the addition of enzyme contained no rac-2-deoxyE4P, but were otherwise identical to the experimental assays. The decrease in absorbance due to the lost of PEP was monitored at 232 nm (ε = 2.8 x 10^3 $M^{-1}cm^{-1}$ at 25°C) to completion and the concentration of 2-deoxyE4P consumed by the enzyme calculated from the change in absorbance observed after correction for the blank assay containing no 2-deoxyE4P. Assays were carried out in duplicate and averaged.

Results:

Average [rac-2-deoxyE4P] determined from enzyme assay = 13.2 mM

[rac-2-deoxyE4P] determined from Lanzetta assay = 23.6 mM

From these results we can see that the concentration determined from the use of 2-deoxyE4P in solution is approximately half (0.56) that of the total concentration consistent with the enzyme (*M. tuberculosis* DAH7P synthase) only using one enantiomer of the racemic mixture.

6.2.9 Thiobarbituric assay

Thiobarbituric acid assay reagents:

25 mM sodium periodate ($NaIO_4$) in 0.0625 M H_2SO_4

Sodium metaarsenite ($NaAsO_2$) 2% w/v in 0.5 N HCl

Thiobarbituric acid solution (0.36 % w/v, pH = 9 adjusted with NaOH)

A standard enzyme assay was carried out with 3-deoxyE4P (~150 μM), PEP (200 μM) and $MnSO_4$ (100 μM). The reaction was initiated with enzyme (3 μL). When the assay had completed, an aliquot (100 μL) of the assay mixture was transferred to a small round bottom flask. Water (50 μL) and $NaIO_4$ (100 μL in 0.0625 M H_2SO_4) were added. The mixture was stirred and heated at 60°C for one hour. The excess oxidising agent was reduced by the addition of 200 μL of $NaAsO_2$. Following the disappearance of the yellow colour, 1 mL of thiobarbituric acid solution was added and the reaction mixture was then stirred and heated at

100°C for 10 minutes. Once the sample was cool, the absorbance at 549 nm was measured ($\varepsilon = 1.03 \times 10^5 M^{-1}cm^{-1}$).[24,96]

6.2.10 Biological structures

All protein structures were drawn from files downloaded from the Protein Data Bank and drawn using the PyMol Molecular Graphics System Version 1.3, Schrödinger, LLC.

6.3 Experimental procedures

6.3.1 Experimental for Chapter 2

Synthesis of 2.1

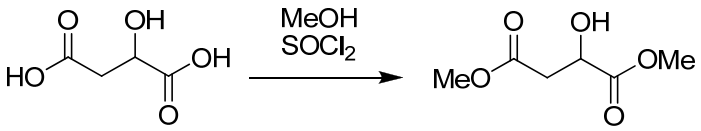

DL-malic acid **2.1**

$SOCl_2$ (2.40 mL) was added dropwise to a solution of DL-malic acid (2.0024 g, 15 mmol) in MeOH (20 mL) at 0°C. The solution was stirred at room temperature for 24 hours then concentrated under reduced pressure. Flash chromatography (1:1 EtOAc:Pet ether) gave **2.1** (2.4034 g, 99%) as a light yellow oil with spectral data in accordance with the literature.[194,195]

^{1}H NMR (500 MHz, *$CDCl_3$*) ppm 4.52 (q, *J* = 5.5 Hz, 1H, H2), 3.82 (s, 3H, OCH_3), 3.72 (s, 3H, OCH_3), 2.95-2.74 (m, 2H, H3).
^{13}C NMR (126 MHz, *$CDCl_3$*) δ ppm 173.9, 171.2, 67.4, 53.1, 52.2, 38.6.
HRMS (ESI): calc. $C_6H_{10}NaO_5$ $[M+Na]^+$: 185.0420; found: 185.0427.
R_f (1:1 EtOAc:Pet ether) = 0.3.

Synthesis of 2.2

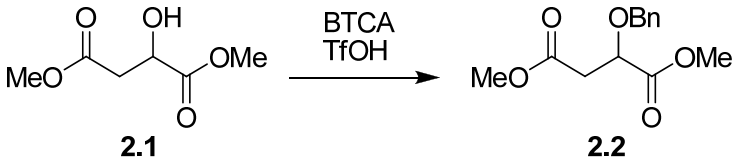

2.1 **2.2**

Alcohol **2.1** (1.0063 g, 6.0 mmol) was dissolved in DCM (40 mL) and cyclohexane (20 mL) and cooled to 0°C. Benzyl 2,2,2-trichloroacetimidate (BTCA, 2.90 mL, 16 mmol) was added followed by dropwise addition of TfOH (270 µL, 3.0 mmol). The mixture was stirred overnight at room temperature before additional BTCA (1.2 mL, 6.0 mmol) and TfOH (140 µL, 1.6 mmol) were added at 0°C. After a further 24 hours of stirring at room temperature the reaction was quenched by the addition of sat. $NaHCO_3$, extracted with DCM, dried and concentrated. Flash chromatography (10 to 20% EtOAc:Pet ether) gave **2.2** (1.1746 g, 75%) as an oil with spectral data in accordance with the literature.[102]

^{1}H NMR (500 MHz, *$CDCl_3$*) δ ppm 7.48-7.20 (m, 5H, Ph), 4.77 (d, *J* = 11.4 Hz, 1H, C$\underline{H}_2$Ph), 4.54 (d, *J* = 11.4 Hz, 1H, C$\underline{H}_2$Ph), 4.40 (dd, *J* = 5.1, 7.7 Hz, 1H, H2), 3.77 (s, 3H, OCH_3), 3.69 (s, 3H, OCH_3), 2.89-2.75 (m, 2H, H3).
^{13}C NMR (126 MHz, $CDCl_3$) δ ppm 172.1, 170.7, 137.4, 128.6, 128.3, 128.2, 74.7 (C2), 73.3 ($\underline{C}H_2$Ph), 52.5 (OCH_3), 52.2 (OCH_3), 38.0 (C3).
HRMS (ESI): calc. $C_{13}H_{16}NaO_5$ $[M+Na]^+$: 275.0890; found: 275.0897.
R_f (20% EtOAc:Pet ether) = 0.3.

Synthesis of 2.3

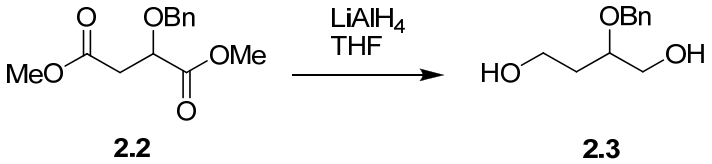

2.2 **2.3**

$LiAlH_4$ (0.9351 g, 25 mmol) was suspended in THF (30 mL) and cooled to 0°C. Compound **2.2** (2.0692 g, 8.0 mmol) in THF (20 mL) was added dropwise to this cooled suspension over 10 minutes. The reaction was then heated to reflux for four hours. After cooling to 0°C the solution was quenched slowly by the addition of ice, followed by 3 M NaOH, until

effervescence had ceased and a white solid had formed. The mixture was filtered through celite, the celite washed with ether and the filtrate dried and evaporated. Flash chromatography (3:1 EtOAc:Pet ether) gave **2.3** (1.0082 g, 63%) with spectral data in accordance with the literature.[102]

^{1}H NMR (500 MHz, *CDCl$_3$*) δ ppm 7.54-7.22 (m, 5H, Ph), 4.66-4.59 (m, 2H, C$\underline{H}_2$Ph), 3.83-3.70 (m, 4H, H1, H2, H4a), 3.62 (dd, *J* = 4.4, 11.7 Hz, 1H, H4b), 1.96-1.79 (m, 2H, H3).
^{13}C NMR (126 MHz, *CDCl$_3$*) δ ppm 138.3, 128.8, 128.2, 128.1, 78.0 (C2), 71.9 (C$\underline{H}_2$Ph), 64.2 (C4), 59.8 (C1), 34.1 (C3).
HRMS (ESI): calc. $C_{11}H_{16}NaO_3$ $[M+Na]^+$: 219.0992; found: 219.0996.
R_f (2:1 EtOAc:Pet ether) = 0.1.

Synthesis of 2.4

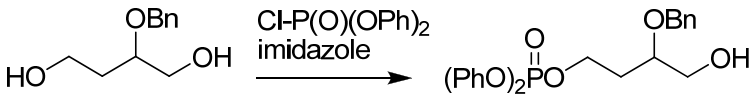

2.3 **2.4**

To a solution of diol **2.3** (0.2236 g, 1.14 mmol) in DCM (10 mL) was added diphenylchlorophosphate (210 µL, 1.01 mmol) and imidazole (0.3099 g, 4.55 mmol) at 0°C. The solution was allowed to warm slowly to room temperature by allowing the cooling bath to melt, and stirred overnight. The reaction was quenched with H_2O and washed with sat. $NaHCO_3$, sat. NaCl and extracted with DCM. The combined organic extracts were dried over $MgSO_4$ and the solvent removed *in vacuo*. Flash chromatography (gradient elution 30 to 75% EtOAc:Pet ether) gave **2.4** (87.2 mg, 18%) as well as the diphosphorylated compound **2.6** (45.6 mg, 6%, R_f (2:1 EtOAc:Pet ether) = 0.8), a further monophosphorylated compound **2.5** (28.7 mg, 6%, R_f (2:1 EtOAc:Pet ether) = 0.4) and starting material **2.3** (52.8 mg, 24% recoverd).

^{1}H NMR (500 MHz, *CDCl$_3$*) δ ppm 7.51-7.05 (m, 15H, Ph), 4.53 (ABq, *J* = 11.4 Hz, 2H, C$\underline{H}_2$Ph), 4.44-4.36 (m, 2H, H4), 3.75 (dd, *J* = 3.7, 11.7 Hz, 1H, H1), 3.65 (dq, *J* = 4.2, 8.0 Hz, 1H, H2), 3.50 (dd, *J* = 4.8, 11.7 Hz, 1H, H1), 2.07-1.89 (m, 2H, H3), 1.62 (br. s, 1H, OH).

^{13}C NMR (126 MHz, *CDCl$_3$*) δ ppm 150.7 (d, *J* = 7.4 Hz), 138.2, 130.0, 128.8, 128.1, 128.0, 125.6, 120.3 (d, *J* = 5.1 Hz), 76.0 (C2), 72.3 (CH_2Ph), 66.2 (d, $^2J_{POC}$ = 6.1 Hz, C4), 63.9 (C1), 32.3 (d, $^3J_{POCC}$ = 7.0 Hz , C3).

^{31}P NMR (121 MHz, *CDCl$_3$*) δ ppm −11.90.

HRMS (ESI): calc. $C_{23}H_{25}NaO_6P$ $[M+Na]^+$: 451.1281; found: 451.1296.

R_f (2:1 EtOAc:Pet ether) = 0.5.

Synthesis of 2.7

2.4 **2.7**

Compound **2.4** (0.2090 g, 0.49 mmol) was dissolved in DCM (15 mL) and freshly prepared Dess-Martin periodinane (0.4184 g, 0.99 mmol) was added. The mixture was stirred overnight at room temperature before an additional portion of Dess-Martin periodinane (0.2088 g, 0.49 mmol) was added. After a further five hours of stirring, sat. $Na_2S_2O_3$ and sat. $NaHCO_3$ were added and stirred till the solution was clear. The aqueous layer was extracted with DCM (3x) and the combined organic extracts were dried over $MgSO_4$. Removal of the solvent *in vacuo*, followed by flash chromatography (30 to 50% EtOAc:Pet ether) gave **2.7** (0.1762 g, 85%).

^{1}H NMR (500 MHz, *CDCl$_3$*) δ ppm 9.62 (s, 1H, H1), 7.47-7.10 (m, 15H, Ph), 4.64 (d, *J* = 11.4 Hz, 1H, CH_2Ph), 4.52 (d, *J* = 11.4 Hz, 1H, CH_2Ph), 4.46-4.39 (m, 2H, H4), 3.92 (dd, *J* = 4.0, 8.4 Hz, 1H, H2), 2.19-2.09 (m, 1H, H3a), 2.02-1.93 (m, 1H, H3b).

^{13}C NMR (126 MHz, $CDCl_3$) δ ppm 202.5, 150.4 (d, *J* = 7.4 Hz), 136.9, 129.8, 128.6, 128.3, 128.1, 125.5, 120.1 , 79.6 (C2), 73.1 (CH_2Ph), 64.6 (d, $^2J_{POC}$ = 6.0 Hz, C4), 31.0 (d, $^3J_{POCC}$ = 7.0 Hz, C3).

^{31}P NMR (121 MHz, *CDCl$_3$*) δ ppm −11.99.

HRMS (ESI): calc. $C_{23}H_{23}NaO_6P$ $[M+Na]^+$: 449.1124; found: 449.1138.

R_f (30% EtOAc:Pet ether) = 0.2.

Synthesis of 2.8

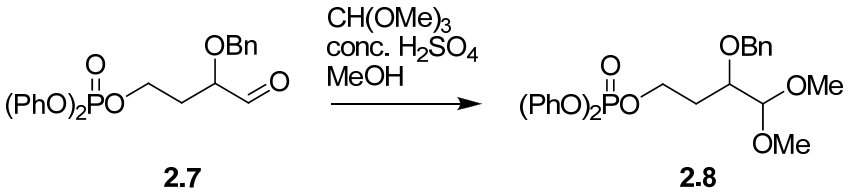

2.7 **2.8**

To **2.7** (0.1673 g, 0.39 mmol) in MeOH (8.0 mL) was added trimethyl orthoformate (430 µL, 3.93 mmol) and conc. H_2SO_4 (4.20 µL, 0.079 mmol). After stirring overnight, the mixture was transferred into a separating funnel containing sat. $NaHCO_3$ and Et_2O. The aqueous layer was washed with Et_2O (3x). The combined organic extracts were washed with sat. NaCl, dried ($MgSO_4$) and the solvent removed *in vacuo*. Flash chromatography using deactivated silica (30% EtOAc:Pet ether) gave **2.8** (0.1735 g, 94%).

^{1}H NMR (500 MHz, *CDCl*$_3$) δ ppm 7.41-7.09 (m, 15H, Ph), 4.69 (d, *J* = 11.0 Hz, 1H, C$\underline{H}_2$Ph), 4.49 (d, *J* = 11.4 Hz, 1H, C$\underline{H}_2$Ph), 4.43-4.38 (m, 2H, H4), 4.24 (d, *J* = 5.1 Hz, 1H, H1), 3.63-3.57 (m, 1H, H2), 3.43 (s, 3H, OCH_3), 3.39 (s, 3H, OCH_3), 2.13-2.03 (m, 1H, H3a), 1.90-1.80 (m, 1H, H3b).

^{13}C NMR (126 MHz, *CDCl*$_3$) δ ppm 150.8 (d, *J* = 7.4 Hz), 138.5, 130.0, 128.6, 128.2, 127.9, 125.5, 120.3 (d, *J* = 5.1 Hz), 106.9 (C1), 75.8 (C2), 73.6 (C$\underline{H}_2$Ph), 66.3 (d, $^2J_{POC}$ = 6.5 Hz, C4), 56.0 (OCH_3), 55.5 (OCH_3), 31.2 (d, $^3J_{POCC}$ = 7.4 Hz, C3).

^{31}P NMR (121 MHz, *CDCl*$_3$) δ ppm −11.94.

HRMS (ESI): calc. $C_{25}H_{29}NaO_7P$ $[M+Na]^+$: 495.1543; found: 495.1553.

R$_f$ (1:1 EtOAc:Pet ether) = 0.6.

Synthesis of rac-3-deoxyE4P

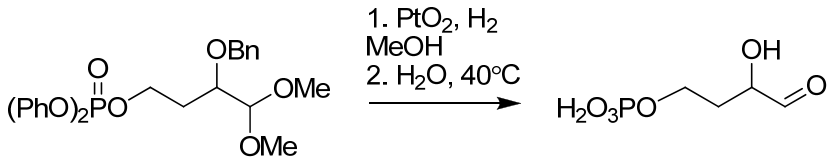

2.8 rac-3-deoxyE4P

To the protected analogue **2.8** (0.1028 g, 0.22 mmol) in MeOH (5.0 mL) was added PtO_2 (0.0491 g, 0.22 mmol). After three vacuum/H_2 cycles, to flush the flask with H_2, the mixture was vigorously stirred at room temperature under hydrogen (balloon) till TLC analysis

showed no UV active compound was on the TLC plate (2 days). The PtO_2 was filtered through a fine sintered funnel and the funnel washed with a small quantity of MeOH. The filtrate was then concentrated *in vacuo*, giving a clear colourless oil (56.8 mg). The oil was dissolved in H_2O (0.70 mL) and heated to 40°C. The solution was stirred overnight and transferred into an eppendorf tube and made up to a final volume of 1.0 mL. The tube was snap frozen using liquid nitrogen and stored at −80°C. Standard enzyme assay conditions using *E. coli* DAH7P synthase (phe) determined the presence and yield of rac-3-deoxyE4P to be 28% over two steps.

HRMS (ESI): calc. $C_4H_9NaO_6P$ $[M+Na]^+$: 207.0029; found: 207.0038.

Synthesis of 2.11

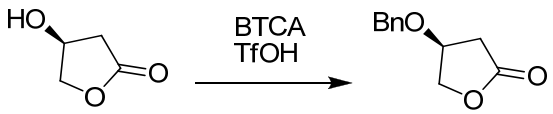

2.11

β-Hydroxy-γ-butyrolactone (0.1191 g, 6.0 mmol) was dissolved in a mixture of DCM (20 mL) and cyclohexane (10 mL), then cooled to 0°C. BTCA (460 µL, 2.48 mmol) was added followed by dropwise addition of TfOH (50 µL, 0.51 mmol). The mixture was stirred overnight at room temperature before the reaction was quenched by the addition of sat. $NaHCO_3$ and extracted with DCM. The organic layer was dried with anhydrous Na_2SO_4, concentrated under reduced pressure and flash chromatography (30% EtOAc:Pet ether) afforded **2.11** (0.1583 g, 71%) as an oil.

^{1}H NMR (500 MHz, *$CDCl_3$*) δ ppm 7.41-7.24 (m, 5H, Ph), 4.53 (ABq, *J* = 11.0 Hz, 2H, C$\underline{H_2}$Ph), 4.41-4.32 (m, 3H, H3, H4), 2.73-2.59 (m, 2H, H2).
^{13}C NMR (126 MHz, *$CDCl_3$*) δ ppm 175.6 (C1), 137.1, 128.8, 128.3, 127.9, 74.0 (C4), 73.3 (C3), 71.3 (C$\underline{H_2}$Ph), 35.1 (C2).
HRMS (ESI): calc. $C_{11}H_{12}NaO_3$ $[M+Na]^+$: 215.0679; found: 215.0686.
R_f (30% EtOAc:Pet ether) = 0.2.

Synthesis of 2.12

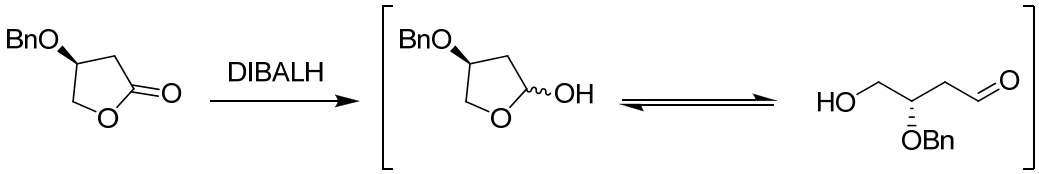

2.11 **2.12**

Compound **2.11** (0.4876 g, 2.53 mmol) was dissolved in dry DCM (40 mL) and cooled to −78°C. DIBALH (3.0 mL, 1 M in THF) was added dropwise and the solution was stirred at −78°C. Once the starting material was undetectable by TLC (1:1 EtOAc:Pet ether, $KMnO_4$), the reaction was quenched by the addition of 10% HCl (5.0 mL) and allowed to warm to room temperature. The solution was diluted with sat. $NaHCO_3$ and extracted with DCM. The organic layer was washed with sat. Rochelle's salt, water and finally sat. NaCl. The combined aqueous extracts were extracted with DCM and the combined organic extracts were dried with anhydrous $MgSO_4$ and the solvent removed *in vacuo*. The product was purified by flash chromatography (30% EtOAc:Pet ether to 100% EtOAc) to give **2.12** (0.3045 g, 62%) as a pair of inseparable diastereoisomers (ratio 3:2).

Major diastereoisomer:

^{1}H NMR (500 MHz, *$CDCl_3$*) δ ppm 7.50-7.17 (m, 5H, Ph), 5.84-5.61 (m, 1H, H1), 4.56 (ABq, *J* = 11.7 Hz, 2H), 4.36-4.30 (m, 1H, H3), 4.07 (dd, *J* = 4.8, 9.5 Hz, 1H, H4a), 3.97 (ap.d, *J* = 9.5 Hz, 1H, H4b), 3.07 (br. s, 1H, OH), 2.28-2.18 (m, 1H, H2a), 2.15-2.07 (m, 1H, H2b).

^{13}C NMR (126 MHz, $CDCl_3$) δ ppm 137.5, 128.8, 128.7, 128.2, 127.9, 127.9, 98.8 (C1), 78.5 (C3), 71.6 ($\underline{C}H_2Ph$), 71.3 (C4), 39.8 (C2).

Minor diastereoisomer:

^{1}H NMR (500 MHz, *$CDCl_3$*) δ ppm 7.44-7.22 (m, 5H, Ph), 5.43 (dd, *J* = 5.1, 10.6 Hz, 1H, H1'), 4.48 (s, 2H, $C\underline{H}_2Ph$), 4.27 (d, *J* = 9.9 Hz, 1H, H4a'), 4.23 (t, *J* = 4.6 Hz, 1H, H3'), 3.88 (dd, *J* = 4.0, 9.9 Hz, 1H, H4b'), 3.73 (ap.d, *J* = 11.0 Hz, 1H, OH), 2.27-2.18 (m, 1H, H2a'), 2.00 (td, *J* = 5.0, 13.8 Hz, 1H, H2b').

^{13}C NMR (126 MHz, *$CDCl_3$*) δ ppm 138.1, 128.8, 128.7, 128.2, 127.9, 127.9, 99.1 (C1'), 78.3 (C3'), 72.6 (C4'), 71.6 ($\underline{C}H_2Ph$), 40.6 (C2').

HRMS (ESI): calc. $C_{11}H_{14}NaO_3$ $[M+Na]^+$: 217.0835; found: 217.0837.
R_f (1:1 EtOAc:Pet ether) = 0.4.

Synthesis of 2.14

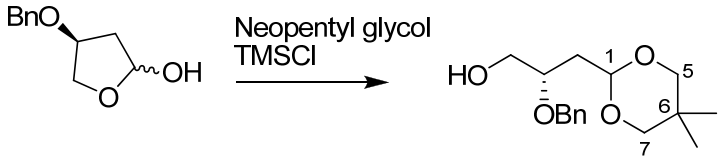

2.12 **2.14**

Neopentyl glycol (0.2088 g, 2.0 mmol) and TMSCl (560 µL, 4.41 mmol) were dissolved in dry DCM (20 mL) at 0°C and stirred for 15 minutes at this temperature. Lactol **2.12** (0.1911 g, 0.98 mmol) in DCM (15 mL) was then added to the reaction mixture and stirred for two hours at 0°C. The reaction was quenched by the addition of sat. $NaHCO_3$. The solution was extracted with DCM (3x) and the organic extracts were washed with water and sat. NaCl. The combined aqueous extracts were extracted with DCM and the combined organic extracts were dried with anhydrous $MgSO_4$. The solvent was removed *in vacuo* and flash chromatography (30 to 50% EtOAc:Pet ether) gave **2.14** (0.2178 g, 79%).

^{1}H NMR (500 MHz, *$CDCl_3$*) δ ppm 7.39-7.25 (m, 5H, Ph), 4.65-4.53 (m, 3H, C$\underline{H}_2$Ph, H1), 3.80-3.71 (m, 2H, H3, H4a), 3.63-3.53 (m, 3H, H4b, H5/7), 3.41 (dd, *J* = 11.0, 16.9 Hz, 2H, H5/7), 2.19 (br. s, 1H, OH), 2.08-2.00 (m, 1H, H2a), 1.87 (td, *J* = 5.7, 14.3 Hz, 1H, H2b), 1.19 (s, 3H, CH_3), 0.72 (s, 3H, CH_3).
^{13}C NMR (126 MHz, *$CDCl_3$*) δ ppm 138.6, 128.7, 128.1, 128.0, 99.9 (C1), 77.4 (C5/7), 76.0 (C3), 71.8 (C$\underline{H}_2$Ph), 64.6 (C4), 36.8 (C2), 30.3 (C6), 23.3 (CH_3), 22.1 (CH_3).
HRMS (ESI): calc. $C_{16}H_{24}NaO_4$ $[M+Na]^+$: 303.1567; found: 303.1572.
R_f (1:1 EtOAc:Pet ether) = 0.5.

Synthesis of 2.16

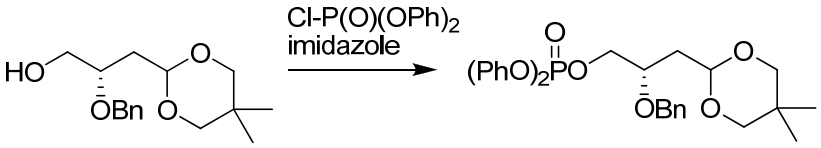

2.14 **2.16**

To a solution of **2.14** (0.0917 g, 0.33 mmol) in anhydrous DCM (5.0 mL) was added diphenylchlorophosphate (140 µL, 0.68 mmol) and imidazole (0.0458 g, 0.67 mmol) at 0°C. The reaction was stirred overnight at room temperature before additional diphenylchlorophosphate (70 µL, 0.33 mmol) and imidazole (0.0215 g, 0.32 mmol) was added and stirred for a further six hours before quenching with sat. NH_4Cl. The reaction was extracted with DCM, dried with $MgSO_4$ and the solvent removed *in vacuo*. The product was purified by two flash columns (20 to 30% EtOAc:Pet ether followed by 20% EtOAc:Pet ether for the second column) to give **2.16** (0.1588 g, 95%) as an oil.

^{1}H NMR (500 MHz, *$CDCl_3$*) δ ppm 7.37-7.14 (m, 15H, Ph), 4.62 (d, *J* = 11.4 Hz, 1H, C$\underline{H}_2$Ph), 4.54 (dd, *J* = 4.0, 6.2 Hz, 1H, H1), 4.50 (d, *J* = 11.7 Hz, 1H, C$\underline{H}_2$Ph), 4.47-4.38 (m, 1H, H4a), 4.24 (td, *J* = 6.4, 11.0 Hz, 1H, H4b), 3.94-3.88 (m, 1H, H3), 3.60-3.52 (m, 2H, H5/7), 3.38 (d, *J* = 11.4 Hz, 1H, H5/7), 3.32 (d, *J* = 11.0 Hz, 1H, H5/7), 1.96 (ddd, *J* = 3.9, 7.7, 14.1 Hz, 1H, H2a), 1.85 (td, *J* = 5.7, 14.2 Hz, 1H, H2b), 1.16 (s, 3H, CH_3), 0.71 (s, 3H, CH_3).

^{13}C NMR (126 MHz, *$CDCl_3$*) δ ppm 150.8 (d, *J* = 7.4 Hz), 138.4, 130.1, 130.0 (d, *J* = 2.8 Hz), 128.6, 128.1, 127.9, 126.2, 125.5, 120.3, 99.4, 77.4 (C5/7), 77.3 (C5/7), 74.0 (d, $^3J_{POCC}$ = 7.9 Hz, C3), 72.4 (C$\underline{H}_2$Ph), 70.8 (d, $^2J_{POC}$ = 6.5 Hz, C4), 36.8 (C2), 30.3 (C6), 23.2 (CH_3), 22.1 (CH_3).

^{31}P NMR (121 MHz, *$CDCl_3$*) δ ppm −11.85.

HRMS (ESI): calc. $C_{28}H_{33}NaO_7P$ $[M+Na]^+$: 535.1856; found: 535.1870.

R_f (30% EtOAc:Pet ether) = 0.4.

Synthesis of (3*S*)-2-deoxyE4P

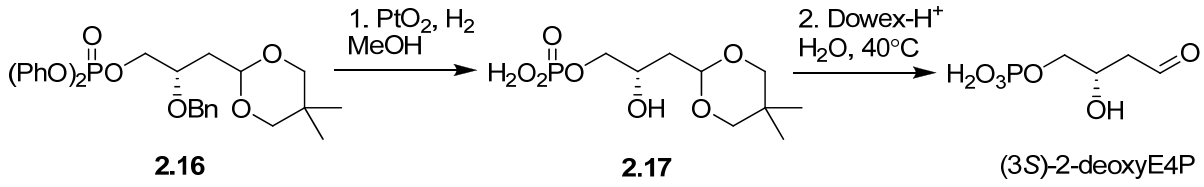

2.16 **2.17** (3*S*)-2-deoxyE4P

To compound **2.16** (0.1512 g, 0.30 mmol) in MeOH (8.0 mL) was added PtO_2 (66 mg, 0.29 mmol). After three vacuum/H_2 cycles, to flush the flask with H_2, the mixture was vigorously stirred at room temperature under hydrogen (balloon) overnight. The PtO_2 was filtered through a small pad of celite and the pad washed with MeOH. The filtrate was then concentrated *in vacuo*, giving a clear colourless oil (98 mg). At this point, a small sample was taken for ^{1}H NMR and mass spectrometry analysis which confirmed the deprotected intermediate **2.17**. The clear colourless oil (82.7 mg) was dissolved in water (1.0 mL) and freshly activated Dowex-H^+ resin was added to give a pH of 2. The solution was heated at 40°C overnight and the Dowex-H^+ resin removed by filtration. The pH of the filtrate was adjusted using 1 M NaOH to give a pH of 6.8 and final volume of 1.0 mL. The solution was frozen till use in enzyme assays. Standard enzyme assay conditions using *E. coli* DAH7P synthase (phe) determined the presence and yield of (3*S*)-2-deoxyE4P to be 22% over two steps.

Intermediate **2.17**:

Crude ^{1}H NMR (500 MHz, D_2O) δ ppm 4.64-4.60 (m, 1H, H1), 3.89-3.81 (m, 1H), 3.81-3.74 (m, 1H), 3.71-3.62 (m, 1H), 3.57-3.40 (m, 5H), 1.68 (ap.t, J = 5.9 Hz, 2H, H2), 0.98 (s, 3H, CH_3), 0.59 (s, 3H, CH_3).

HRMS (ESI): calc. $C_9H_{17}Na_3O_7P$ $[M+Na]^+$: 337.0399; found: 337.0405.

(3*S*)-2-DeoxyE4P:

HRMS (ESI): calc. $C_4H_8O_6P$ $[M-H]^-$: 183.0064; found: 183.0060.

6.3.2 Experimental for Chapter 3

Synthesis of 3.1

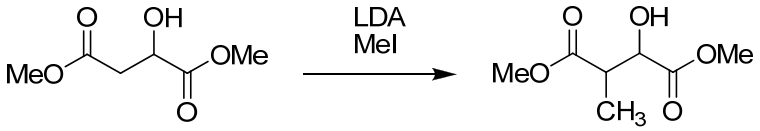

2.1 **3.1**

n-BuLi (1.50 M in hexane, 90 mL, 135 mmol) was slowly added to a solution of diisopropylamine (22 mL, 156 mmol) in THF (200 mL) at −78°C. The solution was then allowed to warm by removing the dry ice bath. After 45 minutes the solution was cooled to −78°C and a solution of **2.1** (10.0255 g, 62 mmol) in THF (5 mL) was added dropwise over 10 minutes. The dry ice cooling bath was then replaced by an ice–salt bath (−15 to −20°C) and the solution was stirred at this temperature for one hour. The solution was cooled to −78°C and MeI (4.30 mL, 69 mmol) was added dropwise over five minutes. The solution was then stirred overnight as the temperature rises from −78°C to room temperature. The reaction mixture was quenched by the addition of glacial acetic acid (40 mL) in ether (40 mL) at −78°C and is then poured into a separating funnel containing ether (500 mL) and H_2O (70 mL). The organic layer is washed successively with sat. $NaHCO_3$ (40 mL), sat. NaCl (40 mL) and the aqueous phases were extracted with ether (2x 200 mL). The combined ethereal solutions were dried using $MgSO_4$ and the solvent removed *in vacuo*. Flash chromatography (30% EtOAc:Pet ether) gave **3.1** (7.2182 g, 66%) as a pair of inseparable diastereoisomers (ratio 6:1).

Major diastereoisomer:

^{1}H NMR (500 MHz, *$CDCl_3$*) δ ppm 4.25 (d, *J* = 3.7 Hz, 1H, H2), 3.77 (s, 3H, OCH_3), 3.66 (s, 3H, OCH_3), 3.01 (qd, *J* = 3.7, 7.2 Hz, 1H, H3), 1.26 (d, *J* = 7.3 Hz, 3H, CH_3).

^{13}C NMR (75 MHz, *$CDCl_3$*) δ ppm 173.9, 173.7, 72.7 (C2), 53.0 (OMe), 52.3 (OMe), 43.4 (C3), 13.3 (CH_3).

Minor diastereoisomer:

^{1}H NMR (500 MHz, *$CDCl_3$*) δ ppm 4.59 (d, *J* = 3.7 Hz, 1H, H2'), 3.78 (s, 3H, OCH_3'), 3.70 (s, 3H, OCH_3'), 2.94-2.87 (m, 1H, H3'), 1.14 (d, *J* = 7.3 Hz, 3H, CH_3').

^{13}C NMR (75 MHz, *$CDCl_3$*) δ ppm 173.9, 173.7, 71.7 (C2'), 53.1 (OMe'), 52.4 (OMe'), 43.2 (C3'), 10.9 (CH_3').

HRMS (ESI): calc. $C_7H_{12}NaO_5$ $[M+Na]^+$: 199.0582; found: 199.0575.
R_f (30% EtOAc:Pet ether) = 0.2.

Synthesis of 3.2

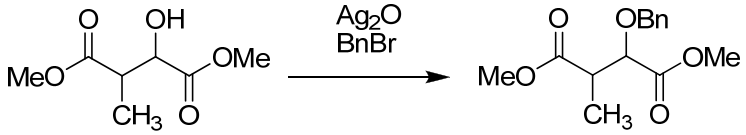

3.1 **3.2**

To a solution of **3.1** (6.08 g, 35 mmol) in anhydrous DCM (100 mL) was added Ag_2O (27.9918 g, 121 mmol), BnBr (14.5 mL, 121 mmol) and KI (0.20 equiv.). The mixture was stirred for three days before another portion of Ag_2O (4.01 g, 17 mmol), BnBr (2.10 mL, 18 mmol) and KI (0.20 equiv.) were added and stirred for a further two days. The mixture was filtered through celite and the filtrate washed successively with sat. $NaHCO_3$, H_2O, and sat. NaCl. The organic extracts were dried ($MgSO_4$) and the solvent removed *in vacuo*. Flash chromatography (10 to 20% EtOAc:Pet ether) afforded **3.2** (7.22 g, 79%) as a pair of inseparable diastereoisomers (ratio 6:1).

Major diastereoisomer:
^{1}H NMR (500 MHz, *$CDCl_3$*) δ ppm 7.35-7.26 (m, 5H, Ph), 4.72 (d, *J* = 11.7 Hz, 1H, C$\underline{H}_2$Ph), 4.48 (d, *J* = 11.7 Hz, 1H, C$\underline{H}_2$Ph), 4.15 (d, *J* = 7.0 Hz, 1H, H2), 3.75 (s, 3H, OCH_3), 3.68 (s, 3H, OCH_3), 2.99 (q, *J* = 7.2 Hz, 1H, H3), 1.15 (d, *J* = 7.0 Hz, 3H, CH_3).
^{13}C NMR (126 MHz, *$CDCl_3$*) δ ppm 173.6, 171.6, 137.3, 128.6, 128.3, 128.2, 80.1 (C2), 73.3 (C$\underline{H}_2$Ph), 52.2, 43.1 (C3), 13.1 (CH_3).

Minor diastereoisomer:
^{1}H NMR (500 MHz, *$CDCl_3$*) δ ppm 7.35-7.26 (m, 5H, Ph), 4.78 (d, *J* = 11.7 Hz, 1H, C$\underline{H}_2$Ph), 4.45 (d, *J* = 11.7 Hz, 1H, C$\underline{H}_2$Ph), 4.37 (ap.d, *J* = 5.1 Hz, 1H, H2'), 3.77 (s, 3H, OCH_3'), 3.63 (s, 3H, OCH_3'), 1.22 (d, *J* = 7.3 Hz, 3H, CH_3').

^{13}C NMR (126 MHz, *$CDCl_3$*) δ ppm 173.6, 171.6, 137.3, 128.6, 128.3, 128.2, 78.7 (C2'), 73.3 ($\underline{C}H_2Ph$), 52.2, 42.7 (C3'), 11.6 (CH_3').

HRMS (ESI): calc. $C_{14}H_{19}O_5$ $[M+H]^+$: 267.1232; found: 267.1228.
R_f (20% EtOAc:Pet ether) = 0.3.

Synthesis of 3.3

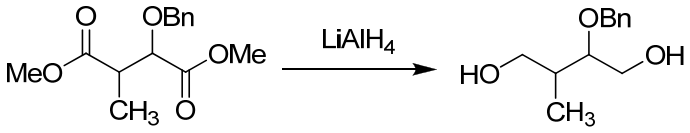

3.2 **3.3**

$LiAlH_4$ (2.3152 g, 61 mmol) was suspended in THF (20 mL) and cooled to 0°C. Compound **3.2** (5.36 g, 20 mmol) in THF (30 mL) was added dropwise to this suspension over 10 minutes. The reaction was then heated to reflux for three hours. After cooling to 0°C the solution was quenched slowly by the addition of ice, followed by 3 M NaOH until effervescence had ceased and a white solid had formed. The mixture was filtered through celite, the celite washed with ether (3x 20 mL) and the filtrate was dried over $MgSO_4$. The solvent was removed *in vacuo* and flash chromatography (1:1 to 2:1 EtOAc:Pet ether) gave **3.3** (3.44 g, 81%).

^{1}H NMR (500 MHz, *$CDCl_3$*) δ ppm 7.39-7.29 (m, 5H, Ph), 4.67 (d, J = 11.4 Hz, 1H, $C\underline{H}_2Ph$), 4.58 (d, J = 11.7 Hz, 1H, $C\underline{H}_2Ph$), 3.87 (dd, *J* = 3.7, 12.1 Hz, 1H, H1), 3.69-3.59 (m, 3H, H1, H4), 3.49-3.45 (m, 1H, H2), 3.22 (br. s, 2H, OH), 2.10-2.01 (m, 1H, H3), 0.95 (d, *J* = 7.0 Hz, 3H, CH_3).
^{13}C NMR (126 MHz, *$CDCl_3$*) δ ppm 138.0, 128.8, 128.2, 128.1, 83.3 (C2), 72.5 ($\underline{C}H_2Ph$), 65.8 (C4), 61.6 (C1), 37.1 (C3), 14.2 (CH_3).
HRMS (ESI): calc. $C_{12}H_{19}O_3$ $[M+H]^+$: 211.1334; found: 211.1344.
R_f (2:1 EtOAc:Pet ether) = 0.3.

Synthesis of 3.4

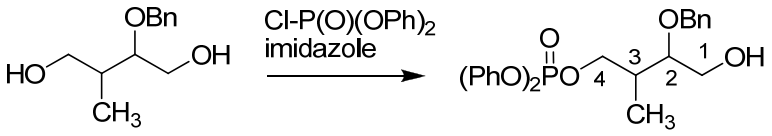

3.3 **3.4**

To a solution of **3.3** (1.0104 g, 4.80 mmol) in anhydrous DCM (20 mL) was added diphenylchlorophosphate (900 μL, 4.4 mmol) and imidazole (1.2983 g, 19 mmol) at 0°C. The solution was allowed to warm slowly to room temperature. After stirring overnight, the solution was diluted with DCM, quenched with water and washed with sat. $NaHCO_3$ and sat. NaCl. The combined aqueous extracts were extracted with DCM. The combined organic extracts were dried over $MgSO_4$ and the solvent removed *in vacuo*. Flash chromatography (30 to 45% EtOAc:Pet ether) gave **3.4** (0.4599, 22%) as a pair of inseparable diastereoisomers (ratio 3:1), the diphosphorylated compound **3.6** (0.6681 g, 21%, R_f (1:1 EtOAc:Pet ether) = 0.6) and **3.3** (0.2967 g, 30% recovered).

Major diastereoisomer:

^{1}H NMR (500 MHz, *$CDCl_3$*) δ ppm 7.38-7.15 (m, 15H, Ph), 4.57-4.46 (m, 2H, C$\underline{H}_2$Ph), 4.43-4.27 (m, 2H, H4), 3.81 (dd, *J* = 3.3, 12.1 Hz, 1H, H1a), 3.67-3.61 (m, 1H, H1b), 3.41 (td, *J* = 3.8, 7.9 Hz, 1H, H2), 2.50 (br. s, 1H, OH), 2.24-2.16 (m, 1H, H3), 1.00 (d, *J* = 7.0 Hz, 3H, CH_3).

^{13}C NMR (75 MHz, *$CDCl_3$*) δ ppm 150.8 (m), 138.4, 130.1, 128.8, 128.1, 125.7, 120.3 (d, *J* = 4.4 Hz, Ph), 80.4 (C2), 72.7 (C$\underline{H}_2$Ph), 71.5 (d, $^2J_{POC}$ = 6.6 Hz, C4), 61.2 (C1), 35.6 (d, $^3J_{POCC}$ = 7.6 Hz, C3), 13.5 (CH_3).

Minor diastereoisomer:

^{1}H NMR (500 MHz, *$CDCl_3$*) δ ppm 7.38-7.15 (m, 15H, Ph), 4.69 (ap.d, *J* = 11.0 Hz, 1H, C$\underline{H}_2$Ph), 4.48-4.44 (m, 1H, C$\underline{H}_2$Ph), 4.42-4.28 (m, 2H, H4'), 3.66-3.52 (m, 3H, H1', H2'), 2.50 (br. s, 1H, OH), 2.02-1.92 (m, 1H, H3'), 0.91 (d, *J* = 7.0 Hz, 3H, CH_3').

^{13}C NMR (75 MHz, *$CDCl_3$*) δ ppm 150.8 (m), 137.9, 130.1, 128.8, 128.1, 125.7, 120.3 (d, *J* = 4.4 Hz), 81.5 (d, *J* = 7.2 Hz), 73.1 (C$\underline{H}_2$Ph'), 69.1 (d, $^2J_{POC}$ = 6.1 Hz, C4'), 65.6 (C1'), 36.9 (C3'), 14.0 (CH_3').

^{31}P NMR (121 MHz, *CDCl$_3$*) δ ppm −10.42, −10.64.

HRMS (ESI): calc. $C_{24}H_{28}O_6P$ $[M+H]^+$: 443.1624; found: 443.1626.

R_f (1:1 EtOAc:Pet ether) = 0.3.

Synthesis of 3.7

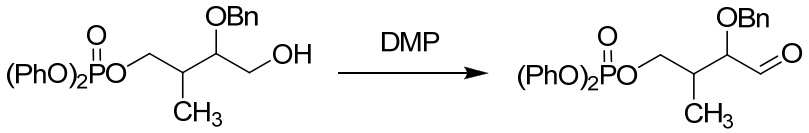

3.4 **3.7**

3.4 (1.0328 g, 2.35 mmol) was dissolved in DCM (40 mL) and freshly prepared DMP (2.4761 g, 5.84 mmol) was added. The mixture was stirred overnight at room temperature before an additional portion of DMP (0.4970 g, 1.17 mmol) was added. After a further five hours of stirring, sat. $Na_2S_2O_3$ and sat. $NaHCO_3$ were added and stirred till the solution was clear. The aqueous layer was extracted with DCM and the combined organic extracts were dried over $MgSO_4$. Removal of the solvent *in vacuo*, followed by flash chromatography (30% EtOAc:Pet ether) gave **3.7** (0.8290 g, 81%), a clear colourless oil, as a pair of inseparable diastereoisomers (ratio 2:1).

Major diastereoisomer:

^{1}H NMR (500 MHz, *CDCl$_3$*) δ ppm 9.60 (d, *J* = 2.6 Hz, 1H, H1), 7.35-7.17 (m, 10H, Ph), 4.63 (d, *J* = 11.4 Hz, 1H, C$\underline{H}_2$Ph), 4.48 (d, *J* = 11.7 Hz, 1H, C$\underline{H}_2$Ph), 4.35-4.27 (m, 1H, H4), 3.63 (dd, *J* = 2.6, 5.9 Hz, 1H, H2), 2.35 (spt, *J* = 6.4 Hz, 1H, H3), 1.00 (d, *J* = 7.3 Hz, 3H, CH_3).

^{13}C NMR (126 MHz, *CDCl$_3$*) δ ppm 203.4 (C1), 150.7, 137.2, 130.1, 128.8, 128.7, 128.4, 128.3, 128.2, 125.7, 120.3, 84.4 (C2), 73.5 (C$\underline{H}_2$Ph), 69.4 (d, $^2J_{POC}$ = 6.2 Hz, C4), 36.4 (d, $^3J_{POCC}$ = 8.1 Hz, C3), 13.1 (CH_3).

Minor diastereoisomer:

^{1}H NMR (500 MHz, *CDCl$_3$*) δ ppm 9.69 (d, *J* = 1.8 Hz, 1H, H1'), 7.35-7.17 (m, 15H, Ph), 4.68 (d, *J* = 11.4 Hz, 1H, C$\underline{H}_2$Ph), 4.54-4.46 (m, 1H, H4a'), 4.49 (d, *J* = 11.4 Hz, 1H, C$\underline{H}_2$Ph), 4.35-4.27 (m, 1H, H4b'), 3.86-3.82 (m, 1H, H2'), 2.75-2.68 (m, 1H, H3'), 1.07 (d, *J* = 7.3 Hz, 3H, CH_3').

^{13}C NMR (126 MHz, *CDCl$_3$*) δ ppm 203.0 (C1'), 150.7, 137.5, 130.1, 128.8, 128.7, 128.4, 128.3, 128.2, 125.7, 120.3, 78.2 (d, *J* = 7.9 Hz, C2'), 72.7 (C$\underline{H}_2$Ph), 67.6 (d, $^2J_{POC}$ = 6.4 Hz, C4'), 47.8 (C3'), 10.6 (CH$_3$').

^{31}P NMR (121 MHz, *CDCl$_3$*) δ ppm −11.68, −12.14.

HRMS (ESI): calc. $C_{24}H_{26}O_6P$ $[M+H]^+$: 441.1467; found: 441.1481.

R$_f$ (30% EtOAc:Pet ether) = 0.2.

Synthesis of 3.8

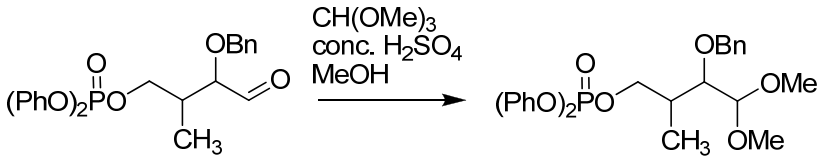

3.7 **3.8**

To **3.7** (1.5379 g, 3.49 mmol) in MeOH (50 mL) was added trimethyl orthoformate (3.90 mL, 35.6 mmol) and conc. H_2SO_4 (40 μL, 0.75 mmol). After stirring overnight, the mixture was transferred into a separating funnel containing sat. $NaHCO_3$ and Et_2O. The aqueous layer was washed with Et_2O (3x). The combined organic extracts were washed with sat. NaCl, dried ($MgSO_4$) and the solvent removed *in vacuo*. Flash chromatography using deactivated silica (20% EtOAc:Pet ether) gave **3.8** (1.4817 g, 87%), a clear colourless oil, as a pair of inseparable diastereoisomers (ratio 2:1).

Major diastereoisomer:

^{1}H NMR (500 MHz, *CDCl$_3$*) δ ppm 7.34-7.16 (m, 15H, Ph), 4.77 (d, *J* = 11.4 Hz, 1H, C$\underline{H}_2$Ph), 4.51 (d, *J* = 11.4 Hz, 1H, C$\underline{H}_2$Ph), 4.44-4.39 (m, 1H, H4a), 4.37-4.34 (m, 1H, H1), 4.23 (td, *J* = 6.6, 9.9 Hz, 1H, H4b), 3.44 (s, 3H, OCH$_3$), 3.40 (s, 3H, OCH$_3$), 3.39-3.36 (m, 1H, H2), 2.33-2.23 (m, 1H, H3), 1.02 (d, *J* = 7.0 Hz, 3H, CH$_3$).

^{13}C NMR (126 MHz, *CDCl$_3$*) δ ppm 150.9, 138.8, 130.0, 128.5, 128.1, 127.8, 125.5, 120.3, 106.5 (C1), 81.2 (C2), 74.6 (C$\underline{H}_2$Ph), 71.2 (d, $^2J_{POC}$ = 6.6 Hz, C4), 56.2 (OCH$_3$), 55.8 (OCH$_3$), 35.8 (d, $^3J_{POCC}$ = 7.8 Hz, C3), 14.3 (CH$_3$).

Minor diastereoisomer:

^{1}H NMR (500 MHz, *$CDCl_3$*) δ ppm 7.34-7.16 (m, 15H, Ph), 4.65 (d, *J* = 11.4 Hz, 1H, C$\underline{H}_2$Ph), 4.54-4.48 (m, 1H, H4a'), 4.46 (d, *J* = 11.4 Hz, 1H, C$\underline{H}_2$Ph), 4.37-4.34 (m, 1H, H1'), 4.34-4.28 (m, 1H, H4b'), 3.71-3.66 (m, 1H, H2'), 3.34 (s, 3H, OCH_3'), 3.32 (s, 3H, OCH_3'), 2.12 (dq, *J* = 6.6, 12.9 Hz, 1H, H3'), 0.92 (d, *J* = 7.0 Hz, 3H, CH_3').

^{13}C NMR (126 MHz, *$CDCl_3$*) δ ppm 150.9, 138.5, 130.0, 128.5, 128.1, 127.8, 125.5, 120.3, 106.1 (C1'), 79.2 (d, *J* = 7.9 Hz, C2'), 72.8 (C$\underline{H}_2$Ph), 69.7 (d, $^{2}J_{POC}$ = 6.6 Hz, C4'), 55.6 (OCH_3'), 54.9 (OCH_3'), 38.2 (C3'), 10.2 (CH_3').

^{31}P NMR (121 MHz, *$CDCl_3$*) δ ppm −11.70, −11.97.

HRMS (ESI): calc. $C_{26}H_{32}O_7P$ $[M+H]^+$: 487.1886; found: 487.1901.

R_f (30% EtOAc:Pet ether) = 0.3.

Synthesis of 3-methylE4P

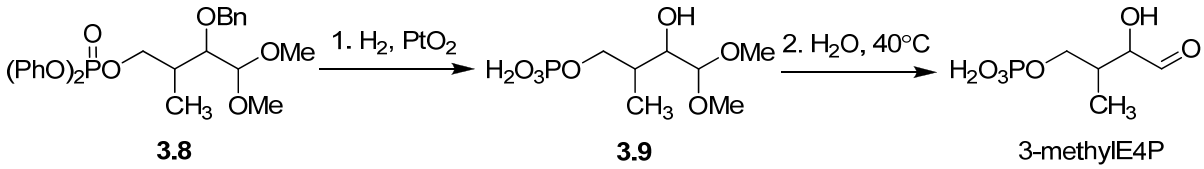

3.8 **3.9** 3-methylE4P

To the protected analogue **3.8** (1.4645 g, 3.01 mmol) in MeOH (40 mL) was added PtO_2 (0.2946 g, 1.29 mmol). After three vacuum/H_2 cycles, to flush the flask with H_2, the mixture was vigorously stirred at room temperature under hydrogen (balloon) for three days. The PtO_2 was filtered through a small pad of celite and the pad washed with MeOH (3x). The filtrate was then concentrated *in vacuo* to give intermediate **3.9** as a clear colourless oil. The oil was dissolved in H_2O and heated overnight at 40°C to afford 3-methylE4P that was used in enzyme assays without further purification.

Intermediate **3.9**:

HRMS (ESI): calc. $C_7H_{16}O_7P$ $[M-H]^-$: 243.0634; found: 243.0623.

3-MethylE4P:

HRMS (ESI): calc. $C_5H_{10}O_6P$ $[M-H]^-$: 197.0215; found: 197.0223.

Synthesis of 3.11

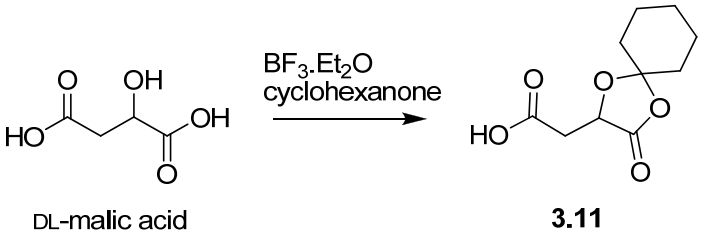

To a suspension of DL-malic acid (5.0557 g, 37.7 mmol) in dry THF (50 mL) containing 4 Å molecular sieves was added, dropwise via syringe, freshly distilled cyclohexanone (12 mL, 115.9 mmol) and $BF_3.Et_2O$ (10 mL, 78.9 mmol) at 0°C. The ice bath was then removed and the mixture was stirred at room temperature overnight. The reaction mixture was quenched with water and the molecular sieves were filtered off. The filtrate was diluted with ether and washed with sat. NaCl. The combined aqueous phases were extracted with ether (3x) and the combined organic phases dried over anhydrous $MgSO_4$. Removal of the solvent *in vacuo* followed by flash chromatography (10 to 30% EtOAc:Pet ether) gave **3.11** (5.31 g, 66%), with spectral data in accordance with the literature.[126,127]

^{1}H NMR (500 MHz, *$CDCl_3$*) δ ppm 4.72 (dd, *J* = 3.9, 6.4 Hz, 1H, H2), 3.00, 2.85 (d of ABq, *J* = 3.9, 6.6, 17.2 Hz, 1H, H3), 1.93-1.80 (m, 2H, cyclic CH_2's), 1.80-1.57 (m, 6H, cyclic CH_2's), 1.55-1.46 (m, 1H, cyclic CH_2's), 1.46-1.33 (m, 1H, cyclic CH_2's).
^{13}C NMR (126 MHz, *$CDCl_3$*) δ ppm 174.5, 172.2, 112.5, 70.2, 36.4, 36.3, 35.6, 24.7, 23.3, 23.2.
HRMS (ESI): calc. $C_{10}H_{14}NaO_5$ $[M+Na]^+$: 237.0733; found: 237.0737.
R_f (30% EtOAc:Pet ether) = 0.3.

Synthesis of 3.12

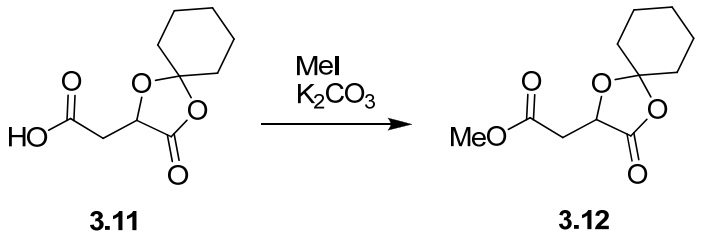

To a solution of **3.11** (5.0023 g, 23.4 mmol) in anhydrous DMF (20 mL) was added K_2CO_3 (4.8493 g, 35.1 mmol) and MeI (2.90 mL, 46.6 mmol) and stirred at room temperature overnight. K_2CO_3 (1.5169 g, 11 mmol) and MeI (0.80 mL, 12.8 mmol) were added and the solution was stirred for a further 24 hours before quenching with sat. $NaHCO_3$. The mixture was diluted with EtOAc and the organic layer washed with H_2O (3x). The combined aqueous phases were extracted with EtOAc (3x) and the combined organic phases dried over anhydrous $MgSO_4$. Removal of the solvent *in vacuo* followed by flash chromatography (10% EtOAc:Pet ether) gave **3.12** (5.0734 g, 95%).

^{1}H NMR (500 MHz, *$CDCl_3$*) δ ppm 4.70 (dd, *J* = 4.0, 6.2 Hz, 1H, H1), 3.71 (s, 3H, OCH_3), 2.91, 2.78 (ABq x2, *J* = 3.7, 7.0, 16.9 Hz, 1H, H3), 1.92-1.77 (m, 2H, cyclic CH_2's), 1.77-1.55 (m, 6H, cyclic CH_2's), 1.53-1.43 (m, 1H, cyclic CH_2's), 1.42-1.32 (m, 1H, cyclic CH_2's).

^{13}C NMR (126 MHz, *$CDCl_3$*) δ ppm 172.3, 169.8, 112.2, 70.4, 52.3, 36.4, 36.4, 35.5, 24.6, 23.2, 23.1.

HRMS (ESI): calc. $C_{11}H_{16}NaO_5$ $[M+Na]^+$: 251.0890; found: 251.0902.

R_f (20% EtOAc:Pet ether) = 0.4.

Synthesis of 3.22

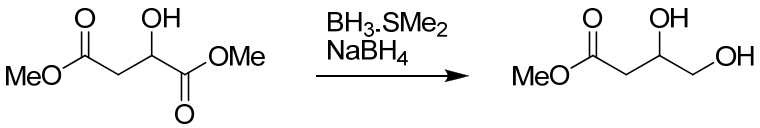

2.1 **3.22**

Diester **2.1** (5.0145 g, 30.9 mmol) was dissolved in THF (50 mL) at 0°C. $BH_3.SMe_2$ (4.0 mL, 10 M in Me_2S) was added dropwise as gas evolved. The solution was stirred at 0°C for 30 minutes before the addition of $NaBH_4$ (41.1 mg, 1.1 mmol). The ice bath was removed and the solution was stirred for one hour at room temperature before quenching with EtOH (2.0 mL). The solution was concentrated *in vacuo* and flash chromatography (2:1 EtOAc:Pet ether to 5% MeOH:EtOAc) gave **3.22** (3.91 g, 94%) as a clear oil, with spectral data in accordance with the literature.[131]

^{1}H NMR (500 MHz, *CDCl$_3$*) δ ppm 4.18-4.09 (m, 1H, H3), 3.71 (s, 3H, OCH_3), 3.67 (dd, *J* = 3.3, 11.4 Hz, 1H, H4a), 3.52 (dd, *J* = 6.4, 11.6 Hz, 1H, H4b), 3.09 (br. s, 2H, OH), 2.59-2.47 (m, 2H, H2).

^{13}C NMR (126 MHz, *CDCl$_3$*) δ ppm 173.3, 68.7, 65.9, 52.2, 37.6.

HRMS (ESI): calc. $C_5H_{10}NaO_4$ $[M+Na]^+$: 157.0471; found: 157.0475.

R$_f$ (5% MeOH:EtOAc) = 0.6.

Synthesis of 3.29

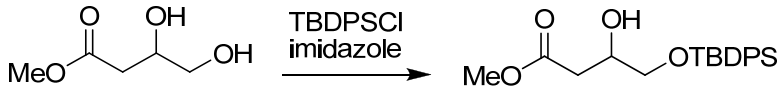

3.22 **3.29**

A mixture of **3.22** (0.8647 g, 6.45 mmol), *tert*-butyldiphenylchlorosilane (TBDPSCl, 2.10 mL, 8.08 mmol) and imidazole (0.5712 g, 8.39 mmol) in DCM (100 mL) was stirred at room temperature for 2.5 hours. The reaction was then quenched with sat. NH_4Cl (30 mL) and transferred to a separating funnel. The organic layer was washed with water and sat. NaCl, dried over $MgSO_4$ and the solvent removed *in vacuo*. Flash chromatography (20% EtOAc:Pet ether) gave **3.29** (2.1522 g, 90%) as a clear oil.

^{1}H NMR (500 MHz, *CDCl$_3$*) δ ppm 7.70-7.62 (m, 4H, Ph), 7.48-7.35 (m, 6H, Ph), 4.21-4.14 (m, 1H, H3), 3.70 (s, 3H, OCH_3), 3.68-3.61 (m, 2H, H4), 2.61-2.50 (m, 2H, H2), 1.07 (s, 9H, $SiC(CH_3)_3$).

^{13}C NMR (126 MHz, *CDCl$_3$*) δ ppm 172.7 (C=O), 135.8, 133.2, 130.1, 128.0 (Ph), 68.9 (C3), 67.1 (C4), 52.0 (OCH_3), 38.1 (C2), 27.1 ($SiC(\underline{C}H_3)_3$), 19.5 ($Si\underline{C}(CH_3)_3$).

HRMS (ESI): calc. $C_{21}H_{29}O_4Si$ $[M+H]^+$: 373.1835; found: 373.1837.

R$_f$ (20% EtOAc:Pet ether) = 0.2.

Synthesis of 3.31

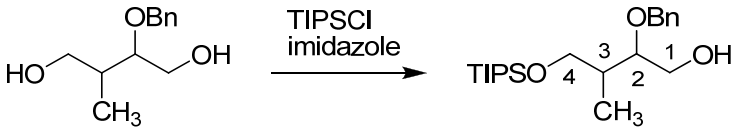

3.3 **3.31**

A mixture of **3.3** (0.1065 g, 0.51 mmol), triisopropylsilyl chloride (TIPSCl, 115 µL, 0.54 mmol) and imidazole (67 mg, 0.98 mmol) in DMF (5.0 mL) was stirred at room temperature for 4.5 hours. The reaction was then quenched with sat. NH_4Cl (2.0 mL) and H_2O (5.0 mL). The solution was then transferred into a separating funnel containing ether (20 mL) and H_2O (20 mL). The organic layer was washed with H_2O (2x 30 mL) and the combined aqueous extracts were washed with Et_2O (2x 20 mL). The combined organic extracts were then dried over $MgSO_4$ and the solvent was removed *in vacuo*. Flash chromatography (15% EtOAc:Pet ether) gave **3.31** (95.4 mg, 51%) as a colourless oil, the disilylated compound **3.33** (53.9 mg, 20%, R_f (1:9 EtOAc:Pet ether) = 0.58) and starting material **3.4** (30 mg, 28% recovered). Compound **3.31** was isolated as pair of inseparable diastereoisomers (ratio 2:1).

Major diastereoisomer:

^{1}H NMR (500 MHz, *CDCl$_3$*) δ ppm 7.37-7.26 (m, 5H, Ph), 4.82-4.73 (m, 1H, C$\underline{H}_2$Ph), 4.64-4.54 (m, 1H, C$\underline{H}_2$Ph), 3.82-3.77 (m, 1H, H1a), 3.80-3.74 (m, 1H, H4a), 3.73-3.68 (m, 1H, H4b), 3.67-3.60 (m, 1H, H1b), 3.59-3.54 (m, 1H, H2), 2.10-2.02 (m, 1H, H3), 1.12-1.05 (m, 21H, SiC$\underline{H}$(CH$_3$)$_2$, SiCH(C$\underline{H}_3$)$_2$), 0.98 (d, *J* = 7.0 Hz, 3H, CH$_3$).

^{13}C NMR (126 MHz, *CDCl$_3$*) δ ppm 138.8, 128.7, 128.2, 128.0, 127.9, 81.2 (C2), 72.3 (C$\underline{H}_2$Ph), 65.3 (C4), 61.8 (C1), 37.9 (C3), 18.2 (SiCH(C$\underline{H}_3$)$_2$), 13.4 (CH$_3$), 12.2 (Si$\underline{C}$H(CH$_3$)$_2$).

Minor diastereoisomer:

^{1}H NMR (500 MHz, *CDCl$_3$*) δ ppm 7.37-7.26 (m, 5H, Ph), 4.82-4.73 (m, 1H, C$\underline{H}_2$Ph), 4.64-4.54 (m, 1H, C$\underline{H}_2$Ph), 3.93-3.88 (m, 1H, H1a'), 3.85-3.80 (m, 1H, H1b'), 3.70-3.63 (m, 1H, H4a'), 3.62-3.57 (m, 1H, H4b'), 3.48 (q, *J* = 5.1 Hz, 1H, H2'), 2.03-1.97 (m, 1H, H3'), 1.12-1.05 (m, 21H, SiC$\underline{H}$(CH$_3$)$_2$, SiCH(C$\underline{H}_3$)$_2$), 0.99 (d, *J* = 7.0 Hz, 1H, CH$_3$').

^{13}C NMR (126 MHz, *CDCl$_3$*) δ ppm 138.8, 128.7, 128.2, 128.0, 127.9, 84.9 (C2'), 73.3 (C$\underline{H}_2$Ph), 66.2 (C4'), 64.4 (C1'), 36.9 (C3'), 18.2 (SiCH(C$\underline{H}_3$)$_2$), 14.2 (CH$_3$'), 12.2 (Si$\underline{C}$H(CH$_3$)$_2$).

HRMS (ESI): calc. $C_{21}H_{39}O_3Si$ $[M+H]^+$: 367.2668; found: 367.2655.

R_f (1:9 EtOAc:Pet ether) = 0.1.

Synthesis of 3.34

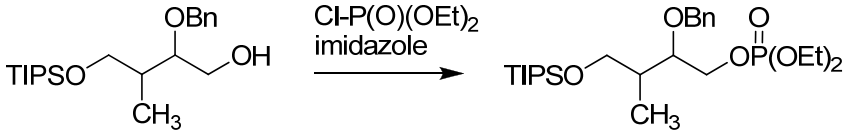

3.31 **3.34**

To a solution of **3.31** (0.3618 g, 0.99 mmol) in anhydrous DCM (7.0 mL) was added diethyl chlorophosphate (360 µl, 2.49 mmol) and imidazole (0.1680 g, 2.48 mmol) at 0°C. The solution was allowed to warm slowly to room temperature. After stirring overnight, additional diethyl chlorophosphate (140 µL, 0.97 mmol) was added. The solution was stirred overnight before it was diluted with DCM, quenched with H_2O and washed with sat. $NaHCO_3$ and sat. NaCl. The combined aqueous extracts were extracted with DCM (3x). The combined organic extracts were dried over $MgSO_4$ and the solvent removed *in vacuo*. Flash chromatography (20 to 50% EtOAc:Pet ether) gave **3.34** (0.3548 g, 72%) as a pair of inseparable diastereoisomers (ratio 2:1).

Major diastereoisomer:

^{1}H NMR (500 MHz, *CDCl$_3$*) δ ppm 7.37-7.24 (m, 5H, Ph), 4.79-4.71 (m, 1H, C$\underline{H}_2$Ph), 4.61-4.50 (m, 1H, C$\underline{H}_2$Ph), 4.30 (ddd, *J* = 2.8, 5.6, 11.1 Hz, 1H, H1a), 4.17-4.14 (m, 1H, H1b), 4.14-4.06 (m, 4H, OC$\underline{H}_2$CH$_3$), 3.73 (ap.dd, *J* = 5.3, 1.3 Hz, 2H, H4), 3.68-3.62 (m, 1H, H2), 2.03-1.96 (m, 1H, H3), 1.31 (t, *J* = 7.3 Hz, 6H, OCH$_2$C$\underline{H}_3$), 1.09-1.04 (m, 21H, SiC$\underline{H}$(CH$_3$)$_2$, SiCH(C$\underline{H}_3$)$_2$), 0.98 (d, *J* = 7.0 Hz, 3H, CH$_3$).

^{13}C NMR (126 MHz, *CDCl$_3$*) δ ppm 138.8, 128.5, 128.0, 127.7, 79.6 (d, $^3J_{POCC}$ = 7.4 Hz, C2), 72.9 (C$\underline{H}_2$Ph), 68.2 (d, $^2J_{POC}$ = 6.5 Hz, C1), 65.1 (C4), 63.9 (m, O$\underline{C}$H$_2$CH$_3$), 38.1 (C3), 18.3 (SiCH(C$\underline{H}_3$)$_2$), 16.4 (m, OCH$_2\underline{C}$H$_3$), 13.6 (CH$_3$), 12.2 (Si$\underline{C}$H(CH$_3$)$_2$).

Minor diastereoisomer:

^{1}H NMR (500 MHz, *CDCl$_3$*) δ ppm 7.37-7.24 (m, 5H, Ph), 4.79-4.72 (m, 1H, C$\underline{H}_2$Ph), 4.61-4.51 (m, 1H, C$\underline{H}_2$Ph), 4.17-4.06 (overlap. m, 6H, OC$\underline{H}_2$CH$_3$, H1'), 3.92-3.87 (m, 1H, H4a'), 3.83-3.78 (m, 1H, H4b'), 3.46-3.41 (m, 1H, H2'), 2.20-2.11 (m, 1H, H3'), 1.31 (t, *J* = 7.3 Hz, 6H, OCH$_2$C$\underline{H}_3$), 1.09-1.04 (overlap. m, 24H, SiC$\underline{H}$(CH$_3$)$_2$, SiCH(C$\underline{H}_3$)$_2$, CH$_3$').

^{13}C NMR (126 MHz, *CDCl$_3$*) δ ppm 139.0, 128.5, 128.0, 127.7, 81.4 (C2'), 73.1 (CH_2Ph), 69.8 (d, $^2J_{POC}$ = 6.0 Hz, C1'), 64.2 (C4'), 63.9 (m, OCH_2CH$_3$), 36.9 (C3'), 18.3 (SiCH(CH_3)$_2$), 16.4 (m, OCH$_2$CH_3), 13.9 (CH$_3$'), 12.2 (SiCH(CH$_3$)$_2$).

^{31}P NMR (121 MHz, *CDCl$_3$*) δ ppm −0.33 (br. s).

HRMS (ESI): calc. $C_{25}H_{48}O_6SiP$ $[M+H]^+$: 503.2958; found: 503.2937.

R_f (1:1 EtOAc:Pet ether) = 0.4.

Synthesis of 3.35

3.34 **3.35**

A solution of **3.34** (0.0918 g, 0.18 mmol) in THF (2.5 mL) was treated with tetra-*n*-butylammonium fluoride (TBAF, 280 μL, 1 M solution in THF, 0.28 mmol). After stirring at room temperature for one hour the reaction mixture was quenched with H_2O and the aqueous mixture extracted with Et_2O (3x). The combined organic extracts were washed with sat. NaCl, dried ($MgSO_4$) and the solvent removed *in vacuo*. Flash chromatography (2:1 EtOAc:Pet ether to 100% EtOAc) gave **3.35** (56.7 mg, 90%) as a pair of inseparable diastereoisomers (ratio 2:1).

Major diastereoisomer:

^{1}H NMR (500 MHz, *CDCl$_3$*) δ ppm 7.45-7.20 (m, 5H, Ph), 4.82-4.73 (m, 1H, CH_2Ph), 4.65-4.52 (m, 1H, CH_2Ph), 4.36-4.30 (m, 1H, H1a), 4.17-4.06 (overlap. m, 5H, OCH_2CH$_3$, H1b), 3.83 (dd, *J* = 3.5, 11.9 Hz, 1H, H4a), 3.69-3.64 (m, 1H, H4b), 3.63-3.57 (m, 1H, H2), 2.06-1.99 (m, 1H, H3), 1.36-1.30 (m, 6H, OCH$_2$CH_3), 0.96 (d, *J* = 7.0 Hz, 3H, CH$_3$).

^{13}C NMR (126 MHz, *CDCl$_3$*) δ ppm 137.9, 128.8, 128.3, 128.2, 128.1, 128.0, 82.0 (d, $^3J_{POCC}$ = 7.0 Hz, C2), 73.0 (CH_2Ph), 67.3 (d, $^2J_{POC}$ = 6.0 Hz, C1), 64.1 (m, OCH_2CH$_3$), 61.4 (C4), 36.8 (C3), 16.4 (m, OCH$_2$CH_3), 14.0 (CH$_3$).

Minor diastereoisomer:

^{1}H NMR (500 MHz, *CDCl$_3$*) δ ppm 7.45-7.20 (m, 5H, Ph), 4.82-4.73 (m, 1H, C$\underline{H}_2$Ph), 4.65-4.52 (m, 1H, C$\underline{H}_2$Ph), 4.17-4.06 (overlap. m, 6H, OC$\underline{H}_2$CH$_3$, H1'), 3.70-3.57 (m, 2H, H4'), 3.52-3.46 (m, 1H, H2'), 2.25-2.16 (m, 1H, H3'), 1.36-1.30 (m, 6H, OCH$_2$C$\underline{H}_3$), 1.03 (d, *J* = 7.0 Hz, 3H, CH$_3$').

^{13}C NMR (126 MHz, *CDCl$_3$*) δ ppm 138.4, 128.8, 128.3, 128.2, 128.1, 128.0, 80.5 (C2'), 72.7 (C$\underline{H}_2$Ph), 69.6 (d, $^{2}J_{POC}$ = 6.0 Hz, C1'), 66.0 (C4'), 64.1 (m, O$\underline{C}$H$_2$CH$_3$), 35.5 (d, *J* = 7.4 Hz, C3'), 16.4 (m, OCH$_2\underline{C}$H$_3$), 13.4 (CH$_3$').

R$_f$ (2:1 EtOAc:Pet ether) = 0.2.

Synthesis of 3.36

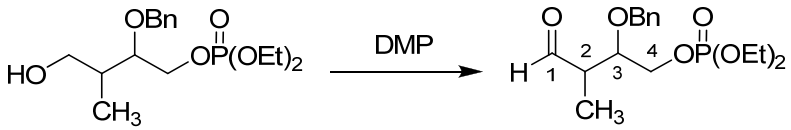

3.35 **3.36**

Compound **3.35** (0.1877 g, 0.54 mmol) was dissolved in DCM (10 mL) and freshly prepared DMP (0.5754 g, 1.36 mmol) was added. The mixture was stirred for 2.5 hours, after which DCM, sat. NaHCO$_3$ and sat. Na$_2$S$_2$O$_3$ were added and the mixture was stirred till the solution was clear. The mixture was transferred to a separating funnel and the aqueous layer extracted with DCM (3x). The combined organic extracts were washed with sat. NaCl, dried (MgSO$_4$) and the solvent removed *in vacuo*. Flash chromatography (2:1 EtOAc:Pet ether) gave aldehyde **3.36** (0.1347 g, 72%) as a pair of inseparable diastereoisomers (ratio 2:1).

Major diastereoisomer:

^{1}H NMR (500 MHz, *CDCl$_3$*) δ ppm 9.74 (d, *J* = 1.5 Hz, 1H, H1), 7.38-7.26 (m, 5H, Ph), 4.79-4.69 (m, 1H, C$\underline{H}_2$Ph), 4.63-4.53 (m, 1H, C$\underline{H}_2$Ph), 4.30 (ddd, *J* = 4.0, 6.3, 10.9 Hz, 1H, H4a), 4.19-4.01 (overlap. m, 5H, OC$\underline{H}_2$CH$_3$, H4b), 3.88-3.83 (m, 1H, H3), 2.76 (quin, *J* = 6.6 Hz, 1H, H2), 1.36-1.28 (m, 6H, OCH$_2$C$\underline{H}_3$), 1.13 (d, *J* = 7.3 Hz, 3H, CH$_3$).

^{13}C NMR (126 MHz, *CDCl$_3$*) δ ppm 203.2 (C1), 137.7, 130.0, 128.7, 128.6, 128.5, 128.3, 128.1, 128.0, 127.8, 78.2 (d, $^{3}J_{POCC}$ = 7.9 Hz, C3), 72.6 (C$\underline{H}_2$Ph), 66.0 (d, $^{2}J_{POC}$ = 6.0 Hz, C4), 64.3 (m, O$\underline{C}$H$_2$CH$_3$), 47.9 (C2), 16.3 (m, OCH$_2\underline{C}$H$_3$), 10.5 (CH$_3$).

Minor diastereoisomer:

^{1}H NMR (500 MHz, *$CDCl_3$*) δ ppm 9.70 (d, *J* = 1.8 Hz, 1H, H1'), 7.38-7.26 (m, 5H, Ph), 4.79-4.69 (m, 1H, C$\underline{H}_2$Ph), 4.63-4.53 (m, 1H, C$\underline{H}_2$Ph), 4.19-4.01 (overlap. m, 5H, OC$\underline{H}_2$CH$_3$, H4'), 3.69 (dd, *J* = 2.2, 5.1 Hz, 1H, H3'), 2.88 (quin, *J* = 7.1 Hz, 1H, H2'), 1.37-1.28 (m, 6H, OCH$_2$C$\underline{H}_3$), 1.06 (d, *J* = 7.3 Hz, 3H, CH$_3$').

^{13}C NMR (126 MHz, *$CDCl_3$*) δ ppm 203.2 (C1'), 137.7, 130.0, 128.7, 128.6, 128.5, 128.3, 128.1, 128.0, 127.8, 79.5 (d, $^{3}J_{POCC}$ = 7.9 Hz, C3'), 73.4 ($\underline{C}$H$_2$Ph), 66.6 (d, $^{2}J_{POC}$ = 6.0 Hz, C4'), 64.3 (m, O$\underline{C}$H$_2$CH$_3$), 41.7 (C2'), 16.3 (m, OCH$_2\underline{C}$H$_3$), 13.2 (CH$_3$').

HRMS (ESI): calc. $C_{16}H_{26}O_6P$ $[M+H]^+$: 345.1467; found: 345.1475.

R_f (2:1 EtOAc:Pet ether) = 0.3.

Synthesis of 3.37

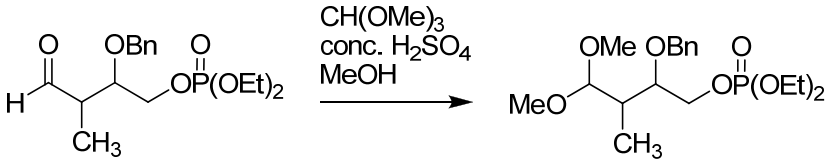

3.36 **3.37**

To **3.36** (0.1341 g, 0.39 mmol) in MeOH (8.0 mL) was added trimethyl orthoformate (430 µL, 3.93 mmol) and conc. H_2SO_4 (10 µL, 0.19 mmol). After stirring overnight, the mixture was transferred to a separating funnel containing sat. $NaHCO_3$ and Et_2O. The aqueous layer was extracted with Et_2O (3x). The combined organic extracts were washed with sat. NaCl, dried ($MgSO_4$) and the solvent removed *in vacuo*. Flash chromatography using deactivated silica, (1:1 EtOAc:Pet ether) gave **3.37** (0.1177 g. 77%) as a pair of inseparable diastereoisomers (ratio 2:1).

Major diastereoisomer:

^{1}H NMR (500 MHz, *CDCl$_3$*) δ ppm 7.37-7.26 (m, 5H, Ph), 4.72 (d, *J* = 11.7 Hz, 1H, C$\underline{H}_2$Ph), 4.52 (d, *J* = 11.7 Hz, 1H, C$\underline{H}_2$Ph), 4.38 (ap.t, *J* = 5.9 Hz, 1H, H1), 4.28 (ddd, *J* = 3.1, 5.7, 11.0 Hz, 1H, H4a), 4.14-4.07 (overlap. m, 5H, OC$\underline{H}_2$CH$_3$, H4b), 3.69-3.62 (m, 1H, H3), 3.36 (s, 3H, OMe), 3.33 (s, 3H, OMe), 2.18-2.10 (m, 1H, H2), 1.32 (t, *J* = 7.0 Hz, 6H, OCH$_2$C$\underline{H}_3$), 0.94 (d, *J* = 7.0 Hz, 3H, CH$_3$).

^{13}C NMR (126 MHz, *CDCl$_3$*) δ ppm 138.6, 128.5, 128.0, 127.8, 127.7, 106.2 (C1), 79.3 (d, $^{3}J_{POCC}$ = 7.4 Hz, C3), 72.7 (C$\underline{H}_2$Ph), 67.9 (d, $^{2}J_{POC}$ = 6.0 Hz, C4), 63.9 (m, O$\underline{C}$H$_2$CH$_3$), 55.6 (OMe), 55.0 (OMe), 38.2 (C2), 16.4 (m, OCH$_2\underline{C}$H$_3$), 10.0 (CH$_3$).

Minor diastereoisomer:

^{1}H NMR (500 MHz, *CDCl$_3$*) δ ppm 7.37-7.26 (m, 5H, Ph), 4.80 (d, *J* = 11.4 Hz, 1H, C$\underline{H}_2$Ph), 4.58-4.50 (m, 1H, C$\underline{H}_2$Ph), 4.38 (ap.t, *J* = 5.9 Hz, 1H, H1'), 4.19-4.05 (overlap. m, 5H, OC$\underline{H}_2$CH$_3$, H4a'), 3.98 (td, *J* = 6.3, 9.8 Hz, 1H, H4b'), 3.47 (s, 3H, OMe), 3.43 (s, 3H, OMe), 3.41-3.37 (m, 1H, H3'), 2.26-2.18 (m, 1H, H2'), 1.32 (t, *J* = 7.0 Hz, 6H, OCH$_2$C$\underline{H}_3$), 1.04 (d, *J* = 7.0 Hz, 3H, CH$_3$).

^{13}C NMR (126 MHz, *CDCl$_3$*) δ ppm 138.9, 128.5, 128.0, 127.8, 127.7, 106.5 (C1'), 81.3 (C3'), 74.6 (C$\underline{H}_2$Ph), 69.4 (d, $^{2}J_{POC}$ = 6.0 Hz, C4'), 63.9 (m, O$\underline{C}$H$_2$CH$_3$), 56.2 (OMe), 55.7 (OMe), 35.8 (d, *J* = 7.9 Hz, C2), 16.4 (m, OCH$_2\underline{C}$H$_3$), 14.3 (CH$_3$').

^{31}P NMR (121 MHz, *CDCl$_3$*) δ ppm −0.76, −0.85.

HRMS (ESI): calc. $C_{18}H_{32}O_7P$ $[M+H]^+$: 391.1886; found: 391.1883.

R$_f$ (1:1 EtOAc:Pet ether) = 0.1.

Synthesis of 3.38

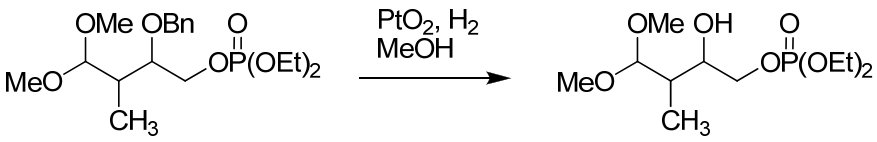

3.37 **3.38**

To the protected analogue **3.37** (0.1125 g, 0.29 mmol) in MeOH (8.0 mL) was added PtO_2 (0.0676 g, 0.30 mmol). After three vacuum/H_2 cycles, to flush the flask with H_2, the mixture

was vigorously stirred at room temperature under hydrogen (balloon) for three days. The PtO_2 was filtered through a small pad of celite and the pad washed with MeOH (3x). The filtrate was concentrate *in vacuo* followed by flash chromatography (2:1 EtOAc:Pet ether) gave **3.38** (82.5 mg, 95%) as a pair of inseparable diastereoisomers (ratio 2:1).

Major diastereoisomer:

^{1}H NMR (500 MHz, $CDCl_3$) δ ppm 4.37 (d, *J* = 5.1 Hz, 1H, H1), 4.19 (ddd, *J* = 2.9, 5.5, 11.0 Hz, 1H, H4a), 4.15-4.07 (m, 4H, $OC\underline{H}_2CH_3$), 4.00 (ap.td, *J* = 5.6, 11.1 Hz, 1H, H4b), 3.40-3.37 (overlap. m, 7H, OMe, H3), 2.10-2.04 (m, 1H, H2), 1.73 (t, *J* = 7.2 Hz, 6H, $OCH_2C\underline{H}_3$), 0.91 (d, *J* = 7.3 Hz, 1H, CH_3).

^{13}C NMR (126 MHz, $CDCl_3$) δ ppm 106.3, 79.8, 67.6, 64.0, 55.7, 55.0, 38.1, 16.4, 10.0 (CH_3).

Minor diastereoisomer:

^{1}H NMR (500 MHz, $CDCl_3$) δ ppm 4.69 (d, *J* = 5.5 Hz, 1H, H1'), 4.55-4.47 (overlap. m, 5H, H4a', $OC\underline{H}_2CH_3$), 4.37-4.31 (m, 1H, H4b'), 3.84 (s, 3H, OMe), 3.80 (s, 3H, OMe), 3.62-3.53 (m, 1H, H3'), 2.60-2.52 (m, 1H, H2'), 1.73 (t, *J* = 7.2 Hz, 6H, $OCH_2C\underline{H}_3$), 1.42 (d, *J* = 7.0 Hz, 1H, CH_3).

^{13}C NMR (126 MHz, $CDCl_3$) δ ppm 106.4, 81.7, 76.6, 64.0, 55.7, 55.0, 35.8, 16.4, 14.3 (CH_3).

^{31}P NMR (121 MHz, *$CDCl_3$*) δ ppm −0.77, −0.83.

R_f (2:1 EtOAc:Pet ether) = 0.3.

6.3.3 Experimental for Chapter 4

Preparation of E4P[90]

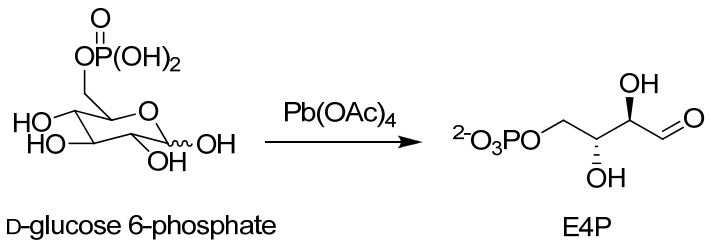

D-glucose 6-phosphate E4P

D-Glucose 6-phosphate (0.34 g, 1.0 mmol) was moistened with 2.0 mL of H_2O and 5.0 mL of glacial acetic acid was added to the reaction mixture. A 0.17 mL aliquot of 3 M H_2SO_4 and 245 mL of glacial acetic acid were then added to the reaction mixture. A mixture containing 3 M H_2SO_4 (0.60 mL), glacial acetic acid (40 mL), and lead tetraacetate (1.70 mmol) was prepared before use and added drop wise to the D-glucose 6-phosphate solution over 30 minutes with vigorous stirring. The reaction mixture was then filtered through a celite pad. The celite was washed with 100 mL of H_2O (3x) and the filtrate was concentrated until the volume of the solution reached approximately 20 mL. The concentrate was then extracted continuously with ether for 15 hours and the volume of the aqueous solution was reduced *in vacuo* to give a final volume of 25 mL. This solution was stored in the refrigerator or frozen and stored at −20ºC. Standard enzyme assay conditions determined the yield of E4P to be 48%.

Synthesis of 4.1

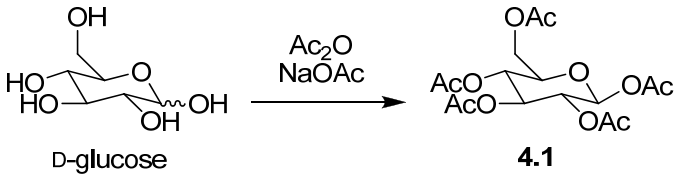

D-glucose **4.1**

Following the procedure by Tsuji *et al.*[148]: A mixture of D-glucose (30.13 g, 0.17 mol), Ac_2O (100 mL), NaOAc (5.2104 g, 0.06 mol) and toluene (2.50 mL) was refluxed with stirring for three hours. H_2O (100 mL) was added to this solution and the mixture was stirred and neutralised with a 3% (w/v) NaOH solution. The organic layer was concentrated to give

crude crystals. Recrystallisation from EtOH gave pure **4.1** (28.5932 g, 44%) as a white solid with spectral data in accordance with the literature.[196]

^{1}H NMR (300MHz, *$CDCl_3$*) δ ppm 5.70 (d, *J* = 7.8 Hz, 1H), 5.29-5.19 (m, 1H), 5.17-5.06 (m, 2H), 4.28 (dd, *J* = 4.4, 12.7 Hz, 1H), 4.14-4.06 (m, 1H), 3.88-3.78 (m, 1H), 2.10 (s, 3H), 2.07 (s, 3H), 2.02 (s, 6H), 2.00 (s, 3H).
HRMS (ESI): calc. $C_{16}H_{22}O_{11}Na$ $[M+Na]^+$: 413.1054; found: 413.1061.
M.p. 126–128°C; lit.[196] 131°C.

Synthesis of 4.2

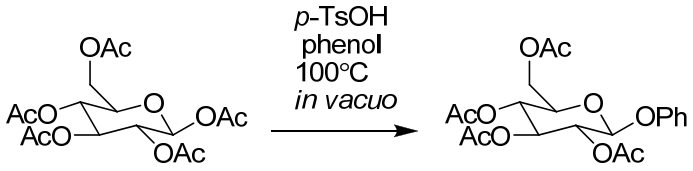

Following the procedure by Montgomery *et al.*[149]: A mixture of **4.1** (9.9895 g, 30 mmol), phenol (11.5182 g, 120 mmol), *p*-tolunesulfonic acid (0.1795 g, 0.94 mmol) was prepared in a Claisen flask. The mixture was heated at 100°C *in vacuo* for one hour where $N_{2(g)}$ was bubbled through the solution. The resulting dark red syrup was dissolved in 1,2 dichloroethane, washed with 3 M NaOH and the organic layer collected and concentrated. Recrystallisation from EtOH gave **4.2** (3.5046 g, 32%) as a white solid with spectral data in accordance with the literature.[197]

^{1}H NMR (300MHz, *$CDCl_3$*) δ ppm 7.34-7.25 (m, 2H), 7.11-7.04 (m, 2H), 7.02-6.96 (m, 1H), 5.32-5.27 (m, 1H), 5.21-5.13 (m, 1H), 5.11-5.06 (m, 1H), 4.30 (dd, *J* = 5.4, 12.2 Hz, 1H), 4.17 (dd, *J* = 2.4, 12.2 Hz, 1H), 3.86 (ddd, *J* = 2.4, 5.2, 9.9 Hz, 1H), 2.08 (s, 2H), 2.06 (s, 3H), 2.05 (s, 3H), 2.04 (s, 3H).
M.p. 123–125°C; lit.[197] 124–125°C.

Synthesis of 4.4

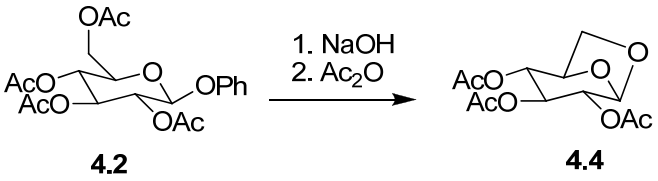

4.2 **4.4**

Following the procedure outlined by Lu *et al.*[150]: In a round bottom flask was added the β-phenylglycoside **4.2** (8.7228 g, 20.6 mmol), 40 mL of a 3 M solution of NaOH (120 mmol) and the mixture was refluxed for 24 hours in an oil bath. After cooling, the mixture was neutralised with conc. H_2SO_4 and diluted with ice of the same volume. The solution was concentrated on a rotary evaporator, extracted with 50 mL of boiling EtOH, filtered, and the filter cake was washed with hot EtOH (2x 10 mL). The combined EtOH solution was concentrated and acetylised by heating at 100°C in an oil bath for one hour with 30 mL of Ac_2O. The excess Ac_2O was decomposed with 10 mL of H_2O. AcOH was removed under reduced pressure. Then the mixture was extracted with $CHCl_3$ (2x 20 mL). The salt suspended in the solution was washed off with water. The $CHCl_3$ was removed under vacuum, and then 10 mL of EtOH was added to the residue. After 8–10 hrs in the fridge, a white solid was obtained with vacuum filtration. The mother liquid was concentrated, and 10 mL ether was added. After crystallising in the fridge, more solid was obtained. The combined solids were triturated in 10 mL of 0°C ether and then filtered to give compound **4.4** (2.3239 g, 39%). The spectral data was in accordance with that reported in the literature.[151]

^{1}H NMR (300MHz, *CDCl$_3$*) δ ppm 5.47 (br. s, 1H), 4.86 (ap.s, 1H), 4.66-4.56 (m, 3H), 4.10 (d, *J* = 7.3 Hz, 1H), 3.81 (dd, *J* = 5.4, 7.8 Hz, 1H), 2.17 (s, 3H), 2.15 (s, 3H), 2.12 (s, 3H).
M.p. 107–110°C; lit.[151] 110–112°C.

Synthesis of 4.5

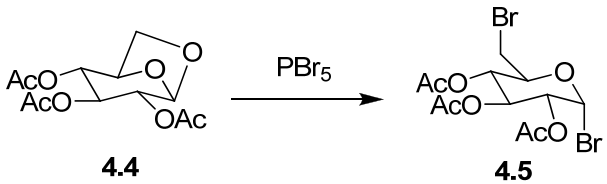

4.4 **4.5**

Following the procedure by Irvine *et al.*[152]: Sugar **4.4** (1.0807 g, 3.75 mmol) was heated on an oil bath at 80–90°C with PBr_5 (2.3471 g, 5.45 mmol) with stirring. The flask was fitted with a reflux condenser and performed under nitrogen. When effervescence had nearly ceased, the contents of the flask were poured into crushed ice and thoroughly disintegrated by a glass rod. The solution was filtered, the filter cakes was washed with H_2O until free of phosphoric acid and thereafter with EtOH until the washings were nearly colourless giving a fine white solid. Purification was effected by dissolving the solid in a small quantity of $CHCl_3$ and precipitated with pet ether giving the dibromo-derivative **4.5** (0.5451 g, 34%) as a very light brown to white solid.

^{1}H NMR (500 MHz, *$CDCl_3$*) δ ppm 6.63 (d, *J* = 4.0 Hz, 1H, H1), 5.56 (t, *J* = 9.7 Hz, 1H, H3), 5.18 (t, *J* = 9.5 Hz, 1H, H4), 4.84 (dd, *J* = 4.0, 9.9 Hz, 1H, H2), 4.33 (ddd, *J* = 2.9, 4.8, 9.9 Hz, 1H, H5), 3.57-3.52 (m, 1H, H6a), 3.47-3.42 (m, 1H, H6b), 2.10 (s, 3H, Ac), 2.08 (s, 3H, Ac), 2.04 (s, 3H, Ac).
^{13}C NMR (126 MHz, *$CDCl_3$*) δ ppm 170.2, 170.0, 169.5, 86.4 (C1), 72.7 (C5), 70.8 (C2), 70.3 (C3), 69.9 (C4), 30.3 (C6), 20.9 (Ac x3).
HRMS (ESI): calc. $C_{12}H_{16}Br_2NaO_7$ $[M+Na]^+$: 452.9155; found: 452.9158.
M.p. 173–174°C; lit.[152] 173°C.

Synthesis of 4.6

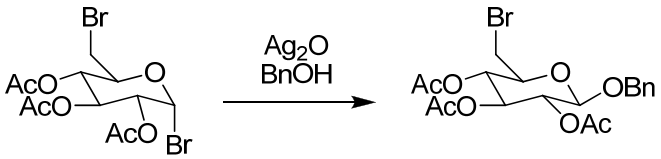

4.5 **4.6**

In a round bottom flask containing freshly activated 4Å molecular sieves was added the dibromo-derivative **4.5** (0.2554 g, 0.59 mmol), Ag_2O (0.1357 g, 0.59 mmol), BnOH (1 mL, 9.65 mmol) and anhydrous DCM (5 mL). The solution was stirred at −10°C (MeOH/ice bath) and stirred for twohours. The mixture was then filtered through celite to remove silver salts. The filtrate was then washed with H_2O, extracted with DCM and dried over Na_2SO_4. The solvent was removed *in vacuo* and the residue was purified by flash chromatography (1:1 EtOAc:Pet ether) and then recrystallised from EtOH to give pure **4.6** (50 mg, 18%) as a white solid.

^{1}H NMR (500 MHz, *$CDCl_3$*) δ ppm 7.39-7.29 (m, 5H, Ph), 5.17 (ap.t, *J* = 9.2 Hz, 1H, H3), 5.09-5.03 (m, 1H, H2), 4.98 (t, *J* = 9.5 Hz, 1H, H4), 4.92 (d, *J* = 12.5 Hz, 1H, C$\underline{H}_2$Ph), 4.68 (d, *J* = 12.1 Hz, 1H, C$\underline{H}_2$Ph), 4.55 (d, *J* = 8.1 Hz, 1H, H1), 3.67 (m, 1H, H5), 3.51-3.37 (m, 2H, H6a, H6b), 2.05 (s, 3H, Ac), 2.01 (s, 3H, Ac), 2.00 (s, 3H, Ac).

^{13}C NMR (126 MHz, *$CDCl_3$*) δ ppm 136.7, 128.7, 128.3, 128.2, 99.0 (C1), 73.7 (C5), 72.9 (C3), 71.6 (C2), 71.4 (C4), 70.8 (C$\underline{H}_2$Ph), 31.0 (C6), 20.9 (Ac x3).

HRMS (ESI): calc. $C_{19}H_{23}BrNaO_6$ $[M+Na]^+$: 481.0469; found: 481.0478.

R_f (1:1 EtOAc:Pet ether) = 0.7.

Synthesis of 4.15

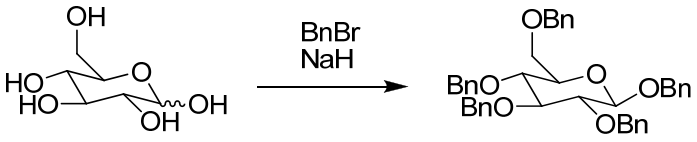

D-glucose **4.15**

Following the procedure by Lu *et al.*[158]: To a solution of D-glucose (9.65 g, 54 mmol) in dry DMF (250 mL) was added NaH (5.97 g, 249 mmol) at room temperature. This solution was stirred for 30 minutes then cooled in an ice bath. BnBr (21 mL, 177 mmol) was added dropwise over five minutes, and after ten minutes the ice bath was removed. After 2.5 hours stirring at room temperature additional NaH (5.94 g, 250 mmol) and BnBr (21 mL, 175 mmol) was added and stirred. After another 2.5 hours the final batch of NaH (3.98g, 165mmol) and BnBr (12 mL, 101 mmol) was added. The reaction mixture was stirred overnight, and then quenched slowly with MeOH. The solution was poured into H_2O (500 mL) and extracted with DCM (3x 150 mL). The combined organic layers were washed with H_2O (3x 300 mL), then sat. NaCl (300 mL) and dried over $MgSO_4$. The solvent was removed *in vacuo* to give the crude product. Flash chromatography (1:9 EtOAc:Pet ether) followed by recrystallisation from MeOH gave **4.15** (10.92 g , 32%) as a white solid with spectral data in accordance with the literature.[158]

^{1}H NMR (500 MHz, *$CDCl_3$*) δ ppm 7.47-7.16 (m, 25H, Ph), 5.03-4.55 (m, 10H, C$\underline{H}_2$Ph), 4.54 (d, *J* = 7.7 Hz, 1H, H1), 3.81-3.71 (m, 2H, H6), 3.69-3.61 (m, 2H, H3, H4), 3.55 (m, 1H, H2), 3.49 (ddd, *J* = 1.8, 4.8, 9.5 Hz, 1H).

^{13}C NMR (126 MHz, *CDCl$_3$*) δ ppm 138.8, 138.6, 138.4, 138.3, 137.7, 128.6, 128.4, 128.1, 128.1, 128.0, 127.8, 102.8 (C1), 84.9, 82.5 (C2), 78.1, 75.9, 75.2 (C5), 75.1, 73.7, 71.4, 69.1 (C6).

HRMS (ESI): calc. $C_{41}H_{42}NaO_6$ $[M+Na]^+$: 653.2879; found: 653.2865.

M.p.: 82–85°C, lit.[198] 83–83.5°C.

R$_f$ (1:9 EtOAC:Pet ether) = 0.2.

Synthesis of 4.16

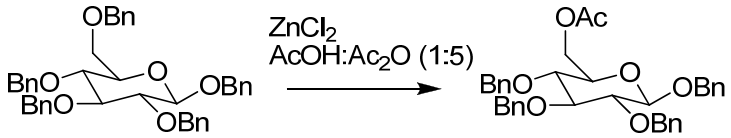

4.15 **4.16**

Following the procedure from Lu *et al.*[158]: To freshly fused $ZnCl_2$ (4.4385 g, 33 mmol) (under high vacuum overnight prior to use) was added AcOH:Ac_2O (1:5, 30 mL). The mixture was cooled down to 0°C and then a solution of **4.15** (4.01 g, 6.4 mmol) in AcOH:Ac_2O (1:5, 30 mL) was added dropwise. The reaction was stirred at room temperature for 1.5 hours and then 180 mL of ice-water was added. The resulting brownish precipitate was filtered and washed with H_2O. Purification by flash chromatography (1:5:1 $CHCl_3$:Pet ether:EtOAc) yielded **4.16** (2.3799 g, 64%) as a white solid.

^{1}H NMR (500 MHz, *CDCl$_3$*) δ pppm 7.40-7.24 (m, 20H, Ph), 5.00-4.55 (m, 8H, C$\underline{H_2}$Ph), 4.52 (d, *J* = 8.1 Hz, 1H, H1), 4.41-4.23 (m, 2H, H6), 3.71-3.65 (m, 1H, H3), 3.60-3.49 (m, 3H, H2, H4, H5), 2.07 (s, 3H, CH_3).

^{13}C NMR (126 MHz, *CDCl$_3$*) δ ppm 171.0, 138.6, 138.4, 137.9, 137.3, 128.7, 128.6, 128.6, 128.6, 128.4, 128.3, 128.2, 128.1, 127.9, 102.6 (C1), 84.9 (C3), 82.4, 77.6, 75.9, 75.2, 73.1, 71.4, 63.3 (C6), 21.1 (CH_3).

HRMS (ESI): calc. $C_{36}H_{38}NaO_7$ $[M+Na]^+$: 605.2515; found: 605.2528.

M.p. 112–113°C; lit.[199] 116–117°C.

R$_f$ (1:5:1 $CHCl_3$:Pet ether: EtOAc) = 0.5.

Synthesis of 4.17

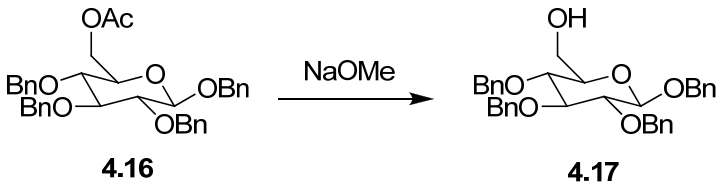

4.16 **4.17**

Following the procedure from Lu *et al.*[158]: A suspension of **4.16** (2.3799 g, 4.1 mmol) in 20 mL of 0.035 M NaOMe in MeOH was stirred for five hours at room temperature. The reaction mixture was then poured into 50 mL of ice-water and stirred for 30 minutes. The resulting precipitate was filtered and washed with sat. $NaHCO_3$, H_2O and then dried under high vacuum to give crude **4.17**. Recrystallisation from EtOH gave 4.18 (2.1211 g, 96%) as white solid with spectral data in accordance with the literature.[158]

^{1}H NMR (500 MHz, *$CDCl_3$*) δ ppm 7.40-7.26 (m, 20H, Ph), 4.99-4.63 (m, 8H, C$\underline{H}_2$Ph), 4.59 (d, *J* = 8.1 Hz, 1H, H1), 3.89 (ddd, *J* = 2.6, 5.9, 11.7 Hz, 1H, H6a), 3.75-3.66 (m, 2H, H6b, H3), 3.59 (t, *J* = 9.4 Hz, 1H, H4), 3.50 (t, *J* = 8.4 Hz, 1H, H2), 3.38 (ddd, *J* = 2.8, 4.4, 9.4 Hz, 1H, H5), 1.86 (t, *J* = 6.8 Hz, 1H), 1.61 (br. s, 1H, OH).

^{13}C NMR (75 MHz, *$CDCl_3$*) δ ppm 138.8, 138.6, 138.3, 137.6, 128.9, 128.8, 128.7, 128.5, 128.4, 128.3, 128.2, 128.1, 128.0, 103.2 (C1), 84.9, 82.7 (C2), 77.9, 76.1, 75.4, 72.0, 62.5 (C6).

HRMS (ESI): calc. $C_{34}H_{36}NaO_6$ $[M+Na]^+$: 563.2410; found: 563.2389.

M.p. 101–103°C; lit.[199] 104–106°C.

Synthesis of 4.18

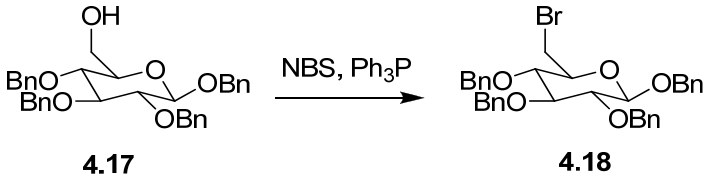

4.17 **4.18**

To a solution of **4.17** (2.001 g, 3.7 mmol) in dry DCM (20 mL) was added Ph_3P (2.9142 g, 11.1 mmol) at 0°C. To this cooled solution was added, portion wise and slowly, NBS (1.9797 g, 11.1 mmol) at a rate to maintain the exothermic reaction. The solution was stirred over

night with a drying tube attached, concentrated and filtered through a pad of celite. The celite was washed with ether (3x 50 mL) and the combined organic extracts were concentrated *in vacuo*. Flash chromatography (1:9 EtOAc:Pet ether) gave **4.18** (2.0651 g, 92%) as a white solid.

^{1}H NMR (500 MHz, *$CDCl_3$*) δ ppm 7.42-7.26 (m, 20H, Ph), 5.01-4.89 (m, 4H, C$\underline{H}_2$Ph), 4.81-4.64 (m, 4H, C$\underline{H}_2$Ph), 4.55 (d, *J* = 7.7 Hz, 1H, H1), 3.71-3.65 (m, 2H, H3, H6a), 3.58-3.45 (m, 4H, H2, H4, H5, H6b).

^{13}C NMR (75 MHz, *$CDCl_3$*) δ ppm 138.8, 138.7, 138.2, 137.5, 128.9, 128.8, 128.8, 128.7, 128.6, 128.5, 128.3, 128.1, 102.5 (C1), 84.9 (C3), 82.7 (C4), 80.0 (C2), 76.1, 75.6, 75.3, 74.4 (C5), 71.5, 33.2 (C6).

HRMS (ESI): calc. $C_{34}H_{35}NaO_5Br$ $[M+Na]^+$: 625.1566; found: 625.1573.

M.p. 103–106°C.

R_f (1:9 EtOAc:Pet ether) = 0.3.

Synthesis of 4.22

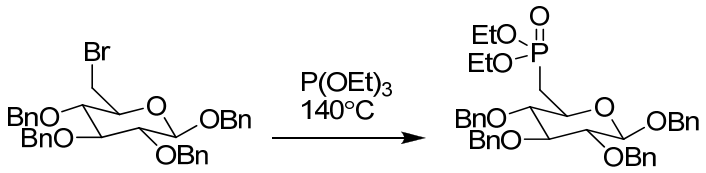

4.18 **4.22**

A mixture of **4.18** (1.0034 g, 1.7 mmol) and triethyl phosphite (14.5 mL, 84.5 mmol) was heated and stirred at 140°C. After three days the solution was subjected to high vacuum overnight. Flash chromatography (1:1 to 2:1 EtOAc:Pet ether) gave **4.22** (0.7526 g, 69%).

Alternative method:

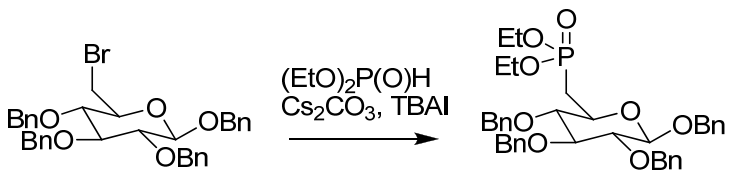

4.18 **4.22**

To a solution of diethyl phosphite (50 μL, 0.33 mmol) in DMF (5 mL) was added tetrabutylammonium iodide (TBAI, 0.1888 g, 0.51 mmol) and Cs_2CO_3 (0.1785 g, 0.55 mmol). The solution was stirred vigorously for one hour at room temperature before the addition of **4.18** (99.6 mg, 0.17 mmol) in DMF (5 mL). The reaction was stirred at room temperature for three days before the solution was poured into H_2O (30 mL) and extracted with EtOAc (3x 30 mL). The combined organic layers were dried over $MgSO_4$ and concentrated *in vacuo*. Flash chromatography (30% EtOAc:Pet ether to 100% EtOAc) gave **4.22** (44.7 mg, 41%) as a white solid.

^{1}H NMR (500 MHz, *$CDCl_3$*) δ ppm 7.51-7.14 (m, 20H, Ph), 5.04-4.90 (m, 4H, C$\underline{H}_2$Ph), 4.84-4.70 (m, 3H, C$\underline{H}_2$Ph), 4.65 (d, *J* = 11.0 Hz, 1H, C$\underline{H}_2$Ph), 4.57 (d, *J* = 7.7 Hz, 1H, H1), 4.19-4.07 (m, 4H, OC$\underline{H}_2$CH$_3$), 3.77-3.64 (m, 2H, H3, H5), 3.60-3.52 (m, 1H, H2), 3.35 (t, *J* = 9.0 Hz, 1H, H4), 2.33 (ap.dd., *J* = 16.9, 18.3 Hz, 1H, H6a), 1.92 (dt, *J* = 10.6, 15.6 Hz, 1H, H6b), 1.39-1.29 (m, 6H, OCH$_2$C$\underline{H}_3$).

^{13}C NMR (126 MHz, *$CDCl_3$*) δ ppm 138.6, 138.5, 138.0, 137.3, 128.6, 128.6, 128.5, 128.5, 128.2, 128.2, 128.1, 128.0, 128.0, 127.8, 102.2 (C1), 84.7 (d, *J* = 2.6 Hz, C3), 82.5 (C2), 81.7 (d, $^3J_{PCCC}$ = 14.8 Hz, C4), 75.8, 75.2, 74.9, 71.0, 70.6 (d, $^2J_{PCC}$ = 7.0 Hz, C5), 61.9 (d, $^2J_{POC}$ = 2.3 Hz, O$\underline{C}$H$_2$CH$_3$), 61.8 (d, $^2J_{POC}$ = 2.8 Hz, O$\underline{C}$H$_2$CH$_3$'), 28.4 (d, $^1J_{PC}$ = 142.9 Hz, C6, C6'), 16.8 (d, $^3J_{POCC}$ = 4.19 Hz, OCH$_2\underline{C}$H$_3$), 16.7 (d, $^3J_{POCC}$ = 4.19 Hz, OCH$_2\underline{C}$H$_3$').

^{31}P NMR (121 MHz, *$CDCl_3$*) δ ppm 29.57.

HRMS (ESI): calc. $C_{38}H_{46}O_8P$ $[M+H]^+$: 661.2930; found: 661.2961.

M.p. 96–98°C.

R_f (2:1 EtOAc:Pet ether) = 0.5.

Synthesis of 4.23

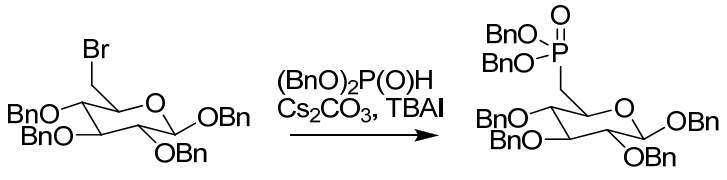

4.18 **4.23**

To a solution of dibenzyl phosphite (80 μL, 0.36 mmol) in DMF (5 mL) was added TBAI (0.1813 g, 0.49 mmol) and Cs_2CO_3 (0.1792 g, 0.55 mmol). The solution was stirred

vigorously for one hour at room temperature before the addition of **4.18** (102 mg, 0.17 mmol) in DMF (5 mL). The reaction was stirred at room temperature for five days before the solution was poured into H_2O (50 mL) and extracted with EtOAc (3x 30 mL). The combined organic layers were dried over $MgSO_4$ and concentrated in vacuo. Flash chromatograph (30% EtOAc:Pet ether to 100% EtOAc) gave **4.23** (48 mg, 36%) as a white solid.

^{1}H NMR (500 MHz, *CDCl$_3$*) δ ppm 7.39-7.22 (m, 30H, Ph), 5.11-5.00 (m, 4H, C$\underline{H}_2$Ph), 4.98-4.88 (m, 4H, C$\underline{H}_2$Ph), 4.79 (t, *J* = 11.0 Hz, 2H, C$\underline{H}_2$Ph), 4.72 (d, *J* = 10.6 Hz, 1H, C$\underline{H}_2$Ph), 4.61 (d, *J* = 11.0 Hz, 1H, C$\underline{H}_2$Ph), 4.53 (d, *J* = 11.7 Hz, 1H, C$\underline{H}_2$Ph), 4.50 (d, *J* = 7.7 Hz, 1H, H1), 3.70 (q, *J* = 9.9 Hz, 1H, H5), 3.64 (t, *J* = 8.8 Hz, 1H, H3), 3.53 (t, *J* = 8.4 Hz, 0H, H2), 3.34 (t, *J* = 9.2 Hz, 1H, H4), 2.45-2.33 (m, 1H, H6), 1.99 (dt, *J* = 10.3, 15.6 Hz, 1H, H6').
^{13}C NMR (75 MHz, *CDCl$_3$*) δ ppm 138.7, 138.6, 138.2, 137.5, 128.9, 128.8, 128.8, 128.7, 128.7, 128.5, 128.3, 128.2, 128.2, 128.0, 128.0, 102.6 (C1), 84.8 (C3), 82.7 (C2), 81.8 (d, $^3J_{PCCC}$ = 14.7 Hz, C4), 76.0, 75.3, 75.1, 71.2, 70.7 (d, $^2J_{PCC}$ = 7.2 Hz, C5), 68.0, 67.9, 67.5, 67.5, 67.4, 67.3, 29.10 (d, $^1J_{PC}$ = 142.7 Hz, C6, C6').
^{31}P NMR (121 MHz, *CDCl$_3$*) δ ppm 30.59.
HRMS (ESI): calc. $C_{48}H_{50}O_8P$ $[M+H]^+$: 785.3243; found: 785.3240.
M.p. 76–79°C.
R_f (30% EtOAc:Pet ether) = 0.2.

Synthesis of 4.24

4.22 **4.24**

To a solution of **4.22** (0.2060 g, 0.31 mmol) in DCM (10 mL) was added TMSBr (200 µL, 1.52 mmol) and the mixture was stirred for 24 hours at room temperature. After removal of the solvent *in vacuo*, the remaining residue was treated with a solvent mixture of MeOH:DCM (5:1, 10 mL) and stirred vigorously for 12 hours. The solvent was then removed *in vacuo* to give **4.24** (0.1854g, 98%) as a pale white-yellow solid that was spectroscopically pure by ^{1}H NMR.

^{1}H NMR (500 MHz , *$CDCl_3$*) δ ppm 7.43-7.03 (m, 20H, Ph), 4.96-4.79 (m, 4H, C$\underline{H_2}$Ph), 4.74-4.65 (m, 2H, C$\underline{H_2}$Ph), 4.59 (d, *J* = 12.1 Hz, 1H, C$\underline{H_2}$Ph), 4.51 (d, *J* = 11.0 Hz, 1H, C$\underline{H_2}$Ph), 4.46 (d, *J* = 7.7 Hz, 1H, H1), 3.65-3.51 (m, 2H, H3, H5), 3.51-3.44 (m, 1H, H2), 3.23 (t, *J* = 9.0 Hz, 1H, H4), 2.34-2.19 (m, 1H, H6), 1.91-1.78 (m, 1H, H6').

^{13}C NMR (126 MHz, *$CDCl_3$*) δ ppm 138.6, 138.5, 137.8, 137.4, 128.7, 128.6, 128.5, 128.5, 128.5, 128.2, 128.2, 128.1, 128.0, 127.8, 127.8, 102.4 (C1), 84.5 (C3), 82.4 (C2), 81.34 (d, $^{3}J_{PCCC}$ = 14.8 Hz, C4), 75.9, 75.2, 74.9, 71.3, 70.20-70.10 (m, C5), 28.42 (d, $^{1}J_{PC}$ = 151.3 Hz, C6, C6').

^{31}P NMR (121 MHz, *$CDCl_3$*) δ ppm 34.82.

HRMS (ESI): calc. $C_{34}H_{38}O_8P$ $[M+H]^+$: 605.2304; found: 605.2297.

M.p. 179–181°C

Synthesis of 4.14

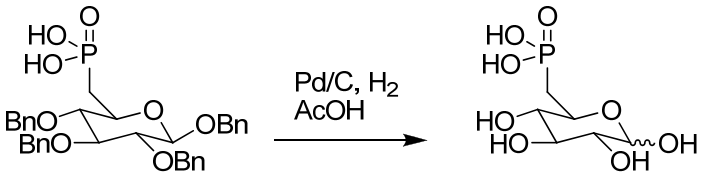

4.24 **4.14**

To **4.24** (81.4 mg, 0.13 mmol) in AcOH (3 mL) was added 10% Pd/C (20% wt of 4.25). After three vacuum/H_2 cycles, to flush the flask with H_2, the mixture was vigorously stirred at room temperature under hydrogen (balloon) for 48 hours. The Pd/C was filtered through a small pad of celite and the pad washed with MeOH (3x). The filtrate was concentrate *in vacuo* to give crude **4.14** as an oil. The oil was purified using a reverse phase C18 silica column eluting with 10% MeOH:H_2O. The relevant fractions were collected and freeze dried to give **4.14** as a sticky white-yellow semi-solid (29.8 mg, 100%) containing both α- and β-anomers (1:1.3 ratio, respectively).

^{1}H NMR (500 MHz, *D_2O*) δ ppm 5.07 (d, *J* = 3.3 Hz, 1H, H1α), 4.53 (d, *J* = 7.7 Hz, 1H, H1β), 3.96 (q, *J* = 9.8 Hz, 1H, H5α), 3.60-3.46 (m, 2H, H3α and H5β), 3.42 (dd, *J* = 3.3, 9.9 Hz, 1H, H2α), 3.34 (ap.t, *J* = 9.5 Hz, 1H, H3β), 3.16-3.07 (m, 3H, H4α, H2β, H4β), 2.25-2.13 (m, 2H, H6α, H6β), 1.87-1.76 (m, 3H, H6'α, H6'β).

^{13}C NMR (126 MHz, D_2O) δ ppm 96.0 (C1β), 92.1 (C1α), 75.5, 74.3, 74.1, 74.0, 72.7, 71.7, 67.1, 29.7 (d, $^1J_{PC}$ = 137.7 Hz, C6β, C6'β), 29.6 (d, $^1J_{PC}$ = 137.7 Hz, C6α, C6'α).

^{31}P NMR (121 MHz, $CDCl_3$) δ ppm 26.07, 25.49.

HRMS (ESI): calc. $C_6H_{12}O_8P$ $[M-H]^-$: 243.0270; found: 243.0267.

Synthesis of 4.26

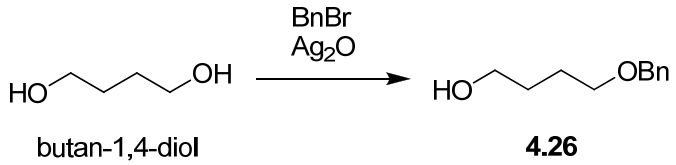

butan-1,4-diol **4.26**

To a solution of butan-1,4-diol (5.0385 g, 56 mmol) in DCM (100 mL) was added Ag_2O (19.3293 g, 83.4 mmol) and BnBr (7.30 mL, 61.4 mmol) at room temperature. The mixture was stirred for four hours before the residual Ag_2O was filtered through celite. The resulting filtrate was concentrated *in vacuo* and purified by flash chromatography (10 to 30% EtOAc:Pet ether) to give **4.26** (7.5065 g, 75%) as a colourless oil with spectral data in accordance with the literature.[169]

^{1}H NMR (500 MHz, $CDCl_3$) δ ppm 7.38-7.26 (m, 5H, Ph), 4.53 (s, 2H, C$\underline{H_2}$Ph), 3.65 (t, J = 5.9 Hz, 2H, H4), 3.53 (t, J = 5.7 Hz, 2H, H1), 2.35 (br. s, 1H, OH), 1.77-1.63 (m, 4H, H2, H3).

^{13}C NMR (126 MHz, $CDCl_3$) δ ppm 171.4, 138.4, 128.7, 127.9, 73.3, 70.6 (C1), 62.9 (C4), 30.4 (C3), 26.9 (C2).

R_f (30% EtOAc:Pet ether) = 0.15

Synthesis of 4.27

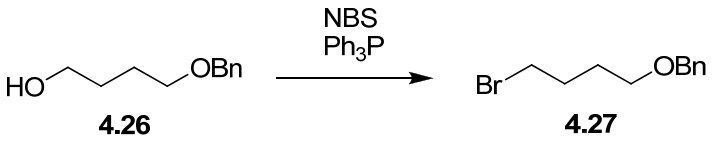

4.26 **4.27**

To a solution of **4.26** (1.5020 g, 8.33 mmol) in DCM (25 mL) was added Ph_3P (3.2773 g, 12.5 mmol) and the solution was cooled to 0°C. To this cooled solution was added NBS

(2.2252 g, 12.5 mmol) portionwise. The mixture was then stirred for five hours at room temperature, concentrated *in vacuo* and filtered through a pad of celite to remove triphenylphosphine oxide. The pad was washed with ether, the filtrate collected, concentrated *in vacuo* and purified by flash chromatography (5% EtOAc:Pet ether) to give **4.27** (1.7419 g, 86 %) as a colourless oil with spectral data in accordance with literature.[173]

^{1}H NMR (500 MHz, *CDCl$_3$*) δ ppm 7.38-7.25 (m, 5H, Ph), 4.51 (s, 2H, C$\underline{H}_2$Ph), 3.51 (t, *J* = 6.1 Hz, 2H, H1), 3.44 (t, *J* = 6.8 Hz, 2H, H4), 2.03-1.94 (m, 2H, H3), 1.82-1.72 (m, 2H, H2).
^{13}C NMR (126 MHz, *CDCl$_3$*) δ ppm 138.6, 128.6, 127.8, 73.2 (C$\underline{H}_2$Ph), 69.5 (C1), 34.0 (C4), 29.9 (C3), 28.6 (C2).
R$_f$ (10% EtOAc:Pet ether) = 0.60.

Synthesis of 4.28

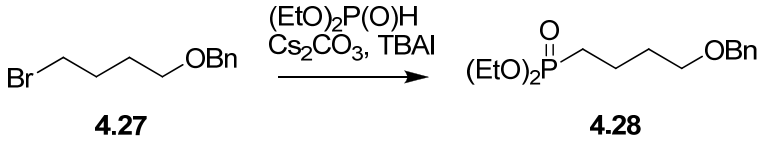

4.27 **4.28**

To a solution of diethyl phosphite (530 µL, 4.11 mmol) in DMF (20 mL) was added TBAI (4.5576 g, 12.3 mmol) and Cs_2CO_3 (4.0153 g, 12.3 mmol). The solution was stirred vigorously for one hour at room temperature before the addition of **4.27** (0.5021 g, 2.07 mmol) in DMF (5 mL). The reaction was stirred at room temperature for three days before the solution was poured into H_2O and extracted with EtOAc (3x). The combined organic layers were washed with sat. NaCl, dried over $MgSO_4$ and concentrated *in vacuo*. Flash chromatography (2:1 EtOAc:Pet ether to 5% MeOH:EtOAc) gave **4.28** (0.5170 g, 83%).

^{1}H NMR (500 MHz, *CDCl$_3$*) δ ppm 7.37-7.26 (m, 5H, Ph), 4.50 (s, 2H, C$\underline{H}_2$Ph), 4.16-4.02 (m, 4H, OC$\underline{H}_2$CH$_3$), 3.51-3.45 (m, 2H, H1), 1.81-1.67 (m, 6H, H2, H3, H4), 1.32 (t, *J* = 7.2 Hz, 6H, OCH$_2$C$\underline{H}_3$).
^{13}C NMR (126 MHz, *CDCl$_3$*) δ ppm 138.7, 128.6, 127.8, 127.8, 73.2 (C$\underline{H}_2$Ph), 69.8 (C1), 61.7 (d, $^2J_{POC}$ = 6.5 Hz, O$\underline{C}$H$_2$CH$_3$), 30.8 (d, $^3J_{PCCC}$ = 16.7 Hz, C2), 25.7 (d, $^1J_{PC}$ = 141.0 Hz, C4), 19.7 (d, $^2J_{PCC}$ = 5.1 Hz, C3), 16.7 (d, $^3J_{POCC}$ = 6.0 Hz, OCH$_2$C$\underline{H}_3$).
^{31}P NMR (121 MHz, *CDCl$_3$*) δ ppm 32.18.

HRMS (ESI): calc. $C_{15}H_{25}NaO_4P$ $[M+Na]^+$: 323.1383; found: 323.1382.

R_f (5% MeOH:EtOAc) = 0.6.

Synthesis of 4.34

Method 1:

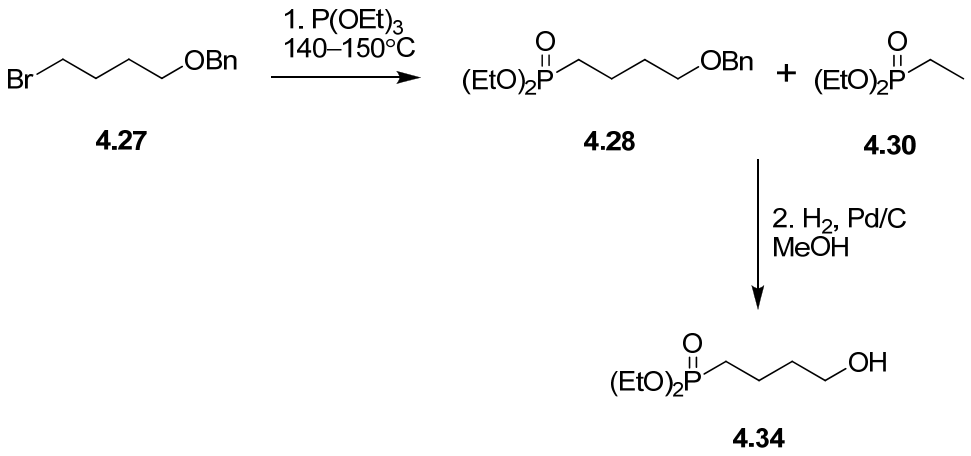

4.27 **4.28** **4.30** **4.34**

To **4.27** (0.5010 g, 2.06 mmol) was added $P(OEt)_3$ in excess (52.5 mmol). The mixture was heated to 140–150°C on an oil bath. After three days the mixture was quenched with H_2O and extracted with ether. The organic layer was washed with sat. $NaHCO_3$, sat. NaCl and dried over $MgSO_4$. The organic layer was concentrated to give a mixture of **4.28** and side-product **4.30** that was inseparable by column chromatography. To the inseparable mixture of **4.28** and **4.30** was added MeOH and 10% Pd/C (2% wt of mixture). After three vacuum/H_2 cycles, to flush the flask with H_2, the mixture was vigorously stirred at room temperature under hydrogen (balloon) for four days. The Pd/C was filtered through a small pad of celite and the pad washed with MeOH (3x). The filtrate was concentrate *in vacuo* and purified by flash chromatography (5% MeOH:EtOAc) to give **4.34** (86.9 mg, 20% over 2 steps) as a colourless oil.

Method 2:

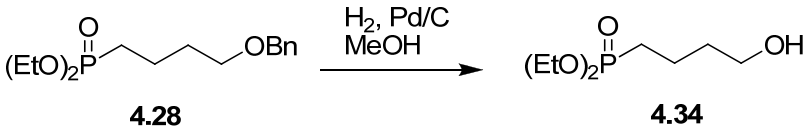

4.28 **4.34**

A mixture of **4.28** (0.5017 g, 1.63 mmol) in MeOH (20 mL) was added 10% Pd/C (10% wt of **4.28**). The mixture was hydrogenated at 30 atm and 45°C using a Parr hydrogenator

overnight. The Pd/C was filtered through a small pad of celite and the pad washed with MeOH (3x). The filtrate was concentrate *in vacuo* and purified by flash chromatography (5% MeOH:EtOAc) to give **4.34** (85.2 mg, 24%).

Method 3:

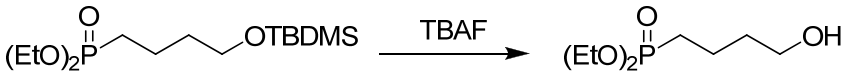

4.33 **4.34**

A solution of **4.33** (0.5450 g, 1.68 mmol) in THF (10 mL) was treated with TBAF (2.5 mL, 1 M solution in THF, 2.5 mmol). After stirring at room temperature for two hours, the reaction mixture was quenched with H_2O and the aqueous mixture extracted with DCM (3x). The combined organic extracts were washed with sat. NaCl, dried ($MgSO_4$) and the solvent removed *in vacuo*. Flash chromatography (5% MeOH:EtOAc) gave **4.34** (0.1879 g, 52%).

^{1}H NMR (500 MHz, *$CDCl_3$*) δ ppm 4.18-4.02 (m, 4H, $OC\underline{H}_2CH_3$), 3.67 (t, *J* = 6.1 Hz, 2H, H1), 1.84-1.63 (m, 6H, H2, H3, H4), 1.33 (t, *J* = 7.2 Hz, 6H, $OCH_2C\underline{H}_3$).
^{13}C NMR (126 MHz, *$CDCl_3$*) δ ppm 62.3 (C1), 61.7 (d, $^2J_{POC}$ = 6.5 Hz, $O\underline{C}H_2CH_3$), 33.5 (, $^3J_{PCCC}$ = 14.9 Hz, C2), 25.5 (d, $^1J_{PC}$ = 141.0 Hz, C4), 19.1 (d, $^2J_{PCC}$ = 5.1 Hz, C3), 16.7 (d, $^3J_{POCC}$ = 6.0 Hz, $OCH_2\underline{C}H_3$).
^{31}P NMR (121 MHz, *$CDCl_3$*) δ ppm 32.34.
HRMS (ESI): calc. $C_8H_{20}O_4P$ $[M+H]^+$: 211.1099; found: 211.1098.
R_f (5% MeOH:EtOAc) = 0.2.

Synthesis of 4.36

4.34 **4.36**

Compound **4.34** (0.3029 g, 1.44 mmol) was dissolved in DCM (10 mL) and freshly prepared DMP (1.2258 g, 2.89 mmol) was added. The mixture was stirred overnight, after which Et_2O, sat. $NaHCO_3$ and sat. NaS_2O_3 were added and the mixture was stirred till the solution was

clear. The mixture was transferred to a separating funnel and the aqueous layer extracted with Et_2O (3x). The combined organic extracts were washed with sat. NaCl, dried ($MgSO_4$) and the solvent removed *in vacuo*. Flash chromatography (5% MeOH:EtOAc) gave the aldehyde **4.36** (0.2192 g, 73%) as a yellowish clear oil.

^{1}H NMR (500 MHz, *$CDCl_3$*) δ ppm 9.79 (s, 1H, H1), 4.19-4.04 (m, 4H, $OC\underline{H}_2CH_3$), 2.62 (t, *J* = 7.0 Hz, 2H, H2), 1.95 (dq, *J* = 7.3, 14.6 Hz, 2H, H3), 1.84-1.73 (m, 2H, H4), 1.33 (t, *J* = 7.0 Hz, 6H, $OCH_2C\underline{H}_3$).

^{13}C NMR (126 MHz, *$CDCl_3$*) δ ppm 201.5 (C1), 61.9 (d, $^2J_{POC}$ = 6.5 Hz, $O\underline{C}H_2CH_3$), 44.1 (d, $^3J_{PCCC}$ = 14.0 Hz, C2), 25.0 (d, $^1J_{PC}$ =141.9 Hz, C4), 16.7 (d, $^3J_{POCC}$ = 6.0 Hz, $OCH_2\underline{C}H_3$), 15.6 (d, $^2J_{PCC}$ = 5.1 Hz, C3).

^{31}P NMR (121 MHz, *$CDCl_3$*) δ ppm 30.99.

HRMS (ESI): calc. $C_8H_{18}O_4P$ $[M+H]^+$: 209.0943; found: 209.0943.

R_f (5% MeOH:EtOAc) = 0.2.

Synthesis of 4.29

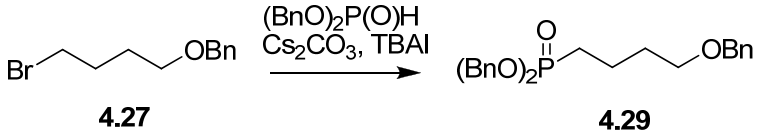

4.27 **4.29**

To a solution of dibenzyl phosphite (0.8145 g, 3.11 mmol) in DMF (20 mL) was added TBAI (3.4179 g, 9.25 mmol) and Cs_2CO_3 (3.0164 g, 9.26 mmol). The solution was stirred vigorously for one hour at room temperature before the addition of **4.27** (0.5019 g, 2.06 mmol) in DMF (1 mL). The reaction was stirred at room temperature for six days before the solution was poured into water and extracted with EtOAc (3x). The combined organic layers were washed with H_2O, sat. NaCl, dried over $MgSO_4$ and concentrated *in vacuo*. Flash chromatography (30 to 50% EtOAc:Pet ether) gave **4.29** (0.3517 g, 49%).

^{1}H NMR (500 MHz, *$CDCl_3$*) δ ppm 7.47-7.20 (m, 15H, Ph), 5.08-4.93 (m, 4H, $C\underline{H}_2Ph$), 4.46 (s, 2H, $C\underline{H}_2Ph$), 3.42 (t, *J* = 5.9 Hz, 2H, H1), 1.84-1.60 (m, 6H, H2, H3, H4).

^{13}C NMR (126 MHz, $CDCl_3$) δ ppm 138.7, 136.7 (d), 128.8, 128.6 (d), 128.1, 127.8, 127.8, 73.1 ($\underline{C}H_2Ph$), 69.7 (C1), 67.3 (d, J = 6.5 Hz, $\underline{C}H_2Ph$), 30.7 (d, $^3J_{PCCC}$ = 16.7 Hz, C2), 26.0 (d, $^1J_{PC}$ =140.0 Hz, C4), 19.5 (d, $^2J_{PCC}$ = 5.1 Hz, C3).

^{31}P NMR (121 MHz, *$CDCl_3$*) δ ppm 33.32.

HRMS (ESI): calc. $C_{25}H_{29}NaO_4P$ $[M+Na]^+$: 447.1696; found: 447.1703.

R_f (1:1 EtOAc:Pet ether) = 0.2.

Synthesis of 4.35

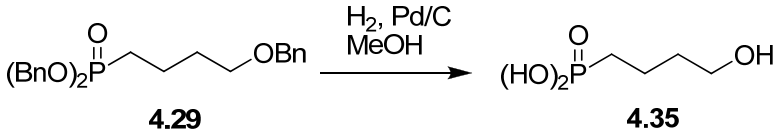

4.29 **4.35**

To a solution of **4.29** (0.3505 g, 0.83 mmol) was added MeOH (5 mL) and 10% Pd/C (37.5 mg, 10% wt of **4.29**). After three vacuum/H_2 cycles, to flush the flask with H_2, the mixture was vigorously stirred at room temperature under hydrogen (balloon) for four hours. The Pd/C was filtered through a small pad of celite and the pad washed with MeOH (3x 10 mL). The filtrate was concentrate *in vacuo* to give spectroscopically pure **4.35** (0.1413 g, 100%).

^{1}H NMR (500 MHz, *MeOH-d_4*) δ ppm 3.58 (t, J = 5.9 Hz, 2H, H1), 1.79-1.58 (m, 6H, H2, H3, H4).

^{13}C NMR (126 MHz, *MeOH-d_4*) δ ppm 61.1 (C1), 33.3 (d, $^3J_{PCCC}$ = 16.3 Hz, C2), 26.7 (d, $^1J_{PC}$ = 138.6 Hz, C4), 19.3 (d, $^2J_{PCC}$ = 4.7 Hz, C3).

^{31}P NMR (121 MHz, *$CDCl_3$*) δ ppm 26.60.

HRMS (ESI): calc. $C_4H_{10}O_4P$ $[M-H]^-$: 153.0317; found: 153.0311.

Synthesis of 4.31

butan-1,4-diol **4.31**

TBDMSCl (12.4210 g, 82 mmol) in dry DCM (40 mL) was added dropwise to a solution of butan-1,4-diol (22.0162 g, 240 mmol) and imidazole (12.1774 g, 180 mmol) in DCM (60 mL) at 0°C over 15 minutes. The solution was stirred overnight at room temperature then quenched using sat. NH_4Cl, extracted with DCM and dried over $MgSO_4$. The crude product was purified by flash chromatography (10 to 30% EtOAc:Pet ether) to give **4.31** (11.77 g, 70%) as a colourless oil with spectral data in accordance with the literature.[170]

^{1}H NMR (500 MHz, *$CDCl_3$*) δ ppm 3.72-3.60 (m, 4H, H1, H4), 2.35 (br. s, 1H, OH), 1.73-1.57 (m, 4H, H2, H3), 0.90 (s, 9H, ^{t}Bu), 0.07 (s, 6H, $SiMe_2$).
^{13}C NMR (126 MHz, $CDCl_3$) δ ppm 63.6 (C4), 63.0 (C1), 30.5 (C3), 30.1 (C2), 26.1 (^{t}Bu, 3C), 18.5 (^{t}Bu, 1C), -5.2 ($SiMe_2$).
HRMS (ESI): calc. $C_{10}H_{24}NaO_2Si$ $[M+Na]^+$:227.1438; found: 227.1438.
R_f (30% EtOAc:Pet ether) = 0.3.

Synthesis of 4.32

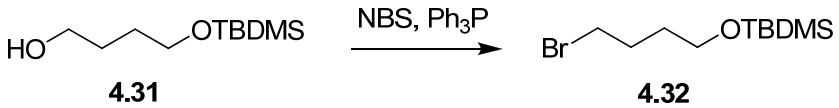

4.31 **4.32**

To a solution of **4.31** (0.5025 g, 2.46 mmol) in DCM (10 mL) was added triphenylphosphine (0.9654 g, 3.68 mmol) at 0°C. To this cooled solution was added, portion wise and slowly, NBS (0.6524 g, 3.67 mmol) at a rate to maintain the exothermic reaction. The solution was stirred overnight then concentrated and filtered through a pad of celite to remove triphenylphosphine oxide. The celite was washed with ether (3x) and the combined organic extracts were concentrated *in vacuo*. Flash chromatography (100% Pet ether to 30% EtOAc:Pet ether) gave **4.32** (0.2057 g, 31%) with spectral data in accordance with the literature.[172]

^{1}H NMR (500 MHz, *$CDCl_3$*) δ ppm 3.65 (t, *J* = 6.2 Hz, 2H, H1), 3.45 (t, *J* = 6.8 Hz, 2H, H4), 1.95 (quin, *J* = 7.2 Hz, 2H, H3), 1.71-1.61 (m, 2H, H2), 0.90 (s, 9H, ^{t}Bu), 0.05 (s, 6H, $SiMe_2$).
^{13}C NMR (126 MHz, *$CDCl_3$*) δ ppm 62.4 (C1), 34.2 (C4), 31.5 (C2), 29.7 (C3), 26.2 (^{t}Bu, 3C), 18.5 (^{t}Bu, 1C), -5.1 ($SiMe_2$).

HRMS (ESI): calc. $C_{10}H_{23}BrNaOSi$ $[M+Na]^+$: 289.0594; found: 289.0595.

R_f (Pet ether) = 0.2.

Synthesis of 4.33

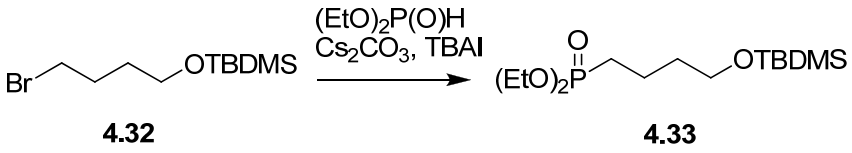

4.32 **4.33**

To a solution of diethyl phosphite (470 µL, 3.65 mmol) in DMF (20 mL) was added TBAI (3.9965 g, 10.8 mmol) and Cs_2CO_3 (3.5292 g, 10.8 mmol). The solution was stirred vigorously for one hour at room temperature before the addition of 4.32 (0.4823 g, 1.80 mmol) in DMF (1.0 mL). The reaction was stirred at room temperature for three days before the solution was poured into H_2O and extracted with EtOAc (3x). The combined organic layers were washed with sat. NaCl, dried over $MgSO_4$ and concentrated *in vacuo*. Flash chromatography (2:1 EtOAc:Pet ether to 5% MeOH:EtOAc) gave 4.33 (0.2866 g, 49%).

^{1}H NMR (500 MHz, *$CDCl_3$*) δ ppm 4.26-3.95 (m, 4H, OCH_2CH_3), 3.62 (t, *J* = 6.1 Hz, 2H, H1), 1.86-1.53 (m, 6H, H2, H3, H4), 1.32 (t, *J* = 7.2 Hz, 6H, OCH_2CH_3), 0.89 (s, 9H, ^{t}Bu), 0.04 (s, 6H, $SiMe_2$).

^{13}C NMR (126 MHz, *$CDCl_3$*) δ ppm 62.6 (C1), 61.6 (d, $^2J_{POC}$ = 6.5 Hz, OCH_2CH_3), 33.7 (d, $^3J_{PCCC}$ = 16.3 Hz, C2), 26.2 (^{t}Bu, 3C), 25.7 (d, $^1J_{PC}$ = 140.5 Hz, C4), 19.2 (d, $^2J_{PCC}$ = 5.1 Hz, C3), 18.5 (^{t}Bu, 1C), 16.7 (d, $^3J_{POCC}$ = 6.0 Hz, OCH_2CH_3), -5.1 ($SiMe_2$).

^{31}P NMR (121 MHz, *$CDCl_3$*) δ ppm 32.35.

HRMS (ESI): calc. $C_{14}H_{34}O_4SiP$ $[M+H]^+$: 325.1964; found: 325.1969.

R_f (5% MeOH:EtOAc) = 0.5.

Synthesis of 4.37

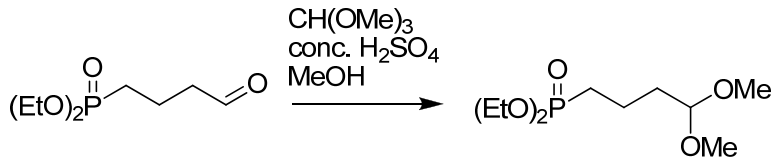

4.36 **4.37**

To **4.36** (0.1120 g, 0.54 mmol) in MeOH (8 mL) was added trimethyl orthoformate (590 µL, 5.39 mmol) and conc. H_2SO_4 (6 µL, 0.11 mmol). After stirring overnight, an addition aliquot of trimethyl orthoformate (560 µL, 5.11 mmol) and conc. H_2SO_4 (10 µL, 0.19 mmol) was added and stirred for a further 24 hours. The mixture was transferred to a separating funnel containing sat. $NaHCO_3$ and EtOAc. The aqueous layer was extracted with EtOAc (3x). The combined organic extracts were washed with sat. NaCl, dried ($NaSO_3$) and the solvent removed *in vacuo* to give spectroscopically pure **4.37** (99 mg, 72%).

^{1}H NMR (500 MHz, *$CDCl_3$*) δ ppm 4.33 (ap.t, *J* = 4.6 Hz, 2H, H1), 4.14-4.00 (m, 4H, $OC\underline{H}_2CH_3$), 3.29 (s, 6H, OMe), 1.79-1.59 (m, 6H, H2, H3, H4), 1.30 (t, *J* = 7.2 Hz, 6H, $OCH_2C\underline{H}_3$).

^{13}C NMR (126 MHz, *$CDCl_3$*) δ ppm 104.2 (C1), 61.7 (d, $^2J_{POC}$ = 6.5 Hz, $O\underline{C}H_2CH_3$), 53.0 (OMe), 33.4 (d, $^3J_{PCCC}$ = 15.8 Hz, C2), 25.6 (d, $^1J_{PC}$ = 140.0 Hz, C1), 18.1 (d, $^2J_{PCC}$ = 5.1 Hz, C3), 16.7 (d, $^3J_{POCC}$ = 6.0 Hz, $OCH_2\underline{C}H_3$).

^{31}P NMR (121 MHz, *$CDCl_3$*) δ ppm 31.85.

HRMS (ESI): calc. $C_{10}H_{23}NaO_5P$ $[M+Na]^+$: 277.1175; found: 277.1178.

R_f (1:1 EtOAc:Pet ether) = 0.1.

Synthesis of 2,3-dideoxyerythrose 4-phosphonate 4.38

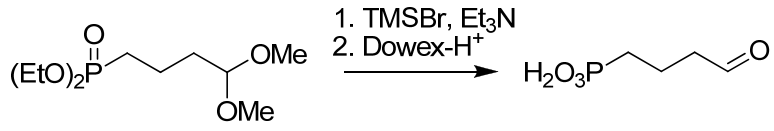

4.37 **4.38**

To a solution of **4.37** (0.040 g, 0.16 mmol) in DCM (2.0 mL) was added Et_3N (130 µL, 0.93 mmol) and TMSBr (90 µL, 0.68 mmol). The mixture was stirred at room temperature over night before additional Et_3N (50 µL, 0.36 mmol) and TMSBr (50 µL, 0.38 mmol) was added and stirred for 24 hours. The mixture was then reduced to dryness *in vacuo*. H_2O (2.0 mL) and freshly activated Dowex-H+ resin was then added. The solution was stirred overnight, reduced *in vacuo* and made up to 1.0 mL in H_2O. This solution was used in enzyme assays without further purification.

HRMS (ESI): calc. $C_4H_9O_4P$ $[M+H]^+$: 153.0311; found: 153.0311.

References

1. Herrmann, K. M.; Weaver, L. M., The shikimate pathway. *Annu. Rev. Plant Physiol. Plant Mol. Biol.* **1999,** 50, (1), 473-503.
2. Woodard, R. W., Unique biosynthesis of dehydroquinic acid. *Bioorg. Chem.* **2004,** 32, 309-315.
3. Knaggs, A. R., The biosynthesis of shikimate metabolites. *Nat. Prod. Rep.* **2001,** 18, (3), 334-355.
4. Jiang, S.; Singh, G., Chemical synthesis of shikimic acid and its analogues. *Tetrahedron* **1998,** 54, 4697-4753.
5. Fischer, H.; Dangschat, G.; Taube, C.; Radt, F.; Stettiner, H., Quinic acid and derivatives. II. Constitution and configuration of quinic acid. *Chemistry of Berlin* **1932,** 65B.
6. Davis, B. D., Isolation of biochemically deficient mutants of bacteria by penicillin. *J. Am. Chem. Soc.* **1948,** 70, 4267-4268.
7. Ducati, R. G.; Basso, L. A.; Santos, D. S., Mycobacterial shikimate pathway enzymes as targets for drug design. *Curr. Drug Targets* **2007,** 8, (3), 423-435.
8. Roberts, C. W.; Roberts, F.; Lyons, R. E.; Kirisits, M. J.; Mui, E. J.; Finnerty, J.; Johnson, J. J.; Ferguson, D. J. P.; Coggins, J. R.; Krell, T.; Coombs, G. H.; Milhous, W. K.; Kyle, D. E.; Tzipori, S.; Barnwell, J.; Dame, J. B.; Carlton, J.; McLeod, R., The shikimate pathway and its branches in apicomplexan parasites. *J. Infect. Dis.* **2002,** 185, (Suppl. 1), S25-S36.
9. Kishore, G. M.; Shah, D. M., Amino acid biosynthesis inhibitors as herbicides. *Annu. Rev. Biochem* **1988,** 57, 627-63.
10. O'Callaghan, D.; Maskell, D.; Liew, F. Y.; Easmon, C. S. F.; Dougan, G., Characterization of aromatic- and purine-dependent Salmonella typhimurium: attenuation, persistence, and ability to induce protective immunity in BALB/c mice. *Infect. Immun.* **1988,** 56, (2), 419-23.
11. Baillie, A. C.; Corbett, J. R.; Dowsett, J. R.; McCloskey, P., Inhibitors of shikimate dehydrogenase as potential herbicides. *Pestic. Sci.* **1972,** 3, (2), 113-120.
12. Bentley, R., The shikimate pathway - a metabolic tree with many branches. *Crit. Rev. Biochem. Mol. Biol.* **1990,** 25, (5), 307-84.
13. Roberts, F.; Roberts, C. W.; Johnson, J. J.; Kyle, D. E.; Krell, T., Evidence for the shikimate pathway in apicomplexan parasites. *Nature* **1998,** 393, 801-805.
14. Steinrucken, H. C.; Amrhein, N., The herbicide glyphosate is a potent inhibitor of 5-enolpyruvylshikimic acid 3-phosphate synthase. *Biochem. Biophys. Res. Commun.* **1980,** 94, 1207-1212.
15. Abell, C., Enzymology and molecular biology of the shikimate pathway. *Comprehensive Natural Products Chemistry* **1999,** 1, 573-607.
16. Srinivasan, P. R.; Katagiri, M.; Sprinson, D. B., Conversion of pyruvic acid phosphate and D-erythrose 4-phosphate to 5-dehydroquinic acid. *J. Biol. Chem.* **1959,** 234, 713-15.
17. Srinivasan, P. R.; Sprinson, D. B., 2-Keto-3-deoxy-D-*arabo*-heptonic acid 7-phosphate synthetase. *J. Biol. Chem.* **1959,** 234, 716-22.
18. Walker, G. E.; Dunbar, B.; Hunter, I. S.; Nimmo, H. G.; Coggins, J. R., Evidence for a novel class of microbial 3-deoxy-D-*arabino*-heptulosonate 7-phosphate synthase in *Streptomyces coelicolor* A3(2), *Streptomyces rimosus* and *Neurospora crassa*. *Microbiology (Reading, United Kingdom)* **1996,** 142, (8), 1973-1982.

19. Gosset, G.; Bonner, C. A.; Jensen, R. A., Microbial origin of plant-type 2-keto-3-deoxy-D-*arabino*-heptulosonate 7-phosphate synthases, exemplified by the chorismate- and tryptophan-regulated enzyme from *Xanthomonas campestris*. *J. Bacteriol.* **2001,** 183, (13), 4061-4070.
20. Subramaniam, P. S.; Xie, G.; Xia, T.; Jensen, R. A., Substrate ambiguity of 3-deoxy-D-*manno*-octulosonate 8-phosphate synthase from *Neisseria gonorrhoeae* in the context of its membership in a protein family containing a subset of 3-deoxy-D-*arabino*-heptulosonate 7-phosphate synthases. *J. Bacteriol.* **1998,** 180, (1), 119-127.
21. Shumilin, I. A.; Kretsinger, R. H.; Bauerle, R. H., Crystal structure of phenylalanine-regulated 3-deoxy-D-*arabino*-heptulosonate 7-phosphate synthase from *Escherichia coli*. *Structure (London)* **1999,** 7, (7), 865-875.
22. Schoner, R.; Herrmann, K. M., 3-Deoxy-D-*arabino*-heptulosonate 7-phosphate synthase. Purification, properties, and kinetics of the tyrosine-sensitive isoenzyme from *Escherichia coli*. *J. Biol. Chem.* **1976,** 251, (18), 5440-7.
23. Ray, J. M.; Bauerle, R., Purification and properties of tryptophan-sensitive 3-deoxy-D-*arabino*-heptulosonate 7-phosphate synthase from *Escherichia coli*. *J. Bacteriol.* **1991,** 173, (6), 1894-901.
24. Sheflyan, G. Y.; Howe, D. L.; Wilson, T. L.; Woodard, R. W., Enzymatic synthesis of 3-deoxy-D-*manno*-octulosonate 8-phosphate, 3-deoxy-D-*altro*-octulosonate 8-phosphate, 3,5-dideoxy-D-gluco(*manno*)-octulosonate 8-phosphate by 3-deoxy-D-*arabino*-heptulosonate 7-phosphate synthase. *J. Am. Chem. Soc.* **1998,** 120, (43), 11027-11032.
25. Hartmann, M.; Schneider, T. R.; Pfeil, A.; Heinrich, G.; Lipscomb, W. N.; Braus, G. H., Evolution of feedback-inhibited β/α barrel isoenzymes by gene duplication and a single mutation. *Proc. Natl. Acad. Sci. U. S. A.* **2003,** 100, (3), 862-867.
26. Paravicini, G.; Schmidheini, T.; Braus, G., Purification and properties of the 3-deoxy-D-*arabino*-heptulosonate 7-phosphate synthase (phenylalanine-inhibitable) of *Saccharomyces cerevisiae*. *Eur. J. Biochem.* **1989,** 186, (1-2), 361-6.
27. Schnappauf, G.; Hartmann, M.; Kunzler, M.; Braus, G. H., The two 3-deoxy-D-*arabino*-heptulosonate 7-phosphate synthase isoenzymes from *Saccharomyces cerevisiae* show different kinetic modes of inhibition. *Arch. Microbiol.* **1998,** 169, (6), 517-524.
28. Birck, M. R.; Woodard, R. W., *Aquifex aeolicus* 3-deoxy-D-*manno*-2-octulosonic acid 8-phosphate synthase: a new class of KDO8P synthase. *J. Mol. Evol.* **2001,** 52, (2), 205-214.
29. Jensen, R. A.; Xie, G.; Calhoun, D. H.; Bonner, C. A., The correct phylogenetic relationship of KdsA (3-deoxy-D-*manno*-octalosonate 8-phosphate synthase) with one of two independently evolved classes of AroA (3-deoxy-D-*arabino*-heptulosonate 7-phosphate synthase). *J. Mol. Evol.* **2002,** 54, (3), 416-423.
30. Krosky, D. J.; Alm, R.; Berg, M.; Carmel, G.; Tummino, P. J.; Xu, B.; Yang, W., *Helicobacter pylori* 3-deoxy-D-*manno*-octulosonate 8-phosphate (KDO-8-P) synthase is a zinc-metalloenzyme. *Biochim. Biophys. Acta, Protein Struct. Mol. Enzymol.* **2002,** 1594, (2), 297-306.
31. Ray, P. H., Purification and characterization of 3-deoxy-D-*manno*-octulosonate 8-phosphate synthetase from *Escherichia coli*. *J. Bacteriol.* **1980,** 141, (2), 635-44.
32. Schofield, L. R. A., B F; Patchett, M. L.; Norris, G. E.; Jameson, G. B.; Parker, E. J., Substrate ambiguity and crystal structure of *Pyrococcus furiosus* 3-deoxy-D-*arabino*-heptulosonate 7-phosphate synthase: an ancestral 3-deoxyald-2-ulosonatephosphate synthase? *Biochemistry* **2005,** 44, (36), 11950-11962.
33. Ogino, T.; Garner, C.; Markley, J. L.; Herrmann, K. M., Biosynthesis of aromatic compounds: carbon-13 NMR spectroscopy of whole *Escherichia coli* cells. *Proc. Natl. Acad. Sci. U. S. A.* **1982,** 79, (19), 5828-32.

34. Blattner, F. R.; Plunkett, G., III; Bloch, C. A.; Perna, N. T.; Burland, V.; Riley, M.; Collado-Vides, J.; Glasner, J. D.; Rode, C. K.; Mayhew, G. F.; Gregor, J.; Davis, N. W.; Kirkpatrick, H. A.; Goeden, M. A.; Rose, D. J.; Mau, B.; Shao, Y., Complete genome sequence of *Escherichia coli* K-12. *Science (Washington, D. C.)* **1997,** 277, (5331), 1453-1462.
35. Schofield, L. R.; Patchett, M. L.; Parker, E. J., Expression, purification, and characterization of 3-deoxy-D-*arabino*-heptulosonate 7-phosphate synthase from *Pyrococcus furiosus*. *Protein Expression Purif.* **2004,** 34, (1), 17-27.
36. Tribe, D. E.; Camakaris, H.; Pittard, J., Constitutive and repressible enzymes of the common pathway of aromatic biosynthesis in *Escherichia coli* K-12: regulation of enzyme synthesis at different growth rates. *J. Bacteriol.* **1976,** 127, (3), 1085-97.
37. Webby, C. J. Structural & functional characterization of 3-deoxy-D-*arabino*-heptulosonate 7-phosphate synthase from *Helicobacter pylori* & *Mycobacterium tuberculosis*. PhD, Massey University, New Zealand, 2006.
38. Webby, C. J.; Baker, H. M.; Lott, J. S.; Baker, E. N.; Parker, E. J., The structure of 3-deoxy-D-*arabino*-heptulosonate 7-phosphate synthase from *Mycobacterium tuberculosis* reveals a common catalytic scaffold and ancestry for type I and type II enzymes. *J. Mol. Biol.* **2005,** 354, (4), 927-939.
39. Webby, C. J.; Jiao, W.; Hutton, R. D.; Blackmore, N. J.; Baker, H. M.; Baker, E. N.; Jameson, G. B.; Parker, E. J., Synergistic allostery, a sophisticated regulatory network for the control of aromatic amino acid biosynthesis in *Mycobacterium tuberculosis*. *J. Biol. Chem.* **2010,** 285, (40), 30567-30576.
40. Ahn, M. Substrate analogues as mechanistic probes for 3-deoxy-D-*arabino*-heptulosonate 7-phosphate synthase and 3-deoxy-D-*manno*-octulosonate 8-phosphate synthase. PhD, Massey University, New Zealand, 2007.
41. Shumilin, I. A.; Zhao, C.; Bauerle, R.; Kretsinger, R. H., Allosteric inhibition of 3-deoxy-D-*arabino*-heptulosonate 7-phosphate synthase alters the coordination of both substrates. *J. Mol. Biol.* **2002,** 320, 1147-1156.
42. Staub, M.; Denes, G., Purification and properties of the 3-deoxy-D-*arabino*-heptulosonate 7-phosphate synthase (phenylalanine sensitive) of *Escherichia coli* K-12. II. Inhibition of activity of the enzyme with phenylalanine and functional group-specific reagents. *Biochimica et Biophysica Acta, Enzymology* **1969,** 178, (3), 599-608.
43. Simpson, R. J.; Davidson, B. E., Studies on 3-deoxy-D-*arabino*-heptulosonate-7-phosphate synthetase(phe) from *Escherichia co*li K12. 2. Kinetic properties. *Eur. J. Biochem.* **1976,** 1976, (70), 2.
44. Jensen, R. A.; Nester, E. W., Regulatory enzymes of aromatic amino acid biosynthesis in *Bacillus subtilis*. I. Purification and properties of 3-deoxy-D-*arabino*-heptulosonate 7-phosphate synthetase. *J. Biol. Chem.* **1966,** 241, (14), 3365-3372.
45. DeLeo, A. B.; Dayan, J.; Sprinson, D. B., Purification and kinetics of tyrosine-sensitive 3-deoxy-D-*arabino*-heptulosonic acid 7-phosphate synthetase from *Salmonella*. *J. Biol. Chem.* **1973,** 248, (7), 2344-53.
46. Wu, J.; Howe, D. L.; Woodard, R. W., *Thermotoga maritima* 3-deoxy-D-*arabino*-heptulosonate 7-phosphate (DAHP) Synthase: The ancestral eubacterial DAHP synthase? *J. Biol. Chem.* **2003,** 278, (30), 27525-27531.
47. Webby, C. J.; Patchett, M. L.; Parker, E. J., Characterization of a recombinant type II 3-deoxy-D-*arabino*-heptulosonate 7-phosphate synthase from *Helicobacter pylori*. *Biochem. J* **2005,** 390, (1), 223-230.
48. Stephens, C. M.; Bauerle, R., Analysis of the metal requirement of 3-deoxy-D-*arabino*-heptulosonate 7-phosphate synthase from *Escherichia coli*. *J. Biol. Chem.* **1991,** 266, (31), 20810-17.

49. Furdui, C.; Zhou, L.; Woodard, R. W.; Anderson, K. S., Insights into the mechanism of 3-deoxy-D-*arabino*-heptulosonate 7-phosphate synthase (Phe) from *Escherichia coli* using a transient kinetic analysis. *J. Biol. Chem.* **2004,** 279, (44), 45618-45625.
50. McCandliss, R. J.; Herrmann, K. M., Iron, an essential element for biosynthesis of aromatic compounds. *Proc. Natl. Acad. Sci. U. S. A.* **1978,** 75, (10), 4810-4813.
51. Baasov, T.; Knowles, J. R., Is the first enzyme of the shikimate pathway, 3-deoxy-D-*arabino*-heptulosonate 7-phosphate synthase (tyrosine sensitive), a copper metalloenzyme? *J. Bacteriol.* **1989,** 171, (11), 6155-60.
52. Park, O. K.; Bauerle, R., Metal-catalyzed oxidation of phenylalanine-sensitive 3-deoxy-D-*arabino*-heptulosonate 7-phosphate synthase from *Escherichia coli*: inactivation and destabilization by oxidation of active-site cysteines. *J. Bacteriol.* **1999,** 181, (5), 1636-1642.
53. Stephens, C. M.; Bauerle, R., Essential cysteines in 3-deoxy-D-*arabino*-heptulosonate 7-phosphate synthase from *Escherichia coli*. Analysis by chemical modification and site-directed mutagenesis of the phenylalanine-sensitive isozyme. *J. Biol. Chem.* **1992,** 267, (9), 5762-7.
54. Floss, H. G.; Onderka, D. K.; Carroll, M., Stereochemistry of the 3-deoxy-D-*arabino*-heptulosonate 7-phosphate synthetase reaction and the chorismate synthetase reaction. *J. Biol. Chem.* **1972,** 247, (3), 736-44.
55. Onderka, D. K.; Floss, H. G., Steric course of the chorismate synthetase reaction and the 3-deoxy-D-*arabino*-heptulosonate 7-phosphate (DAHP) synthetase reaction. *J. Am. Chem. Soc.* **1969,** 91, (21), 5894-6.
56. DeLeo, A. B.; Sprinson, D. B., Mechanism of 3-deoxy-D-*arabino*-heptulsonate 7-phosphate synthetase. *Biochem. Biophys. Res. Commun.* **1968,** 32, (5), 873-7.
57. Wanke, C.; Amrhein, N., Evidence that the reaction of the UDP-*N*-acetylglucosamine 1-carboxyvinyltransferase proceeds through the *O*-phosphothioketal of pyruvic acid bound to Cys115 of the enzyme. *Eur. J. Biochem.* **1993,** 218, (3), 861-70.
58. Asojo, O.; Friedman, J.; Adir, N.; Belakhov, V.; Shoham, Y.; Baasov, T., Crystal structures of KDOP synthase in Its binary complexes with the substrate phosphoenolpyruvate and with a mechanism-based inhibitor. *Biochemistry* **2001,** 40, (21), 6326-6334.
59. Staub, M.; Denes, G., A kinetic study of the mechanism of action of 3-deoxy-D-*arabino*-heptulosonate 7-phosphate synthase in *Escherichia coli* K12. *Biochimica et Biophysica Acta, Enzymology* **1967,** 132, (2), 528-30.
60. Lambert, J. M.; Boocock, M. R.; Coggins, J. R., The 3-dehydroquinate synthase activity of the pentafunctional arom enzyme complex of *Neurospora crassa* is zinc-dependent. *Biochem. J* **1985,** 226, (3), 817-29.
61. Konig, V.; Pfeil, A.; Braus, G. H.; Schneider, T. R., Substrate and metal complexes of 3-deoxy-D-*arabino*-heptulosonate 7-phosphate synthase from *Saccharomyces cerevisiae* provide new insights into the catalytic mechanism. *J. Mol. Biol.* **2004,** 337, (3), 675-690.
62. Shumilin, I. A.; Bauerle, R.; Wu, J.; Woodard, R. W.; Kretsinger, R. H., Crystal structure of the reaction complex of 3-deoxy-D-*arabino*-heptulosonate 7-phosphate synthase from *Thermotoga maritima* refines the catalytic mechanism and indicates a new mechanism of allosteric regulation. *J. Mol. Biol.* **2004,** 341, (2), 455-466.
63. Wagner, T.; Shumilin, I. A.; Bauerle, R.; Kretsinger, R. H., Structure of 3-Deoxy-D-*arabino*-heptulosonate 7-phosphate synthase from *Escherichia coli*: Comparison of the Mn^{2+}-2-phosphoglycolate and the Pb^{2+}-2-phosphoenolpyruvate complexes and implications for catalysis. *J. Mol. Biol.* **2000,** 301, (2), 389-399.
64. Sheffer-Dee-Noor, S.; Belakhov, V.; Baasov, T., Insight into the catalytic mechanism of KDO8P synthase. Synthesis and evaluation of the isosteric phosphonate mimic of the putative cyclic intermediate. *Bioorg. Med. Chem. Lett.* **1993,** 8, (3), 1583-8.

65. Walker, S. R. Design, synthesis and characterisation of inhibitors of 3-deoxy-D-*arabino*-heptulosonate 7-phosphate synthase. PhD, University of Canterbury, New Zealand, 2007.
66. Pietersma, A. L. Using substrate analogues to probe the mechansims of two biosynthetic enzymes. PhD, Massey University, New Zealand, 2007.
67. Shumilin, I. A.; Bauerle, R.; Kretsinger, R. H., The high-resolution structure of 3-deoxy-D-*arabino*-heptulosonate 7-phosphate synthase reveals a twist in the plane of bound phosphoenolpyruvate. *Biochemistry* **2003,** 42, (13), 3766-76.
68. Muday, G. K.; Herrmann, K. M., Regulation of the *Salmonella typhimurium* aroF gene in *Escherichia coli*. *J. Bacteriol.* **1990,** 172, 2259-2266.
69. Meredith, T. C.; Woodard, R. W., Characterization of *Escherichia coli* D-arabinose 5-phosphate isomerase encoded by kpsF: implications for group 2 capsule biosynthesis. *Biochem. J* **2006,** 395, (2), 427-432.
70. Rick, P. D.; Osborn, M. J., Lipid A mutants of *Salmonella typhimurium*. Characterization of a conditional lethal mutant in 3-deoxy-D-*manno*-octulosonate 8-phosphate synthetase. *J. Biol. Chem.* **1977,** 252, (14), 4895-903.
71. Raetz, C., Biochemistry of endotoxins. *Annu. Rev. Biochem* **1990,** 59, 129-70.
72. Kohen, A.; Jakob, A.; Baasov, T., Mechanistic studies of 3-deoxy-D-*manno*-2-octulosonate 8-phosphaste synthase from *Escherichia coli*. *Eur. J. Biochem.* **1992,** 208, 443-449.
73. Staub, M.; Denes, G., Kinetic study on the inactivation of 3-deoxy-D-*arabino*-heptulosonate 7-phosphate synthase by bromopyruvate. *Biochimica et Biophysica Acta, Enzymology* **1967,** 139, (2), 519-521.
74. Forlani, G.; Lejczak, B.; Kafarski, P., The herbicidally active compound *N*-2-(6-methylpyridyl)aminomethylenebisphosphonic acid inhibits in vivo aromatic biosynthesis. *J. Plant Growth Regul.* **1999,** 18, (2), 73-79.
75. Grison, C.; Petek, S.; Finance, C.; Coutrot, P., Synthesis and antibacterial activity of mechanism-based inhibitors of KDO8P synthase and DAH7P synthase. *Carbohydr. Res.* **2005,** 340, (4), 529-537.
76. Baasov, T.; Belakhov, V., Studies towards the synthesis and evaluation of mechanism-based inhibitors of KDO8P synthase - a key enzyme in the biosynthesis of lipopolysaccharides. *Recent Research Developments in Organic Chemistry* **1999,** 3, (Pt. 1), 195-206.
77. Belakhov, V.; Dovgolevsky, E.; Rabkin, E.; Shulami, S.; Shoham, Y.; Baasov, T., Synthesis and evaluation of a mechanism-based inhibitor of KDO8P synthase. *Carbohydr. Res.* **2004,** 339, (2), 385-392.
78. Singh, V.; Evans, G. B.; Lenz, D. H.; Mason, J. M.; Clinch, K.; Mee, S.; Painter, G. F.; Tyler, P. C.; Furneaux, R. H.; Lee, J. E.; Howell, P. L.; Schramm, V. L., Femtomolar transition state analogue inhibitors of 5'-methylthioadenosine/*S*-adenosylhomocysteine nucleosidase from *Escherichia coli*. *J. Biol. Chem.* **2005,** 280, (18), 18265-18273.
79. Walker, S. R.; Parker, E. J., Synthesis and evaluation of a mechanism-based inhibitor of a 3-deoxy-D-*arabino* heptulosonate 7-phosphate synthase. *Bioorg. Med. Chem. Lett.* **2006,** 16, (11), 2951-2954.
80. Cumming, H. Probing the substrate specificity of 3-deoxy-D-*arabino*-heptulsonate 7-phosphate synthase and 3-deoxy-D-*manno*-octulosonate 8-phosphate synthase using analogues of phosphoenolpyruvate. Masters, University of Canterbury, New Zealand, 2007.
81. Walker, S. R.; Cumming, H.; Parker, E. J., Substrate and reaction intermediate mimics as inhibitors of 3-deoxy-D-*arabino*-heptulosonate 7-phosphate synthase. *Org. Biomol. Chem.* **2009,** 7, (15), 3031-3035.

82. Nowak, T.; Mildvan, A. S., Stereoselective interactions of phosphoenolpyruvate analogs with phosphoenolpyruvate-utilizing enzymes. *J. Biol. Chem.* **1970,** 245, (22), 6057-64.
83. Parker, E. J. Mechanistic studies on shikimate pathway enzymes. PhD, University of Cambridge, United Kingdom, 1996.
84. Blackmore, P. F.; Williams, J. F.; MacLeod, J. K., Dimerization of erythrose 4-phosphate. *FEBS Lett.* **1976,** 64, (1), 222-226.
85. Duke, C. C.; MacLeod, J. K., Nuclear magnetic resonance studies of D-erythrose 4-phosphate in aqueous solution. Structures of the major contributing monomeric and dimeric forms. *Carbohydr. Res.* **1981,** 95, 1-26.
86. Williams, J. F.; Blackmore, P. F.; Duke, C. C.; MacLeod, J. K., Fact, uncertainty and speculation concerning the biochemistry of D-erythrose-4-phosphate and its metabolic roles. *Int. J. Biochem.* **1980,** 12, (3), 339-44.
87. Reimer, L. M.; Conley, D. L.; Pompliano, D. L.; Frost, J. W., Construction of an enzyme-targeted organophosphonate using immobilized enzyme and whole-cell synthesis. *J. Am. Chem. Soc.* **1986,** 108, (25), 8010-15.
88. Ballou, C. E.; Fischer, H. O. L.; MacDonald, D. L., The synthesis and properties of D-erythrose 4-phosphate. *J. Am. Chem. Soc.* **1955,** 77, 5967-70.
89. Sieben, A. S.; Perlin, A. S.; Simpson, F. J., An improved preparative method for D-erythrose 4-phosphate. *Can. J. Biochem.* **1966,** 44, 663-669.
90. Simpson, F. J.; Perlin, A. S.; Sieben, A. S., Erythrose 4-phosphate. *Methods Enzymol.* **1966,** 9, 35-38.
91. Perlin, A. S., Reducing Sugars. *Adv. Carbohydr. Chem. Biochem.* **2006,** 60, 183-230.
92. Williamson, R. M.; Pietersma, A. L.; Jameson, G. B.; Parker, E. J., Stereospecific deuteration of 2-deoxyerthrose 4-phosphate using 3-deoxy-D-*arabino*-heptulosnate 7-phosphate synthase. *Bioorg. Med. Chem. Lett.* **2005,** 15, (9), 2339.
93. Lanzetta, P. A.; Alvarez, L. J.; Reinach, P. S.; Candia, O. A., An improved assay for nanomole amounts of inorganic phosphate. *Anal. Biochem.* **1979,** 100, 95-97.
94. Tanabe, M.; Peters, R. H., (*R,S*)-mevalonolactone-2-^{13}C. *Org. Synth.* **1981,** 60, 92-101.
95. Chan, T. H.; Brook, M. A.; Chaly, T., A simple procedure for the acetalization of carbonyl compounds. *Synthesis* **1983,** 3, 203-5.
96. Aminoff, D., Methods for the quantitative estimation of *N*-acetyl-neuraminic acid and their application to hydrolyzates of sialomucoids. *Biochem. J* **1961,** 81, 384-392.
97. Unger, F. M., The chemistry and biological significance of 3-deoxy-D-*manno*-2-octulosonic acid (KDO). *Adv. Carbohydr. Chem. Biochem.* **1981,** 38, 324-387.
98. Weissbach, A.; Hurtwitz, J., The formation of 2-keto-3-deoxyheptonic acid in extracts of *Escherichia coli* B. *J. Biol. Chem.* **1959,** 234, 705-709.
99. Aussenac, F.; Lavigne, B.; Dufourc, E. J., Toward bicelle stability with ether-linked phospholipids: Temperature, composition, and hydration diagrams by ^{2}H and ^{31}P solid-state NMR. *Langmuir* **2005,** 21, 7129-7135.
100. Bravo, J.; Cativiela, C.; Chaves, J. E.; Navarro, R.; Urriolabeitia, E. P., ^{31}P NMR spectroscopy as a powerful tool for the determination of enantiomeric excess and absolute configurations of α-amino acids. *Inorg. Chem.* **2003,** 42, 1006-1013.
101. Gorenstein, D. G.; Rowell, R., Isotopic oxygen-18 shifts in phosphorus-31 NMR as a probe of stereochemistry of hydrolysis in phosphate triesters. *J. Am. Chem. Soc.* **1980,** 102, 6165-6166.
102. Gmeiner, P.; Junge, D., Regioselective transformation of malic acid: A practical method for the construction of enantiomerically pure indolizidines. *J. Org. Chem.* **1995,** 60, (12), 3910-15.

103. Kocienski, P. J., *Protecting groups*. 1st ed.; Thieme: 2000.
104. Fessner, W. D., Enzyme mediated C-C bond formation. *Curr. Opin. Chem. Biol.* **1998,** 2, 85-97.
105. Aehle, W., *Enzymes in industry: production and applications*. 2nd ed.; Wiley-VCH: 2004.
106. Seebach, D.; Johannes, A.; Wasmuth, D., Diastereoselective α-alkylation of β-hydroxycarboxylic esters through alkoxide enolates: Diethyl (2*S*, 3*R*)-(+)-3-allyl-2-hydroxysuccinate from diethyl (*S*)-(-)-malate. *Organic syntheses collective* **1990,** 7, 153.
107. Seebach, D.; Johannes, A.; Wasmuth, D., Diastereoselective α-alkylation of β-hydroxycarboxylic esters through alkoxide enolates: Diethyl (2*S*, 3*R*)-(+)-3-allyl-2-hydroxysuccinate from diethyl (*S*)-(-)-malate. *Organic syntheses collective* **1985,** 63, 109.
108. Nicolaou, K. C.; Pavia, M. R.; Seitz, S. P., Synthesis of 16-membered-ring macrolide antibiotics. Carbomycin B and leucomycin A3: total synthesis of cyclic key intermediate. *J. Am. Chem. Soc.* **1981,** 103, (5), 1224-6.
109. Mori, S.; Ohno, T.; Harada, H.; Aoyama, T.; Shioiri, T., New methods and reagents in organic synthesis. 92. A stereoselective synthesis of tilivalline and its analogs. *Tetrahedron* **1991,** 47, (27), 5051-5070.
110. Larsen, C. H.; Ridgway, B. H.; Shaw, J. T.; Woerpel, K. A., A stereoelectronic model to explain the highly stereoselective reactions of nucleophiles with five-membered-ring oxocarbenium ions. *J. Am. Chem. Soc.* **1999,** 121, (51), 12208-12209.
111. Trappeniers, M.; Goormans, S.; Van Beneden, K.; Decruy, T.; Linclau, B.; Al-Shamkhani, A.; Elliott, T.; Ottensmeier, C.; Werner, J. M.; Elewaut, D.; Van Calenbergh, S., Synthesis and *in vitro* evaluation of α-GalCer epimers. *ChemMedChem* **2008,** 3, (7), 1061-1070.
112. Widmer, U., A convenient benzylation procedure for β-hydroxy esters. *Synthesis* **1987**, (6), 568-70.
113. Bouzide, A.; LeBerre, N.; Sauve, G., Silver(I) oxide-mediated facile and practical sulfonylation of alcohols. *Tetrahedron Lett.* **2001,** 42, (50), 8781-8783.
114. Bouzide, A.; Sauve, G., Highly selective silver(I) oxide mediated monoprotection of symmetrical diols. *Tetrahedron Lett.* **1997,** 38, (34), 5945-5948.
115. Bouzide, A.; Sauve, G., Silver(I) oxide mediated highly selective monotosylation of symmetrical diols. Application to the synthesis of polysubstituted cyclic ethers. *Org. Lett.* **2002,** 4, (14), 2329-2332.
116. Cunningham, A. F., Jr.; Kuendig, E. P., An efficient synthesis of both enantiomers of trans-1,2-cyclopentanediol and their conversion to two novel bidentate phosphite and fluorophosphinite ligands. *J. Org. Chem.* **1988,** 53, (8), 1823-5.
117. Nemoto, H.; Takamatsu, S.; Yamamoto, Y., An improved and practical method for the synthesis of optically active diethyl tartrate dibenzyl ether. *J. Org. Chem.* **1991,** 56, (3), 1321-2.
118. Dess, D. B.; Martin, J. C., A useful 12-I-5 triacetoxyperiodinane (the Dess-Martin periodinane) for the selective oxidation of primary or secondary alcohols and a variety of related 12-I-5 species. *J. Am. Chem. Soc.* **1991,** 113, (19), 7277-7287.
119. Corey, E. J.; Suggs, J. W., Pyridinium chlorochromate. An efficient reagent for oxidation of primary and secondary alcohols to carbonyl compounds *Tetrahedron Lett.* **1975,** 16, (31), 2647-2650.
120. Ireland, R. E.; Liu, L., An improved procedure for the preparation of the Dess-Martin periodinane. *J. Org. Chem.* **1993,** 58, 2899.
121. Frigerio, M.; Santagostino, M.; Sputore, S., A user friendly entry to 2-iodoxybenzoic acid (IBX). *J. Org. Chem.* **1999,** 64, 4537-4538.

122. Pfitzner, K. E.; Moffatt, J. G., A new and selective oxidation of alcohols. *J. Am. Chem. Soc.* **1963,** 85, (19), 3027-3028.
123. Omura, K.; Swern, D., Oxidation of alcohols by "activated" dimethyl sulfoxide. a preparative, steric and mechanistic study. *Tetrahedron* **1978,** 34, (11), 1651-1660.
124. Mancuso, A. J.; Brownfain, D. S.; Swern, D., Structure of the dimethyl sulfoxide-oxalyl chloride reaction product. Oxidation of heteroaromatic and diverse alcohols to carbonyl compounds. *J. Org. Chem.* **1979,** 44, (23), 4148-4150.
125. Araki, K.; Suenaga, K.; Sengoku, T.; Uemura, D., Total synthesis of attenols A and B. *Tetrahedron* **2002,** 58, (10), 1983-1995.
126. Monma, S.; Sunazuka, T.; Nagai, K.; Arai, T.; Shiomi, K.; Matsui, R.; Acemura, S., Verticilide: Elucidation of absolute configuration and total synthesis. *Org. Lett.* **2006,** 8, (24), 5601-5604.
127. Hanessian, S.; Tehim, A.; Chen, P., Total synthesis of (-)-tetrahydrolipstatin. *J. Org. Chem.* **1993,** 58, (27), 7768-7781.
128. Karanewsky, D. S.; Malley, M. F.; Gougoutas, J. Z., Practical synthesis of an enantiomerically pure synthon for the preparation of mevinic acid analogs. *J. Org. Chem.* **1991,** 56, (11), 3744-7.
129. Casper, D. M.; Hitchcock, S. R., An improved procedure for the asymmetric aldol reaction of the titanium enolate of an N_3-propionyl-3,4,5,6-tetrahydro-^{2}H-1,3,4-oxadiazin-2-one. *Tetrahedron asymmetry* **2003,** 14, 517-521.
130. Tursun, A.; Canet, I.; Aboab, B.; Sinibaldi, M.-E., A short and versatile route to chiral spiroketal skeletons. *Tetrahedron Lett.* **2005,** 46, 2291-2294.
131. White, J. D.; Lincoln, C. M.; Yang, J.; Martin, W. H. C.; Chan, D. B., Total synthesis of solandelactones A, B, E, and F exploiting a tandem Petasisa-Claisen lactonization strategy. *J. Org. Chem.* **2008,** 73, (11), 4139-4150.
132. Miura, T.; Kajimoto, T., Application of L-threonine aldolase-catalyzed reaction to the preparation of protected 3*R*,5*R*-dihydroxy-L-homoproline as a mimetic of idulonic acid. *Chirality* **2001,** 13, (9), 577-580.
133. Saito, S.; Ishikawa, T.; Kuroda, A.; Koga, K.; Moriwake, T., A revised mechanism for chemoselective reduction of esters with boranhdimethyl sulfide complex and catalytic sodium tetrahydroborate directed by adjacent hydroxyl group. *Tetrahedron* **1992,** 48, (20), 4067-4086.
134. Lundy, S. D. Synthetic approaches to the bicyclic core of TEO3.1, hamigerone and embellistatin. PhD, University of Canterbury, New Zealand, 2007.
135. Chouinard, P. M.; Bartlett, P. A., Conversion of shikimic acid to 5-enolpyruvylshikimate 3-phosphate. *J. Org. Chem.* **1986,** 51, (1), 75-78.
136. Engel, R., Phosphonates as analogues of natural phosphates. *Chem. Rev.* **1977,** 77, (3), 349-367.
137. Matulic-Adamic, J.; Haeberli, P.; Usman, N., Synthesis of 5'-deoxy-5'-difluoromethyl phosphonate nucleotide analogs. *J. Org. Chem.* **1995,** 60, 2563-2569.
138. Hecker, S. J.; Erion, M. D., Prodrugs of phosphates and phosphonates. *J. Med. Chem.* **2008,** 51, 2328-2345.
139. Pham, V.; Zhang, W.; Chen, V.; Whitney, T.; Yao, J.; Froese, D.; Friesen, A. D.; Diakur, J. M.; Haque, W., Design and synthesis of novel pyridoxine 5'-phosphonates as potential antiischemic agents. *J. Med. Chem.* **2003,** 46, (17), 3680-3687.
140. Simon, L.; Myers, T.; Mednieks, M., The enzymic synthesis of polyribonucleotides using 5'-adenylmethylenediphosphonate: a phosphonic acid analog of adenosine triphosphate. *Biochim. Biophys. Acta, Nucleic Acids Protein Synth.* **1965,** 103, (2), 189-95.

141. Le Marechal, P.; Froussios, C.; Level, M.; Azerad, R., Enzymic properties of phosphonic analogues of D-erythrose 4-phosphate. *Biochem. Biophys. Res. Commun.* **1980,** 92, (4), 1097.
142. Griffin, B. S.; Burger, A., D-Glucopyranose 6-phosphonic acid. *J. Am. Chem. Soc.* **1956,** 78, 2336-2338.
143. Bhattacharya, A. K.; Thyagarajan, G., Michaelis-Arbuzov rearrangement. *Chem. Rev.* **1981,** 81, (4), 415-430.
144. Arbuzov, B. A., Michaelis-Arbusov- und Perkow-Reaktionen. *Pure Appl. Chem.* **1964,** 9, (2), 307-336.
145. Meyer, B.; Stuike-Prill, R., Syntheses of benzyl 6-*O*-sulfo-β-D-glucopyranoside salts and their *6S*-deuterated analogues. Conformational preferences of their (sulfonyloxy)methyl group. *J. Org. Chem.* **1990,** 55, 902-906.
146. Ogawa, S.; Aoyama, H.; Sato, T., Synthesis of an ether-linked alkyl 5α-carba-β-D-glucoside, a 5α-carba-β-D-galactoside, a 2-acetamido-2-deoxy-5α-carba-β-D-glucoside, and an alkyl 5α-carba-β-lactoside. *Carbohydr. Res.* **2002,** 337, 1979-1992.
147. Koenigs, W.; Knorr, E., Ueber einige Derivate des Traubenzuckers und der Galactose. *Berichte der deutschen chemischen Gesellschaft* **1901,** 34, (1), 957-981.
148. Tsuji, M.; Yamazaki, H. Process for the preparation of pentaacetyl-β-D-glucopyranose. European patent: EP 1041080 A1, 2000.
149. Montgomery, E. M.; Richtmyer, N. K.; Hudson, C. S., The preparation and rearrangment of phenylglycosides. *J. Am. Chem. Soc.* **1942,** 64, 690-694.
150. Lu, S.; Li, X.; Wang, A., A new chiral diphosphine ligand and its asymmetric induction in catalytic hydroformylation of olefins. *Catal. Today* **2000,** 63, 531-536.
151. Lafont, D.; Boullanger, P.; Cadas, O.; Descotes, G., A mild procedure for the preparation of 1,6-Anhydro-β-D-hexopyranoses and derivatives. *Synthesis* **1989**, 191-194.
152. Irvine, J. C.; Oldman, J. W. H., Synthesis of 2:3:5 (or 2:3:4)-trimethyl glucose. *J. Am. Chem. Soc.* **1925,** 127, 2729-2735.
153. Fairbanks, A. J.; Davis, B. G., *Carbohydrate chemistry*. Oxford University Press: 2002.
154. Gan, X. M.; Duesler, E. N.; Paine, R. T., Synthesis and coordination properties of new bis(phosphinomethyl)pyridine *N*,*P*,*P*'-trioxides. *Inorg. Chem.* **2001,** 40, 4420-4427.
155. Young, R. W.; Wood, K. H.; Joyce, R. J.; Anderson, G. W., The use of phosphorous acid chlorides in peptide synthesis. *J. Am. Chem. Soc.* **1956,** 78, 2126-2131.
156. Touchard, F. P., Phosphonate modification for a highly (*Z)*-selective synthesis of unsaturated esters by Horner-Wadsworth-Emmons olefination. *Eur. J. Org. Chem.* **2005**, 1790-1794.
157. Ando, K., Highly selective synthesis of *Z*-unsaturated esters by using new Horner-Emmons reagents, ethyl (diarylphosphono)acetates. *J. Org. Chem.* **1997,** 62, (7), 1934-1939.
158. Lu, W.; Navidpour, L.; Taylor, S., An expedient synthesis of benzyl 2,3,4-tri-*O*-benzyl-β-D-glucopyranoside and benzyl 2,3,4-tri-*O*-benzyl-β-D-mannopyranoside. *Carbohydr. Res.* **2005,** 340, 1213-1217.
159. Zemplen, G.; Pascu, E., Saponification of acetylated sugars and related substances. *Berichte der Deutschen Chemischen Gesellschaft* **1929,** 62B, 1613-1614.
160. Ágoston, K.; Dobó, A.; Rákó, J.; Kerékgyártó, J.; Szurmai, Z., Anomalous Zemplén deacylation reactions of [α]- and [β]-mannopyranoside derivatives. *Carbohydr. Res.* **2001,** 330, (2), 183-190.
161. Yang, G.; Ding, X.; Kong, F., Selective 6-*O*-debenzylation of mono- and disaccharide derivatives using $ZnCl_2$-Ac_2O-HOAc. *Tetrahedron Lett.* **1997,** 38, (38), 6725-6728.
162. Angibeaud, P.; Utille, J. P., Cyclodextrin chemistry. Part I. Application of a regioselective acetolysis method for benzyl ethers. *Synthesis* **1991**, (9), 737-8.

163. Ruiz, J.; Lete, E.; Sotomayor, N., Intramolecular cyclisation of functionalised heteroaryllithiums. Synthesis of novel indolizinone-based compounds. *Tetrahedron Lett.* **2006,** 62, 6182-6189.
164. Vidal, S.; Morere, A.; Montero, J.-L., A convenient synthetic route to mannose 6-phosphonate-cholesteryl conjugate. *Heteroat. Chem* **2003,** 14, (3), 241-246.
165. Brass, S.; Chan, N.-S.; Gerlach, C.; Luksch, T.; Bottcher, J.; Diederich, W. E., Synthesis of 2,3,4,7-tetrahydro-1H-azepines as privileged ligand scaffolds for the design of aspartic protease inhibitors via a ring-closing metathesis approach. *J. Organomet. Chem.* **2006,** 691, 5406-5422.
166. Berkowitz, W. F.; Wu, Y., A C10 Chiron applicable to the synthesis of archaebacterial lipids. *J. Org. Chem.* **1997,** 62, 1536-1539.
167. Cohen, R. J.; Fox, D. L.; Eubank, J. F.; Salvatore, R. N., Mild and efficient Cs_2CO_3-promoted synthesis of phosphonates. *Tetrahedron Lett.* **2003,** 44, 8617-8621.
168. Keen, K.; Parker, E. J., Honours Report. *Massey University, New Zealand* **1999**.
169. Wang, J.; Uttamchandani, M.; Li, J.; Hu, M.; Yao, S. Q., Rapid assembly of matrix metalloprotease inhibitors using click chemistry. *Org. Lett.* **2006,** 8, (17), 3821-3824.
170. Nicolaou, K. C.; Prasad, C. V. C.; Hwang, C. K.; Duggan, M. E.; Veale, C. A., Cyclizations of hydroxy dithioketals. New synthetic technology for the construction of oxocenes and related medium-ring systems. *J. Am. Chem. Soc.* **1989,** 111, 5321-5330.
171. Boomer, J. A.; Qualls, M. M.; Inerowicz, H. D.; Haynes, R. H.; Patri, V. S.; Kim, J.-M.; Thompson, D. H., Cytoplasmic delivery of liposomal contents mediated by an acid-labile cholesterol-vinyl ether-PEG conjugate. *Bioconjugate Chem.* **2009,** 20, (1), 47-59.
172. Tauh, P.; Fallis, A. G., Rate constants for 5-exo secondary alkyl radical cyclizations onto hydrazones and oxime ethers via intramolecular competition experiments. *J. Org. Chem.* **1999,** 64, 6960-6968.
173. Versteegen, R. M.; van Beek, D. J. M.; Sijbesma, R. P.; Vlassopoulos, D.; Fytas, G.; Meijer, E. W., Dendrimer-based transient supramolecular networks. *J. Am. Chem. Soc.* **2005,** 127, (40), 13862-13868.
174. Chacko, A.-M.; Qu, W.; Kung, H. F., Synthesis and in vitro evaluation of 5-[18F]fluoroalkyl pyrimidine nucleosides for molecular imaging of herpes simplex virus type 1 thymidine kinase reporter gene expression. *J. Med. Chem.* **2008,** 51, (18), 5690-5701.
175. Kharrasova, F. M.; Efimova, V. D.; Bikeev, S. S.; Salakhutdinov, R. A., Reaction of carbon tetrachloride with alkyl esters of three-coordinate phosphorus atom acids in the presence of benzaldehyde. *Zh. Obshch. Khim.* **1979,** 49, (11), 2442-6.
176. Arbuzov, B. A.; Vizel, A. O.; Ivanovskaya, K. M.; Gol'dfarb, E. I., Reaction of 2-oxo-2-chloro-3,3,5-trimethyl-1,2-oxa-4-phospholene with ethylene glycol. *Zh. Obshch. Khim.* **1973,** 43, (10), 2134-7.
177. Leonard, J.; Lygo, B.; Procter, G., *Advanced practical organic chemistry*. 2nd ed.; Chapman & Hall: 1995.
178. Tran, D.; Pietersma, A. L.; Schofield, L. R.; Rost, M.; Jameson, G. B.; Parker, E. J., Investigating the role of the hydroxyl groups of substrate erythrose 4-phosphate in the reaction catalysed by the first enzyme of the shikimate pathway. *Bioorg. Med. Chem. Lett.* **2011,** 21, (22), 6838-6841.
179. Nair, V.; Sharma, P. K., Synthesis of the 5'-phosphonate of 4(*S*)-(6-amino-9H-purin-9-yl)tetrahydro-2(*S*)-furanmethanol [*S,S*-IsoddA]. *ARKIVOC (Gainesville, FL, U. S.)* **2003**, (15), 10-14.
180. Kabak, J.; Defilippe, L.; Engel, R.; Tropp, B., Synthesis of the phosphonic acid isostere of glycerol 3-phosphate. *J. Med. Chem.* **1972,** 15, (10), 1074-5.

181. Shopsis, C. S.; Engel, R.; Tropp, B. E., Inhibition of phosphatidylglycerol synthesis in *Escherichia coli* by 3,4-dihydroxybutyl-1-phosphonate. *J. Biol. Chem.* **1974,** 249, (8), 2473-7.
182. Adams, P.; Harrison, R.; Inch, T.; Rich, P., Dehydrogenation of the phosphonate analog of glucose 6-phoshate by glucose 6-phosphate dehydrogenase. *Biochem. J* **1976,** 155, (1), 1-4.
183. Checinska, L.; Kudzin, Z. H.; Malecka, M.; Nazarski, R. B.; Okruszek, A., [(Diphenoxyphosphinyl)methylidene]triphenylphosphorane the double P^+-stabilized carbanion: a crystallographic, computational and solution NMR comparative study on the ylidic bonding. *Tetrahedron* **2003,** 59, (39), 7681-7693.
184. Jones, G. H.; Hamamura, E. K.; Moffatt, J. G., Stable Wittig reagent suitable for the synthesis of α,β-unsaturated phosphonates. *Tetrahedron Lett.* **1968**, (55), 5731-4.
185. Purser, S.; Moore, P. R.; Swallow, S.; Gouverneur, V., Fluorine in medicinal chemistry. *Chem. Soc. Rev.* **2008,** 37, (2), 320-330.
186. Ojima, I., *Fluorine in medicinal chemistry and chemical biology*. John Wiley and Sons: 2009.
187. Kirk, K. L., Fluorine in medicinal chemistry: Recent therapeutic applications of fluorinated small molecules. *J. Fluorine Chem.* **2006,** 127, (8), 1013-1029.
188. Baudoux, J.; Cahard, D., Electrophilic fluorination with N–F reagents. In *Organic Reactions*, John Wiley and Sons: 2004.
189. Be´gue, J.-P.; Bonnet-Delpon, D. l., Recent advances (1995-2005) in fluorinated pharmaceuticals based on natural products. *J. Fluorine Chem.* **2006,** 127, 992-1012.
190. Lal, G. S.; Pez, G. P.; Syvret, R. G., Electrophilic NF fluorinated agents. *Chem. Rev.* **1996,** 96, (5), 1737-1755.
191. Armarego, W. L. F.; Chai, C., *Purification of laboratory chemicals*. 5th ed.; Butterworth-Heinemann: 2003.
192. Li, C.; Li, W.; Wang, J., Gold(I)-catalyzed arylmethylation of terminal alkynes. *Tetrahedron Lett.* **2009,** 50, (21), 2533-2535.
193. Kofron, W. G.; Baclawski, L. M., A convenient method for estimation of alkyllithium concentrations. *J. Org. Chem.* **1976,** 41, (10), 1879-80.
194. Dahlgren, A.; Johansson, P.-O.; Kvarnstro, I.; Musil, D.; Nilsson, I.; Samuelsson, B., Novel morpholinone-based D-phe-pro-arg mimics as potential thrombin inhibitors: design, synthesis, and x-ray crystal structure of an enzyme inhibitor complex. *Biorg. Med. Chem.* **2002,** 10, 1829-1839.
195. Boerjesson, L.; Welch, C. J., Synthesis of 2-hydroxymethyl-1-oxaquinolizidine. *Tetrahedron* **1992,** 48, (30), 6325-34.
196. Jean-Luc, D.; Anne, C.; Céline, H.; Christian, G. B., Photoacylation of alcohols in neutral medium. *Eur. J. Org. Chem.* **2007,** 2007, (13), 2073-2077.
197. Cocinero, E. J.; Gamblin, D. P.; Davis, B. G.; Simons, J. P., The building blocks of cellulose: The intrinsic conformational structures of cellobiose, its epimer, lactose, and their singly hydrated complexes. *J. Am. Chem. Soc.* **2009,** 131, (31), 11117-11123.
198. Petit, J.; Sinay, P., Synthesis of 4-*O*-[(*S*)-1-carboxyethyl]-D-glucose and its (*R*)-isomer. *Carbohydr. Res.* **1978,** 64, 9-16.
199. Zissis, E.; Fletcfher, H. G., Benzyl 2,3,4-tri-*O*-benzyl-β-D-glucopyranosiduronic acid and some related compounds. *Carbohydr. Res.* **1970,** 12, (3), 361.